

DTIC COPY

AFWAL-TR-88-3024

IN-FLIGHT LIGHTNING CHARACTERIZATION PROGRAM ON A  
CV-580 AIRCRAFT



AD-A203 954

H.D. BURKET AND L.C. WALKO  
Flight Dynamics Laboratory  
Wright-Patterson AFB, Ohio 45433-6553

J. REAZER AND A. SERRANO  
Technology/Scientific Services  
Post Office Box 3065, Overlook Branch  
Dayton, Ohio 45431

June 1988

Final Report for Period October 1983 - September 1987

Approved for public release; distribution unlimited

DTIC  
S E C R E T D  
FEB 14 1989  
H

FLIGHT DYNAMICS LABORATORY  
AIR FORCE WRIGHT AERONAUTICAL LABORATORIES  
AIR FORCE SYSTEMS COMMAND  
WRIGHT-PATTERSON AIR FORCE BASE, OHIO 45433-6553

## NOTICE

When Government drawings, specifications, or other data are used for any purpose other than in connection with a definitely Government-related procurement, the United States Government incurs no responsibility or any obligation whatsoever. The fact that the Government may have formulated or in any way supplied the said drawings, specifications, or other data, is not to be regarded by implication, or otherwise in any manner construed, as licensing the holder, or any other person or corporation; or as conveying any rights or permission to manufacture, use, or sell any patented invention that may in any way be related thereto.

This report has been reviewed by the Office of Public Affairs (ASD/PA) and is releasable to the National Technical Information Service (NTIS). At NTIS, it will be available to the general public, including foreign nations.

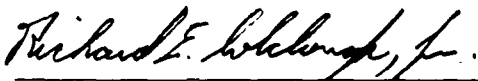
This technical report has been reviewed and is approved for publication.



HAROLD D. BURKET, Project Engineer  
Technology Group  
Survivability Enhancement Branch  
FOR THE COMMANDER



WALLACE C. BUZZARD, Chief  
Survivability Enhancement Branch  
Vehicle Subsystems Division



RICHARD E. COLCLOUGH, JR.  
Chief  
Vehicle Subsystems Division

If your address has changed, if you wish to be removed from our mailing list, or if the addressee is no longer employed by your organization please notify AFWAL/FIES, W-PAFB, OH 45433- 6553 to help us maintain a current mailing list.

Copies of this report should not be returned unless is required by security considerations, contractual obligations, or notice on a specific document.

UNCLASSIFIED

SECURITY CLASSIFICATION OF THIS PAGE

## REPORT DOCUMENTATION PAGE

Form Approved  
OMB No. 0704-0188

1a. REPORT SECURITY CLASSIFICATION UNCLASSIFIED		1b. RESTRICTIVE MARKINGS	
2a. SECURITY CLASSIFICATION AUTHORITY N/A		3. DISTRIBUTION/AVAILABILITY OF REPORT Approved for public release, distribution unlimited.	
2b. DECLASSIFICATION/DOWNGRADING SCHEDULE N/A		5. MONITORING ORGANIZATION REPORT NUMBER(S)	
4. PERFORMING ORGANIZATION REPORT NUMBER(S)  AFWAL-TR-88-3024		7a. NAME OF MONITORING ORGANIZATION	
6a. NAME OF PERFORMING ORGANIZATION Flight Dynamics Laboratory AFWAL AFSC	6b. OFFICE SYMBOL (If applicable) AFWAL/FIES	7b. ADDRESS (City, State, and ZIP Code)	
6c. ADDRESS (City, State, and ZIP Code)  Wright-Patterson Air Force Base, OH 45433-6553		9. PROCUREMENT INSTRUMENT IDENTIFICATION NUMBER	
8a. NAME OF FUNDING/SPONSORING ORGANIZATION	8b. OFFICE SYMBOL (If applicable)	10. SOURCE OF FUNDING NUMBERS	
8c. ADDRESS (City, State, and ZIP Code)		PROGRAM ELEMENT NO. 62201F	PROJECT NO. 2402
		TASK NO. 02	WORK UNIT ACCESSION NO. 43
11. TITLE (Include Security Classification) In-Flight Lightning Characterization Program On A CV-580 Aircraft			
12. PERSONAL AUTHOR(S) Burket, Harold D., Walko, Lawrence C., Reazer, Jean S.*, and Serrano, Arturo V.*			
13a. TYPE OF REPORT Final	13b. TIME COVERED FROM Oct 83 to Sep 87	14. DATE OF REPORT (Year, Month, Day) 1988 June	15. PAGE COUNT 185
16. SUPPLEMENTARY NOTATION *Technology/Scientific Services (T/SS), Dayton, OH 45431			
17. COSATI CODES		18. SUBJECT TERMS (Continue on reverse if necessary and identify by block number)	
FIELD	GROUP	lightning; triggered strike)	
04	01	lightning attachment; intercepted strike	
01	03	direct strike; simulated NEMP <i>electromagnetic pulse</i>	
19. ABSTRACT (Continue on reverse if necessary and identify by block number) A CV-580 aircraft was instrumented with external displacement current density sensors, surface current density sensors, current shunts, and static electric field mill sensors and was flown in active thunderstorms in central Florida during the summers of 1984 and 1985. Electromagnetic data were collected and analyzed for 52 direct lightning strikes to the aircraft flying at altitudes between 2,000 and 18,000 ft. The data consisted of analog records with dc to 2-MHz bandwidth and 10- $\mu$ s windows of digital samples taken at 5-ns intervals. The data show the physical mechanism of lightning attachment to aircraft and suggest three categories of triggered and intercepted lightning strikes to the CV-580. A comparison of aircraft responses to lightning and simulated NEMP is also provided.			
20. DISTRIBUTION/AVAILABILITY OF ABSTRACT <input checked="" type="checkbox"/> UNCLASSIFIED/UNLIMITED <input type="checkbox"/> SAME AS RPT. <input type="checkbox"/> DTIC USERS		21. ABSTRACT SECURITY CLASSIFICATION UNCLASSIFIED	
22a. NAME OF RESPONSIBLE INDIVIDUAL Capt. Harold D. Burket		22b. TELEPHONE (Include Area Code) (513) 255-6823	22c. OFFICE SYMBOL AFWAL/FIES

DD Form 1473, JUN 86

Previous editions are obsolete.

SECURITY CLASSIFICATION OF THIS PAGE

UNCLASSIFIED

## FOREWORD

This report presents the final results of a multiagency lightning measurement program to characterize lightning attachment to a Convair CV-580 aircraft. This effort was managed by the Survivability Enhancement Branch, Vehicle Subsystems Division, Flight Dynamics Laboratory, Air Force Wright Aeronautical Laboratories (AFWAL), Wright-Patterson AFB, Ohio 45433-6553 under Project 2402 Task 02 Work Unit 43, "Lightning/EMP Measurement Program." The CV-580 aircraft and related operational support were provided under the supervision of the Federal Aviation Administration. Lightning acquisition flights were conducted during the summers of 1984 and 1985 in central Florida.

The authors, H.D. Burket and L.C. Walko, wish to thank the numerous agencies that contributed to the success of this program. Participating organizations and key individuals are summarized in Section I and Appendix A. Without the outstanding support and cooperation of everyone involved, it is doubtful that a program of this magnitude could ever have been accomplished. In particular, we wish to acknowledge the efforts of the AFWAL in-house contractor, Technology/Scientific Services (T/SS), whose technical expertise proved invaluable throughout every phase of the program.

Preliminary results from the 1984 portion of this effort were previously published in AFWAL technical report AFWAL-TR-86-3009, Defense Technical Information Center No. A183290.



Accession For	
NTIS GRA&I	<input checked="" type="checkbox"/>
DTIC TAB	<input type="checkbox"/>
Unannounced	<input type="checkbox"/>
Justification	
By	
Distribution/	
Availability Codes	
Avail and/or	
Dist	Special
A-1	

## TABLE OF CONTENTS

SECTION	PAGE
I INTRODUCTION	1
1. General	1
2. Background	2
3. Objectives	5
4. Program Organization	7
II SYSTEMS DESCRIPTION AND PREPARATION	9
1. Test Vehicle	9
2. Aircraft Safety Analysis and Protection	9
3. Tail Boom Design and Analysis	12
4. Airborne Instrumentation	12
a. Sensors	14
(1) Electric Field Sensors	14
(2) Surface Current Sensors	17
(3) Current Shunt	19
(4) Current Probe	20
(5) Magnetic Field Sensor	20
b. VHF Antenna	21
c. Quasi-static Electric Field Measurements	21
d. Internal Induced Transient Measurements	21
e. Cameras	21
f. Recording and Timing Systems	23
(1) Waveform Digitizers	23
(2) Analog Recorder	23
(3) Trigger System and Time Synchronization	23
(4) Strip Chart Recorder	23
5. Ground Station Facility	24
6. Rocket-Triggered Lightning Facility	24
7. Ground Simulation Facilities	25
a. Lightning	25
b. EMP	26

## TABLE OF CONTENTS (Continued)

SECTION	PAGE
III RESULTS	27
1. In-Flight Lightning Characterization	27
a. Summary of Direct Attachments	27
b. Electric Field Measurements	27
c. Electromagnetic Fields and Currents Prior to and During Initial Attachment	34
(1) Negative Leader Intercepts (Category 2)	41
(2) Positive Leader Intercepts (Category 3)	58
(3) Triggered Intracloud Flashes (Category 1)	61
d. Surface Measurements	69
(1) Displacement Currents	69
(2) Surface Currents	70
(3) Rise Times and Rates of Rise	80
e. Current Shunt Measurements	82
(1) Current Pulse Data	82
(2) <i>Continuing Current Data</i>	86
(3) Current Data Summary	89
f. Magnetic Field Measurements	89
g. Quasi-static Electric Fields	95
h. Induced Transients	98
i. Rocket-Triggered Lightning	100
2. Ground Station Far-Field Measurements	103
3. Scale Model Studies	107
4. Ground Simulation Tests	118
a. Lightning	118
b. Simulated Nuclear Electromagnetic Pulse	122
5. CV-580/F-106 Joint Missions	125

## TABLE OF CONTENTS (Concluded)

SECTION	PAGE
IV DISCUSSION OF RESULTS	126
1. General	126
2. Airborne Direct Strikes	126
a. Intercepted Strikes	126
b. Triggered Strikes	128
c. Intracloud Strike Current Measurements	131
3. Instrumentation Considerations	131
4. Predicted Versus Simulated NEMP Responses	133
5. Lightning Versus Simulated NEMP Responses	133
V CONCLUSIONS	135
VI RECOMMENDATION	137
REFERENCES	139
APPENDIX A PROGRAM ORGANIZATIONAL ELEMENTS, RESPONSIBILITIES AND KEY PERSONNEL	143
APPENDIX B ELECTRIC FIELD AT THE FORWARD FUSELAGE AND CURRENT SHUNT DATA FOR LIGHTNING ATTACHMENTS IN 1985	147

## LIST OF FIGURES

FIGURE	PAGE
1 Program Organization	8
2 The CV-580 Aircraft	10
3 External Dimensions of the CV-580 Aircraft	11
4 The Tail Boom Installed on the Aircraft in 1985	13
5 Locations of the Electric Field, Surface Current, Current Shunt, Current Probe, and Magnetic Field Sensors on the Aircraft	15
6 Direction of Negative Charge Flow for a Positive Output From the Surface Current Sensors	18
7 Locations of NRL Field Mills for Quasi-static Measurements on the Aircraft	22
8 The Naval Air Test Center's Electromagnetic Pulse Facility at Patuxent River, Maryland	26
9 Representative Category 1 Waveform With Expansion of Initial 12 ms	33
10 Representative Category 2 Waveform With Expansion of Initial 4 ms	35
11 Representative Category 3 Waveform With Expansion of Initial 4 ms	36
12 Three Category 1 Waveforms Typical of the 32 Waveforms Recorded in This Category at Altitudes Greater Than 14,000 ft	38
13 The Four Category 2 Events Recorded in 1984 and 1985 With Altitudes at Which They Occurred	39
14 Two of the Three Category 3 Events Recorded at Altitudes Above 14,000 ft	40
15 Electromagnetic Field and Current Records at Point A for the Event at 1,500 ft in Figure 13	42
16 Electric Field and Current Records at Point A for the Event at 15,000 ft in Figure 13	43
17 Electromagnetic Field and Current Data During and After Lightning Attachment at 1,500 ft	45
18 A Cloud-To-Ground Channel Passing Close to the Right Wingtip	46

## LIST OF FIGURES (Continued)

FIGURE		PAGE
19	Simultaneous Electric Field and Current Records From a Lightning Attachment in Which the Aircraft Was in a Branch of a Cloud-to-Ground Event	47
20	Lightning Attachment Scenario to Explain the Waveforms Shown in Figure 19	48
21	A Window of 40 $\mu$ s Taken at P in Figure 19 to Show the Absence of Return Stroke Characteristics	49
22	Electric Field and Current Pulses Recorded Digitally as the Branch Attached to the Aircraft Collapses During a Cloud-to-Ground Event	50
23	Stepped Leaders (A) and First Return Stroke (B) Recorded at the Ground Station Simultaneously With the Event in Figure 19	52
24	Electromagnetic Field and Current Data During a Lightning Attachment at 14,400 ft Where the Aircraft Was Part of the Main Channel	53
25	Current Pulses on the Aircraft as the Leader Approaches During the Cloud-to-Ground Event in Figure 24 — Expansion at Point A	54
26	Current Pulses on the Aircraft as the First Return Stroke Passes Through During the Cloud-to-Ground Event in Figure 24 — Expansion at Point B	55
27	Current Pulses on the Aircraft as a Dart Leader (A) and Subsequent Return Stroke (B) Pass Through the Aircraft During the Cloud-to-Ground Event in Figure 24 — Expansion at Point C	57
28	Current Pulses Recorded Digitally During a First Return Stroke of a Cloud-to-Ground Event	59
29	Electric Field and Current Records at Point A in Figure 14	60
30	Initial Portions of Unscaled Electric Field Records Recorded Simultaneously at the Ground Station (Top) and Aircraft (Bottom) During a Strike Triggered by the Aircraft	62
31	Expansion of First Part of Typical Category 1 Electric Field Waveform Shown in Figure 9	64
32	Electric Field and Current Waveforms During the Initial Milliseconds of a Lightning Attachment in Category 1 — Expansion From Figure 31	65

## LIST OF FIGURES (Continued)

FIGURE		PAGE
33	Electric Field and Current Waveforms During the First 12 ms of a Lightning Attachment in Category 1	66
34	Electric Field and Current Waveforms During the First 100 ms of the Lightning Attachment in Figure 9	67
35	Electromagnetic Field and Current Waveforms During a Lightning Attachment in Category 1	68
36	Displacement Current Waveforms Recorded by the Digital System During a Lightning Attachment	72
37	Analog Record for 27 June 1985 Lightning Event Showing Trigger Pulse (A) Which Corresponds to the Time at Which the Data Shown in Figure 36 Was Recorded	73
38	Outputs Expected From Fore and Aft Loop Sensors on Aircraft Fuselage During Four Different Lightning Attachment Scenarios	76
39	Key to Locations of Digital Data Described in Table 10	78
40	Magnetic Field Data Showing Approach of a Stepped Leader, Attachment to the Aircraft and Departure of the Leader	90
41	Electric and Magnetic Field Records During the Initial Attachment Process of an Event Triggered by the Aircraft	92
42	Electromagnetic Field and Current Data During the Initial Attachment Process of an Event Triggered by the Aircraft	93
43	Electromagnetic Field and Current Data During the Initial Attachment Process of Another Event Triggered by the Aircraft	94
44	Return Stroke From Nearby Event Recorded on Magnetic Field Sensor	96
45	Aircraft Potential as Determined From the Quasi-static Electric Fields for an Event Where the Aircraft Was in the Main Channel of a Cloud-to-Ground Discharge	96
46	Aircraft Potential as Determined From the Quasi-static Electric Fields for an Event Where the Aircraft Was in a Branch of a Cloud-to-Ground Discharge	97
47	Aircraft Potential as Determined From the Quasi-static Electric Fields for an Event Triggered by the Aircraft	97
48	Comparison of the Electric Field Record From the Forward Fuselage Sensor With the Field Mill Record Showing Aircraft Potential for an Event Triggered by the Aircraft	99

FIGURE	LIST OF FIGURES (Continued)	PAGE
49	Example of Transient Signals Recorded on Interior Circuits During Lightning Attachments	101
50	Induced Signal on Large Wire Bundle as Compared with Surface Current Recorded on the Forward Upper Fuselage	102
51	Electric Field Produced by a First Return Stroke Recorded at the Ground Station for an Event Where the Aircraft Was in a Branch of a Cloud-to-Ground Discharge	104
52	Digital Data Recorded on the Aircraft at the Time of the Cloud-to-Ground Event Shown in Figure 51.	106
53	Simultaneous Recordings of the Electric Field on the Aircraft and at the Ground Station During an Event Triggered by the Aircraft	108
54	First and Subsequent Return Strokes Recorded at the Ground Station at the End of an Intracloud Event Triggered by the Aircraft	109
55	Scale Model Study Measurement Locations (Not to Scale)	110
56	Comparison of Scale Model Measurements at Three Positions in the Plane of Symmetry Aft of the Aircraft	112
57	Typical CV-580 Response (Taken From Reference 35)	113
58	Predicted Response to the Reciprocal Double Exponential Waveform for the Sensor Location of Figure 57	115
59	Reciprocal Double Exponential and Simulated NEMP Input Waveforms	116
60	Extrapolated Scale Model and Measured Responses of Surface Current Sensor on the Forward Fuselage — Parallel Configuration	117
61	Extrapolated Scale Model and Measured Responses of Left-Wing Electric Field Sensor — Perpendicular Configuration	119
62	Response of the Surface Current Sensors to a Unipolar Current From the 4 $\mu$ F, 200-kV Generator Applied to the Left Wing of the Aircraft	120
63	Response of the Surface Current Sensors to a Unipolar Current From the Fast Rise Time Generator Applied to the Nose of the Aircraft	121

## LIST OF FIGURES (Continued)

FIGURE		PAGE
64	Time and Frequency Domain Responses of the Left Wing Displacement Current Sensor to Simulated NEMP, an Initial Attachment Pulse and a Return Stroke at Altitude	123
65	Time and Frequency Domain Responses of the Aft Fuselage Surface Current Sensor to Simulated NEMP, a Stepped Leader and a Return Stroke at Altitude	124

## LIST OF FIGURES (Concluded)

FIGURE		PAGE
B-1	Event 85-01	148
B-2	Event 85-04	149
B-3	Event 85-05	150
B-4	Event 85-06	151
B-5	Event 85-07	152
B-6	Event 85-08	153
B-7	Event 85-11	154
B-8	Event 85-12	155
B-9	Event 85-13	156
B-10	Event 85-14	157
B-11	Event 85-16	158
B-12	Event 85-17	159
B-13	Event 85-18	160
B-14	Event 85-19	161
B-15	Event 85-20	162
B-16	Event 85-21	163
B-17	Event 85-23	164
B-18	Event 85-24	165
B-19	Event 85-25	166
B-20	Event 85-26	167
B-21	Event 85-27	168
B-22	Event 85-28	169
B-23	Event 85-29	170
B-24	Event 85-30	171
B-25	Event 85-31	172

## LIST OF TABLES

TABLE		PAGE
1	Lightning Mishaps by Type for USAF Aircraft	3
2	Direct Attachments to the Aircraft in 1984	28
3	Direct Attachments to the Aircraft in 1985	29
4	Strike Rates Versus Altitude for the 1984 and 1985 Programs	30
5	Initial Electric Field Changes During the 1984 Events	31
6	Initial Electric Field Changes During the 1985 Events	32
7	Summary of the Average Initial Field Changes for the Three Categories of Electric Field Waveforms	37
8	Leader Velocities During Events Where the Aircraft Intercepted a Negative Leader	44
9	Displacement Current Data	71
10	Digital Data Acquisition in 1984 and 1985	74
11	Surface Currents Measured During Digital Triggers	79
12	Rise Times, Current Levels and Rates of Rise From Digital Data Sets	81
13	Digital Current Data for 1984 and 1985	83
14	Current Pulse Data Summary	85
15	Summary of Current Pulse Interval Data	87
16	Continuing Current Data Summary	88
17	Induced Transients During Lightning Attachments in 1985	101
18	CV-580 Measurement Stations and Excitation Description	114

## SECTION I

## INTRODUCTION

## 1. GENERAL

The Lightning/Electromagnetic Pulse (EMP) Measurement Program was conducted over a 3-yr period which included data acquisition missions during the summers of 1984 and 1985. The program was a multiagency program involving participation by the U.S. Air Force, U.S. Navy, and U.S. Department of Transportation Federal Aviation Administration (FAA), National Aeronautics and Space Administration (NASA), and the French Government research organization, "Office National d'Etudes et de Recherches Aerospatiales" (ONERA). The United States organizations were supported by several contractors and the University of Michigan Radiation Laboratory. The program was managed by the U.S. Air Force Wright Aeronautical Laboratories (AFWAL). The airplane used for this program was an experimentally configured FAA Convair CV-580 flown by FAA Technical Center test pilots. The program was generally conducted according to a test plan entitled "A Program Plan for In-Flight Characterization of Cloud to Ground Lightning Strikes to Aircraft" which was commissioned by the FAA Technical Center at Atlantic City, New Jersey (Reference 1). Participation in the program by U.S. and French Government agencies was in accordance with various agreements which are included in Reference 1. Participation by contractors was under existing or specially executed contracts and subcontracts. In addition to the official participants in the program, support was provided by various lightning researchers in other U.S. Government agencies, U.S. aerospace corporations and U.S. universities. The program was an extremely ambitious one, as detailed in the program plan and this report, whose ambitions were only surpassed by its importance: the protection of future, advanced technology, military and civilian aircraft against the lightning threat without impacting performance or protection against other similar threats. The successes attained by the program would not have been possible without the commitment and dedication of the various organizations and individuals that participated.

The background, objectives and program organization are detailed in the remainder of this section.

## 2. BACKGROUND

The impetus for the program was a result of several factors:

1. The number of lightning-related aircraft mishaps and the attendant costs due to damage, loss of aircraft, and sometimes, loss of life.
2. The on-going conversion from mechanical, electromechanical, and hydraulic flight control systems to electronic (both analog and digital) "fly-by-wire" systems.
3. The increased miniaturization of electronic circuits which operate at very low voltages and currents, making them inherently incapable of experiencing even low-level current and voltage transients without damage or upset.
4. Replacement of traditionally all-metal aircraft skins with advanced composite materials having lower electromagnetic shielding and current carrying capabilities.
5. The redefinition and redistribution of lightning attachment zones resulting from extensive use of advanced composites for external aircraft surfaces.
6. The all-weather capability requirements for a majority of military aerospace vehicles.
7. The fact that, until about 20 yr ago (Reference 2), there was no experimental data from lightning strikes to aircraft. This condition did not change significantly until the advent of the NASA F-106 program (Reference 3).

Several of the fundamental questions that needed to be answered were addressed, and although considerable progress has been made during these and related programs, only some have been answered from the results obtained. Preventing more and conclusive answers are the limited numbers of data points and instrumentation system limitations.

Lightning incident statistics for commercial aircraft from 1950 to 1974 (Reference 4) suggest a lightning strike to aircraft rate of once every 2930 h

(hours). For military aircraft, the same reference cites rates ranging from one per 50,480 h (bombers) to one per 295,600 h (trainers), with an average of one per 137,320 h (including cargo and fighter aircraft), between 1965 and 1969. For USAF aircraft between 1970 and 1982, the breakdown of 877 mishaps as presented in Reference 5 is listed in Table 1.

TABLE 1. Lightning Mishaps by Type for USAF Aircraft  
(Based on 877 Incidents)

<u>Aircraft Type</u>	<u>Percent of Incidents</u>	<u>Aircraft Losses</u>
Cargo	48.9	3
Fighter	31.2	4
Bomber	9.5	-
Trainer	8.3	-
Attack	1.5	-
Helicopter	0.6	-

Several factors other than aircraft type also affect the strike rates to aircraft including geographical area, time of year, and mission flown. As an example, from the data in Reference 5, the highest lightning mishap rates were experienced during the Southeast Asia conflict years when more all-weather missions were probably flown. Nevertheless, from these data covering a 13-yr span, the average number of lightning mishaps per year was 67.5. Reference 6 presents 1967 data, based on USAF and British commercial aircraft, as a function of geographical area as follows: 54 percent in Europe, 29 percent in the U.S. and 17 percent in Asia. The corresponding rates were: one per 1923 h, one per 8333 h, and one per 11,111 h.

The cost of lightning mishaps to aircraft in terms of dollars can be and has been significant. For instance, in Reference 7 which presents data on USAF experience between 1970 and 1975, 55 percent of all aircraft mishaps reported were lightning related and cost an estimated \$7.3 million.

The existing knowledge on the characteristics of cloud-to-ground lightning is based on ground measurements. Statistics from this type data have been used to

derive comprehensive engineering ground lightning environments (Reference 8) and books by Uman (Reference 9) and Golde (Reference 10). In turn, this type of data has been used to develop test waveforms for lightning protection (Reference 11).

The problem is that, at least as far back as 1942 (Reference 12), it has been suspected that most lightning strikes to airplanes involve cloud-to-cloud discharges and that the aircraft triggers many of these discharges. In addition, even when struck by a cloud-to-ground lightning, the characteristics of the lightning channel at the aircraft altitude are expected to be different than on the ground. Quoting from Reference 12: "Thus, if one measures a current of 100,000 A (amperes) in a stroke of lightning, that current peak will presumably have the greatest magnitude at the surface of the earth, with decreasing magnitude upward along the channel."

Aircraft designers are faced with the dilemma of whether to protect aircraft to the most severe lightning threat or to the most probable threat. The most severe threat would be a cloud-to-ground strike when flying at low altitude, while the most probable threat would be a cloud-to-cloud or triggered strike at higher altitudes. The most conservative approach, which has been used to date, is to protect against cloud-to-ground lightning with parameters defined at ground level. This approach, however, does not answer the question as to whether this threat definition provides adequate protection against the most probable threat, for which the amount of experimental data was limited mainly to that from the Rough Rider program (Reference 2).

The need for this program was established on the basis of all the factors discussed above. Several other considerations were involved in determining how the program would be conducted. Among these were how to get the most data in the time available and what measurements needed to be made, without duplicating the objectives of the NASA F-106 in-flight lightning characterization program (Reference 3). From the Table 1 data we see that the largest percentages of mishaps, and also the most severe ones, involve cargo and fighter aircraft. Almost 50 percent of all the incidents involved cargo aircraft. From the Air Force viewpoint, this category included the present C-130, C-141, C-5, and KC-135 fleets, plus special mission aircraft such as Air Force 1, the airborne command posts, AWACS and such. The first choice of aircraft to be used for this program was a C-130 aircraft, since this was

the largest fleet in operation. However, this type of resource was not available for this program. A second choice was a NAVY P-3 aircraft because of its all-weather mission capability, but this type of resource was also not available. Thus the final selection was a commercial type cargo airplane which the FAA could make available for this program.

To enhance the probability of acquiring the maximum amount of data in the least amount of time, it was decided to penetrate thunderstorm clouds (where the occurrence of lightning is most predictable), in central Florida where the most thunderstorm days per year (70-90) occur in the U.S., particularly in the July-August period. This area had the added benefit that Air Force (Patrick AFB) and NASA facilities (Kennedy Space Center) were available for aircraft ground support and weather/aircraft tracking. The best estimate available as to the number of lightning strikes per flight hour was based on data collected between 1964 and 1966 during a multi-aircraft lightning research program (Reference 13). Fitzgerald (Reference 14) estimated the average probability of a lightning strike to the aircraft during storm penetration to be 0.021, based on the ratio of aircraft-strikes to the total number of flashes during the penetration periods. Since there were 33 strikes experienced in 27 penetrations, the average number of strikes per penetration was 1.2. In contrast, Imyanitov (Reference 15) computed the probability of intercepting a strike to be less than  $10^{-4}$  when penetrating a thunderstorm. For this probability, he used a "geometric" model in which he assumed a channel length of 10 km, a cloud volume of  $10 \times 10 \times 10 \text{ km}^3$ , an aircraft length and wing span of 30 m, an aircraft speed of 500 km/h, and a time interval of 10 s (seconds) between discharges. This type of model does not take into consideration strikes that are triggered by the presence of the aircraft, but it may not be an unreasonable way of estimating the probability of intercepting a cloud-to-ground channel. Such a model, however, does not consider the possibility of intercepting a leader from the cloud which does not reach the ground.

### 3. OBJECTIVES

The main objectives of the program were to: (a) obtain a data base of lightning direct strikes to a cargo type aircraft, (b) expand the existing data base and quantify the nature of atmospheric electricity hazards to aircraft, (c) delineate lightning characteristics, and (d) define and validate lightning characterization models and threat definitions.

The first objective was a result of the facts that the only data available for lightning strikes to aircraft was for a fighter (F-100), that NASA was using a fighter (F-106) aircraft to collect additional direct strike data, and that a 13-yr mishap analysis by the Air Force revealed that almost 50 percent of the mishaps involved cargo type aircraft. The second objective related to the fact that the only officially defined lightning threat to aircraft was based on ground measurements of the cloud-to-ground discharges while available data indicated that most strikes to aircraft appear to be triggered intracloud or cloud-to-cloud strikes. The third objective was intended to define the differences between the characteristics of lightning at measured aircraft altitude and on the ground. The fourth objective would result in validation or redefinition of existing lightning models used to define test methods for protection and qualification of aerospace vehicles against atmospheric electricity hazards.

A secondary but important objective was to subject the aircraft to a simulated nuclear EMP (NEMP) environment and compare the response to this threat to the lightning response.

The major objectives of this program were to be accomplished by obtaining time-synchronized measurements of the electromagnetic fields and currents on the aircraft during lightning attachments at altitudes from 2,000 to 20,000 ft. The measurements were to be made by a hybrid instrumentation and data acquisition system capable of recording fast transient processes as well as the entire lightning/aircraft interaction process. The measurements to be made included:

- a. Incident electric and magnetic fields prior to attachments or from nearby flashes.
- b. Surface, displacement, continuing and total currents and current distributions during attachments.
- c. Induced transients on actual aircraft circuits.
- d. Quasi-static ambient electric field conditions both before and after the attachments.

e. Aircraft responses (see a, b, and c) to simulated NEMP.

f. Thunderstorm electrical activity, turbulence, and lightning activity, along with weather radar patterns for correlation purposes.

Data for item d. was not recorded by the USAF system and is documented in Reference 16, although some of this data is presented and discussed in this report. Data for item f. was also not recorded by the USAF system and although referred to (Reference 17), is not presented in this report.

#### 4. PROGRAM ORGANIZATION

The organization of this international, multi-U.S. agency program is illustrated in Fig. 1. Funding responsibility was shared by the U.S. Air Force, DOT/FAA, U.S. Navy, and France. Generally, each of these organizations funded their respective efforts, although there were cases of interagency funding. The primary responsibilities of each of the organizational elements and key participants are detailed in Appendix A.

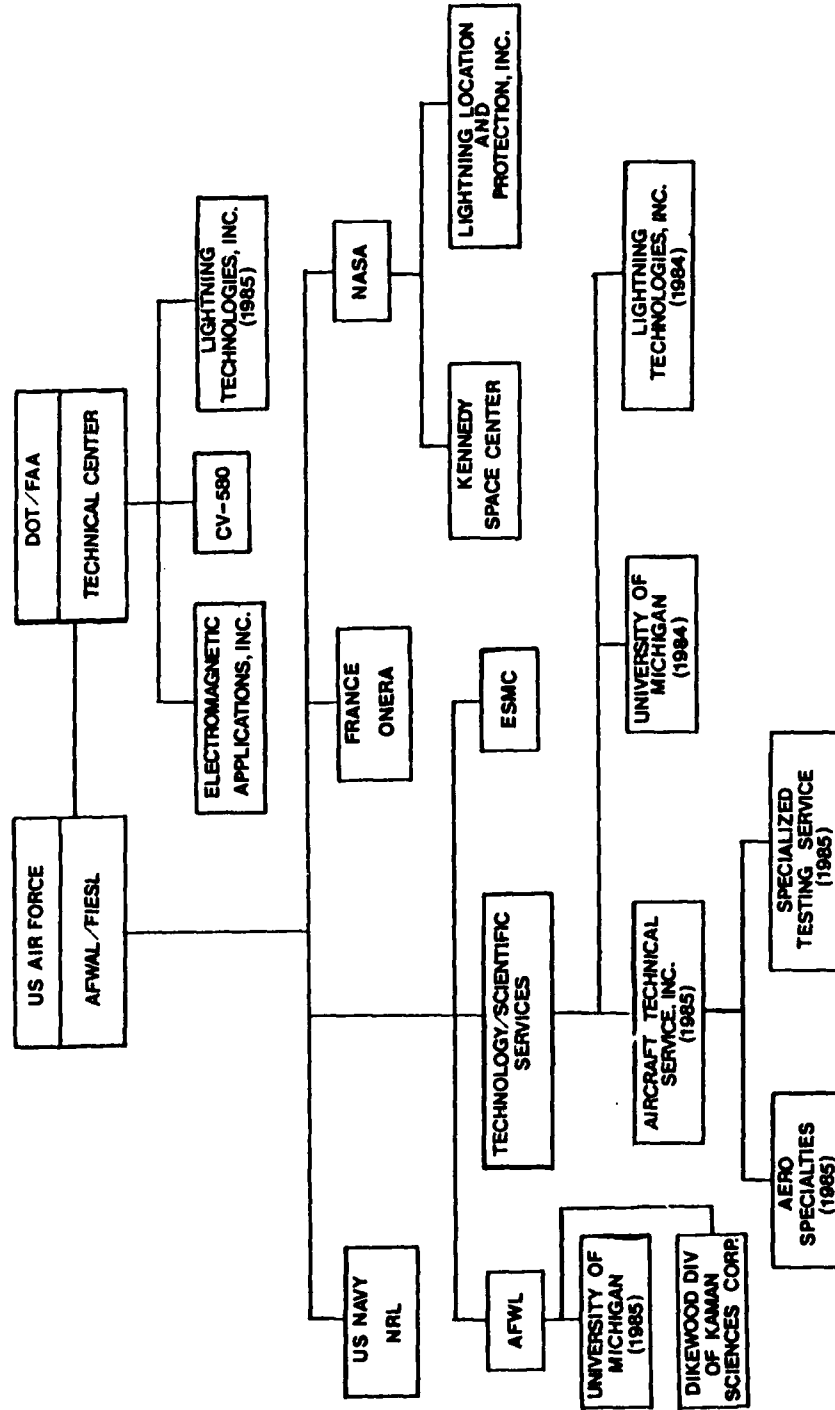


Figure 1. Program Organization

## SECTION II SYSTEMS DESCRIPTION AND PREPARATION

### 1. TEST VEHICLE

The CV-580 aircraft used in both years of the program is shown in Fig. 2. Its exterior dimensions are diagrammed in Fig. 3. The twin-engine, turboprop, low-wing aircraft was flown for over 100 h at altitudes of 1,500 to 18,000 ft and air speeds of 160 to 280 knots in central Florida thunderstorms. A dedicated C-band radar was used to track the aircraft at all times and guide it away from areas of reflectivity exceeding 40 dBZ.

### 2. AIRCRAFT SAFETY ANALYSIS AND PROTECTION

Lightning Technologies, Inc. (LTI) was responsible for the safety of the aircraft. Initial conversations with representatives from airlines flying Convair aircraft showed that lightning strikes usually attached to the rudder, vertical stabilizer, outboard trailing edges of the ailerons and elevators, the fuselage aft of the wing roots, the propeller blades and radome. Other possible problem areas considered in detail by LTI, because of the increased lightning exposure during this mission, were the fuel tanks, wingtip navigation lights, and power distribution busses.

Particular attention was paid to the aircraft fuel tanks. They were drained, then visually inspected to check the condition of the fuel tank sealant, fuel quantity unit wiring and clearances between fuel probes and the adjacent fuel tank skin. Potential spark sources were investigated by injecting current pulses into the wingtip and checking for internal sparking with cameras (Reference 18). Paint was removed from the aircraft wing skin over the fuel tanks to reduce dwell times during swept strokes. Finally, it was recommended that the aircraft be fueled with JP-5 at all times because of its low volatility at the pressure and temperature the fuel would be subjected to during flights.

Prior to flights in 1985, the vertical fin cap was modified to include a boom with a current shunt and the vertical fin strobe light was relocated to the tail cone of the aircraft. The modified fin cap was also evaluated for safety purposes.



Figure 2. The CV-580 Aircraft

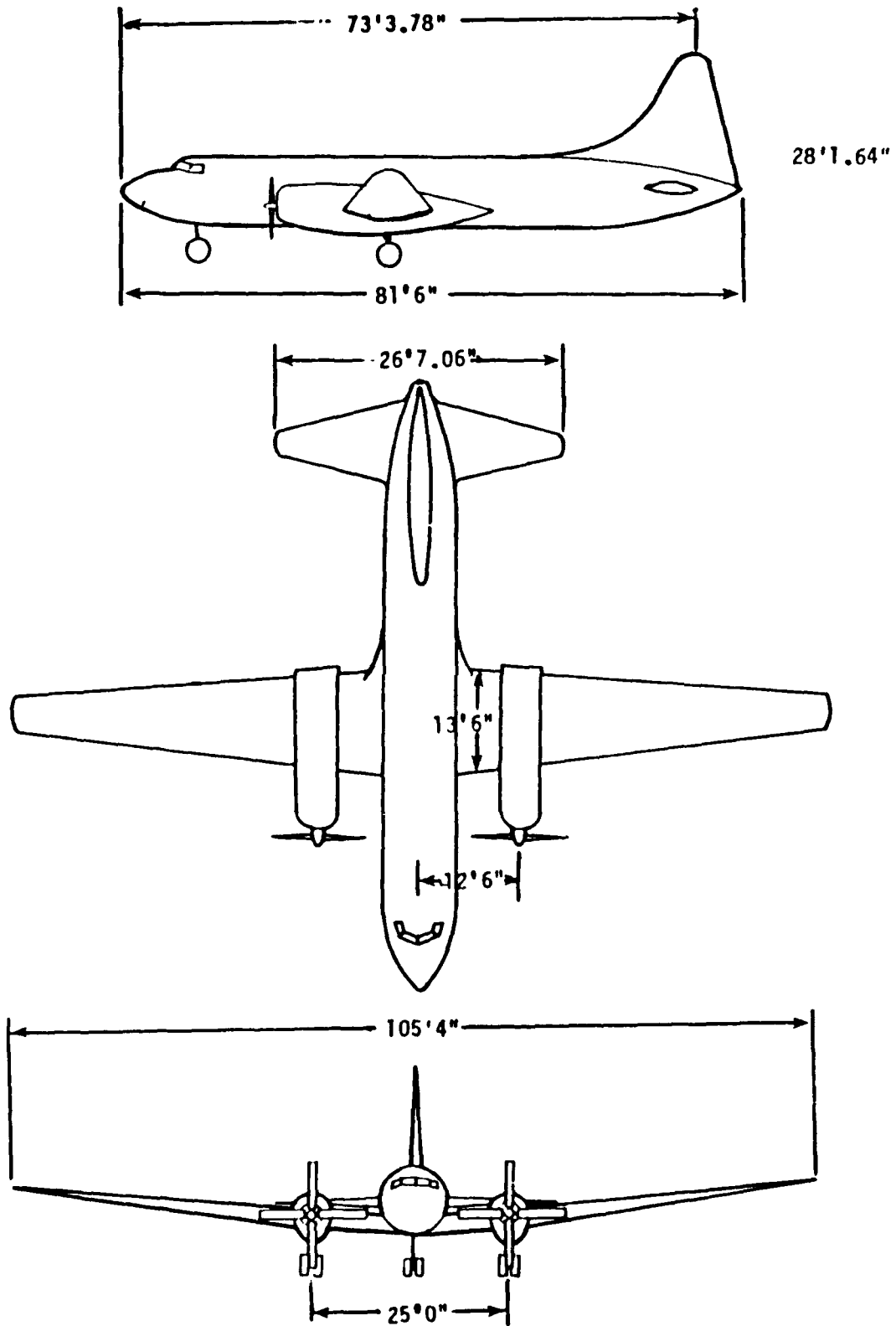


Figure 3. External Dimensions of the CV-580 Aircraft

In other modifications, copper-loaded paint was applied to the rudder cap, diverter strips were added at the wingtips to protect the navigation lights and on the radome, surge protectors were added to the ac and dc power distribution busses and all superfluous antennas were removed.

Ground tests were conducted on the aircraft in 1984 and 1985 by applying impulse currents of up to 100-kA (kiloamperes) peak to the nose or wingtip while all flight-essential electrical and avionics systems were running under engine power. During initial testing, the aircraft fuel tanks were fully fueled and inerted with nitrogen. Subsequent tests were run without inerting. No problems were encountered.

### 3. TAIL BOOM DESIGN AND ANALYSIS

The major addition to the aircraft in 1985 was a boom that protruded 12 ft 8 in from the aft fuselage. The main purpose of the boom, shown in Fig. 4, was to carry a magnetic field sensor at a distance far enough from the aircraft so that it would be suitable for free field measurements. Scale model studies by the University of Michigan (Reference 19) were used to determine the minimum length required.

The boom was designed and fabricated by Technology/Scientific Services, Inc. The boom installation design (Reference 20) was developed by Aircraft Technical Services, Inc. (Van Nuys, CA). Aircraft modification and initial boom installation were performed by Aero Specialties (Van Nuys, CA). After installation of the boom was complete, ground vibration and instrumented flight flutter and vibration tests were conducted on the aircraft by Specialized Testing Service (N. Hollywood, CA) (Reference 21). Results showed the modified aircraft was flutter free within the requirements of all pertinent regulations.

### 4. AIRBORNE INSTRUMENTATION

The frequency content of the electromagnetic fields and currents produced by lightning discharges extends from near dc to hundreds of megahertz (MHz). A typical event lasts about 0.5 s, but some of the pulses in the flash have rise times on the order of tens of nanoseconds (ns). Consequently, to measure the characteristics of individual pulses in a flash and still be able to record the entire event, the



Figure 1. The Tail Boom Installed on the Aircraft in 1936

instrumentation system must have a frequency response from near dc to about 100 MHz. This wideband frequency response was obtained with a combination of analog and digital recorders in the aircraft and at the ground station. This section provides a detailed description of all the sensors, recorders, and other instrumentation on the aircraft.

a. Sensors

The aircraft was instrumented with a variety of sensors. Figure 5 shows the locations of the four electric field sensors, four surface current sensors, four current shunts, one current probe, and one magnetic field sensor.

(1) Electric Field Sensors

The four electric field sensors were flush plate dipole (FPD) designs provided by EG&G. All four had a frequency response greater than 350 MHz and a rise time of 1 ns. The sensors on the left and right wingtips and vertical tail had an equivalent area of 0.01 m<sup>2</sup>, making them more sensitive than the sensor on the forward fuselage with an equivalent area of 0.005 m<sup>2</sup>. This higher sensitivity combined with their location at the extremities of the aircraft (Reference 22) made these three sensors much more responsive to electric field induced displacement currents on the aircraft skin. The less sensitive electric field sensor on the forward upper fuselage was set up to record the ambient electric field. The unintegrated output of each sensor is proportional to the displacement current according to the following relationship:

$$V_o = R A_{eq} \frac{dD}{dt} \cos \theta \quad (1)$$

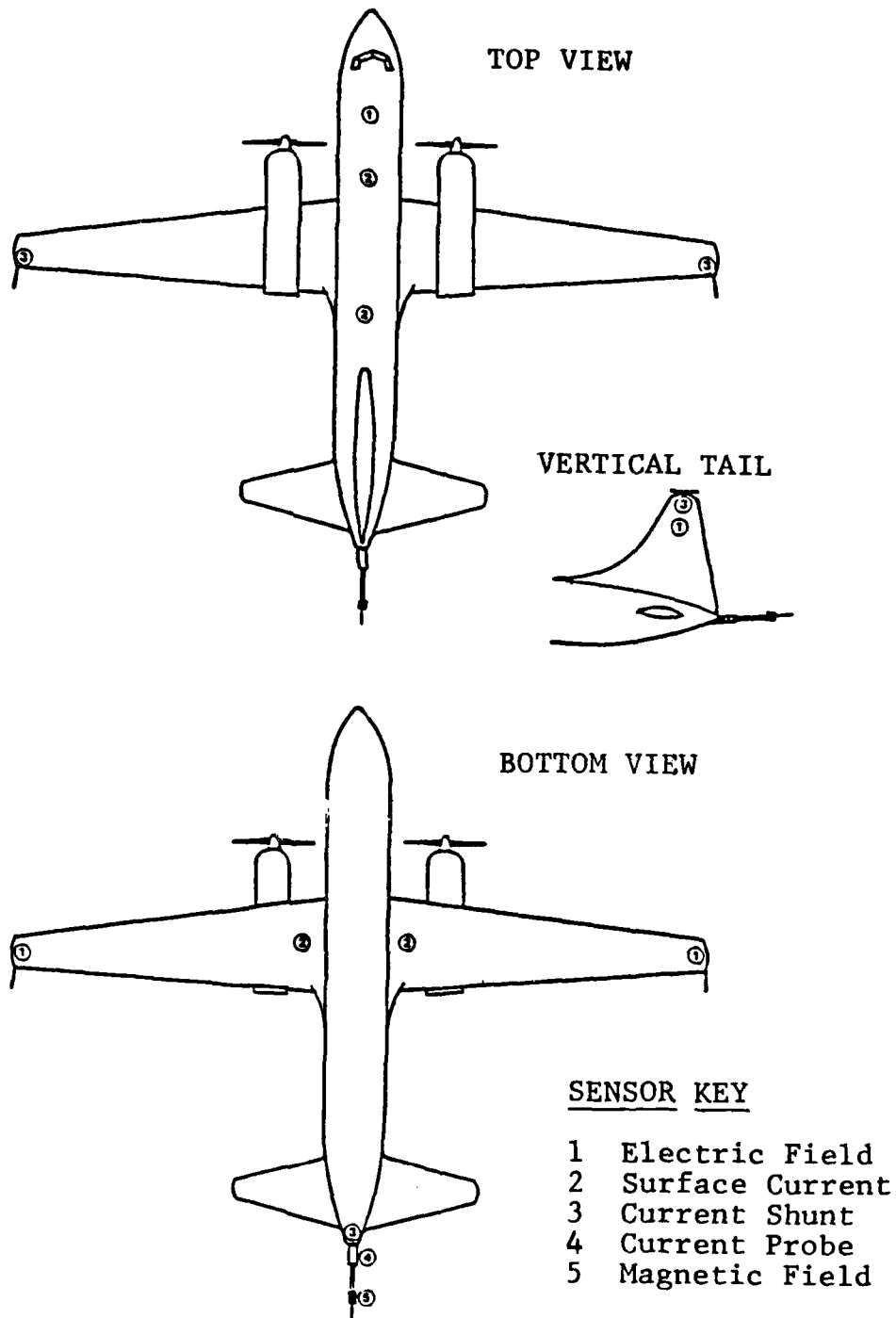


Figure 5. Locations of the Electric Field, Surface Current, Current Shunt, Current Probe, and Magnetic Field Sensors on the Aircraft

Where:

- $V_0$  = sensor output in volts
- $R$  = load impedance ( $50 \Omega$  (ohms))
- $A_{eq}$  = sensor equivalent area in square meter
- $D$  = magnitude of electric displacement vector  $D = \epsilon_0 E$  in  $C/m^2$
- $E$  = electric field magnitude in volt per meter
- $\epsilon_0$  = permittivity of free space ( $8.8 \times 10^{-12}$  F/m)
- $\theta$  = angle between  $E$  and vector normal to sensor surface

The derivative outputs from the three displacement current sensors were sampled at a 5-ns rate and recorded digitally in 10- $\mu$ s (microsecond) windows. For analog recording, the outputs were integrated, as described in Reference 23. The output from the electric field sensor on the forward upper fuselage was integrated with a time constant of 220 ms (milliseconds) to obtain a low frequency response of 1.5 Hz. This provided an overall view of both the slow and fast electric field changes during the event and greatly facilitated interpretation of all the other data.

Since the aircraft received actual attachments of lightning events, the electric field sensors saw large changes due to negative charge flow on or off the aircraft. Interpretation of these changes was facilitated by reporting the results in terms of the charge change in the vicinity of the sensor, rather than the electric field producing the change. The electric field data in this report was presented in this fashion; i.e., an increase in negative charge in the vicinity of the sensor produced a negative excursion in the data while a decrease in negative charge (increase in positive charge) produced a positive excursion. Outputs were scaled in coulombs per square meter ( $C/m^2$ ), without attempting to account for field enhancement due to sensor location on the aircraft. Thus, the actual value of the electric field could be lower by as much as a factor of 3. Field enhancement due to a particular sensor's location on the aircraft must be taken into account before comparing the magnitudes of these electric fields with corresponding measurements at ground level.

Plotting the data required a reversal in polarity since the usual sensor output was in terms of the ambient electric field producing the charge change at the sensor. This reversal was accomplished for the three electric field sensors on the left and right wing and vertical tail by inverting the signal through the electronics. This was not done with the forward fuselage sensor—as a result, data from this sensor was plotted with the negative axis up.

(2) Surface Current Sensors

The four surface current sensors were a multigap loop (MGL) design by EG&G with an equivalent area of 0.001 m<sup>2</sup>, a frequency response greater than 700 MHz, and a rise time of 0.5 ns. Derivative outputs from these sensors were recorded digitally in 10-μs windows. Integrated data from these sensors was recorded on analog tape. However, due to signal conditioning problems, cable shield currents, and signal-to-noise problems, the integrated data could not be processed by conventional methods.

Part of the analysis of the digital surface current data requires a knowledge of the polarities produced as current flows through the particular sensor. Figure 6 shows the sensor locations on the aircraft with arrows indicating the direction of negative charge movement which would produce a positive output. For example a cloud-to-ground return stroke attaching and injecting negative charge into the nose of the aircraft would produce positive outputs on both fuselage sensors. This is discussed in more detail in Section III. The unintegrated sensor output is proportional to the surface current density according to the relationship:

$$V_o = \mu_o A_{eq} \frac{dJ_s}{dt} \sin \theta \quad (2)$$

Where:

- $V_o$  = sensor output in volts
- $\mu_o$  = permeability of free space ( $4\pi \times 10^{-7}$  H/m)
- $A_{eq}$  = sensor equivalent area (0.001 m<sup>2</sup>)
- $J_s$  = surface current density in ampere per meter
- $\theta$  = angle between sensor axis and  $J_s$  vector

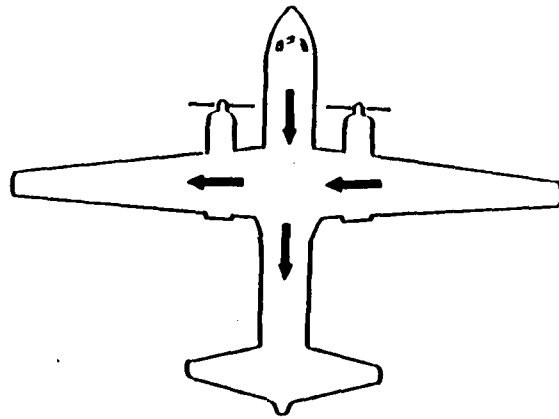


Figure 6. Direction of Negative Charge Flow for a Positive Output From the Surface Current Sensors

The digital output from these sensors was generally scaled in teslas per second (T/s), then integrated for an output in teslas. In many cases, the integrated data was also scaled in amperes per meter (A/m), then multiplied by the fuselage or wing circumference to infer the total current (assuming uniform distribution) in amperes for comparisons with the current shunt data.

### (3) Current Shunts

Resistive current shunts designed by T&M Research Products were mounted at the base of booms on each wingtip (Type K), the tail boom (custom design), and a boom on the vertical tail (Type F). The shunts consisted of  $5 \times 10^{-3}$ - $\Omega$  resistance with a 200-MHz bandwidth and a 2-ns rise time. The sensor output is proportional to the current according to the relationship:

$$V_o = IR \quad (3)$$

Where:

$V_o$  = sensor output in volts

$I$  = current in amperes

$R$  = shunt resistance in ohms

Output from the shunts were recorded digitally in 10-  $\mu$ s windows and on analog tape during the entire event. They provided direct measurements of the current in amperes for comparison with the surface current sensors.

Polarities of the measurements also provided important information for the data analysis in the case of the current shunts. For the shunts at the wingtips and vertical stabilizer, negative charge flowing into the boom and onto the aircraft produced a negative output, while negative charge flowing off the aircraft and out of the boom produced a positive output. The tail boom shunt installation, however, resulted in the polarities being reversed for that particular sensor.

## (4) Current Probe

An outside moebius mutual inductance (OMM) current probe made by EG&G measured the time rate of change of the current through the tail boom. Its derivative output was stored digitally in 10- $\mu$ s windows and in analog form during the entire event. The probe output is proportional to the current according to the relationship:

$$V_o = M \frac{di}{dt} \quad (4)$$

Where:

$V_o$  = sensor output in volts

$M$  = sensor mutual inductance ( $2 \times 10^{-7}$  H)

$I$  = total current in amperes

## (5) Magnetic Field Sensor

A multigap loop (MGL) sensor designed by EG&G was mounted on a 12-ft boom at the tail of the aircraft to minimize aircraft perturbation of the free field measurements (Fig. 4). Because of its orientation, the loop was most sensitive to vertical electric fields off the wingtips and least sensitive to fields off the nose. Vertical negative charge moving downward off the right wingtip produced a positive output from the sensor while the same charge moving downward off the left wingtip produced a negative output.

The derivative output from the sensor was stored digitally in 10- $\mu$ s windows. Integrated output for the entire event was stored on analog tape. The sensor output is proportional to the magnetic field in free space according to the relationship:

$$V_o = A_{eq} \frac{dB}{dt} \quad (5)$$

Where:

$V_o$  = sensor output in volts

$A_{eq}$  = sensor equivalent area ( $10^{-2}$  m<sup>2</sup>)

$B$  = magnetic flux density vector in teslas

b. VHF Antenna

A STAREC Type 2204 VHF antenna was mounted on top of the fuselage to measure the VHF radiation from lightning discharges. The antenna output was connected to a 120-MHz VHF receiver supplied by ONERA. The receiver output was recorded continuously on one channel of the analog recorder.

c. Quasi-static Electric Field Measurements

Four NRL shutter-type field mills were installed on the aircraft as shown in Fig. 7. The use of four field mills allowed determination of the vertical and horizontal external field components and the aircraft charge (potential). Details of the field mill system and its calibration are reported in Reference 24.

d. Internal Induced Transient Measurements

Three types of current probes designed by EG&G were used to measure the current induced by lightning attachments on several circuits in the aircraft during 1985. The specific types were: coaxial current probe (CAP-1, sensitivity  $1 \mu\text{V}/\mu\text{A}$  (microvolt per microampere) into  $50 \Omega$ ), snap-on current probe (SCP-1, sensitivity  $1 \text{ V/A}$  (volt per ampere)), and clip-on probe (COP-1, sensitivity  $1 \text{ mV/mA}$  (millivolt per milliampere)). The data was stored digitally in  $10\text{-}\mu\text{s}$  windows.

e. Cameras

Four video cameras were mounted in the aircraft. Two of the cameras were the solid state, charged coupled device (CCD) type. These cameras were equipped with Nikon Fish Eye - Nikkor 8 mm, f2.8, lenses. In 1984, the effective field of view was about  $90^\circ$  because of the difference in lens format (35 mm) and camera format (16 mm). For 1985 missions, the lenses were modified to attain almost the full  $180^\circ$  field of view. The cameras were mounted on the fuselage, one on top looking up and one on the bottom looking down. The other cameras were of the conventional Vidicon type mounted on instrumentation racks on each side of the aircraft in order to view the wingtips using standard lenses.

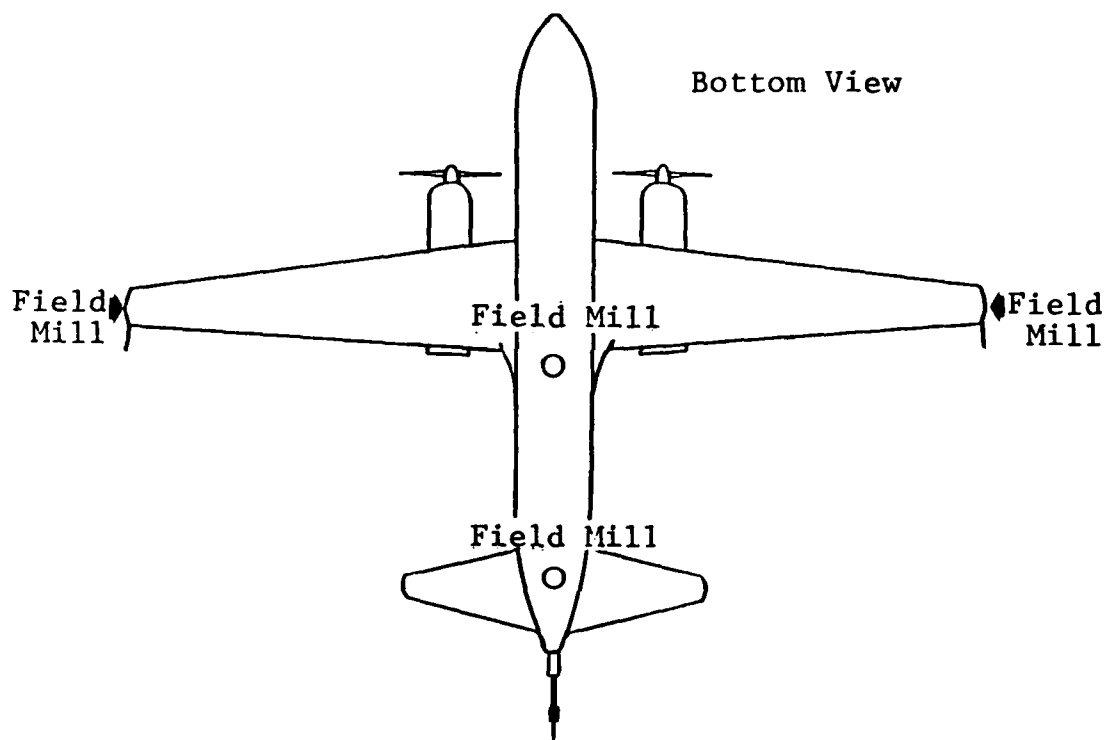


Figure 7. Locations of NRL Field Mills for Quasi-static Measurements on the Aircraft

f. Recording and Timing Systems

(1) Waveform Digitizers

The waveform digitizers were Tektronix 7612Ds with type 7A16P programmable plug-ins. The digitizers were controlled by software developed in the AFWAL/FIESL Research Facility and by a PDP-11/35 minicomputer. The digitizers were triggered simultaneously by a common pulse from the trigger system so that all the digital records were time-synchronized. After the waveform was digitized, we transferred it to a 9-track tape for storage under the automatic control of the computer system. The digitizers were operated at the fastest sampling rate (5 ns) to produce a 10- $\mu$ s window with 2,048 samples at 5-ns intervals.

(2) Analog Recorder

The analog recorder was a Honeywell 101, 28-channel recorder. FM channels had a bandwidth of dc to 500 kHz while direct record channels had a bandwidth of 400 Hz to 2 MHz.

(3) Trigger System and Time Synchronization

The trigger system was activated by preselected signals from the current shunt sensors or the unintegrated output of the surface current sensors. It was set to detect a level change, either positive or negative, from any of their inputs which exceeded a predetermined threshold setting. It would then output a common pulse to each of the digitizers, the system controller, and the analog recorder. Time synchronization between the analog and digital recordings was via the trigger pulse recorded on one analog channel. Time synchronization with the video recording systems was accomplished by recording IRIG B time code on each recorder.

(4) Strip Chart Recorder

A 6-channel Gould ES1000 strip chart recorder was monitored continuously during flight. The time code, electric field and current shunt outputs were displayed here so that events could be located quickly after the flight.

A more detailed explanation of the aircraft instrumentation is provided in Reference 23.

## 5. GROUND STATION FACILITY

A ground station at Cape Canaveral Air Force Station recorded the electric and magnetic fields produced by distant lightning in 1984. Four flush plate dipole electric field sensors and two magnetic field CML-7 loop sensors were mounted on an aluminum wire mesh ground plane extending into the ocean near the instrumentation van. Copper rods were driven into the ground and connected to the mesh to insure a good ground reference. Signal cables from the sensors ran through metallic conduit to the van.

Data from both types of sensors was integrated and stored continuously on a Bell and Howell VR-3700B, 14-channel analog recorder with wideband II electronics. IRIG B time signals from the Kennedy Space Center were recorded at both the ground station and the aircraft to ensure time synchronization. Further information on the 1984 ground station instrumentation is given in Reference 23.

In 1985, the ground station was relocated to another site at Kennedy Space Center where lightning was being triggered by rockets. The same sensors were used but were mounted on the roof of the instrumentation van and therefore required calibration to determine enhancement factors. Otherwise, operations were the same as in 1984.

## 6. ROCKET-TRIGGERED LIGHTNING FACILITY

In 1985, the ground station was collocated with the rocket-triggered lightning facility operated by several French and American scientific groups. Rockets towing lengths of wire were fired into thunderstorm clouds when electric fields in the area reached specified levels, triggering lightning strikes to an instrumented cylinder equipped with an inductive current probe and a current shunt. The aircraft was flown near the facility at low altitude in hopes that a lightning event could be triggered and its current levels recorded simultaneously on the aircraft and at the ground.

## 7. GROUND SIMULATION FACILITIES

### a. Lightning

Lightning simulation tests were performed on the aircraft to verify the integrity of the sensor signal cables, data acquisition equipment, and instrumentation power sources and lines. In addition, electromagnetic and current signals resulting on the aircraft from various current pulses were recorded for comparison with lightning data and to verify the effectiveness of hardening measures.

Tests were performed at Wright-Patterson AFB on three occasions; in June and October of 1984, and in June 1985. In June 1984, the impulse current generator used was a two-stage capacitor bank with a 4- $\mu$ F (microfarad) capacitance and 200 kV charging voltage. The aircraft was isolated from ground by Lexan<sup>®</sup> sheets and a flat, heavy wire mesh screening was placed under the wings and fuselage as a return path. Oscillatory current pulses of up to 115 kA peak were applied in various configurations, including wing-to-wing and nose-to-tail.

Tests conducted in October 1984 employed a fast rise time current generator that produced current pulses with submicrosecond rise times by using a 4-MV (megavolt) Marx generator with a 1 nF (nanofarad) peaking capacitance. The return path was also changed, to a quasi-coaxial screen completely encircling the fuselage or wings of the aircraft, depending on the current injection point. Unipolar pulse currents of 40-kA peak with rise times of 200 ns were applied in various configurations.

Change in instrumentation necessitated further ground tests before the flights in 1985. These tests were performed with the fast rise time generator and flat, wire mesh return path.

---

<sup>®</sup> Registered trademark of the General Electric Company

## b. EMP

In addition to lightning characterization, the program objectives called for comparing the aircraft response to a simulated nuclear electromagnetic pulse (EMP) and to a lightning strike. Ground EMP simulation facilities at the Naval Air Test Center in Patuxent River, Maryland were used for these tests. The EMP simulator consisted of a 5-MV pulse generator suspended above the aircraft in a horizontally polarized dipole configuration. The generator produced a 60- to 65-kV/m electric field with a 7- to 8-ns rise time at a point corresponding to the top of the fuselage. Figure 8 is a diagram of the facility. The aircraft was pulsed with the fuselage parallel or perpendicular to the incident electric field.

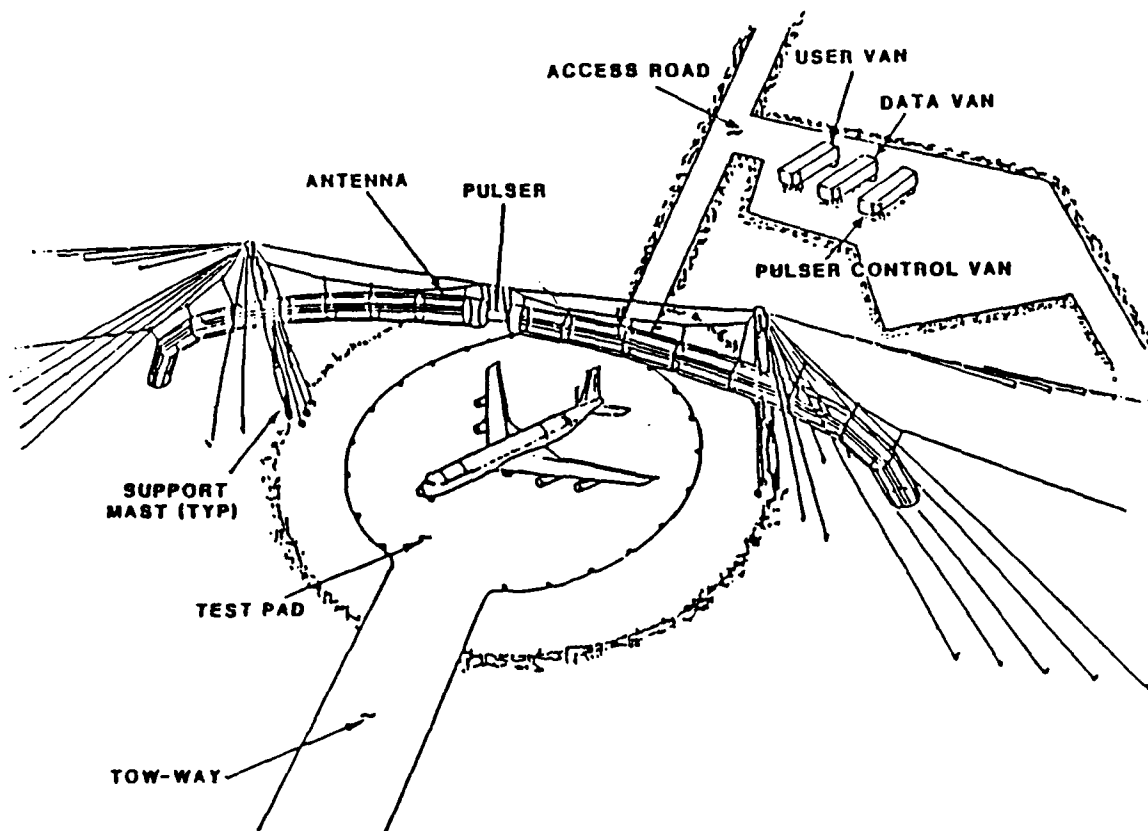


Figure 8. The Naval Air Test Center's Electromagnetic Pulse Facility at Patuxent River, Maryland

### SECTION III RESULTS

#### 1. IN-FLIGHT LIGHTNING CHARACTERIZATION

##### a. Summary Of Direct Attachments

Tables 2 and 3 list the direct attachments to the aircraft in 1984 and 1985, together with the date and time each was obtained; the altitude, outside air temperature and air speed at the time of each strike; the presence of clouds and turbulence; and whether analog and/or digital data sets were recorded for each event.

The aircraft experienced 52 strikes during the 2-yr program. Of these, 47 occurred at altitudes between 14,000 and 19,000 ft. The remaining five were recorded below 4,000 ft. None were recorded at altitudes of 6,000 to 12,000 ft. Table 4 lists the combined total of hours flown at each altitude during both years along with the number of strikes obtained.

Referring to Tables 2 and 3, the aircraft was in cloud for 37 out of the 42 strikes where this data was recorded. The aircraft was in cloud for all but three of the strikes at 14,000 ft and above, and clear of clouds for two out of four strikes at 4,000 ft and below. Light turbulence was reported for 26 strikes, moderate for seven and severe for one. Twenty-five strikes were recorded at 0°C or below. The three strikes below 4,000 ft for which temperature data was not available are assumed to have occurred at temperatures above 5°C.

##### b. Electric Field Measurements

Where analog data was obtained, it was possible to divide 39 of the 41-analog data sets into three categories based on the initial field change measured by the electric field sensor on the forward upper fuselage. The remaining two waveforms could not be classified. Tables 5 and 6 list these categories by events for 1984 and 1985 data, respectively. Figure 9 illustrates a typical electric field waveform for Category 1 and an expansion of the initial change in electric flux

TABLE 2. Direct Attachments to the Aircraft in 1984

EVENT NUMBER	DATE	TIME	AMBIENT AIR TEMPERATURE DEGREES C	AIR SPEED KNOTS	ALTITUDE FEET	CLOUD	TURBULENCE	ANALOG DATA	DIGITAL DATA
1	7/11	21:22:10	5.0	---	14,000	Y	L	Y	N
2	7/11	21:31:01	5.0	---	14,000	Y	L	Y	N
3	7/13	20:46:23	-3.3	229	14,000	Y	L	Y	Y
4	8/06	21:44:05	---	---	14,000	Y	L	N	Y
5	8/07	21:20:56	-7.4	265	18,000	Y	L	Y	N
6	8/07	21:38:24	-6.1	250	18,000	Y	L	Y	N
7	8/07	21:41:23	-8.2	268	14,000	Y	L	Y	Y
8	8/07	21:41:58	-8.2	275	18,000	Y	L	Y	Y
9	8/07	21:43:26	-6.8	252	14,000	Y	L	Y	Y
10	8/07	22:02:01	-8.8	253	18,000	Y	L	Y	Y
11	8/07	22:12:40	-6.4	252	18,000	Y	L	Y	Y
12	8/17	21:36:01	---	---	4,000	Y	M	Y	Y
13	8/18	00:55:26	---	---	4,000	N	N	N	Y
14	8/20	15:37:41	16.6	196	2,000	N	N	N	Y
15	9/05	21:44:00	-4.8	272	18,000	N	N	N	Y
16	9/05	21:52:15	-4.3	266	18,000	---	---	Y	N
17	9/05	21:53:05	-4.2	278	18,000	Y	M	Y	Y
18	9/05	22:34:42	-4.3	290	18,000	Y	L	N	N
19	9/05	23:06:08	-6.2	274	18,000	N	L	Y	N
20	9/05	23:20:36	---	---	18,000	Y	---	Y	N
21	9/05	23:26:54	-2.1	269	18,000	Y	L	Y	N

L - Light  
M - Moderate  
N - None  
S - Severe

TABLE 3. Direct Attachments to the Aircraft in 1985

EVENT NUMBER	DATE	TIME	AMBIENT AIR TEMPERATURE DEGREES C	AIR SPEED KNOTS	ALTITUDE FEET	CLOUD	TURBULENCE	ANALOG DATA	DIGITAL DATA
1	6/21	20:21:49	---	200	14,260	Y	L (R)	Y	Y
2	6/21	21:09:09	---	---	14,176	---	(R)	N	N
3	6/21	21:18:13	---	---	14,358	N	---	N	N
4	6/26	20:40:27	4	200	14,491	Y	L (R)	Y	N
5	6/26	20:55:24	4	180	14,363	---	---	Y	N
6	6/26	21:00:16	3	---	14,567	---	---	Y	N
7	6/27	19:40:20	5	190	14,486	Y	L (R)	Y	N
8	6/27	20:32:44	4	---	14,369	Y	L (R)	Y	Y
9	6/29	17:48:58	4	---	13,700	---	---	N	N
10	6/29	18:49:48	20	---	1,800	Y	M (R)	N	Y
11	7/06	19:40:10	---	---	1,534	---	(R)	N	Y
12	7/15	17:38:44	-5	190	18,870	Y	L	Y	Y
13	7/15	17:42:24	-5	175	18,874	---	---	Y	Y
14	7/15	18:24:20	0	165	16,000	---	---	Y	Y
15	7/15	18:54:39	-2	175	16,456	---	---	Y	Y
16	7/15	19:41:17	1	165	14,411	Y	L (I)	N	Y
17	7/15	19:44:34	2	165	14,335	Y	L (R)	Y	Y
18	7/15	19:49:16	0	165	14,434	Y	L (R)	Y	Y
19	7/15	20:56:26	-4	180	18,857	Y	L (I)	Y	Y
20	7/26	23:21:20	-1	180	14,635	Y	S	Y	N
21	7/26	23:33:23	1	180	14,828	Y	M (R)	Y	N
22	7/26	23:51:58	1	180	14,952	---	N	N	N
23	7/26	00:04:19	1	---	15,822	Y	N (R)	Y	N
24	7/30	00:14:55	---	175	17,321	---	---	Y	N
25	7/30	20:28:18	0	170	14,000	Y	N	Y	Y
26	7/30	21:18:33	0	175	14,121	Y	N	Y	N
27	8/03	19:46:09	---	---	14,000	Y	M (R)	Y	Y
28	8/08	20:33:34	0	---	15,605	Y	N	Y	Y
29	8/08	20:49:46	0	---	15,604	Y	N	Y	Y
30	8/30	22:27:08	---	---	15,341	Y	M	Y	N
31	8/30	22:34:42	---	---	15,111	Y	M	Y	N

L - Light  
M - Moderate  
N - None  
S - Severe  
(I) - In Icing Conditions  
(R) - In Rain

TABLE 4. Strike Rates Versus Altitude  
for the 1984 and 1985 Programs

ALTITUDE ft	TIME AT ALTITUDE h	NUMBER OF STRIKES
17,000 - ABOVE	12.0	16
15,000 - 16,999	7.0	7
13,000 - 14,999	18.0	24
11,000 - 12,999	2.4	0
9,000 - 10,999	2.3	0
7,000 - 8,999	2.3	0
5,000 - 6,999	12.0	0
3,000 - 4,999	5.0	2
BELOW 3,000	17.0	3

TABLE 5. Initial Electric Field Changes During the 1984 Events

EVENT NUMBER	CATEGORY OF EVENT	FIRST FIELD CHANGE			SECOND FIELD CHANGE		
		$\Delta D$ ( $1 \times 10^{-6}$ C/m $^2$ )	$\Delta E$ ( $1 \times 10^5$ V/m)	$\Delta T_1$ (ms)	$\Delta D$ ( $1 \times 10^{-6}$ C/m $^2$ )	$\Delta E$ ( $1 \times 10^5$ V/m)	$\Delta T_1$ (ms)
1	1	-1.8	-204	1.90	+1.7	+195	0.13
2	1	-3.2	-358	2.50	+3.1	+350	0.40
3	1	-1.8	-204	1.50	+3.5	+400	0.32
4	---	---	---	---	---	---	---
5	1	-1.9	-211	1.90	+4.0	+450	0.60
6	1	-1.7	-192	1.60	+3.8	+435	0.60
7	1	-2.0	-224	1.90	+4.0	+460	0.41
8	1	-2.3	-256	2.20	+2.9	+333	0.66
9	1	Saturated	Saturated	---	---	---	---
10	1	-2.0	-230	3.10	+4.0	+448	0.62
11	?	---	---	---	---	---	---
12	2	+0.7	+83	4.40	-1.5	-170	0.06
13	---	---	---	---	---	---	---
14	---	---	---	---	---	---	---
15	---	---	---	---	---	---	---
16	1	-0.7	-84	1.70	+1.0	+109	0.66
17	3	---	---	---	---	---	---
18	---	---	---	---	---	---	---
19	3	-0.4	-48	40.00	+1.2	+131	0.90
20	1	-0.7	-78	1.90	+1.3	+152	0.63
21	3	-0.3	-38	38.00	+1.0	+118	0.31

TABLE 6. Initial Electric Field Changes During the 1985 Events

EVENT NUMBER	CATEGORY OF EVENT	FIRST FIELD CHANGE			SECOND FIELD CHANGE		
		$\Delta D$ ( $1 \times 10^{-6} \text{ C/m}^2$ )	$\Delta E$ ( $1 \times 10^3 \text{ V/m}$ )	$\Delta T_1$ (ms)	$\Delta D$ ( $1 \times 10^{-6} \text{ C/m}^2$ )	$\Delta E$ ( $1 \times 10^3 \text{ V/m}$ )	$\Delta T_1$ (ms)
1	1	-3.9	-441	7.9	+4.0	+452	0.80
2	---	---	---	---	---	---	---
3	---	---	---	---	---	---	---
4	1	-2.0	-226	2.9	+1.7	+192	0.41
5	1	-2.3	-260	3.3	+1.9	+215	0.82
6	1	-2.2	-249	3.7	+1.5	+169	0.84
7	1	-2.0	-226	3.7	+1.8	+203	2.10
8	2	+0.6	+63	7.5	*	*	*
9	---	---	---	---	---	---	---
10	---	---	---	---	---	---	---
11	2	+0.5	+53	6.8	-1.8	-203	0.10
12	?	---	---	---	---	---	---
13	1	-1.1	-124	2.1	+2.2	+249	0.23
14	1	-2.7	-305	6.2	+2.3	+260	1.50
15	---	---	---	---	---	---	---
16	1	-2.2	-249	6.6	+2.6	+294	0.94
17	1	-2.0	-226	1.0	+0.9	+101	0.62
18	1	-1.7	-192	2.5	+0.9	+101	0.69
19	1	-1.7	-192	4.3	+2.4	+271	0.94
20	1	-1.7	-192	3.0	+1.7	+192	1.50
21	1	-1.6	-181	4.4	+0.7	+73	0.33
22	---	---	---	---	---	---	---
23	1	-1.0	-108	2.4	+0.7	+73	0.32
24	1	-1.9	-215	7.4	+1.8	+203	1.30
25	1	-1.4	-158	1.8	+1.4	+158	0.40
26	1	-1.9	-215	4.2	+1.2	+136	1.20
27	1	-3.3	-373	8.3	+2.3	+260	0.70
28	1	-1.7	-192	1.9	+2.3	+260	0.54
29	1	-1.9	-215	1.7	+1.3	+147	0.29
30	1	-2.6	-294	2.8	+1.4	+158	0.82
31	2	+0.5	+53	6.9	*	*	*

? - Not Classified

\* These events are not suitable for this measurement

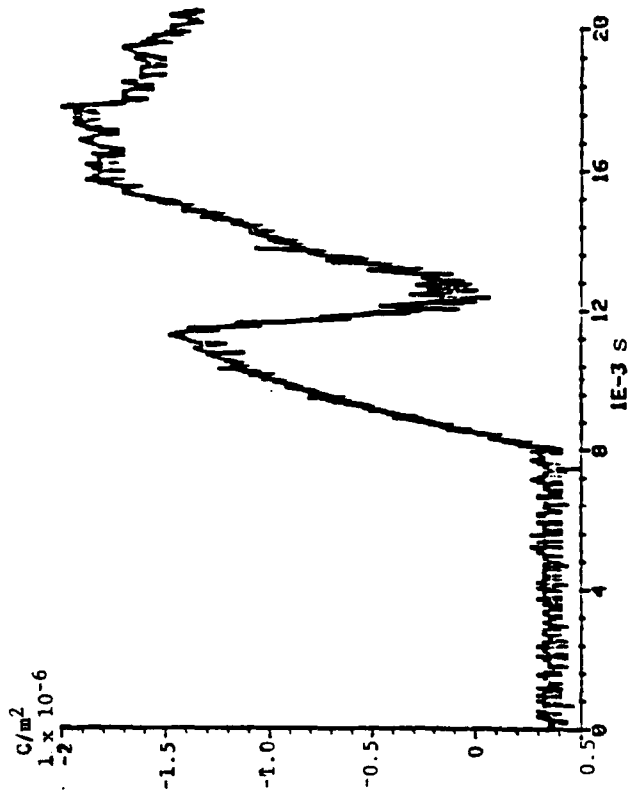
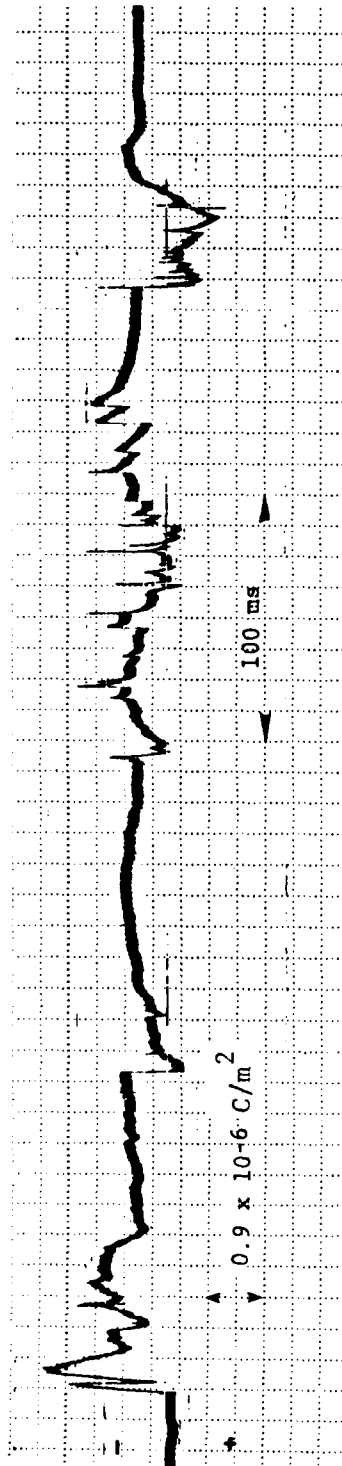


Figure 9. Representative Category 1 Waveform With Expansion of Initial 12 ms

density. Thirty-two of the events could be classified as Category 1. Figure 10 shows one of the four Category 2 waveforms, and Fig. 11 gives one of the three Category 3 waveforms. Average field change values for each category are compared in Table 7.

Three representative Category 1 electric field waveforms are shown in Fig. 12. The durations of the 32 events in this category ranged from 175 to 1766 ms, with an average of 543 ms. All of these waveforms had an initial process similar to that shown in Fig. 9. In addition, they were characterized by a number of sharp, predominantly negative pulses at times later in the flash. All of these events occurred at altitudes above 14,000 ft and we believe that they correspond to intracloud events triggered by the presence of the aircraft. A detailed analysis of these events is presented in Section IV.

The four events in Category 2 shown in Fig. 13 had an average duration of only 56 ms, much shorter than that for Category 1 waveforms. Two lasted only 10 ms and 37 ms, respectively, while the two longer events were 63 ms and 113 ms. These events occurred at both high and low altitude. They appear to be examples of cloud-to-ground discharges in which the aircraft intercepted a negative leader, see Section IV.

Two of the three Category 3 waveforms are shown in Fig. 14. They lasted 188 ms and 288 ms, respectively. They both occurred at an altitude of 18,000 ft and appear to be the result of the aircraft intercepting a positive leader. None of the events in Category 2 or 3 appears to be triggered by the presence of the aircraft. A more detailed discussion of the waveforms in each category is presented in paragraph c.

c. Electromagnetic Fields and Currents Prior to and During Initial attachment

A detailed study of the electromagnetic fields and currents occurring just prior to and during the initial attachment process was performed for all analog data sets. As a result of this analysis, it was possible to classify the data into three different groups: events where the aircraft intercepted a negative leader (Category

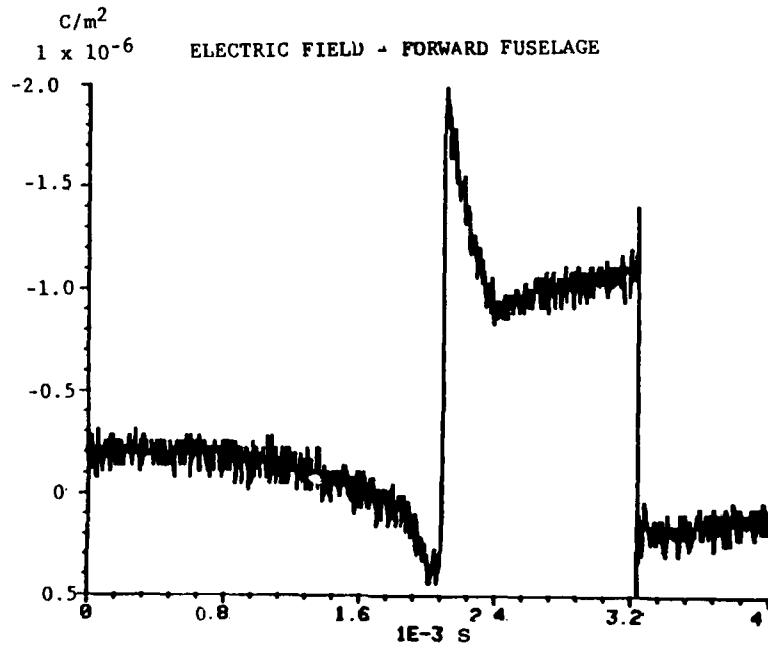
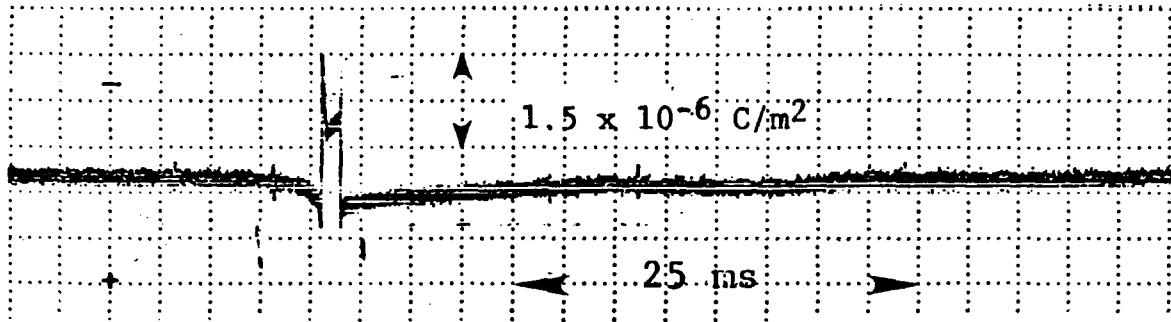


Figure 10. Representative Category 2 Waveform With Expansion of Initial 4 ms

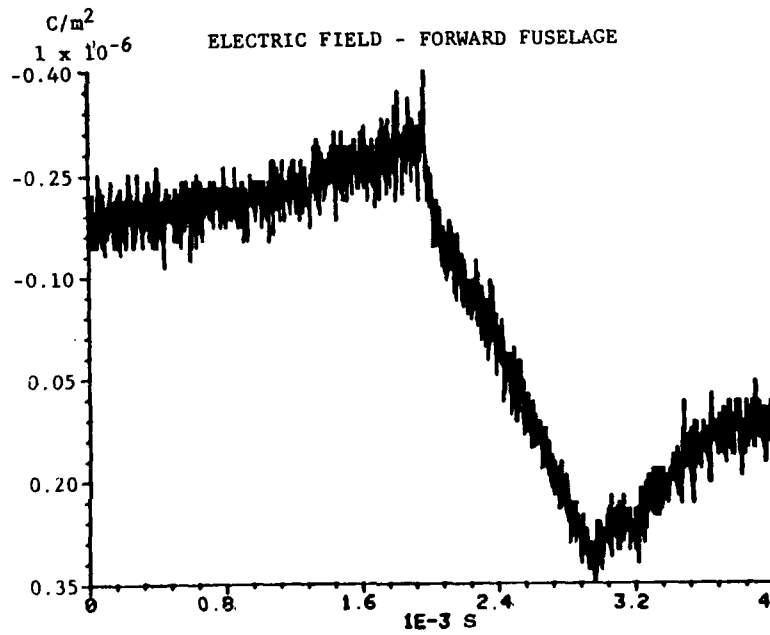
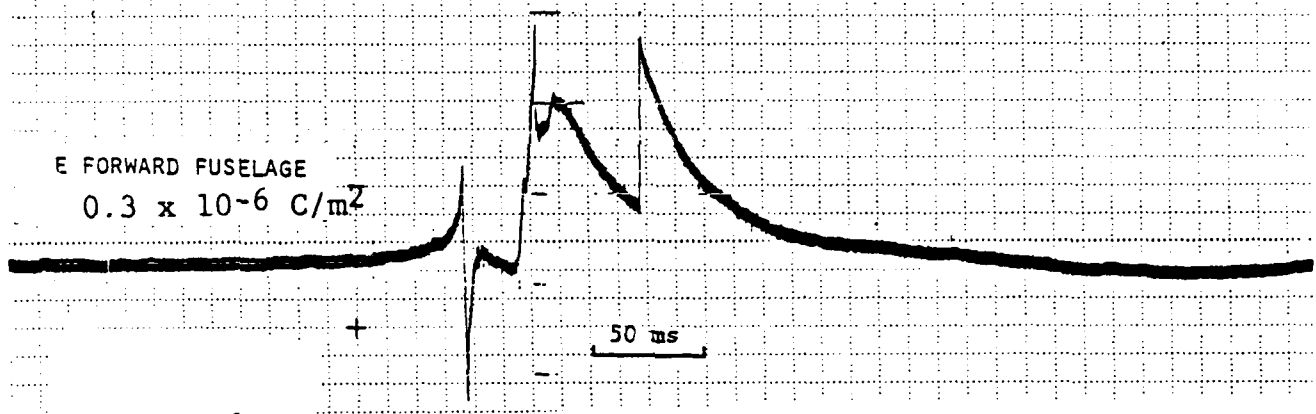
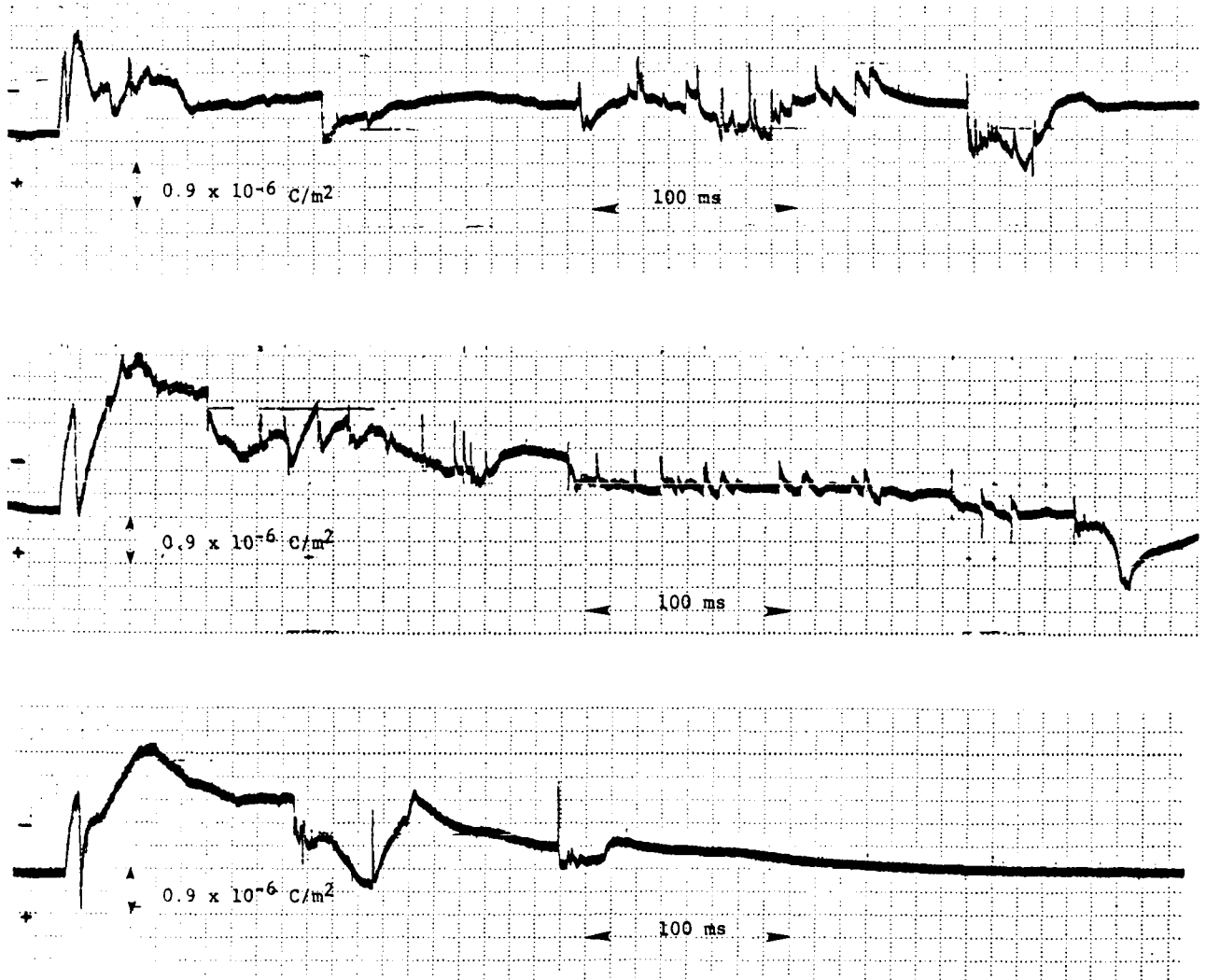


Figure 11. Representative Category 3 Waveform With Expansion of Initial 4 ms

TABLE 7. Summary of the Average Initial Field Changes for the Three Categories of Electric Field Waveforms

CATEGORY	NUMBER OF EVENTS	FIRST FIELD CHANGE		$\Delta T_1$ (ms)	SECOND FIELD CHANGE		$\Delta T_2$ (ms)
		$\Delta D$ ( $1 \times 10^{-6}$ C/m <sup>2</sup> )	$\Delta E$ ( $1 \times 10^3$ V/m)		$\Delta D$ ( $1 \times 10^{-6}$ C/m <sup>2</sup> )	$\Delta E$ ( $1 \times 10^3$ C/m)	
1	31	-2.0	-222	3.2	+2.1	+240	0.70
2	4	+0.6	+63	6.0	-1.6 *	-180 *	0.08 *
3	2	-0.4	-44	39.0	+1.1	+125	0.06

\* Two of these events are not suitable for this measurement



- Figure 12. Three Category 1 Waveforms Typical of the 32 Waveforms Recorded in This Category at Altitudes Greater Than 14,000 ft.

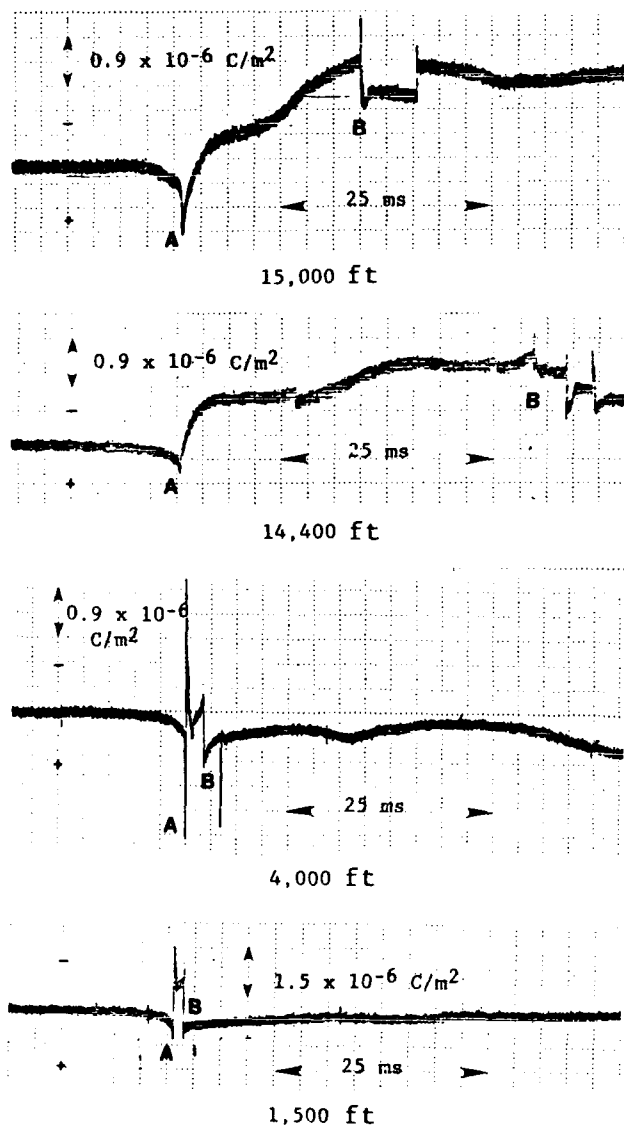


Figure 13. The Four Category 2 Events Recorded in 1984 and 1985 With Altitudes at Which They Occurred

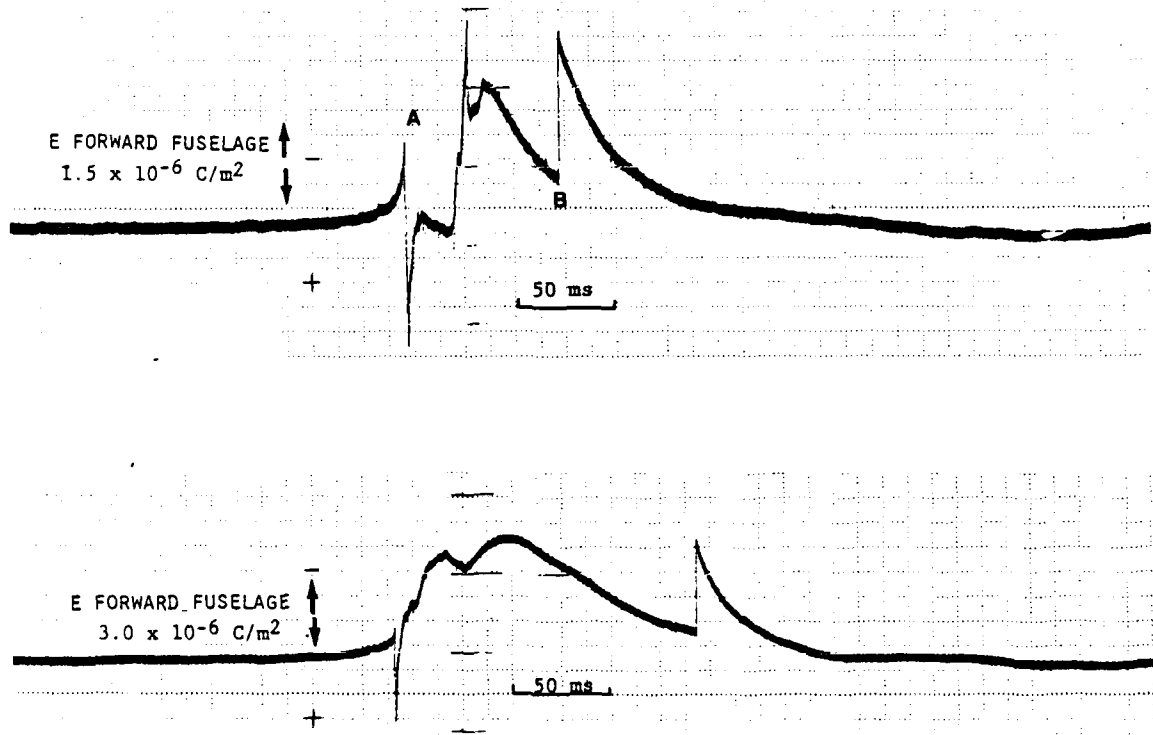


Figure 14. Two of the Three Category 3 Events Recorded at Altitudes Above 14,000 ft

?); events where the aircraft intercepted a positive leader (Category 3); and events where the aircraft triggered an intracloud discharge (Category 1). The analysis technique is discussed next so that subsequent tables of current and other parameters measured on the aircraft can be classified as to the type of event, thus making interpretation of the data more meaningful.

#### (1) Negative Leader Intercepts (Category 2)

The initial portions of the electric field records for the four events in this category were shown in Fig. 13. In all four cases, there was an initial slow positive charge increase, followed by a sharp negative charge increase, which occurred very quickly for the two attachments at low altitude. A slow negative charge increase interrupted many milliseconds later by a sharp negative pulse was observed on the two attachments at high altitude. Figure 15 presents electric field, magnetic field and current measurements corresponding to Point A for the waveform in Fig. 13 obtained at 1,500 ft. It shows relatively fast field changes with a small amount of current flow on the left wing. Figure 16 shows current flow also occurred at this point in the flash for the waveform obtained at 15,000 ft. Small current pulses were observed at this time on the other Category 2 waveforms as well.

It is believed that the aircraft intercepted a negative leader and the initial positive charge increase reflects its approach. When attachment occurred, a small current pulse of approximately 300 to 400 A was produced, depositing negative charge on the aircraft. The leader then continued on toward the ground for a time interval which varied with altitude. Figures 15 and 16 both show negative field changes which coincide with the establishment of current flow on the aircraft.

In Fig. 13, the time from the initial leader attachment to the first subsequent pulse (Point A to Point B) is 20.8 ms for the event at 15,000 ft and 41.9 ms for the event at 14,000 ft. Assuming the leader contacted ground at Point B, these times correspond to leader velocities of  $2.2 \times 10^5$  and  $1.0 \times 10^5$  m/s, respectively, in good agreement with the average velocities given by Uman for a stepped leader (Reference 9). For the events at lower altitudes, the time between initial leader contact at Point A and Point B was 2.1 ms for the event at 4,000 ft

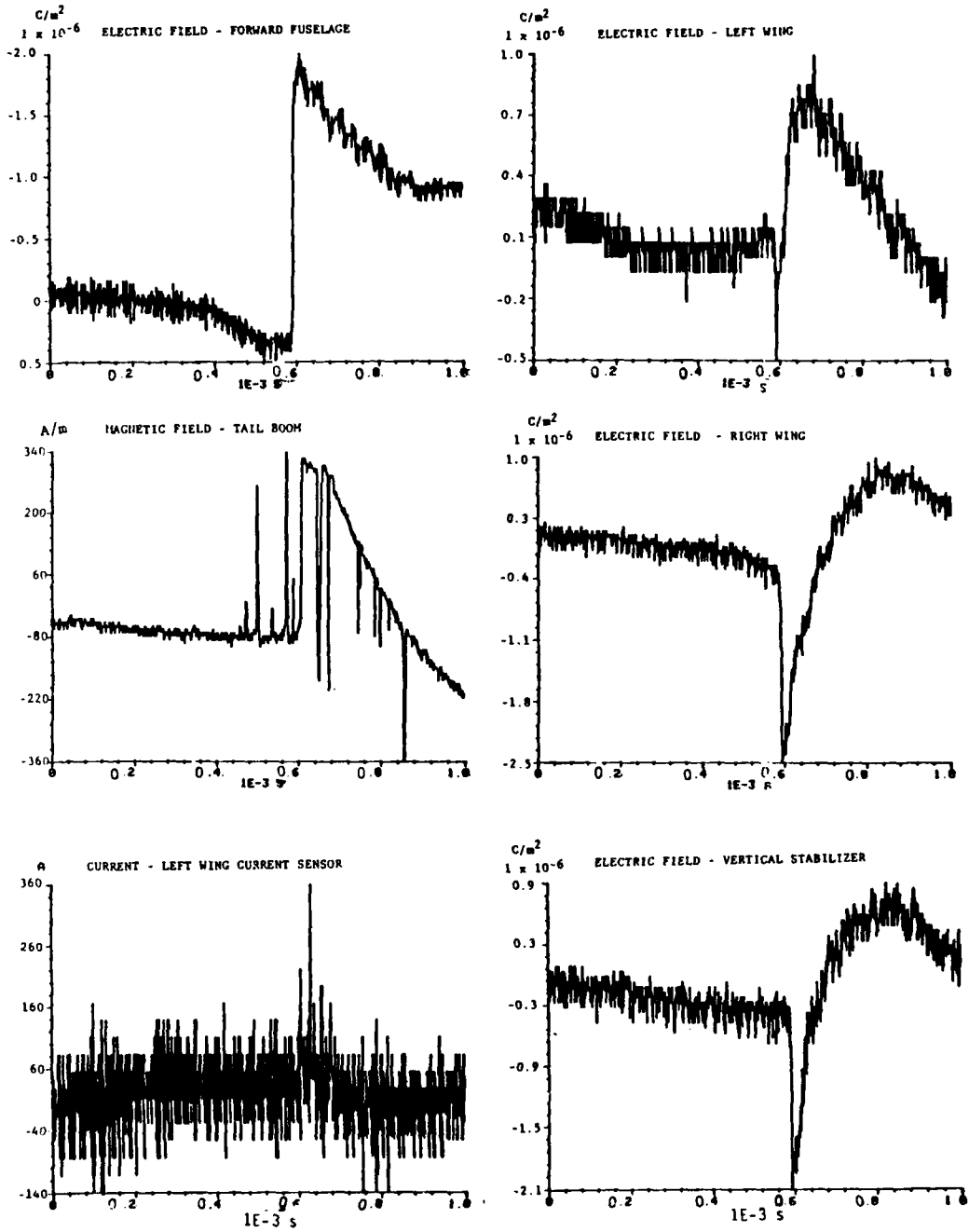


Figure 15. Electromagnetic Field and Current Records at Point A for the Event at 1,500 ft in Figure 13

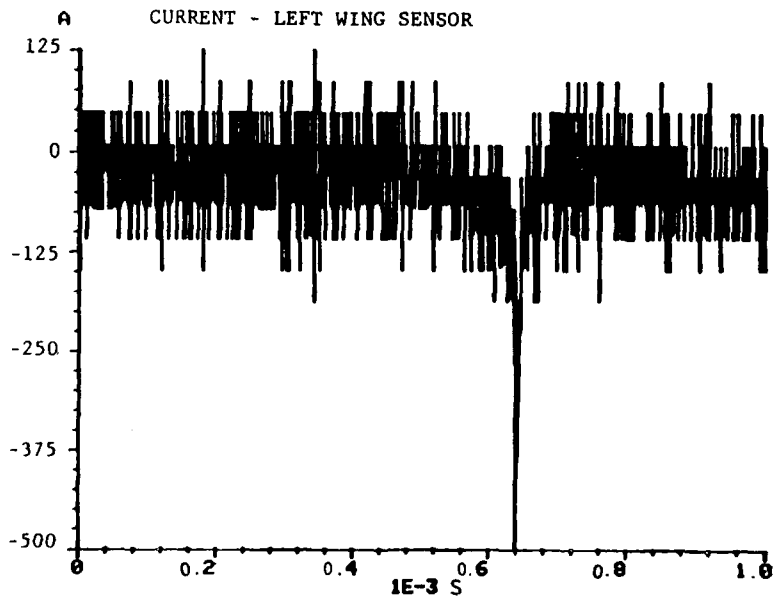
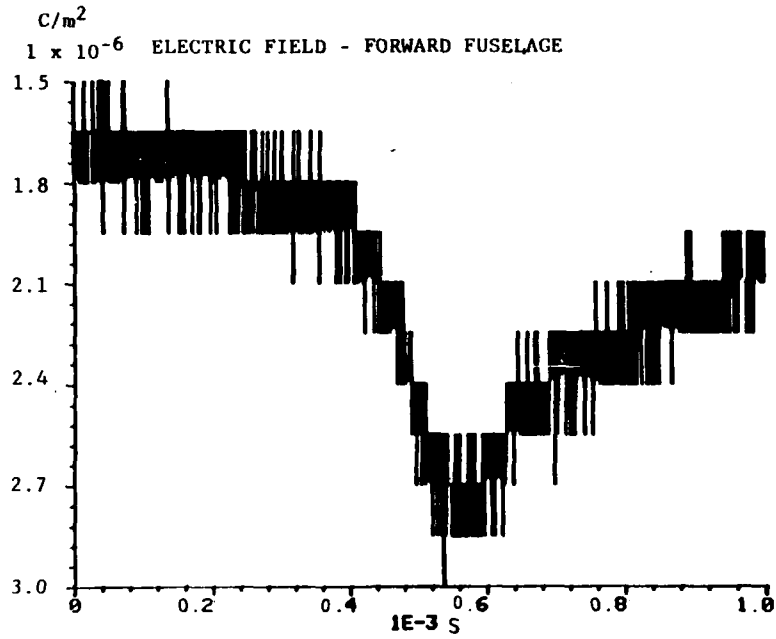


Figure 16. Electric Field and Current Records at Point A for the Event at 15,000 ft in Figure 13

and 1.3 ms for the event at 1,500 ft. These times correspond to leader velocities of  $5.3 \times 10^5$  and  $3.5 \times 10^5$  m/s, respectively, and are also within the range reported in Reference 9. These values are summarized in Table 8.

TABLE 8. Leader Velocities During Events  
Where the Aircraft Intercepted a Negative Leader

<u>Altitude (ft/m)</u>	<u>Time (ms)</u>	<u>Leader Velocity (m/s)</u>
1,500/457	1.3	$3.5 \times 10^5$
4,000/1,220	2.1	$5.3 \times 10^5$
14,400/4,390	41.9	$1.0 \times 10^5$
15,000/4,573	20.8	$2.2 \times 10^5$

Two of these four events are discussed in detail: the one at 1,500 ft and the one at 14,400 ft. The first will be shown to be a cloud-to-ground event in which the aircraft was in a branch rather than the main channel, and the second a cloud-to-ground event in which the aircraft was part of the main channel.

Figure 17 shows the electromagnetic field and current data during and after the lightning attachment at 1,500 ft. Even though the aircraft experienced electric field and current pulses for only a short time, the magnetic field sensor and VHF antenna recorded several more pulses at intervals of 68, 280, 320, and 370 ms, later. Since the magnetic field sensor and VHF antenna acted as free field sensors, the aircraft was apparently involved in only a small portion of the lightning flash. Overall, this event had 12-magnetic field and VHF pulses at intervals which could correspond to intervals between return strokes. Expansion of the magnetic field pulses showed them to have return stroke characteristics. Additionally, the ground station recorded a multistroke cloud-to-ground event at this time and location, as did the Lightning Location and Protection System (LLP). The video recordings on the aircraft showed a large, long-lasting flash close to the right wingtip as shown in Fig. 18.

An explanation of this event is presented by means of Figs. 17, 19, and 20. Figure 19 is an expansion at Point A in Fig. 17 and the lightning attachment scenario is illustrated in Fig. 20. The approach of the lightning leader, in this

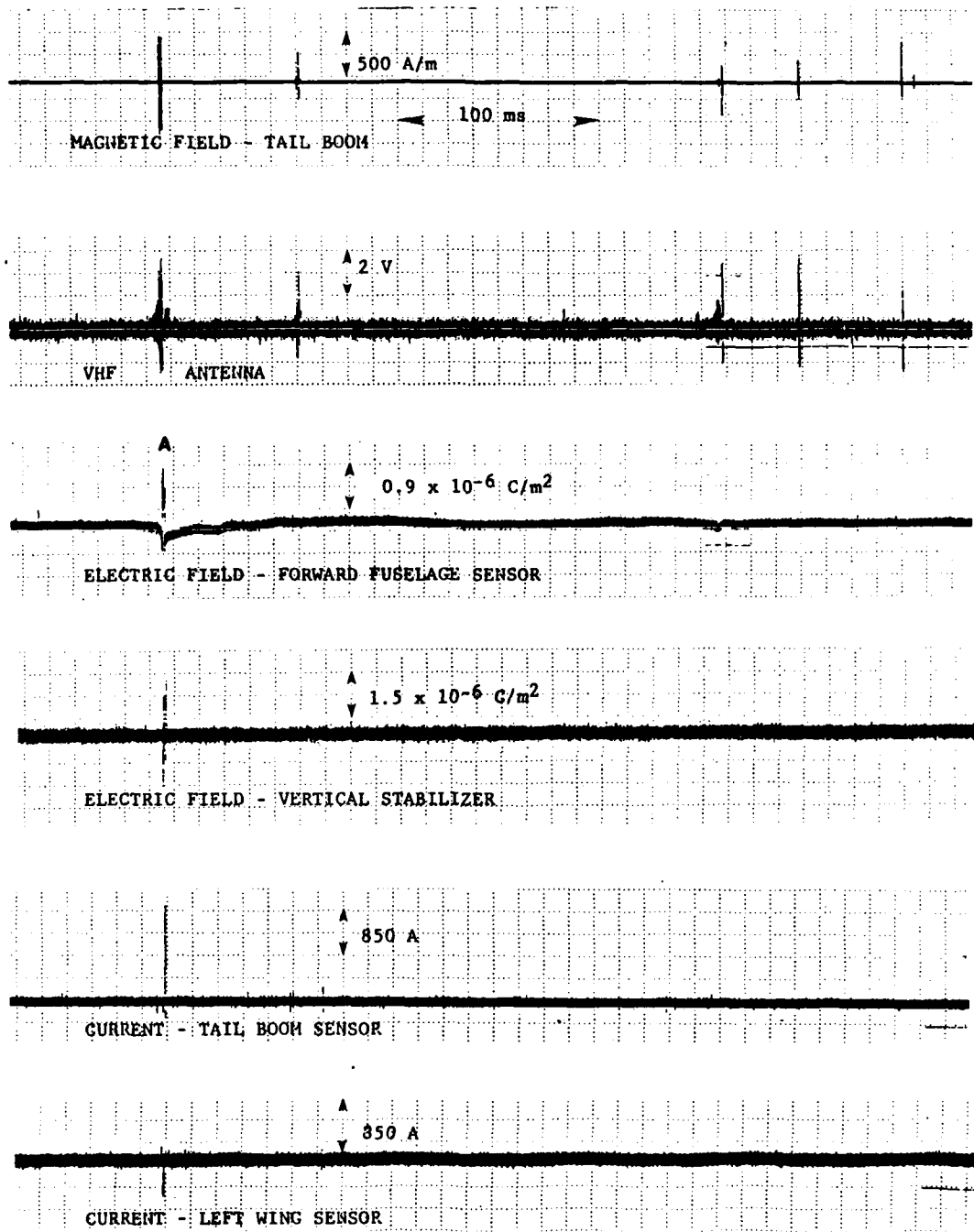


Figure 17. Electromagnetic Field and Current Data During and After Lightning Attachment at 1,500 ft



Figure 1. Ground Channel Passing Close to the Right Wingtip

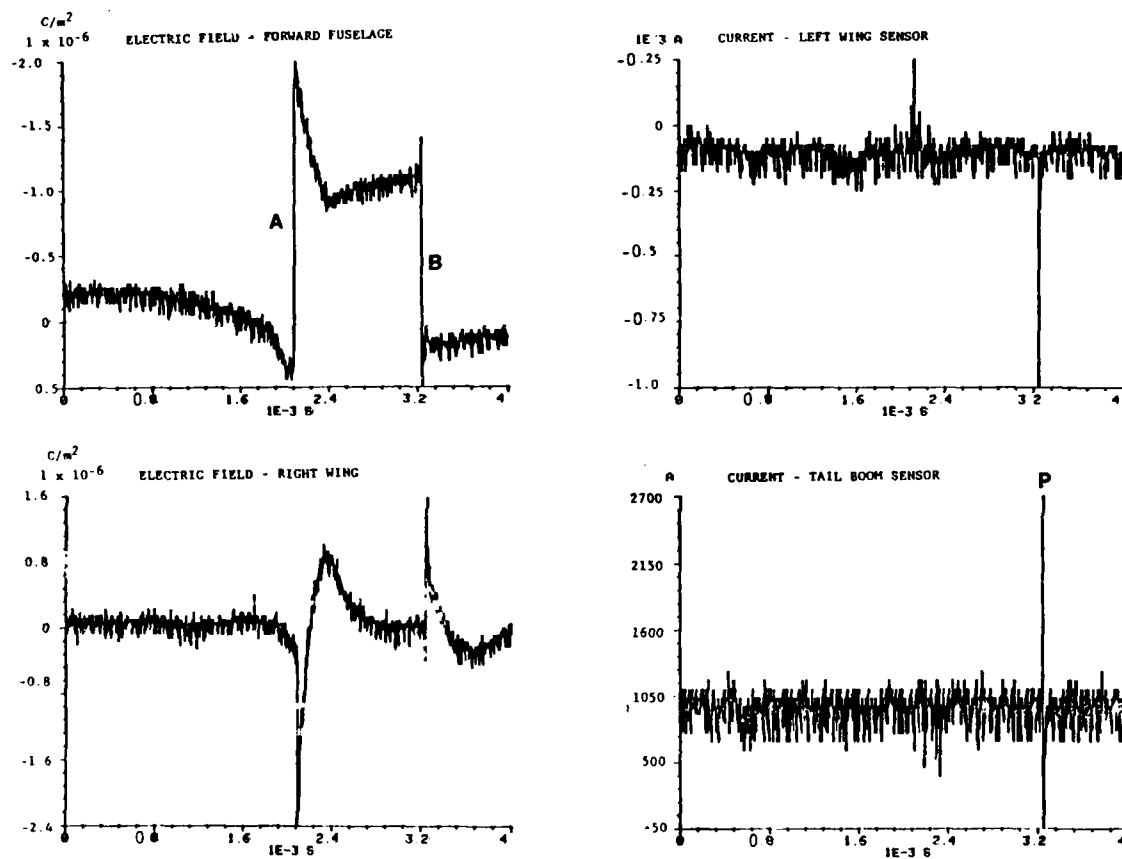


Figure 19. Simultaneous Electric Field and Current Records From a Lightning Attachment in Which the Aircraft Was in a Branch of a Cloud-to-Ground Event

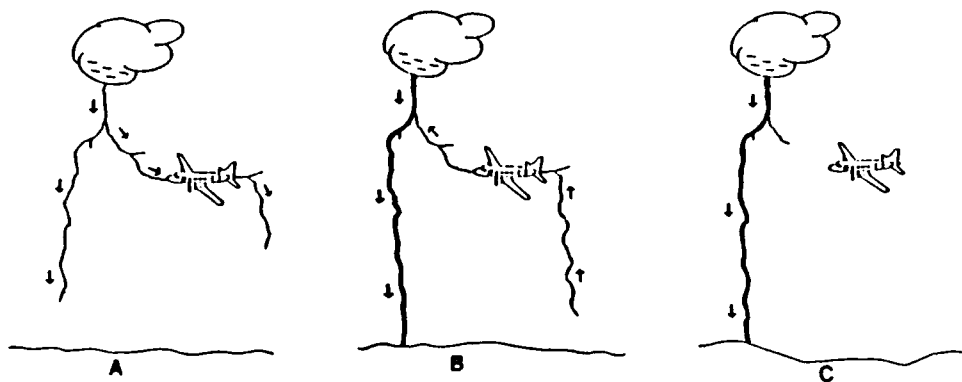


Figure 20. Lightning Attachment Scenario to Explain the Waveforms Shown in Figure 19

case a branch of the main channel, was evidenced by the increase in positive charge at the forward fuselage electric field sensor. The leader attached to the aircraft, resulting in a large negative charge increase which decreased somewhat as the leader passed through and beyond the aircraft, distributing some of the negative charge throughout the rest of the channel. Small current pulses were seen on the left wing and tail boom sensors. The leader passing through the aircraft did not reach the ground before a second leader that formed the main channel. As a result, the branch collapsed, reversing the direction of charge flow on the aircraft and changing the polarity of all the sensor outputs. The time interval between Points A and B in Fig. 19 represents the travel time of the branch leader towards the ground until the main channel is formed, plus the time required for neutralization of the branch. The difference in amplitude of the current pulses reflects the additional amount of charge distributed on the channel after the leader passed through the aircraft and the increased velocity with which charge could move back up the ionized branch. No further current pulses were seen on the aircraft once the branch had collapsed, as shown in Fig. 20C, and subsequent strokes appeared only on the very sensitive magnetic field sensor and VHF antenna. An expansion corresponding to Point P in Fig. 19 is given in Fig. 21. It shows the current pulse on the tail boom as the branch collapsed and bears no resemblance to a return stroke.

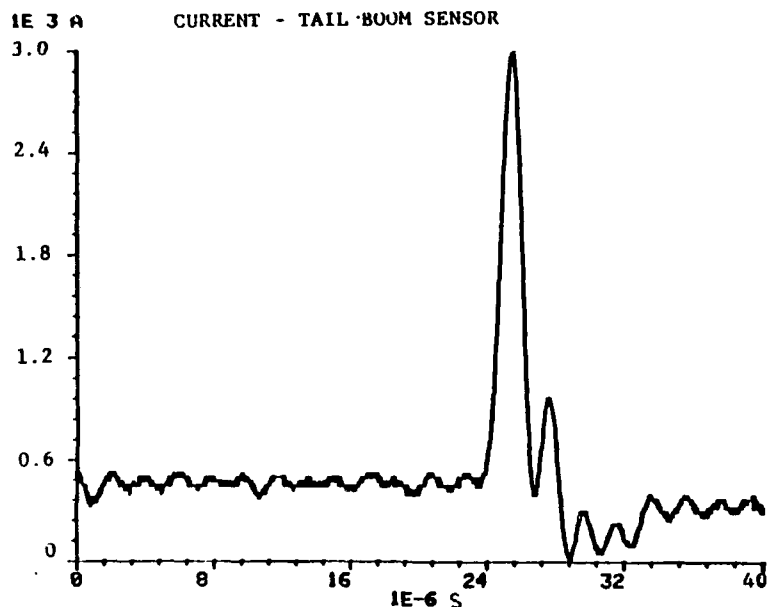


Figure 21. A Window of 40  $\mu$ s Taken at P in Figure 19 to Show the Absence of Return Stroke Characteristics

In Section IV on instrumentation, we found it possible to obtain one set of digital data for each event. A 10- $\mu$ s window of data was obtained at Point P in Fig. 19 and, although limited, this data confirmed the positive field change shown on the analog data. Note the response on the left-wing electric field sensor in Fig. 22, showing decreased negative charge on the aircraft. The tail boom measured 3.2 kA of current as negative charge moved back onto the aircraft. The surface current on the aft fuselage sensor agreed with the tail boom value and was of the correct polarity for negative charge moving from tail to nose. The amplitude and polarity of the surface current on the right wing suggest that a significant quantity of negative charge was also moving from outboard of that sensor toward the fuselage. Although a complete set of digital data is not available, information combined from analog and digital data sets suggests that the attachment occurred somewhere near the nose or top of the fuselage with exit points at the left wing current shunt, tail boom shunt and edge of the right wing.

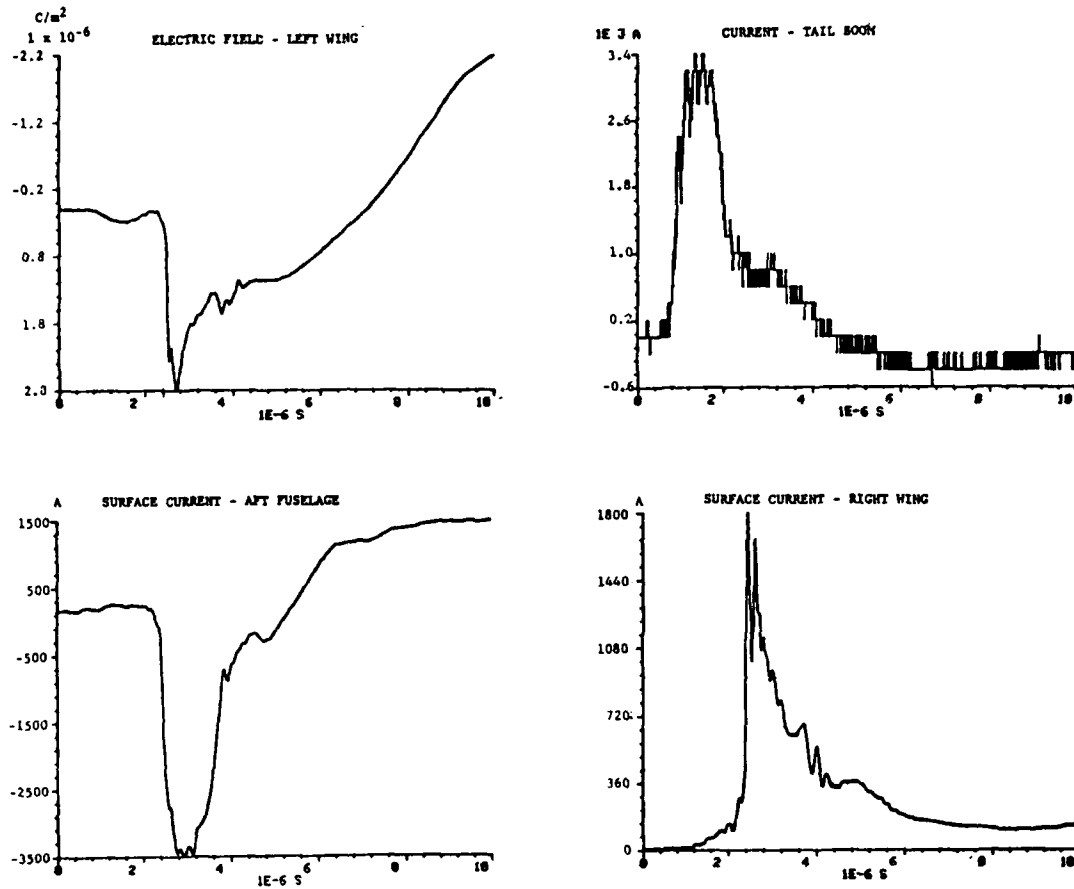


Figure 22. Electric Field and Current Pulses Recorded Digitally as the Branch Attached to the Aircraft Collapses During a Cloud-to-Ground Event.

As mentioned in Section II, the ground station recorded a simultaneous cloud-to-ground event. The stepped leader and first return stroke recorded at the ground are shown in Fig. 23 and confirm the negative polarity of the event (negative charge lowered to ground). The electric field measurement resulting from the return stroke was -6 V/m measured at a horizontal distance of 48 km from the aircraft and can be used to determine the current level using the equation (Reference 25):

$$I = \frac{2\pi R E}{\mu_0 v} \quad (6)$$

Where:

R = the distance from the strike in meters

v = the return stroke velocity in meter per second

E = the electric field in volt per meter

Assuming v to be  $8 \times 10^7$  m/s, the typical velocity for a return stroke (Reference 9), the calculated current level would be about 18 kA. This current level is somewhat low for a first return stroke. Assuming exponential decay with altitude, the current through the aircraft, even if it had been in the main channel, would only have been about 14.2 kA.

Analog records from the strike at 14,400 ft are shown in Fig. 24. As was the case with the waveforms for the previous event (Fig. 17), there was an initial positive charge increase at the forward fuselage sensor as a negative leader approached, passed through the aircraft and proceeded toward the ground. Pulses were then observed on the magnetic field sensor and VHF antenna, corresponding with current pulses and electric field changes on the aircraft throughout the event. We see that this event was a nine stroke cloud-to-ground discharge in which the aircraft was part of the main channel.

Figure 25 shows expansions of the current pulses produced when the leader contacted the aircraft at Point A in Fig. 24. From the polarities of the pulses, we see that the leader attached at the left wing boom and exited through the tail boom. The pulses have amplitudes, rise times, and overall waveshapes typical of leader pulses (Reference 26). Figure 26 shows expansions of the current pulses

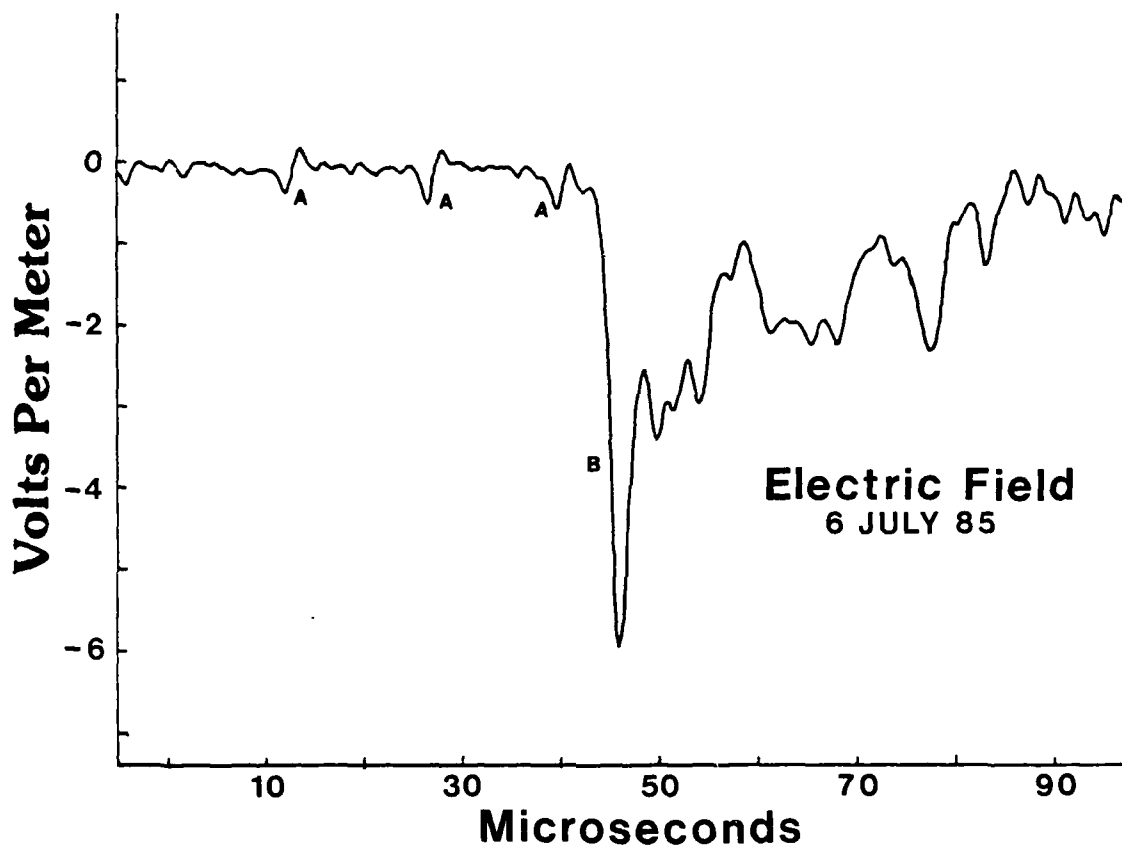


Figure 23. Stepped Leaders (A) and First Return Stroke (B) Recorded at the Ground Station Simultaneously With the Event in Figure 19

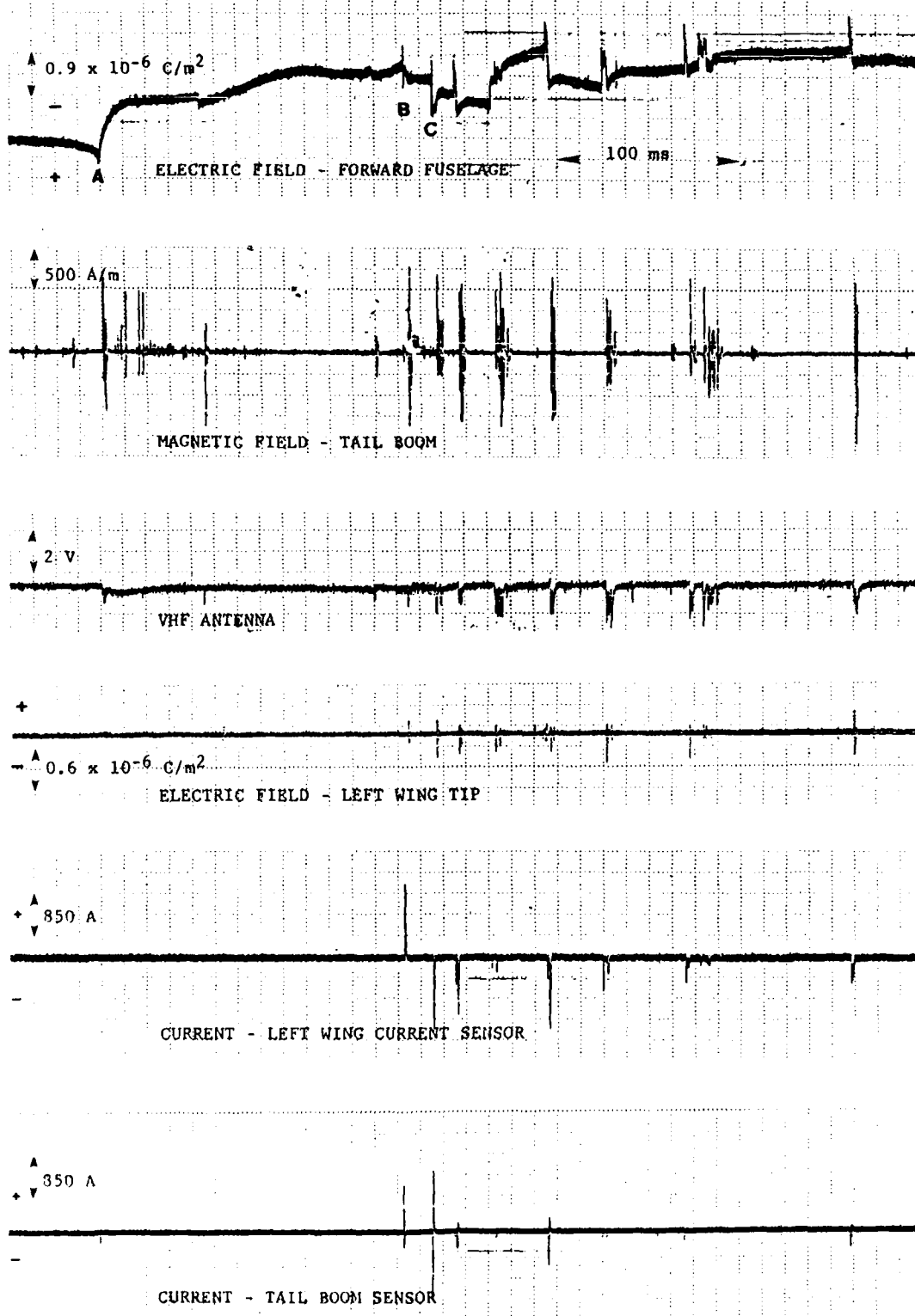


Figure 24. Electromagnetic Field and Current Data During a Lightning Attachment at 14,400 ft Where the Aircraft Was Part of the Main Channel

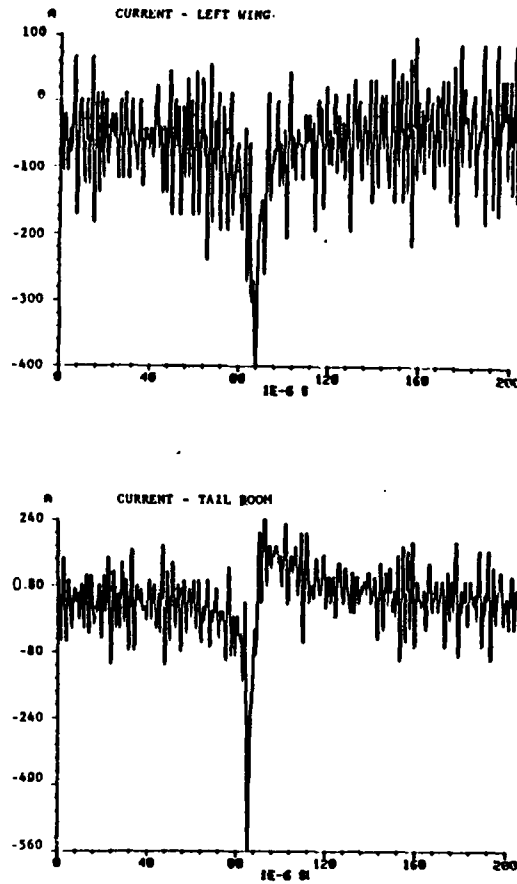
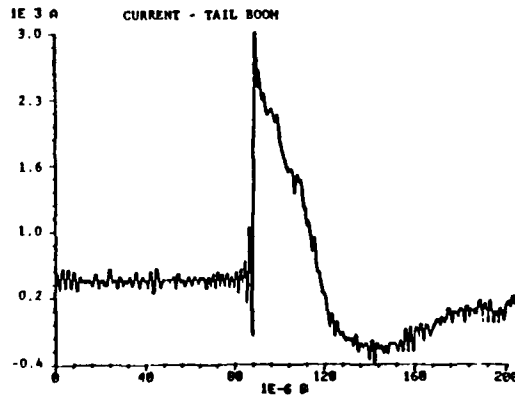
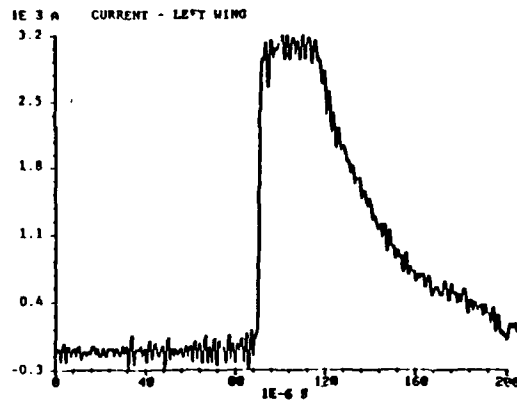


Figure 25. Current Pulses on the Aircraft as the Leader Approaches  
During the Cloud-to-Ground Event in Figure 24 — Expansion  
at Point A



- Figure 26. Current Pulses on the Aircraft as the First Return Stroke Passes Through During the Cloud-to-Ground Event in Figure 24 — Expansion at Point B

for time B in Fig. 24. The amplitudes, rise times, and overall waveshapes are characteristic of a first return stroke, remembering that the aircraft is measuring the channel current at an altitude of 14,400 ft. These current pulses correspond to increases in the negative electric field as negative charge flowed onto the aircraft. The reversal in polarity as compared to the leader pulse can be explained by movement of the channel on the aircraft during the relatively long time (over 160 ms) as the leader approached ground. If the leader temporarily attached at the tail and exited at the left wing, these polarities would be expected.

An interesting set of current waveforms is shown in Fig. 27, which includes an overall 1-ms record and expansions of two pulses, A and B. This type of current response, a fast pulse followed shortly by a slow one, occurred on six of the eight subsequent strokes in this flash. Based on the 300- $\mu$ s time interval between the two pulses, the first fast pulse may have been a dart leader moving through the aircraft to the ground with the second pulse being the return stroke. The expansions of the waveshapes shown in Fig. 27 support this interpretation. The time interval between the first return stroke and this first subsequent stroke was only 8 ms, so we can assume that the channel was still almost completely ionized and the dart leader velocity high. Using the  $2.1 \times 10^7$ -m/s figure given by Uman for the maximum velocity of a dart leader (Reference 9), the time to travel the 14,400-ft distance to ground would be about 200  $\mu$ s. Since the return stroke should require around 50  $\mu$ s to travel back up the channel, based on an average return stroke velocity of  $8 \times 10^7$  m/s, the total time interval between pulses seems appropriate. Later in the flash, when subsequent strokes were separated by somewhat longer intervals of time, the time between dart leaders and return strokes increases from 300 to 400  $\mu$ s, and then to 600  $\mu$ s for subsequent strokes.

Reference to Figs. 24 and 27 shows once again that there had been a reversal in polarity on the current sensors. Again, we assume that the attachment point changed, returning to the left wingtip boom and remaining there for the rest of the flash. Supporting evidence for this supposition is provided by the electric field changes on the aircraft coincident with these current pulses. They are negative for all subsequent pulses, indicating negative charge flowing onto the aircraft in each case. The only way for the current sensors to show a change in

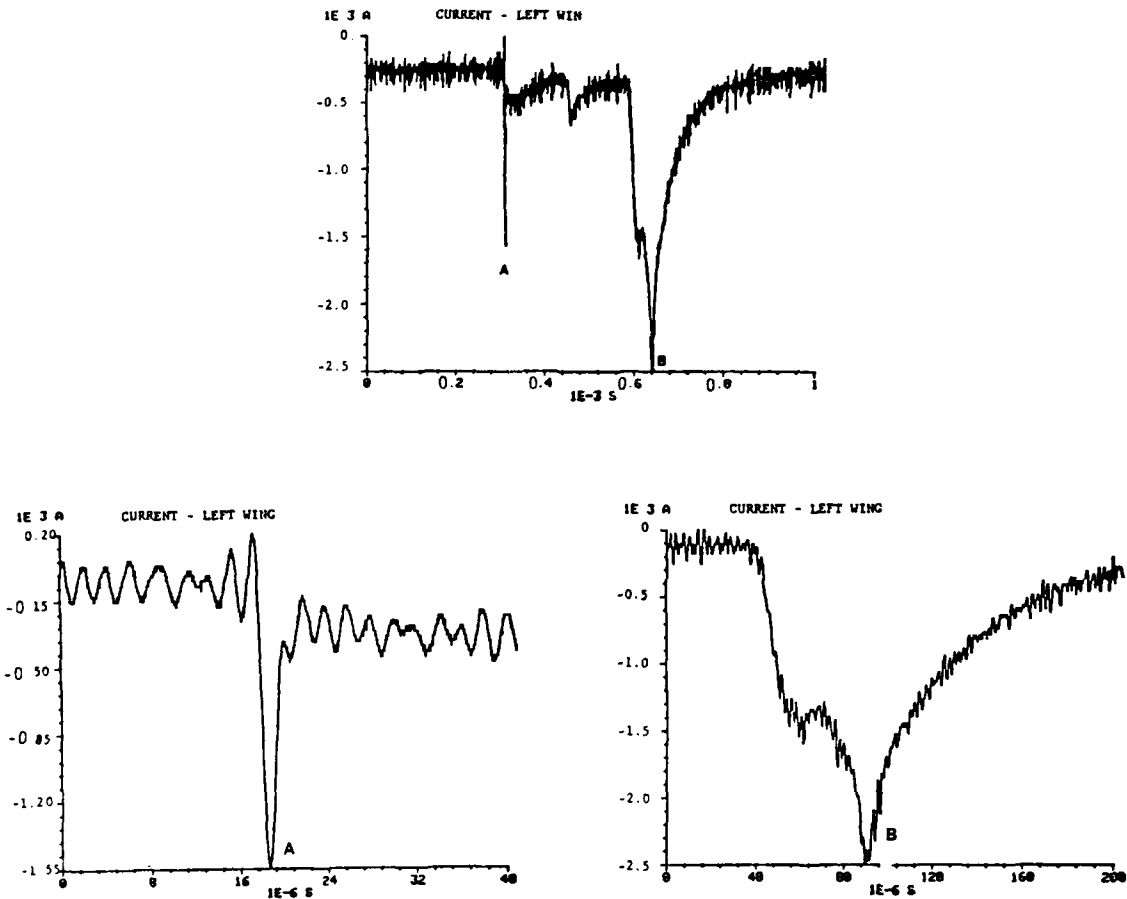


Figure 27. Current Pulses on the Aircraft as a Dart Leader (A) and Subsequent Return Stroke (B) Pass Through the Aircraft During the Cloud-to-Ground Event in Figure 24—Expansion at Point C

polarity, then, is for the direction of current flow through the sensor to reverse. The most logical explanation for such a reversal is a change in attachment point.

A 10- $\mu$ s window of digital data recorded at Point B in Fig. 24 is shown in Fig. 28. The current waveform shown for the tail boom is the integrated output of the current rate-of-change sensor on the tail boom. The polarity of the current pulse indicates that a current of about 4400 A flowed onto the fuselage through the tail boom. The left-wing current sensor saw a current of nearly 3200 A leaving the aircraft. The current of 3200 A, based on the assumption of equal current distribution around the fuselage, that appeared on the aft fuselage surface current sensor was somewhat less than that measured at the tail boom. The forward fuselage recorded 1100 A. The polarities of both surface current pulses confirmed the flow of current from tail to nose. Apparently, 4400 A of current entered the aircraft at the tail boom, with 1100 A exiting through the forward fuselage and 3200 A exiting through the left wing. The rise time calculated from the surface current sensors and the current rate-of-change sensor in the tail boom was 400 ns, with a  $dI/dt$  of  $1.1 \times 10^{10}$  A/s. The left-wing current pulse showed a much slower rise time, due possibly to the fact that the current exited through a resistive current shunt. The current amplitude through the tail boom, based on the analog measurement in Fig. 26, did not agree with the digital record due to the bandwidth limit of the analog system. Pulses with rise times beyond the recorder bandwidth would be reduced in amplitude, as is the case here. Note that the amplitude of the slower left-wing pulse recorded by the analog system (Fig. 26) is in good agreement with the corresponding digital measurement.

## (2) Positive Leader Intercepts (Category 3)

The initial portions of the electric field and current records for one of the events when the aircraft appears to have intercepted a positive leader are shown in Fig. 29. (Figure 14 shows the entire waveform; point A marks the location of Fig. 29.) There was an initial negative field change as the positive leader approached the aircraft. A positive field change was then observed, accompanied by low-level current flow on the aircraft. We see that this positive field change, which also occurred on the other electric field records, was the result of a negative leader moving out from the aircraft to intercept the approaching positive

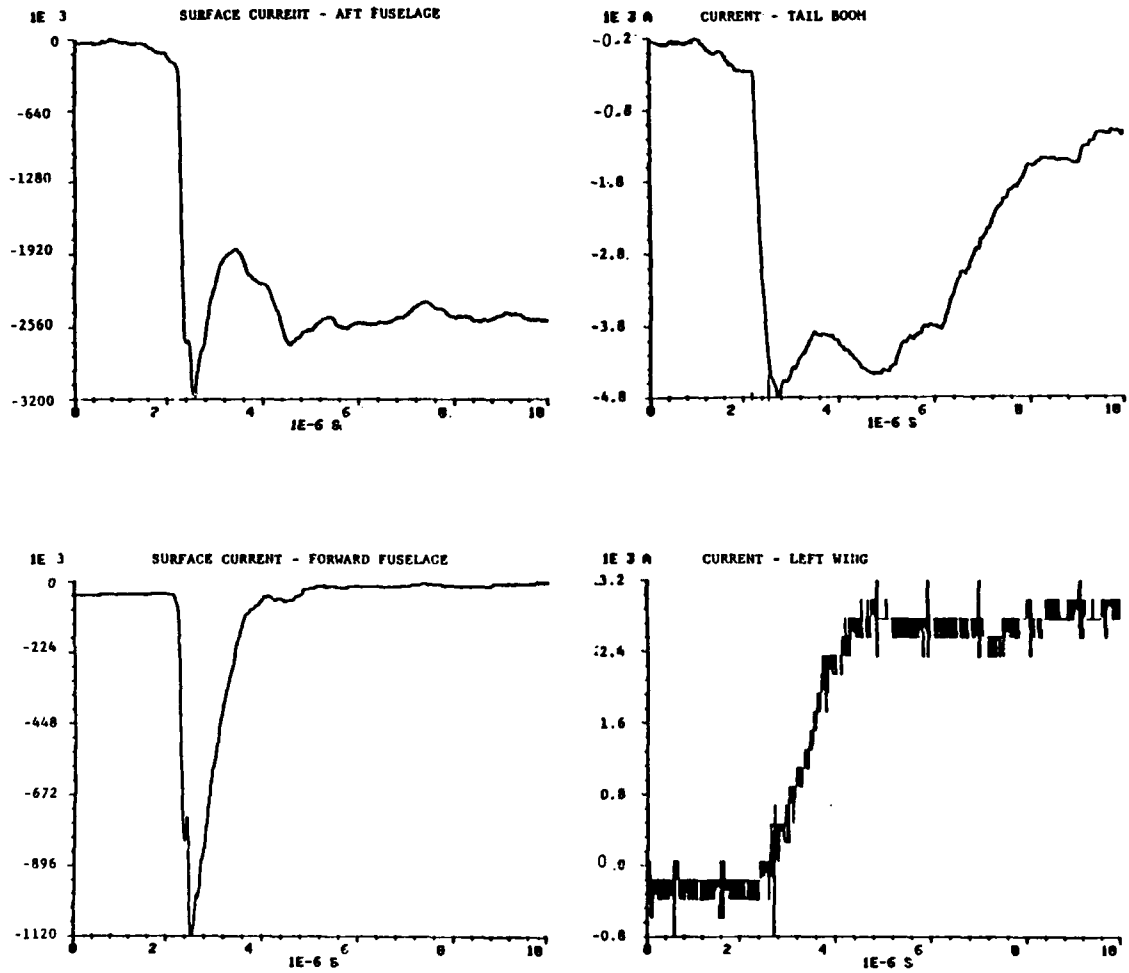
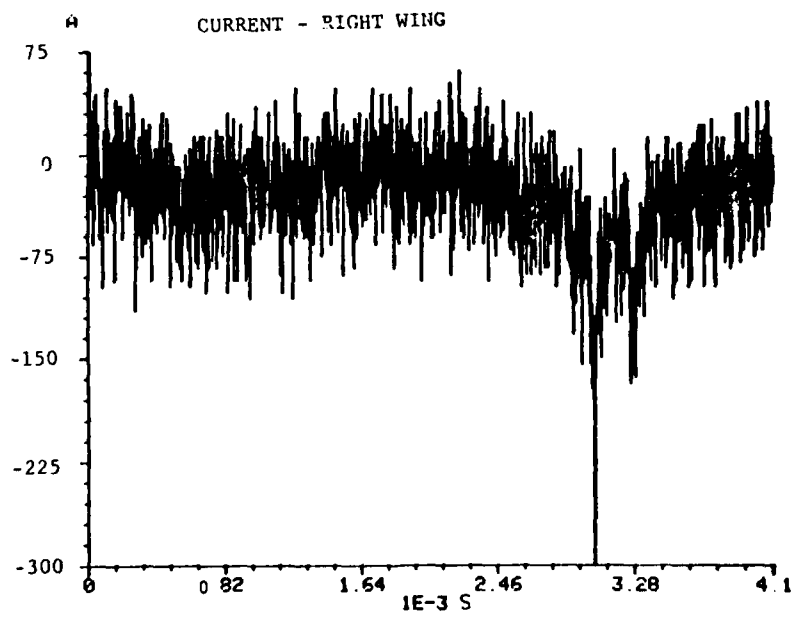
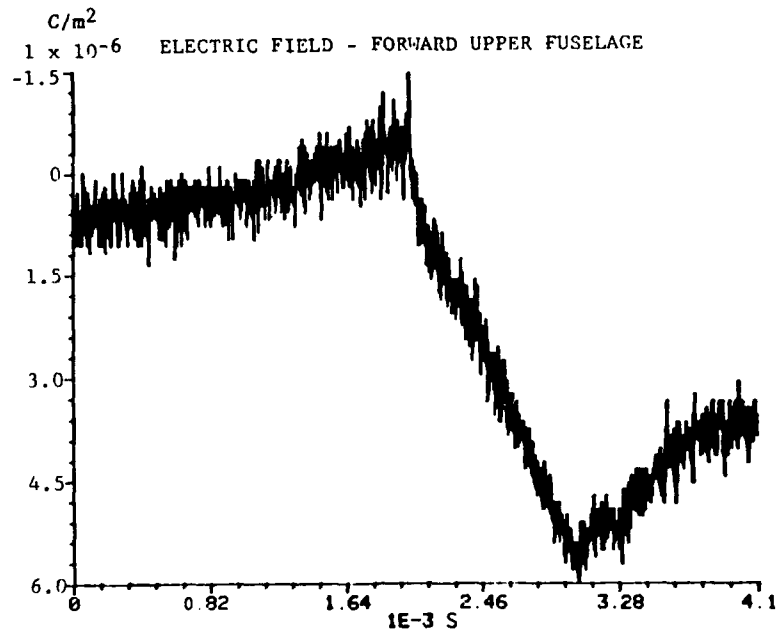


Figure 28. Current Pulses Recorded Digitally During a First Return Stroke of a Cloud-to-Ground Event



- Figure 29. Electric Field and Current Records at Point A in Figure 14.

leader. Upon contact, current flow was established on the aircraft. The other events in this category showed similar behavior.

Later in the event at Point B in Fig. 14, there was a large, fast, negative field change on the electric field sensors. A natural intracloud discharge, according to Ogawa and Brook (Reference 27), typically begins with an advancing leader that lowers positive charge in the cloud. As the leader contacts regions of negative charge, recoil streamers (K-changes) are initiated which travel back along the channel toward the source and produce currents of 1 to 40 kA. It is believed that Point B corresponds to a negative recoil streamer where the aircraft was part of an intracloud event. Unfortunately, the channel did not attach to any of the current shunts during this time and there was no digital trigger so no further information on current levels is available.

In summary, analysis of the 41-analog data sets showed 7 intercepted strikes, 4 negative and 3 positive. Three digital data sets with no accompanying analog data were also analyzed with the aid of strip chart recordings and ground station data and proved to be negative intercepted strikes. For the total of seven negative intercepted strikes, five were in a branch and one or possibly two were in the main channel.

### (3) Triggered Intracloud Flashes (Category 1)

Typical Category 1 waveforms were shown in Figs. 9 and 12. An electric field record measured on the ground from one of these events and the electric field record recorded simultaneously on the aircraft 100 km away are compared in Fig. 30. The initial process on the aircraft record is absent from the ground record and appeared to occur before any activity was detected at the ground. This suggests that the initial field change on the aircraft was a result of charge differences on the aircraft itself rather than of an atmospheric raising or lowering of charge, which would be detectable at both locations. Although one waveform must be inverted due to a polarity difference between the aircraft and ground sensors, the waveforms are similar in shape with many common peaks, valleys and spikes. Some of the dissimilarities are due to the distance and altitude differences between the two

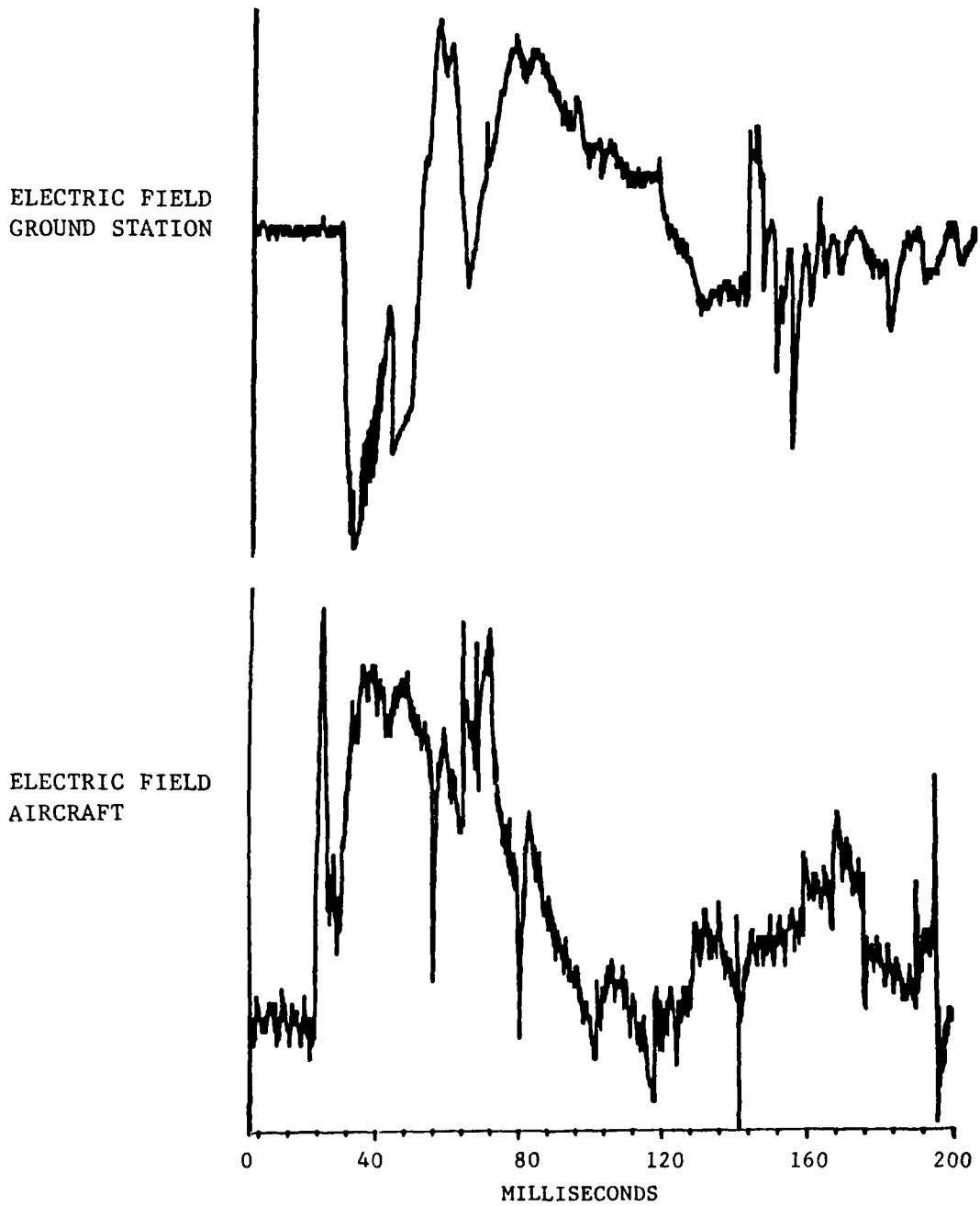


Figure 30. Initial Portions of Unscaled Electric Field Records Recorded Simultaneously at the Ground Station (Top) and Aircraft (Bottom) During a Strike Triggered by the Aircraft

recording sites, and some can be attributed to the fact that the lightning actually attached to the aircraft rather than being just nearby.

Analysis of all the records in Category 1 showed that the slow, initial, negative charge increase averaged  $2.0 \times 10^{-6}$  C/m<sup>2</sup> and lasted between 1 and 10 ms. The more rapid decay in charge occurred within 0.1 to 2 ms to a level more or less than the charge increase in the initial ramp. Individual fast pulses were often observed during both charge changes on electric field records from the fuselage, wingtips, and vertical stabilizer. The expansion of the first part of the electric field waveform from Fig. 9 is shown in Fig. 31, denoting a section of the waveform that is expanded even further in Fig. 32.

Figure 32 includes time-correlated expansions of the right wing electric field and current waveforms that correspond to the bracketed area of Fig. 31. This strike attached to the right wing and produced pulses on the electric field sensors on the right wingtip and forward upper fuselage. Small current pulses on the right wing appeared at a time coincident with the end of the field reversal on the upper fuselage sensor. Figure 32 also shows the beginning of continuing current on the right wing. The 20-ms expansions in Fig. 33 illustrate the existence of continuing current on the right wingtip and the subsidence of pulses on the right wing electric field sensor once continuing current had begun. Figure 34 displays the first 100 ms of the flash and shows approximately 25 ms of continuing current followed by three larger current pulses, coincident with sharp negative increases on the forward fuselage electric field sensor.

Figure 35 shows time-correlated data from all sensors involved in interpreting this flash, which lasted about 450 ms. Similar records have been analyzed for all 32 Category 1 strikes. These strikes occurred in-cloud between 14,000 and 18,000 ft and often in the presence of hail, freezing rain, or other weather phenomena conducive to triboelectric charging.

These data are interpreted below to show that these strikes were triggered by the presence of the aircraft, i.e., they would not have occurred at this time if the aircraft were not there. The triggering process appears to require the presence of an aircraft in close proximity to a positive charge center and

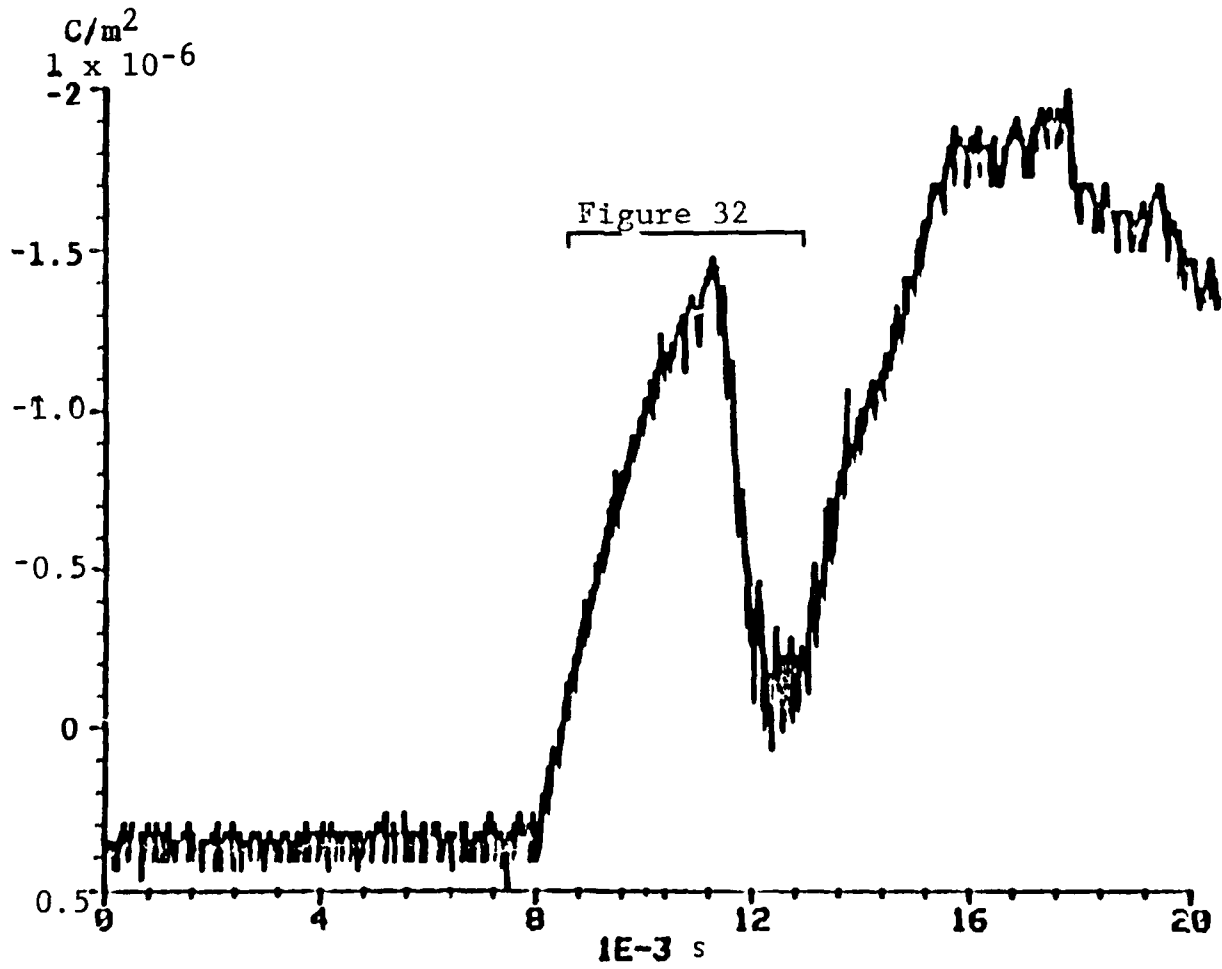


Figure 31. Expansion of First Part of Typical Category 1 Electric Field Waveform Shown in Figure 9

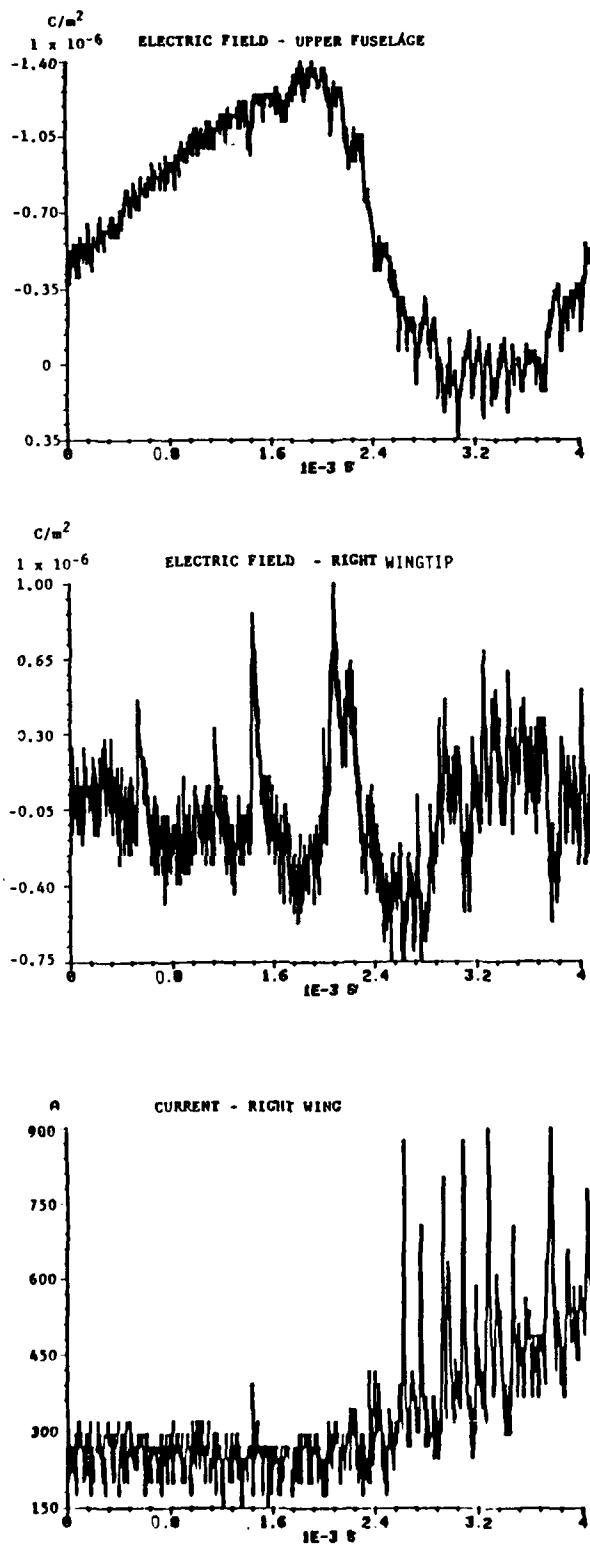


Figure 32. Electric Field and Current Waveforms During the Initial Milliseconds of a Lightning Attachment in Category I—Expansion From Figure 31

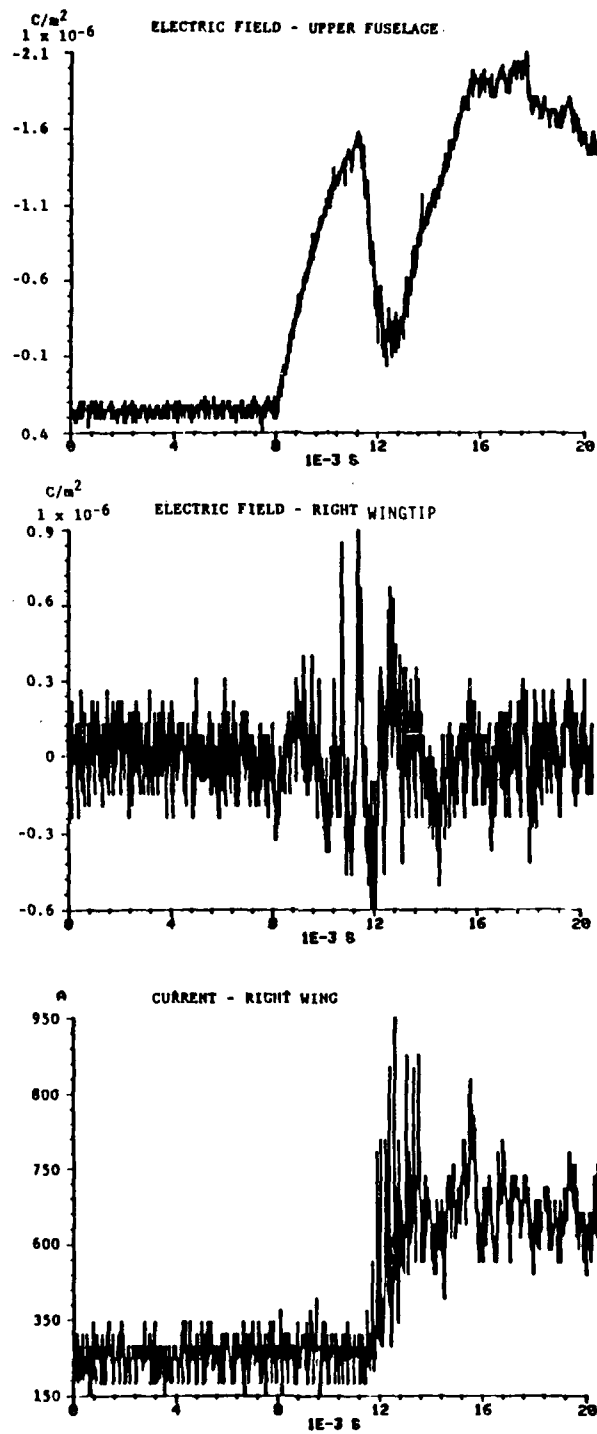


Figure 33. Electric Field and Current Waveforms During the First 12 ms of a Lightning Attachment in Category 1

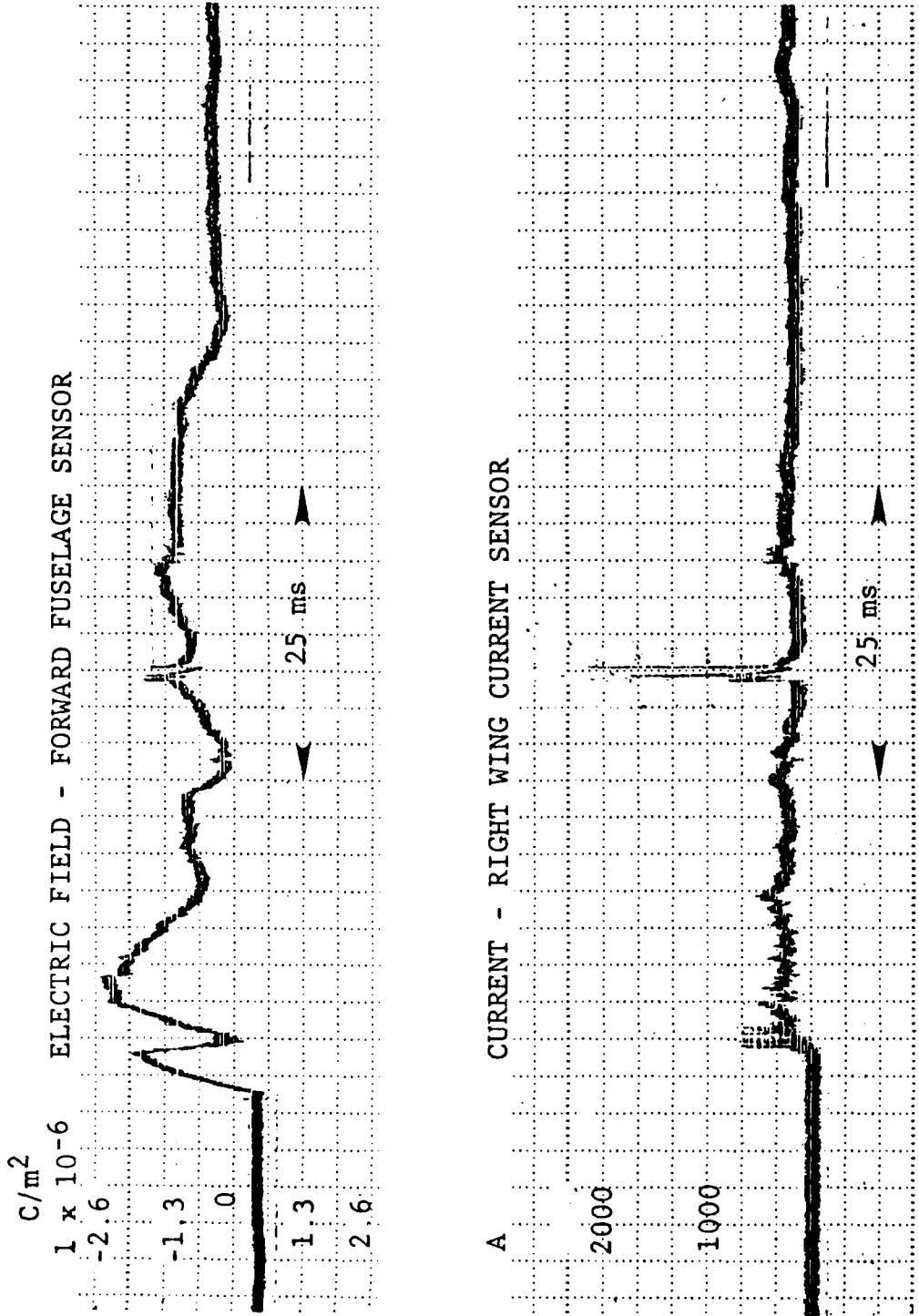


Figure 34. Electric Field and Current Waveforms During the First 100 ms of the Lightning Attachment in Figure 9

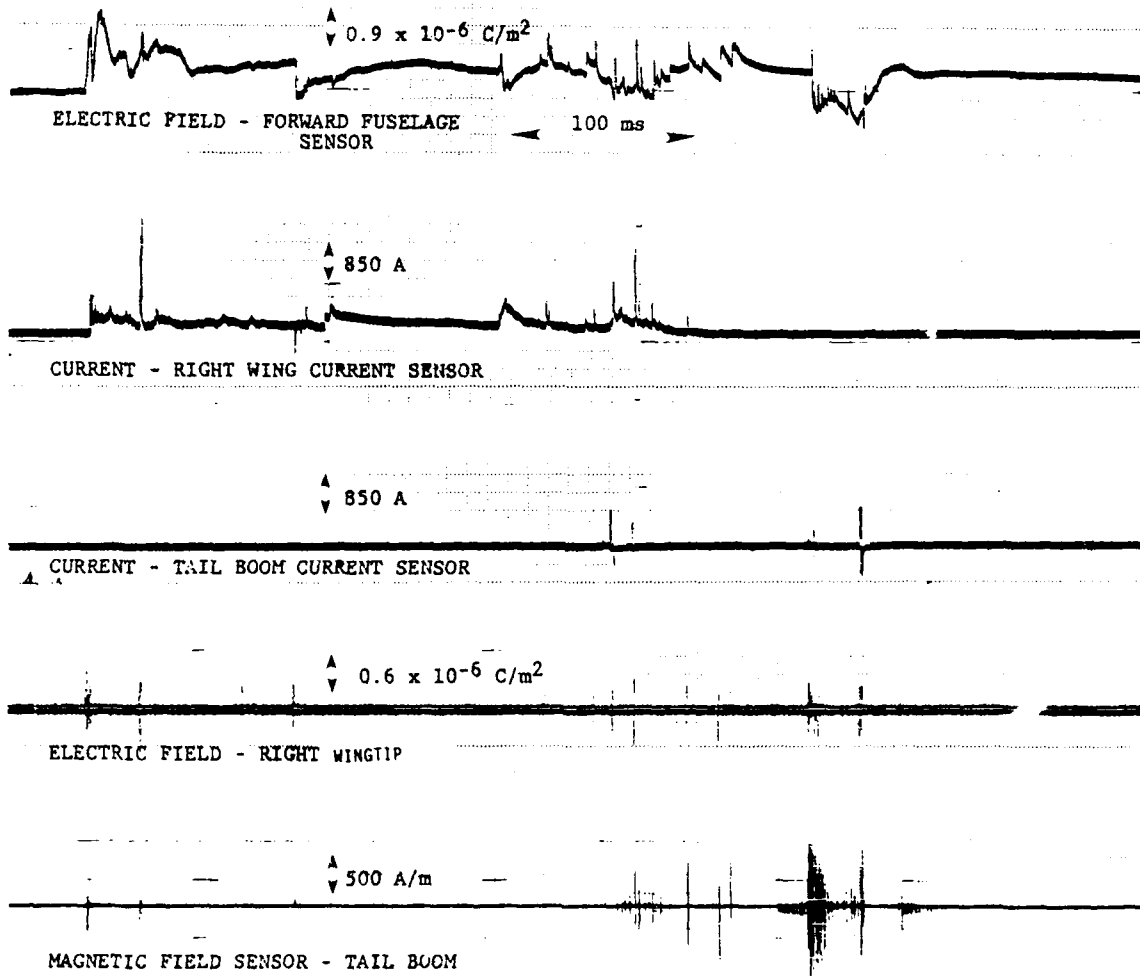


Figure 35. Electromagnetic Field and Current Waveforms During a Lightning Attachment in Category I

climatic conditions capable of causing triboelectric charging. For extended involvement of the aircraft, it is believed that a negative charge center must also be nearby.

The initial slow negative field change is attributed to negative charge accumulation on the aircraft due to triboelectric charging in the vicinity of a positive charge center. As the charge increases, streamering begins at the aircraft extremities and fields increase until a leader propagates from the positive charge center to meet the negative leader from the aircraft. Once the channel is established, the positive leader may continue beyond the aircraft until it contacts other areas of negative charge, producing recoil streamers that appear on the electric field records as sharp negative pulses. From this point on, the aircraft is simply part of an intracloud event.

This triggering mechanism is described and analyzed in more detail in Section IV. Discussions with other investigators have lead to suggestions of other possible mechanisms and these are also presented. In the meantime, data reported in the rest of this section will be categorized according to the previous discussion, as, for example, the result of a recoil streamer, negative leader attachment, positive leader attachment, first return stroke, initial breakdown, etc.

#### d. Surface Measurements

##### (1) Displacement Currents

Maxwell's third equation, which is a generalized form of Ampere's law that satisfies the continuity equation, states that a magnetic field can be produced by moving charges (current) and time-varying electric flux density.

That is  $\nabla \times \dot{H} = \dot{J} + \frac{\partial \dot{D}}{\partial t} = \dot{J} + \dot{J}_D$

where:  $\dot{J}$  = conduction current density

and:  $\dot{J}_D$  = displacement current density

$$\frac{\partial \vec{D}}{\partial t} = \text{time-varying electric flux density}$$

The sensors on the bottom side of the left and right wingtips and the left side of the vertical tail were intended to measure the normal component of the local displacement current density at each of these locations. Table 9 summarizes the displacement current data from 1984 and 1985 events where digital data was recorded. Figure 36 gives a representative set of wing displacement current waveforms. This digital window was obtained at Point A in the analog record shown in Fig. 37.

Since the digital acquisition system was triggered by signals from the current and surface current density sensors, the displacement current data presented in Table 9 should not to be construed as being the largest displacement currents present. The highest levels of displacement current would be expected to occur during and after the initial attachment, due to the enhancement and collapse of the electric field. Half of this data was recorded during triggered strikes at the time of the initial breakdown process, and the other half was recorded during actual attachment. To increase the probability of recording the largest displacement current pulses at the time of attachment, a trigger signal derived from the displacement current sensors would be required.

The highest amplitude of displacement current measured was 30.5 A/m<sup>2</sup> at the left wingtip on 6 July 1985. This corresponded to a peak electric field derivative of  $3.44 \times 10^{12}$  (V/m)/s. The mean magnitudes of nonsaturated displacement current and peak electric field derivative data were 11.95 A/m<sup>2</sup> and  $13.7 \times 10^{12}$  (V/m)/s, respectively.

## (2) Surface Currents

The digital surface current density data obtained consisted of 14 sets (Table 10) that could be used to aid in determining the attachment point, the direction of current flow, and the general current distribution paths on the aircraft. The process for making these determinations is discussed:

The digital records were time-correlated to within 5 ns (Reference 28) corresponding to a distance of 1.5 m at the speed of light. Since the current and

TABLE 9. Displacement Current Data

EVENT	DATE	TIME	PEAK ELECTRIC FIELD DERIVATIVE (V/m)/s			DISPLACEMENT CURRENT AT SENSOR (A/m <sup>2</sup> )			ATTACHMENT AREA	STRIKE TYPE	REMARKS
			LEFT WING	RIGHT WING	VERTICAL TAIL	LEFT WING	RIGHT WING	VERTICAL TAIL			
84-3	7/13/84	20:46:33:200	3.39 (11)	—	+3.85 (11)	1.393	—	3.410	Tail	1	
84-4	8/06/84	21:44:05:210	> +2.86 (11)	—	> +2.81 (11)	> 2.530	—	> 2.488	Right Wing	1	Slight Saturation
84-8	8/07/84	21:41:58:360	+4.55 (11)	+4.26 (11)	+2.22 (12)	4.030	3.77	19.670	Tail	1	
84-9	8/07/84	21:43:26:140	+6.70 (11)	+2.30 (12)	> +1.79 (11)	5.930	20.34	> 1.589	Right Wing	1	Slight Saturation
84-12	8/17/84	21:36:01:380	> -9.45 (11)	> -9.11 (11)	-9.13 (11)	> 8.370	> 8.07	8.080	Nose	2	Saturated
84-14	8/20/84	15:37:41:990	-1.14 (12)	+1.04 (12)	-4.21 (11)	10.090	9.18	3.730	Nose	2	
84-17	9/05/84	21:53:05:400	+9.97 (11)	+2.45 (12)	+5.77 (11)	8.830	21.69	5.110	Right Wing	1	
85-8	6/27/85	20:32:43:760	-2.04 (12)	-2.28 (12)	—	18.060	20.20	—	Tail	2	
85-9	6/29/85	—	-1.43 (12)	-2.47 (12)	—	12.630	21.90	—	Right Wing	2	
85-11	7/06/85	—	+3.44 (12)	—	—	30.500	—	—	Right Wing	2	

1 Triggered  
2 Negative - Cloud to Ground

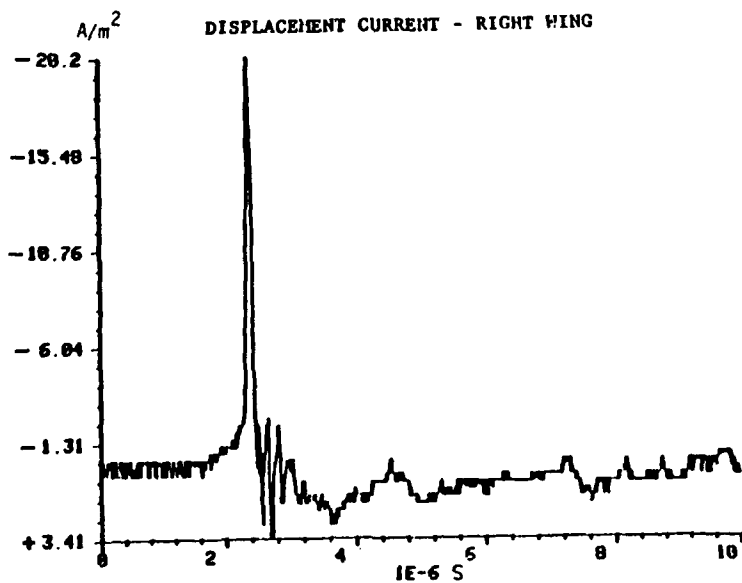
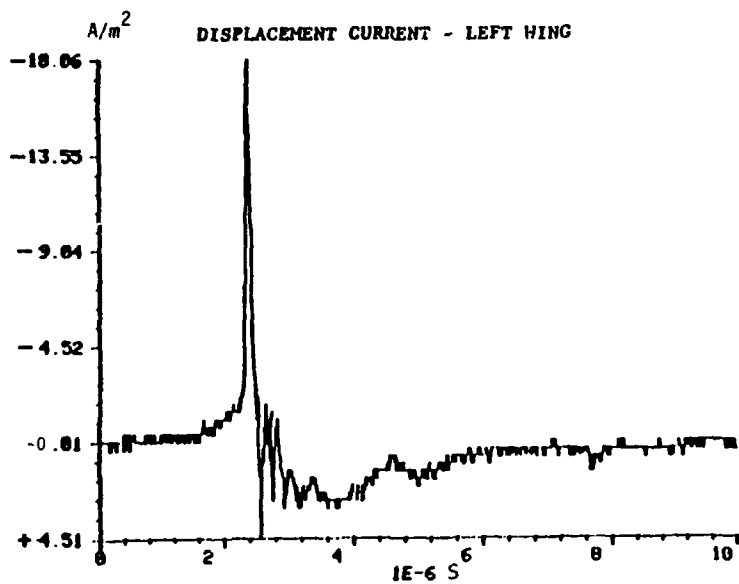


Figure 36. Displacement Current Waveforms Recorded by the Digital System During a Lightning Attachment

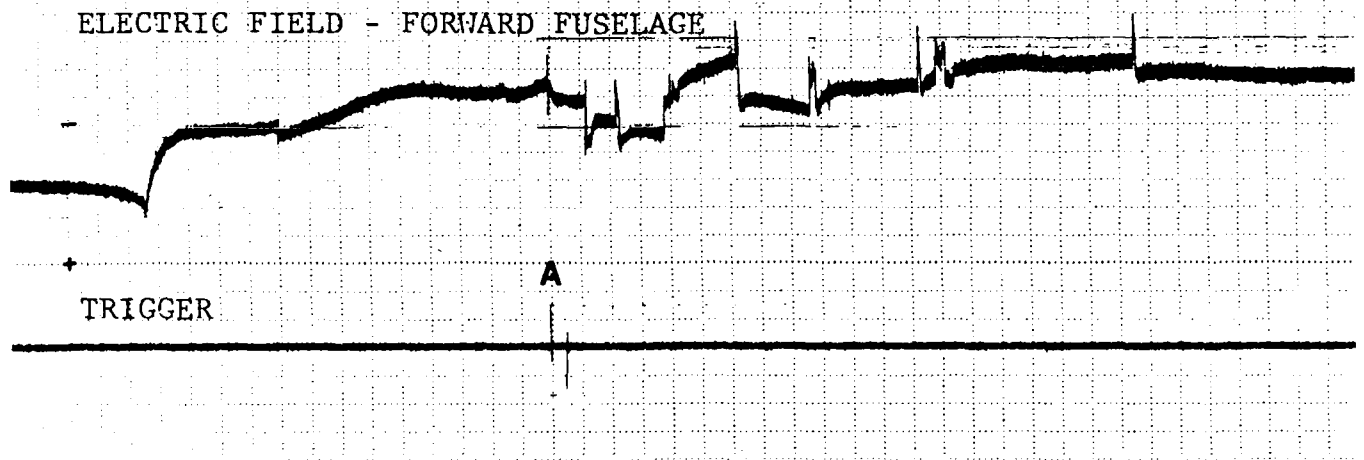


Figure 37. Analog Record for 27 June 1985 Lightning Event Showing Trigger Pulse (A) Which Corresponds to the Time at Which the Data Shown in Figure 36 Was Recorded

TABLE 10. Digital Data Acquisition in 1984 and 1985

EVENT NUMBER	ANALOG DATA	DATE	TYPE OF EVENT	TRIGGER <sup>1</sup> LOCATION	ATTACHMENT POINT	VIDEOD	CHARGE FLOW
84-3	Y	7/13	1	A	Tail	Y	- Out
84-4	N	8/06	---	---	Right Wing	Y	- Out
84-7	Y	8/07	1	A	*	-	* -
84-8	Y	8/07	1	A	Tail	Y	- Out
84-9	Y	8/07	1	A	Right Wing	Y	- Out
84-10	Y	8/07	1	A	*	-	* -
84-11	Y	8/07	1	A	*	-	* -
84-12	Y	8/17	2	C	Nose	Y	- In
84-14	N	8/20	2	C	Nose	Y	- In
84-17	Y	9/05	1	A	Right Wing	Y	- Out
85-1	Y	6/21	1	B	*	-	* -
85-8	Y	6/27	2	E	Tail	N	- In
85-9	N	6/29	2	C	Right Wing	Y	- In
85-11	Y	7/06	2	D	Right Wing	Y	- Out

1 - Triggered Intracloud  
 2 - Negative Cloud to Ground

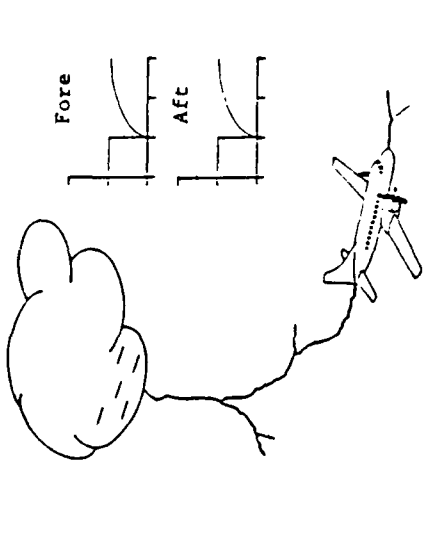
\* - In Noise Level

<sup>1</sup> See Figure 39

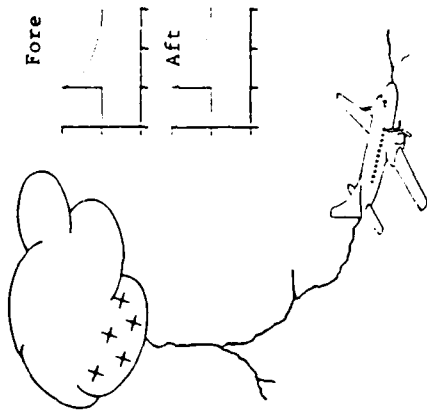
surface current sensors were spaced on the aircraft at least several meters apart, it was possible to determine at which sensor, and hence aircraft location, the current pulse first arrived. Where the pulse appeared on one of the current shunts, an actual attachment point could be identified. Where a pulse was not seen on the current shunts but was seen on several of the surface current sensors, the general area of attachment could be inferred. Once the area of attachment was known and the direction of current flow on the aircraft established, the polarity of the sensor outputs was used to determine whether negative charge had flowed on or off the aircraft. This technique is described as follows:

Consider a hypothetical aircraft fuselage instrumented with two loop type sensors to measure surface current density. One sensor is mounted forward on the fuselage about 15 ft ahead of the wing axis, while the second is aft on the fuselage about 15 ft behind the wing axis. With the sensors 30 ft apart, assuming a propagation velocity equal to the speed of light through the aircraft, a current pulse applied to the nose of the aircraft would reach the forward sensor 30 ns before it reached the aft sensor. With sufficient time resolution in recording the two waveforms, it is possible to tell whether the current pulse was applied to the nose or to the tail.

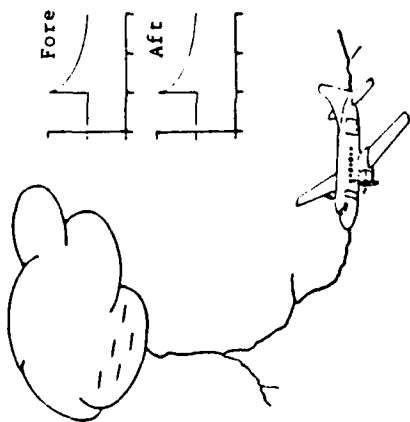
Assume that both sensors were oriented so that negative charge flow from the nose to the tail would produce a positive sensor output. Conversely, negative charge flowing from the tail to the nose will produce a negative output on both sensors. Figure 38 shows four simple scenarios of lightning attachment to an aircraft. In Fig. 38A, negative charge from the cloud is lowered to the aircraft and attaches to the nose, producing negative charge flow toward the tail and positive waveforms on both sensor outputs. In Fig. 38B, negative charge is lowered to the aircraft and there is a strike to the tail, producing negative charge flow toward the nose and negative sensor outputs. In Fig. 38C, positive charge is lowered to the aircraft. In this case, a strike to the nose results in negative charge flow off the aircraft and negative waveforms as sensor outputs. Finally, in Fig. 38D, negative charge flow off the aircraft during a positive strike to the tail produces positive sensor outputs. Thus, identifying the attachment point or area of



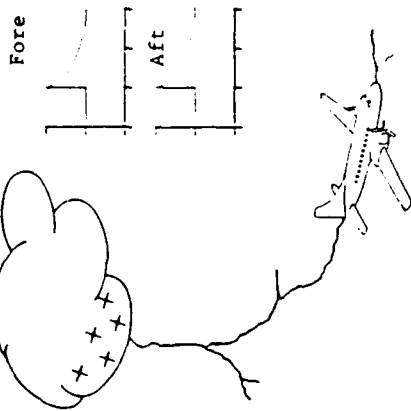
**A NEGATIVE CHARGE FLOW ONTO AIRCRAFT - STRIKE TO NOSE**



**B NEGATIVE CHARGE FLOW ONTO AIRCRAFT - STRIKE TO TAIL**



**C NEGATIVE CHARGE FLOW OFF AIRCRAFT - STRIKE TO NOSE**



**D NEGATIVE CHARGE FLOW OFF AIRCRAFT - STRIKE TO TAIL**

Figure 38. Outputs Expected From Fore and Aft Loop Sensors on Aircraft Fuselage During Four Different Lightning Attachment Scenarios

the lightning event and recording the polarities of the sensor outputs allows determination of whether negative charge was moving onto or off the aircraft during the flash.

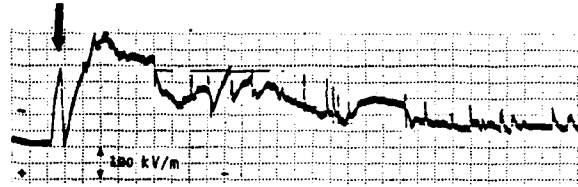
The digital triggers occurred at various times in the events, as shown in Fig. 39. Reference to the analog data showed that seven occurred as shown in Fig. 39A, just at the peak of the initial negative charge increase for a triggered, intracloud strike. One other digital data set was recorded during a triggered, intracloud flash and was on a recoil streamer (K-change). See Fig. 39B. Five digital data sets were recorded during cloud-to-ground events: three on a leader from a branch that did not reach ground (Fig. 39C), one on a collapsing branch (Fig. 39D), and one on a cloud-to-ground return stroke (Fig. 39E).

The digital data sets obtained in 1984 and 1985 are listed in Table 10. The table also lists the attachment points as determined by the time delays between pulses on sensor outputs and by examination of corroborating video data. It also indicates the direction of charge flow on the aircraft at the attachment point.

All the events that were determined to be triggered, intracloud strikes showed negative charge flow off the aircraft whenever the digital trigger occurred during the initial attachment process (Fig. 39A). The three events for which the data was acquired just as a negative leader contacted the aircraft during a cloud-to-ground process showed negative charge flow onto the aircraft (Fig. 39C), as did the event where the digital data was acquired on a first return stroke (Fig. 39E). The digital data set recorded at the time a branch from a cloud-to-ground event collapsed indicated that negative charge flowed off the aircraft (Fig. 39D). The data set recorded during a recoil streamer had a poor signal-to-noise ratio and could not be analyzed (Fig. 39B). These results are discussed further in Section IV.

Table 11 lists the inferred total surface current density values measured during each digital data acquisition, grouped according to the type of event during which the data set was captured. The inferred values were obtained by multiplying the surface current density at the sensor by the circumference of the aircraft or wing at the location of the sensor. The first eight sets occurred

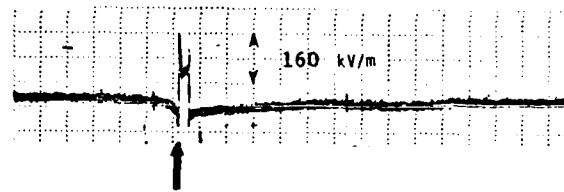
A Initial Current Flow on Aircraft - Triggered Intracloud Event



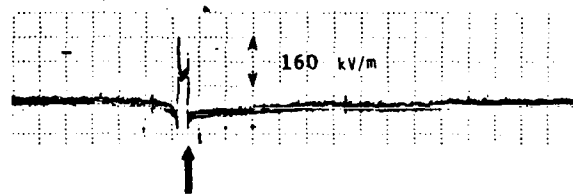
B Recoil Streamer - Triggered Intracloud Event



C Leader - Cloud-to-Ground Event



D Collapsing Branch - Cloud-to-Ground Event



E First Return Stroke - Cloud-to-Ground Event

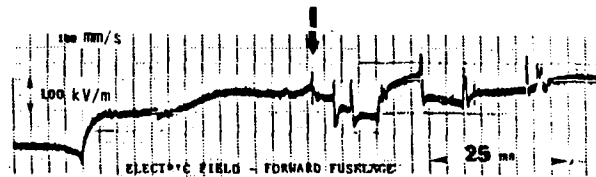


Figure 39. Key to Locations of Digital Data Described in Table 10

TABLE 11. Surface Currents Measured During Digital Triggers

EVENT NUMBER	DATE	ATTACHMENT POINT	SURFACE CURRENT (A)			AFT FUSELAGE
			LEFT WING	RIGHT WING	FORWARD FUSELAGE	
84-3	7/13	Tail	51	47	117	431
84-4	8/06	R Wing	340	431	N/A	235
84-7	8/07	?	N	N	N/A	N
84-8	8/07	Tail	N/A	165	86	272
84-9	8/07	R Wing	N/A	339	149	231
84-10	8/07	?	N	N	N	N
84-11	8/07	?	N	N	N	N
84-17	9/05	R Wing	544	846	279	558
LEADER						
CLOUD-TO-GROUND EVENT						
84-12	8/17	Nose	216	240	2470 (S)	521
84-14	8/20	Nose	252	256	1020 (S)	460
85-9	6/29	R Wing	N/A	1316	N/A	885
FIRST RETURN STROKE						
CLOUD-TO-GROUND EVENT						
8-85	6/27	Tail	329	374	1099	3711
COLLAPSING BRANCH						
CLOUD-TO-GROUND EVENT						
85-II	7/06	R Wing	N/A	1212	N/A	3487

N - In Noise Level  
 N/A - Not Acquired  
 S - Saturated

during triggered, intracloud flashes as illustrated by Fig. 39A. Expansion of the corresponding analog data sets showed that in all cases, these data were recorded exactly at the end of the initial slow negative charge increase on the forward fuselage electric field sensor characteristic of this type of strike. The amplitudes of three of the eight data sets were too low to analyze. In the other five cases, the displacement currents were positive (see Table 9), indicating an increase in positive charge on the aircraft (or loss of negative charge). The inferred total surface current values were low, averaging 294 A. In all cases, the surface current values were largest near the attachment area and decreased as the current flowed through the aircraft to the other sensors. In event 84-3, for example, an attachment to the tail produced 431 A of current on the aft upper fuselage, 117 A on the forward upper fuselage, and approximately equal amounts of current (50 A) on each wing.

Very similar current distributions were observed for two of the cases in which the aircraft made contact with a negative leader. In both cases, the attachment point was to the nose. In event 84-12, at least 2470 A of current flowed onto the forward fuselage, then branched into 521 A at the aft fuselage, 216 A through the left wing, and 240 A through the right wing. A similar distribution occurred for event 84-14.

The return stroke in event 85-8 produced the highest surface current recorded, 3700 A at the aft fuselage. The current distribution during this strike was discussed in this section in paragraph 1(c).

The last data set (event 85-11) is for the aircraft in a collapsing branch of a cloud-to-ground event. The current distribution during this event also was discussed in this section in paragraph 1(c).

### (3) Rise Times and Rates of Rise

Table 12 lists the rise times (10 to 90 percent) and rates of rise obtained for the surface current outputs during the digital data acquisitions. The rise times for the first group, digital data collected during the initial attachment phase in events triggered by the aircraft, were very short, from 14 to 144 ns with an average of 75 ns. Rates of rise, however, were generally slow, ranging from 4.9

TABLE 12. Rise Times, Current Levels and Rates of Rise From Digital Data Sets

EVENT NUMBER	DATE	INITIAL CURRENT FLOW ON AIRCRAFT TRIGGERED INTRACLOUD EVENT															
		FORWARD FUSELAGE				AFT FUSELAGE				LEFT WING				RIGHT WING			
		RISE TIME ns	CURRENT CHANGE A	RATE OF RISE A/S	ns	CURRENT CHANGE A	RATE OF RISE A/S	RISE TIME ns	CURRENT CHANGE A	RATE OF RISE A/S	RISE TIME ns	CURRENT CHANGE A	RATE OF RISE A/S	RISE TIME ns	CURRENT CHANGE A	RATE OF RISE A/S	
84-3	7/13	75	117	$1.5 \times 10^9$	96	431	$4.5 \times 10^9$	63	51	$8.0 \times 10^9$	96	47	$4.9 \times 10^9$				
84-4	8/06	—	N/A	—	77	235	$3.0 \times 10^9$	82	340	$4.1 \times 10^9$	86	431	$5.0 \times 10^9$				
84-7	8/07	—	N	—	—	N	—	—	N	—	—	N	—				
84-8	8/07	14	86	$6.1 \times 10^9$	38	272	$7.2 \times 10^9$	—	N/A	—	14	165	$1.2 \times 10^{10}$				
84-9	8/07	58	149	$2.6 \times 10^9$	91	231	$2.5 \times 10^9$	—	N/A	—	86	339	$3.9 \times 10^9$				
84-10	8/07	—	N	—	—	N	—	—	N/A	—	—	N	—				
84-11	8/07	—	N	—	—	N	—	—	N/A	—	—	N	—				
84-17	9/05	57	279	$4.9 \times 10^9$	96	558	$5.8 \times 10^9$	106	544	$5.1 \times 10^9$	144	846	$5.9 \times 10^9$				
LEADER - CLOUD-TO-GROUND EVENT																	
84-12	8/17	124	2470	$1.8 \times 10^{10}$	206	521	$2.5 \times 10^9$	120	216	$1.8 \times 10^9$	132	240	$1.8 \times 10^9$				
84-14	8/20	96	1020	$1.1 \times 10^{10}$	101	642	$6.4 \times 10^9$	72	252	$3.5 \times 10^9$	96	256	$2.7 \times 10^9$				
85-9	6/29	—	N/A	—	75	885	$1.2 \times 10^{10}$	—	N/A	—	75	1320	$1.8 \times 10^{10}$				
FIRST RETURN STROKE - CLOUD-TO-GROUND EVENT																	
85-8	5/27	408	1099	$2.7 \times 10^9$	326	3711	$1.1 \times 10^{10}$	245	329	$1.3 \times 10^9$	326	374	$1.1 \times 10^9$				
COLLAPSING BRANCH - CLOUD-TO-GROUND EVENT																	
85-11	7/06	—	N/A	—	410	3487	$8.5 \times 10^9$	—	N/A	—	367	1212	$3.3 \times 10^9$				

N - In Noise Level  
 N/A - Not Acquired

$\times 10^8$  to  $1.2 \times 10^{10}$  A/s with an average of  $4.4 \times 10^9$  A/s. This was due to the low current amplitudes. Rise times averaged 120 ns for the two events where leaders from negative cloud-to-ground events attached to the aircraft. Rates of rise averaged  $6.0 \times 10^9$  A/s. The one set of digital data captured during a first return stroke produced an average rise time of 326 ns and an average rate of rise of  $4.0 \times 10^9$  A/s. The digital data acquired during a collapsing branch produced rise times averaging 388 ns and rates of rise averaging  $5.9 \times 10^9$  A/s.

e. Current Shunt Measurements

(1) Current Pulse Data

Current shunt measurements were made using resistive current shunts as described in Section II. In 1984, these measurements were made only at the base of booms installed on the wingtips. In 1985, a tail boom was added which contained a current shunt and other sensors. Also, the vertical fin cap was modified to include a small boom with a current shunt.

The current data presented here are predominantly from the analog recording system. Tables 2 and 3 indicated that digital data was acquired during only 28 of the 52-lightning attachments. Only 13 of the digital sets contained current pulses, all but four of which occurred in 1984 when only the wingtips were instrumented for current measurements.

The digital data that was recorded are presented in Table 13 for both 1984 and 1985. The largest currents, in amperes, measured were 3204 on the left wingtip, 2880 on the right wingtip, 633 on the vertical tail and 3320 on the tail boom. In most cases, the data amplitudes were insufficient for accurate rise time determinations. However, the slowest rise time measured was 3.7  $\mu$ s. Generally, the pulses had short durations (less than 2  $\mu$ s) and the inferred rise times were less than 1  $\mu$ s.

Substantially more data were available from the analog records. Although the data are bandwidth limited and pulse amplitudes are therefore questionable, the pulse data can be used to make some inferences.

TABLE 13. Digital Current Data for 1984 and 1985

EVENT	LEFT WING		RIGHT WING		VERTICAL TAIL		TAIL BOOM	
	+	-	+	-	+	-	+	-
84-7	384	- 406	844	- 736	---	---	---	---
84-8	788	- 990	234	- 556	---	---	---	---
84-9	---	---	782	---	---	---	---	---
84-10	---	---	769	---	---	---	---	---
84-11	---	---	599	-506	---	---	---	---
84-12	570	---	---	---	---	---	---	---
84-13	2000	-2540	1900	-1409	---	---	---	---
84-14	---	---	406	---	---	---	---	---
84-17	---	---	1777	---	---	---	---	---
85-1	650	---	416	- 506	451	---	---	---
85-8	3204	---	672	---	633	---	---	- 818
85-10	---	---	---	-2880	---	---	---	-1633
85-11	---	---	---	- 539	---	---	3320	---

Analog data for each event was rerecorded on strip charts for evaluation. The current trace with the most activity and/or highest signal-to-noise ratio was also selected for each event. These pulses were tabulated in terms of their occurrence with respect to the major phases of the corresponding forward fuselage electric field record. For triggered events, the three phases were labeled: before breakdown, breakdown, and post breakdown. The before breakdown phase corresponds to the period during the negative-going electric field change. The breakdown phase corresponds to the shorter duration positive-going electric field change. The post breakdown phase is the period following the first two phases. For the intercepted strikes, all pulses were placed in the post breakdown category. Again, only those pulses that could be readily identified above noise were counted. In actuality, many more current pulses were present but could not be categorized from the strip chart data. The before breakdown phase pulses are probably streamer pulses while the breakdown phase pulses could be leader pulses. Identification of the post breakdown pulses is a more difficult proposition and requires corroborating data from other sensor channels as well as educated guesswork. However, this type of data, direct current measurements of intracloud strikes or cloud-to-ground strikes at aircraft altitude, is unique. We hope that with time, as other comprehensive lightning characterization programs such as the French Transall C-160 program continue, the data base will expand substantially and the understanding of the data will increase. Table 14 summarizes these results.

Using the selection techniques just discussed, the data that was summarized show that a majority of the current pulses occurred during the post breakdown phase, 96 of 103 in 1984, and 280 of 304 in 1985. The majority of the pulses were of positive polarity, 88 of 103 in 1984, and 195 of 304 in 1985. The smallest amplitude pulse considered was 63 A obtained in 1984, while the largest pulse recorded was 22.5 kA in 1985. Generally, the larger amplitude pulses occurred during the post breakdown phase.

Another parameter of interest related to the current pulse data is the time interval between pulses. Although, the data presented here is not inclusive of all the data that was recorded, we can possibly summarize it into some potentially useful form. The analog recording system was not capable of recording the small fast pulses that are known to be present in lightning events. The digital system,

TABLE 14. Current Pulse Data Summary

	BEFORE BREAKDOWN		BREAKDOWN		POST BREAKDOWN	
	+	-	+	-	+	-
1984						
NO. OF PULSES	2	0	1	4	75	21
MINIMUM (A)	65	---	---	162	63	69
MAXIMUM (A)	165	---	---	255	1,990	1,558
AVERAGE (A)	115	---	178	192	459	256
1985						
NO. OF PULSES	1	2	14	7	180	100
MINIMUM (A)	---	451	227	247	194	216
MAXIMUM (A)	---	741	371	1022	22,500	652
AVERAGE (A)	500	596	333	561	1,248	1,175

being capable of recording only a nominal 10- $\mu$ s window during each flash, was not able to record a statistically significant quantity of these pulses. Thus, the only inferences that can be made from these data are limited until more comprehensive data sets are available. What is important, however, is that current pulses not be indiscriminately grouped together. It would be desirable to be able to identify streamer, leader, recoil streamers, intracloud, cloud to ground, etc., pulses, and group each category individually. This requires that each current parameter be recorded in several amplitude ranges and with sufficient bandwidth. This has not been practical to date. Table 15 summarizes the pulse interval data for those events where a significant number of pulses were available for presentation in this form.

The smallest time interval that could be measured was 10  $\mu$ s, while the longest was 255 ms. Generally, the interval between pulses seemed to increase with time during the post breakdown phase. Table 15 lists the minimum, maximum, and average time interval along with the event duration. The minimum, maximum, and average time interval are also shown for each category. The shortest flash had a duration of 63 ms, the longest lasted 1.171 s, and the average of all events was 488 ms.

## (2) Continuing Current Data

Continuing current was recorded during 4 events in 1984, and 14 events in 1985. In addition, continuing current was observed at two locations during one event (85-20). As with the current pulse data, some discretion was used in selecting and presenting the data. First, the continuing current must be detectable above the noise level, and second, the current must be present between successive pulses or for a significant time after a single pulse (at least 20 ms). The data are summarized in Table 16 for both 1984 and 1985.

The minimum duration was 28 ms and the longest was 506 ms. Charge transfer ranged between 5 and 169 C. The average continuing current ranged between 31.5 and 346 A.

TABLE 15. Summary of Current Pulse Interval Data

EVENT	NO. OF PULSES	INTERVAL (ms)			EVENT DURATION (ms)
		MINIMUM	AVERAGE	MAXIMUM	
84-1	13	0.04	0.32	0.94	975
84-2	8	0.10	3.36	15.80	413
84-5	62	0.03	6.22	142.50	500
84-17	8	0.01	0.06	0.12	182
84-20	4	0.13	0.40	0.63	1171
85-1	29	0.20	17.60	255.00	713
85-4	17	0.20	26.30	139.70	513
85-5	13	1.00	14.80	37.00	500
85-6	25	0.10	16.40	147.10	538
85-7	6	0.30	33.00	99.60	325
85-8	11	0.30	6.10	22.20	113
85-14	21	0.20	23.20	106.70	563
85-16	14	>0.10	16.30	107.40	313
85-18	44	0.10	10.60	80.60	575
85-19	14	>0.10	23.10	163.00	338
85-20	12	0.30	23.40	140.60	738
85-21	3	1.60	2.65	3.70	275
85-23	8	7.50	74.20	227.00	775
85-24	24	0.10	22.60	239.60	588
85-28	7	0.10	20.70	106.60	175
85-29	15	0.10	15.70	101.00	350
85-30	3	1.90	26.60	51.30	525
85-31	3	6.90	13.80	20.60	63
TOTAL PULSES	364	---	---	---	---
MINIMUM	3	0.01	0.06	0.98	63
MAXIMUM	62	7.50	74.20	255.00	1171
AVERAGE	15.8	0.93	17.30	96.00	488

TABLE 16. Continuing Current Data Summary

EVENT	LEFT WING	RIGHT WING	VERTICAL TAIL	TAIL BOOM	CHARGE TRANSFER C	DURATION (ms)	CURRENT (A)		
							MIN	MAX	AVE
84-5	X				90.0	438	42	252	147.0
84-7	X				96.2	419	86	301	193.5
84-11	X				5.0	141	21	42	31.5
84-17		X			7.1	66	41	81	61.0
85-1			X		17.8	28	120	171	145.5
85-4		X			79.5	444	120	223	171.5
85-6		X			98.2	388	171	274	222.5
85-16		X			26.0	94	137	240	188.5
85-18		X			35.2	200	51	137	94.0
85-20	X				34.0	62	124	494	309.0
85-20			X		85.5	188	99	247	173.0
85-23			X		41.4	231	74	296	185.0
85-23	X				109.1	656	74	445	259.5
85-24	X				141.9	506	99	296	197.5
85-25		X			168.6	294	247	445	346.0
85-26			X		8.6	97	74	148	111.0
85-28		X			16.2	131	49	222	135.5
85-29		X			38.7	275	74	198	136.0
85-30		X			17.3	73	49	198	123.5
NO. OF EVENTS	6	9	4	0	19	19	19	19	19.0
MINIMUM					5	28	21	42	31.5
MAXIMUM					169	506	247	494	346.0
AVERAGE					59	249	92	248	170.5

### (3) Current Data Summary

We hoped that the current data available could be suitable for summarizing in a manner similar to that presented by Uman in Table 1.1 of Reference 9 and/or Table II, Appendix E of the same reference. This was not possible with the limited amount of data available for each phase, but should be an objective of future airborne lightning characterization programs, particularly for intracloud, triggered events.

#### f. Magnetic Field Measurements

Magnetic field measurements were only possible in 1985 after the tail boom was installed. In addition, after the flight on 15 July 1985 where eight events were collected, the cable to the sensor was found to be defective and the data for this flight had to be disregarded.

Since the magnetic field sensor was a free field sensor, its measurements are especially important for attempts to analyze what is happening just prior to and during the initial attachment phase. However, a limitation exists in that only one orthogonal component of the magnetic field vector was measured. Figure 15, in the section on electric fields during the initial attachment process (paragraph 1c), includes magnetic field data which show the approach and departure of a leader as a series of pulses that reverse polarity as the leader passes through the aircraft. Figure 40 is the magnetic field record from Fig. 15. The leader steps are from 20 to 40  $\mu$ s apart, within the time frame determined by previous measurements (Reference 29).

Since all of the events involving approaching positive leaders occurred in 1984, before the tail boom was installed, no data for these cases is available.

Many magnetic field data sets were obtained during the initial attachment process for the triggered, intracloud strikes. Although this data is more difficult to interpret due to the many possible orientations within the event, it does seem to provide valuable information on how the triggering process occurs.

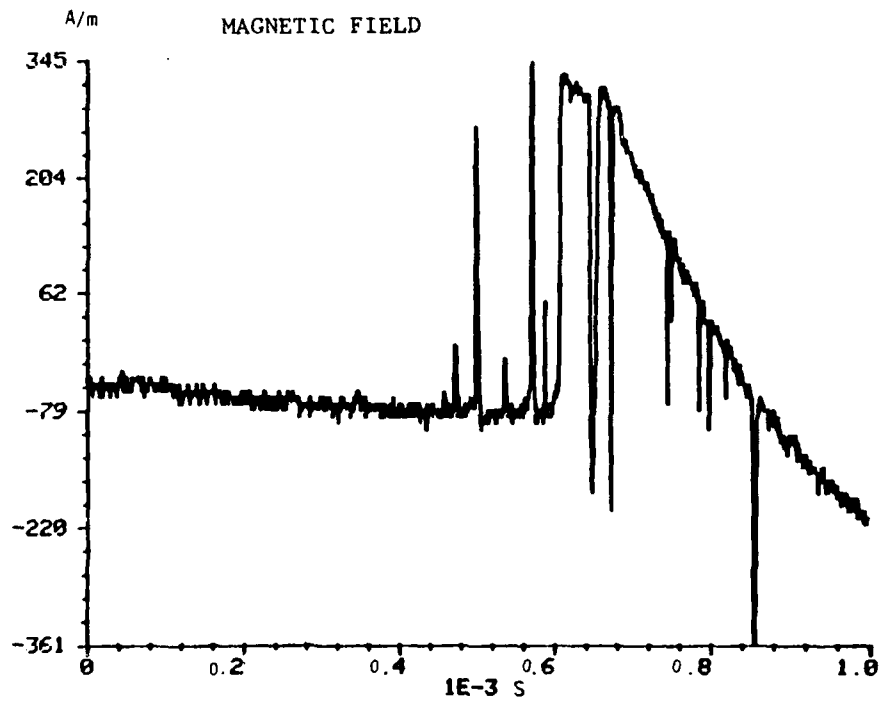


Figure 40. Magnetic Field Data Showing Approach of a Stepped Leader, Attachment to the Aircraft and Departure of the Leader

A typical set of electromagnetic field data is shown in Fig. 41 for a 10-ms window at the beginning of the event. The electric field trace shows the slow negative charge increase and faster, stepped, positive charge increase seen previously. The magnetic field trace shows two large negative pulses which do not correspond to anything obvious on the electric field record, followed by a gradual negative field change which does correspond to the positive charge change on the electric field. Two small, positive polarity pulses on the magnetic field record just before the final negative field change correspond to the first two steps in the positive charge change on the electric field. Careful examination of simultaneously recorded traces for the other three electric field sensors showed that the first two negative magnetic field pulses did not line up with pulses on these records either but often preceded or followed them by very short times. These magnetic field pulses, therefore, appear to be the result of field changes exterior to the aircraft rather than field changes caused by current flow through a channel attached to the aircraft or due to a leader leaving the aircraft.

Figure 42 shows a 4-ms window of magnetic field data time synchronized with electric field and current data. Current flow on the aircraft began at the time of the pulse labeled as A on the right wing current record and corresponds to the step change at A on the electric field record and the pulse at A in the magnetic field record. A small pulse at B on the magnetic field record corresponds to a small pulse on the current record, and a second sharp step on the electric field sensor. A sharp current pulse appears at C, coincident with a sharp field change on the magnetic field record. Pulses A, B, and C on this magnetic field record, therefore, appear to be the result of current movement in the channel during attachment to the aircraft. Pulses 1 and 2 in the magnetic field record, in contrast, are two more examples of the pulses shown in Fig. 41. The pulses do not correspond to any significant electric field changes or current pulses on the aircraft, since no significant streamers from the aircraft are in evidence before breakdown, and thus appear to be due to streamering from a positive charge volume.

An example of two windows of similar data for one other event is presented in Fig. 43. It also clearly shows the correspondence between events on the electric field, magnetic field and current sensor outputs as current flow begins on the aircraft and the lack of correspondence before this point.

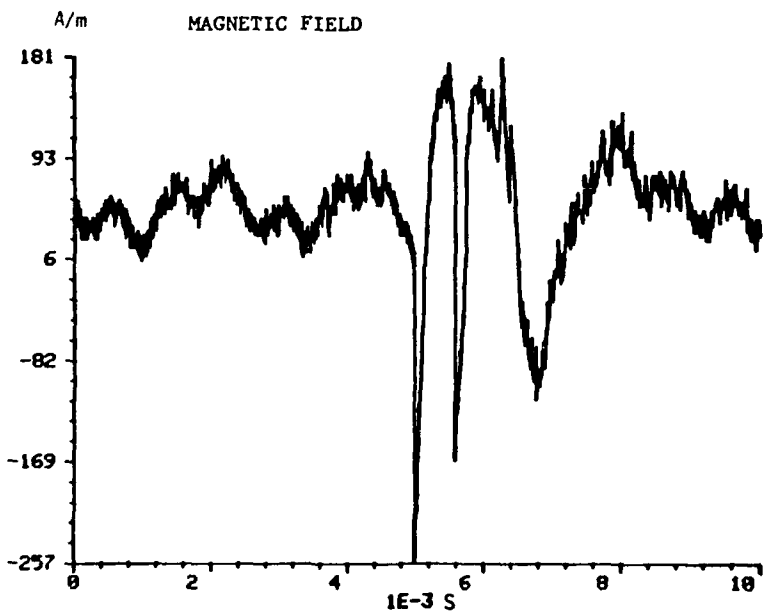
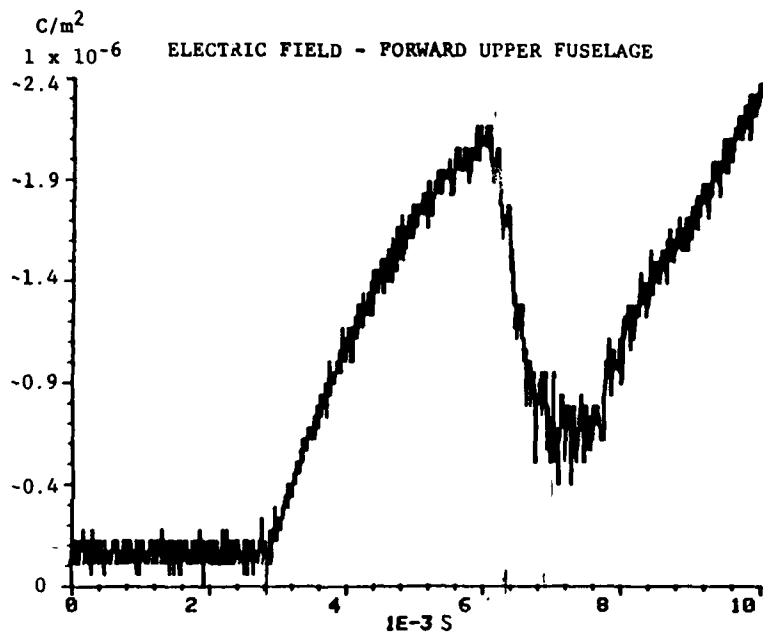


Figure 41. Electric and Magnetic Field Records During the Initial Attachment Process of an Event Triggered by the Aircraft.

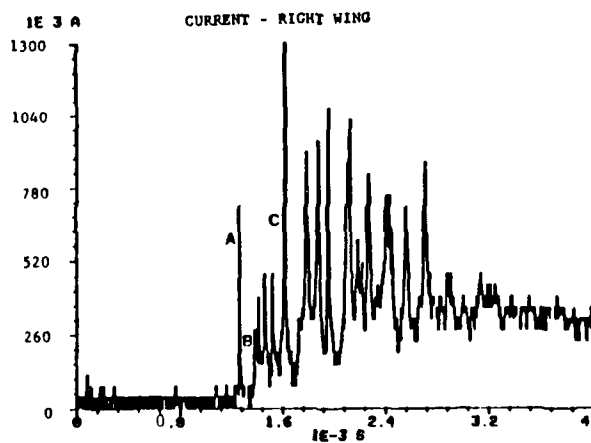
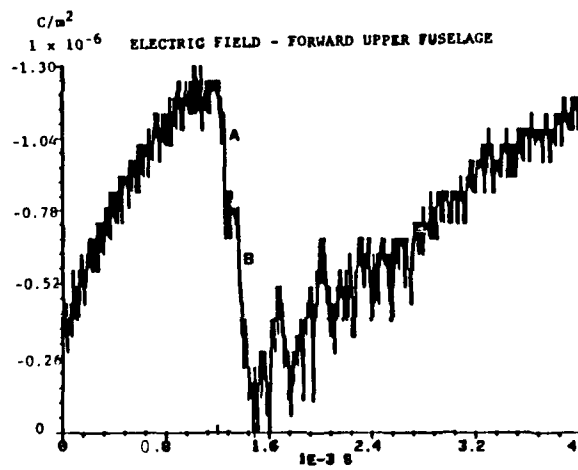
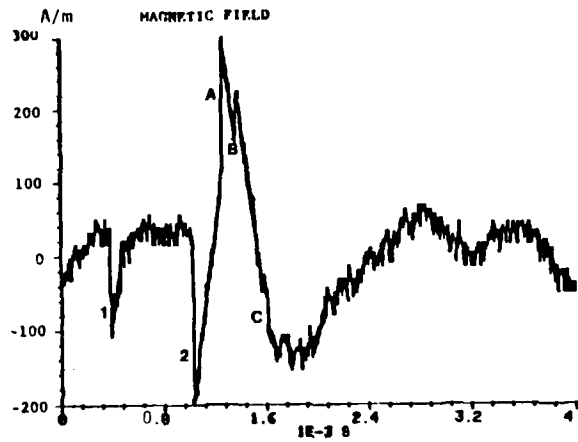


Figure 42. Electromagnetic Field and Current Data During the Initial Attachment Process of an Event Triggered by the Aircraft

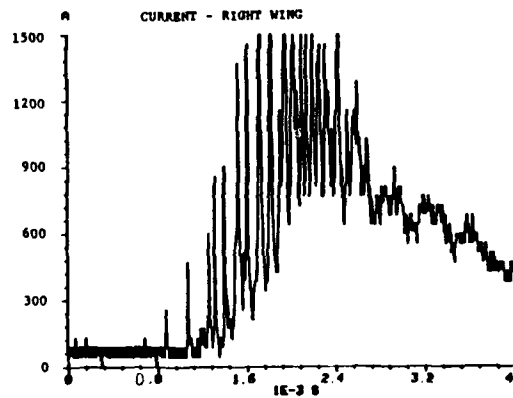
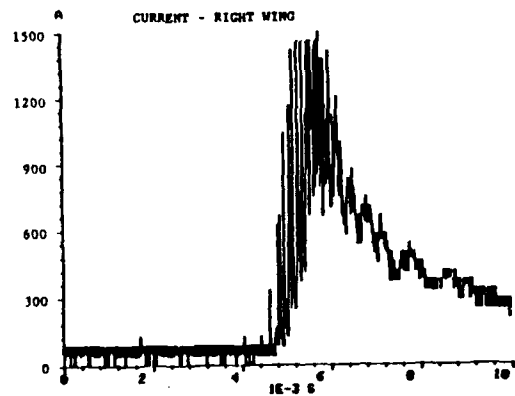
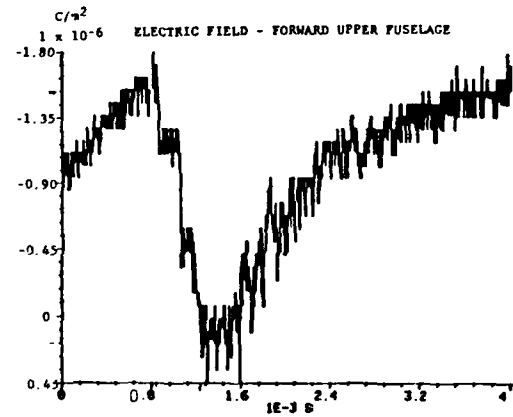
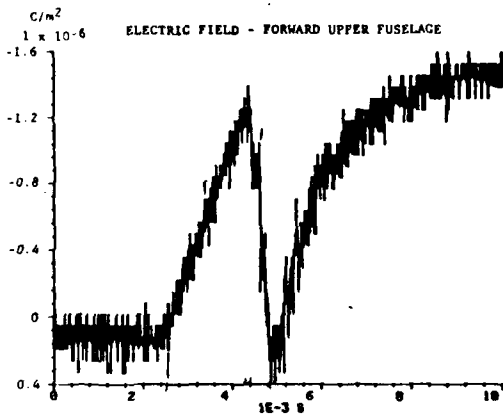
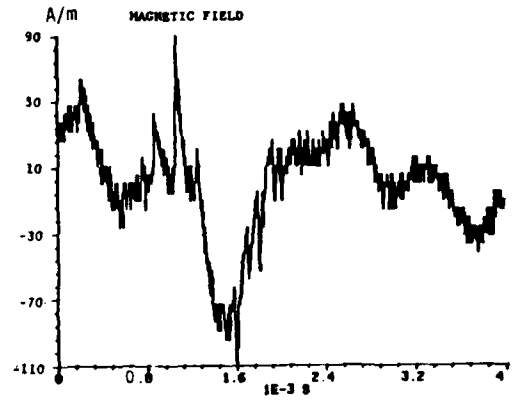
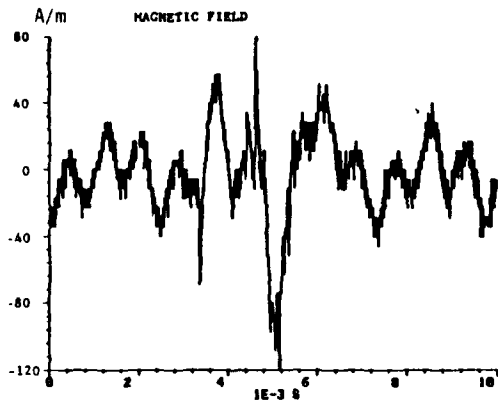


Figure 43. Electromagnetic Field and Current Data During the Initial Attachment Process of Another Event Triggered by the Aircraft

Magnetic field data from the tail boom sensor was used in other ways to aid in the data analysis. For the cloud-to-ground stroke on 6 July 1985 where the aircraft was in a branch, the sensor recorded the nearby subsequent return strokes, an example of which is shown in Fig. 44 where the return stroke itself appears to be preceded by many closely spaced dart stepped leaders.

g. Quasi-Static Electric Fields

The quasi-static electric field measurements were made by the NRL using the system described in Reference 24. The results are documented in Reference 30. In this section, we present and discuss some of the aircraft electric potential data and make some comparisons with the electric field data recorded with the AFWAL system.

Figure 45 illustrates the potential variations for the cloud-to-ground event where the aircraft was in the main channel (event 85-8). No significant change was in the aircraft potential prior to the attachment. At attachment, the aircraft showed an increase in the negative direction indicating negative charging, as would be expected for a cloud-to-ground event. This record supports the supposition that this was an intercepted strike where the aircraft had flown into a leader rather than triggering the event itself.

Figure 46 illustrates the aircraft potential for the cloud-to-ground event where the aircraft was in a branch. There was no change in the amount of charge on the aircraft prior to the attachment, indicating that this was also an intercepted strike. For this one, the aircraft acquired a positive potential. There is not sufficient resolution to see any negative charge due to the leader attachment. The aircraft potential appears to dissipate as the branch is neutralized.

Figure 47 shows the electric field for a discharge that was triggered by the aircraft. Several seconds before the attachment, which occurred at point A in the figure, the aircraft acquired a positive potential while experiencing transient charges that were predominantly negative and of increasing amplitude. Figure 48 compares the electric field record from the forward upper fuselage sensor for the same event with the field mill record showing aircraft potential. The negative

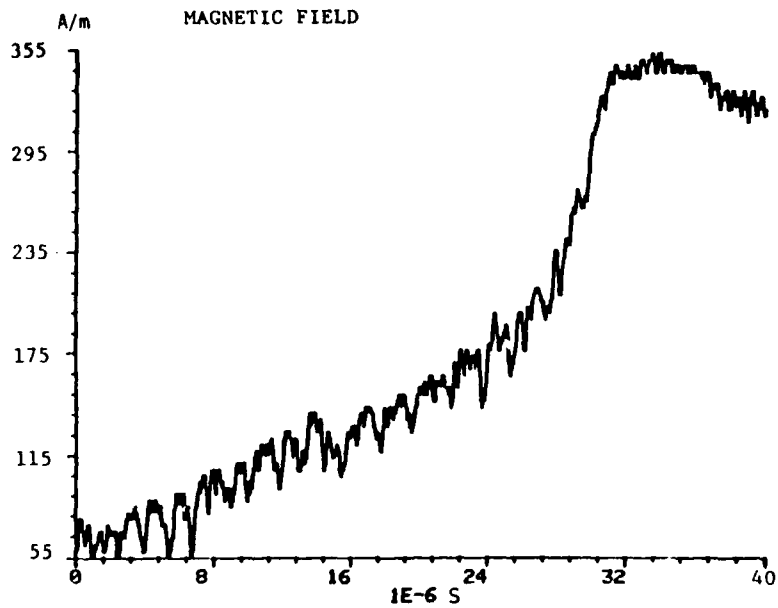


Figure 44. Return Stroke From Nearby Event Recorded on Magnetic Field Sensor

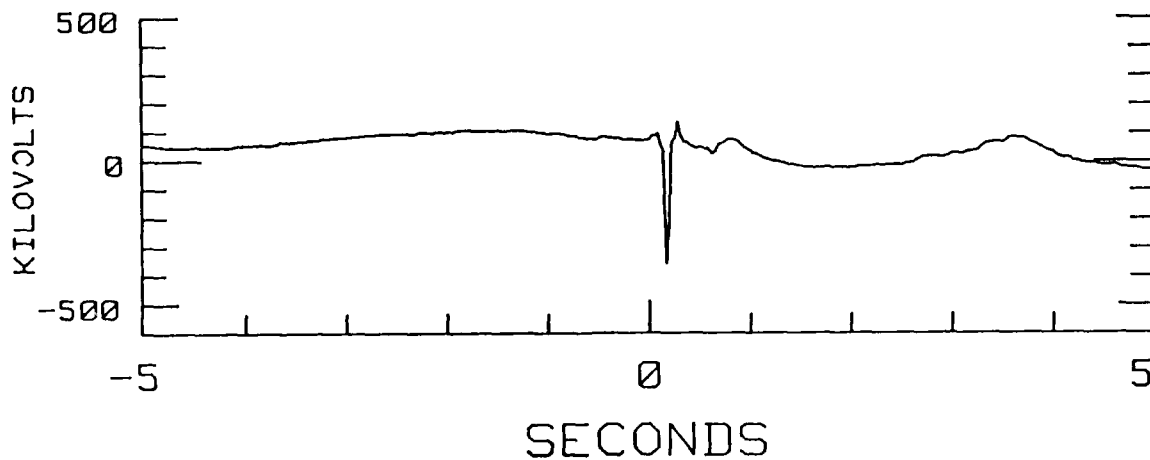


Figure 45. Aircraft Potential as Determined From the Quasi-static Electric Fields for an Event Where the Aircraft Was in the Main Channel of a Cloud-to-Ground Discharge

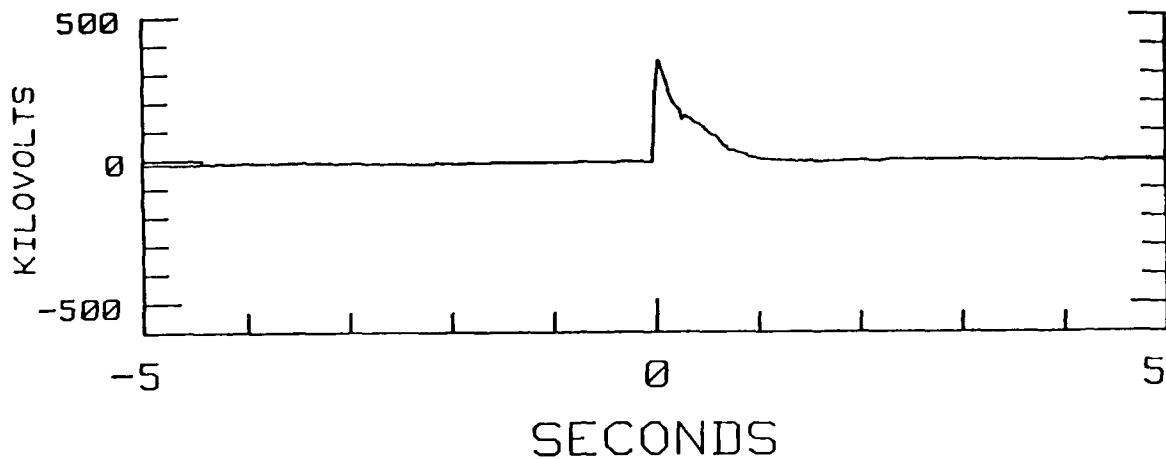


Figure 46. Aircraft Potential as Determined From the Quasi-static Electric Fields for an Event Where the Aircraft Was in a Branch of a Cloud-to-Ground Discharge

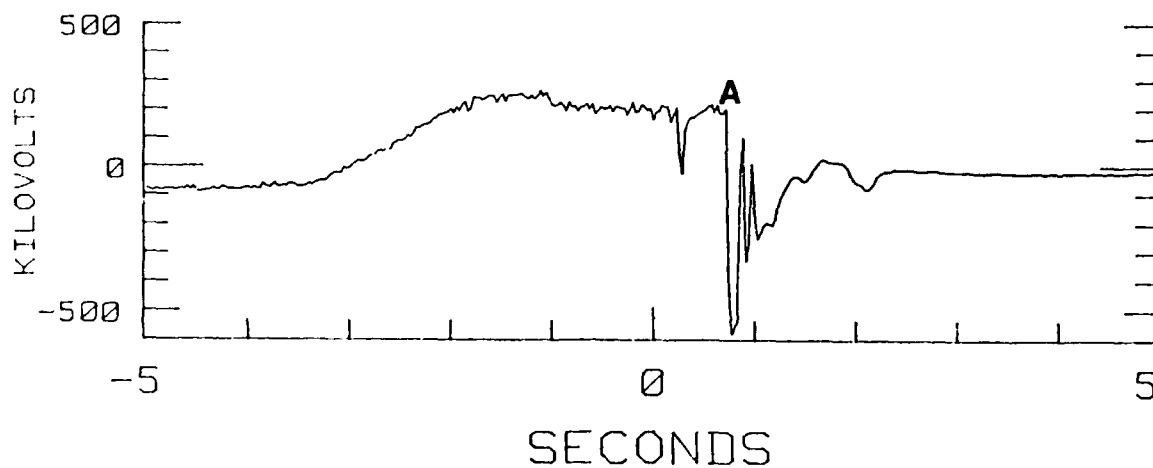


Figure 47. Aircraft Potential as Determined From the Quasi-static Electric Fields for an Event Triggered by the Aircraft

field increase at B corresponds to the increase in negative potential on the field mill record at B.

After the lightning attachment at Point A, the electric field mill record shows three negative excursions, from A to  $A_1$ ,  $A_1$  to  $A_2$ , and  $A_2$  to  $A_3$ . The first excursion lasted approximately 165 ms and corresponds to the first pronounced negative field excursion from A to  $A_1$  on the electric field record for the forward upper fuselage. The second excursion lasted approximately 100 ms and corresponds to the second pronounced negative field excursion on the forward upper fuselage electric field record from  $A_1$  to  $A_2$ . The final slow negative pulse on the electric field record coincides with the third excursion,  $A_2$  to  $A_3$ , on the field mill record. Each negative excursion on the electric field mill record begins with a sharp negative field change. The first can only be seen clearly on expansion but is located at  $K_1$ . The other two appear clearly at  $K_2$  and  $K_3$ . These are believed to be the result of the positive leader contacting successive negative charge volumes and are known as recoil streamers or K-changes. The negative field excursions resulted as negative charge from these areas flowed back through the aircraft to neutralize the positive charge volume from which the leader originated.

Almost all of the events believed to be triggered by the aircraft have electric field mill records similar to those shown in Fig. 48. They show evidence of transient, negative changes in potential for several seconds before the attachment, then an overall negative envelope during the attachment phase that is divided into several individual portions where the aircraft potential briefly becomes almost neutral, then once again becomes sharply negative. The implications of these results are discussed further in Section IV.

#### h. Induced Transients

One objective of the program was the measurement of induced currents on circuits inside the aircraft during lightning attachment. Accordingly, an extra digitizer was added to each of the instrumentation racks so that these inputs could be recorded with the required bandwidth. Problems were experienced throughout the program because of the tendency of the digitizers to overheat and malfunction. When this occurred, the extra digitizers were used to replace those needed for the

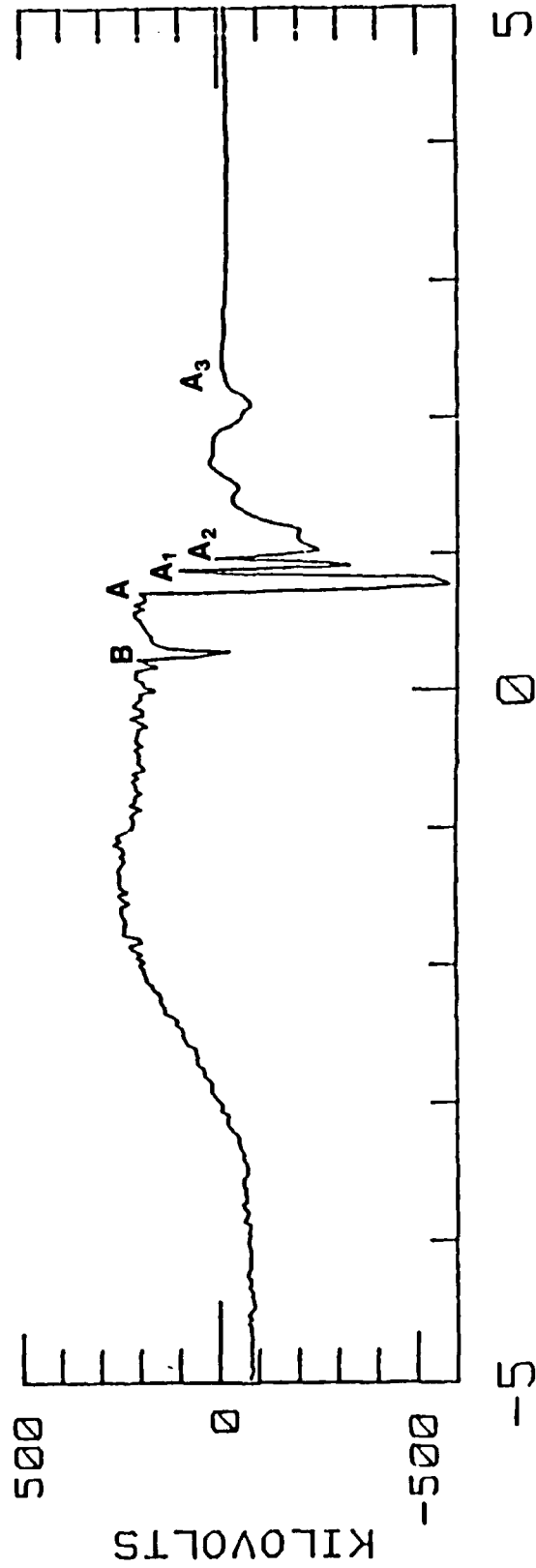
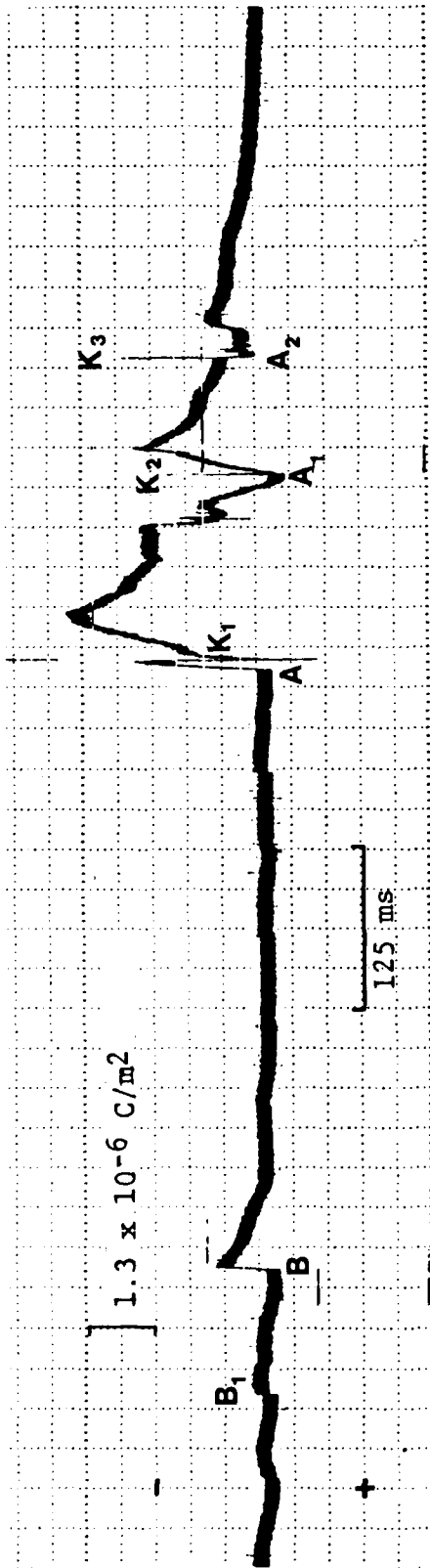


Figure 48. Comparison of the Electric Field Record From the Forward Fuselage Sensor With the Field Mill Record Showing Aircraft Potential for an Event Triggered by the Aircraft

aircraft surface measurements. As a result, only three complete sets of digital data were obtained during which induced transients were recorded. These data are shown in Table 17.

Most of the circuits experienced extremely low current levels, as illustrated by the signal on the right wing light circuit shown in Fig. 49. Only when a snap-on current probe was installed around a large wire bundle running under the forward section of the fuselage was a signal with significant amplitude and waveshape obtained. This signal, shown in Fig. 50, had a comparable rise time to that of the forward fuselage surface current, also shown. The current pulse causing this induced current reached 1099 A in 408 ns for a rate of rise of  $2.7 \times 10^9$  A/s. The resulting induced current level of 11 mA is still very small; however the cable bundle was not close to any apertures.

#### i. Rocket-Triggered Lightning

Another objective of the program was to fire a rocket from the ground station and trigger a cloud-to-ground lightning strike to the aircraft while it was flying above the station at a low altitude. This would result in simultaneous measurements on the ground and at the aircraft altitude. The resulting data could then be used to validate and refine existing models of current variation with altitude. To be successful, this experiment required that the thunderstorm environment over the ground station become favorable for triggering strikes with the rocket while the airplane was in the vicinity.

It was difficult to obtain weather conditions conducive to thunderstorms which would simultaneously allow the aircraft to fly close to the ground station at low altitude under visual flight rules. These conditions did exist, on two occasions of about 2 h each, and the aircraft was flown in a holding pattern above the ground station while ground station personnel waited for the ambient electric field conditions to be high enough for successful rocket-triggering of lightning. A total of five rockets were fired which successfully triggered lightning events, but never when the aircraft was in the correct position over the ground station. Thus, no rocket triggered lightning strikes to the aircraft were obtained.

TABLE 17. Induced Transients During Lightning Attachments in 1985

EVENT NUMBER	DATE	TYPE OF EVENT	CURRENT (mA)					
			POWER RECEPTACLE	UHF CABLE	RIGHT WING LIGHT	AFT RADIO	TACAN	WIRE BUNDLE
8	6/27	Return Stroke	0.255	0.229	0.269	0.370	0.965	11.4
10	6/29	Leader - Cloud-to-Ground Event	0.492	N	N/A	N/A	0.773	N/A
11	6/06	Collapsing Branch - Cloud-to-Ground Event	0.486	N/A	N/A	N/A	N/A	N/A

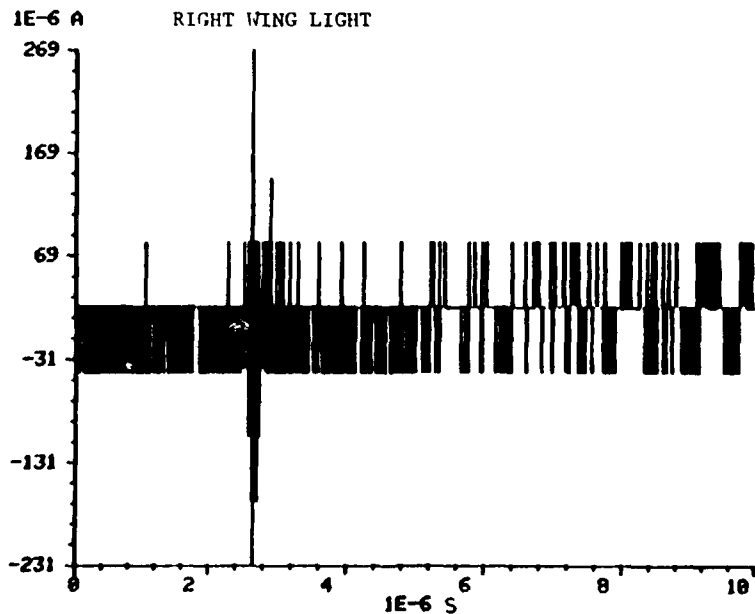


Figure 49. Example of Transient Signals Recorded on Interior Circuits During Lightning Attachments

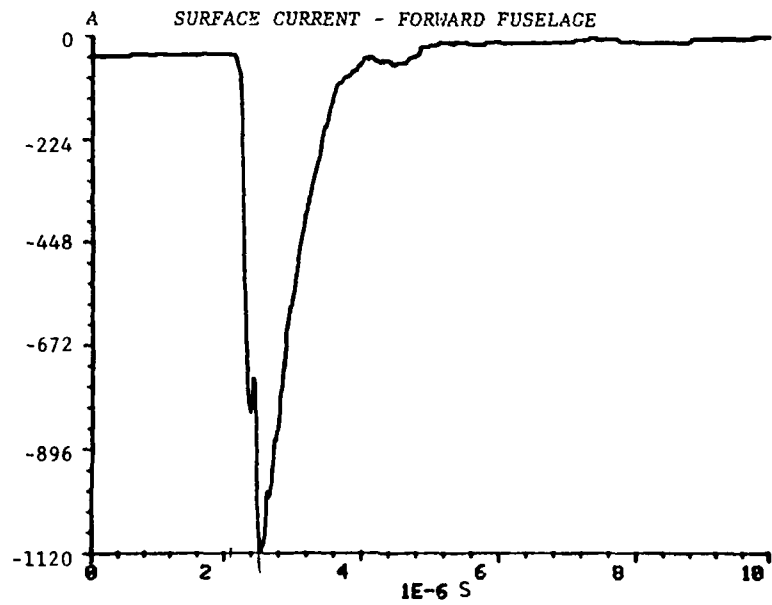
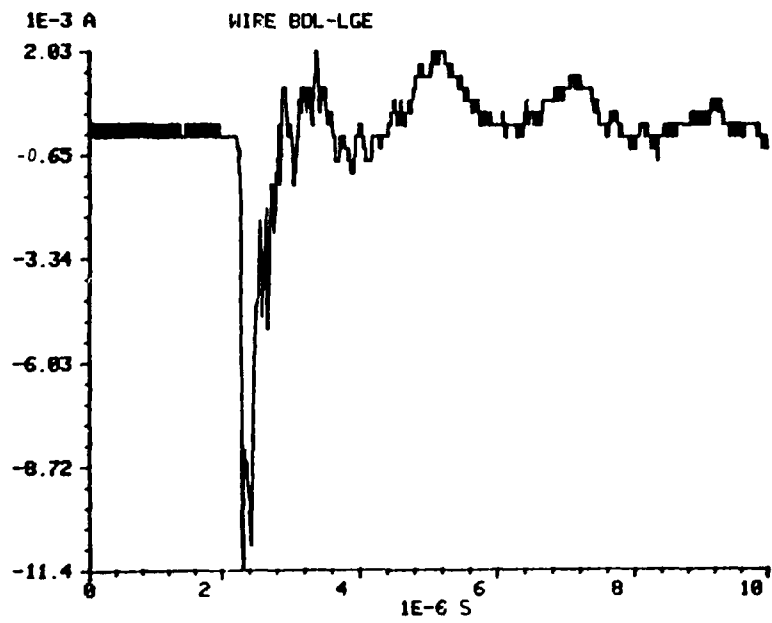


Figure 50. Induced Signal on Large Wire Bundle as Compared with Surface Current Recorded on the Forward Upper Fuselage

## 2. GROUND STATION FAR-FIELD MEASUREMENTS

The ground station was capable of making electromagnetic field measurements from nearby and distant cloud-to-ground lightning strikes. It successfully recorded events simultaneously with an attachment to the aircraft. One of these events was already briefly introduced in a previous section (Fig. 23). The difference in amplitude between the current measured on the aircraft and current calculated from the electric field measured during the first return stroke at the ground was part of the evidence for the aircraft being in a branch rather than the main channel during a cloud-to-ground discharge. The ground record clearly shows a series of stepped leaders preceding a classic first return stroke.

A similar situation occurred during an event on 29 June 1985. As reported in Reference 25, the aircraft instrumentation recorded a lightning attachment at 18:49:49.6 (Z). The aircraft was over the ocean near Melbourne, Florida at an altitude of 1800 ft. The location of the aircraft was 28:17:02 N, 79:57:07 W, placing it about 48 nm (nautical miles) or 90 km from the ground site. The outside air temperature was 20°C and the aircraft was in clouds, rain, and moderate turbulence.

Figure 51 shows a 164- $\mu$ s window of the electric field recorded at the ground station at 18:49:49. This was the only event recorded within several seconds of the time of the attachment to the aircraft.

The polarity of the field indicates that this flash lowered negative charge to ground (in this case, to sea). The measured electric field peak was 9 V/m. Since the actual distance to the flash was known (90 km), an estimate of the ground level return stroke current could be calculated. Dropping the retardation time term in equation 5 of Reference 31, we have

$$I = \frac{2\pi c R B}{\mu_0 V} \quad (7)$$

c = speed of light

B = magnetic flux density

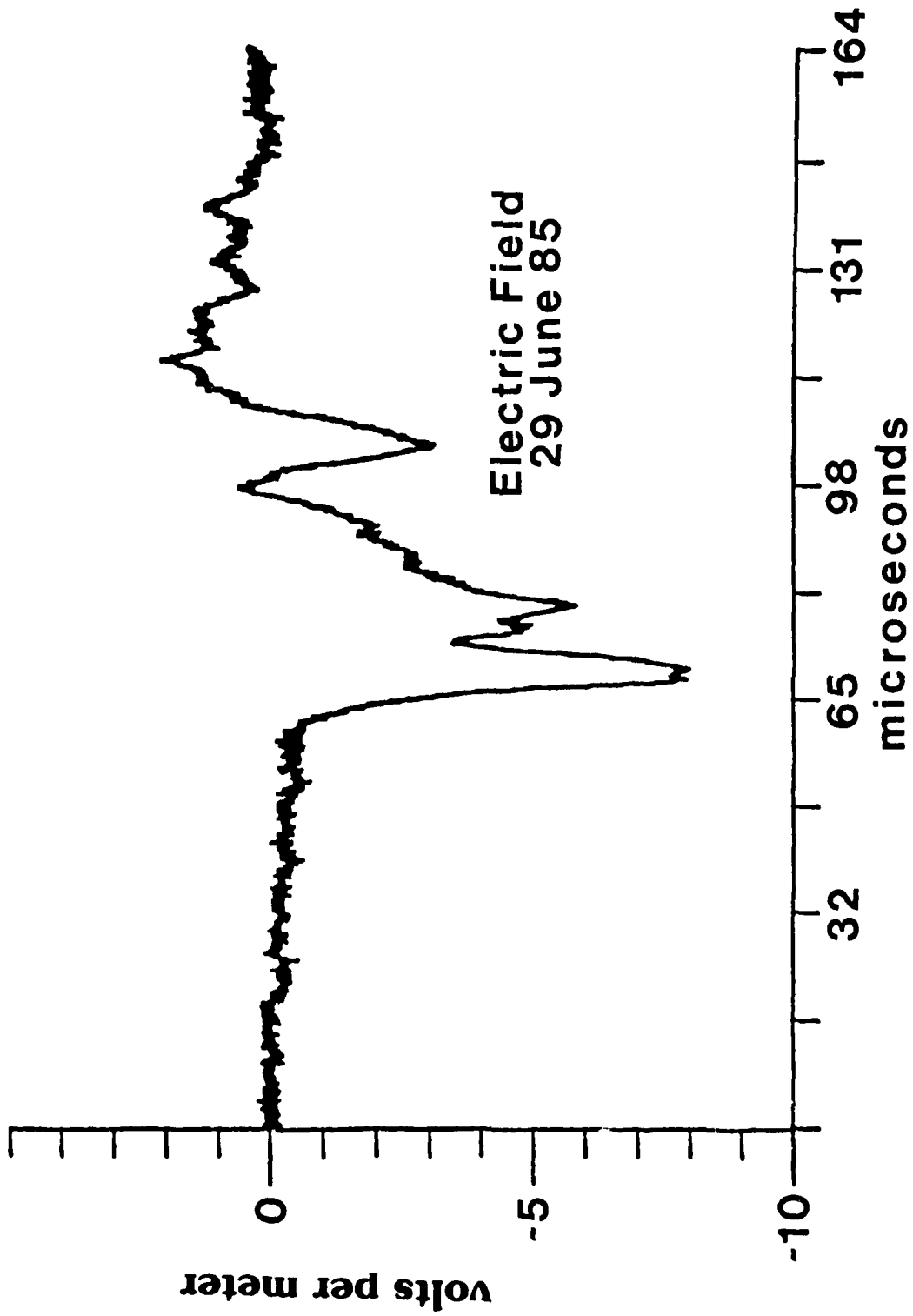


Figure 51. Electric Field Produced by a First Return Stroke Recorded at the Ground Station for an Event Where the Aircraft Was in a Branch of a Cloud-to-Ground Discharge

R = distance (in meters) from the flash  
 v = return stroke velocity (in meter per second)

From Reference 32, a nominal value of  $1.12 \times 10^8$  m/s is used for v. Because these were essentially far-field radiation fields at this distance, the approximation  $E/B = c$  can be used to rewrite this equation:

$$I = \frac{2\pi RE}{\mu_0 v} \quad (8)$$

With the measured value of  $E = 9$  V/m, equation 8 provided a peak current of 33.75 kA at sea level. Assuming an exponential decay of current with height, z, of form

$$I(z) = I(s) \exp(-z/n) \quad (9)$$

with  $n = 2 \times 10^3$  m (Reference 31), the current in the main channel at an altitude of 1800 ft should be 25.6 kA.

Although analog data was not recorded during this event, the electric field was recorded on the aircraft strip chart at 18:49:49. It indicates that the event was very short, but the data was saturated and an actual amplitude could not be obtained. The digital data recorded at the time of the flash, shown in Fig. 52, indicates that a current of 2.8 kA flowed into the right-wing boom sensor and a current of about 1.5 kA flowed out through the tail boom. Expansions of these waveforms showed the delay between the times when the current pulse reached the two sensors, confirming the direction of current flow from right wing to tail. The outputs from the two surface current sensors are also shown in Fig. 52. They show currents of 1.4 kA on the right wing and 0.8 kA on the aft fuselage. The polarities of all the sensor outputs are consistent with negative charge flow onto the aircraft (Reference 28).

The much higher level of current measured at the ground during the first return stroke indicates that, as in the event on 6 July 1985, the aircraft was in a branch rather than the main channel. This explains the short length of the electric field record on the aircraft since the aircraft would not see field changes once the branch collapsed. Since the data showed negative charge flow onto the aircraft, in

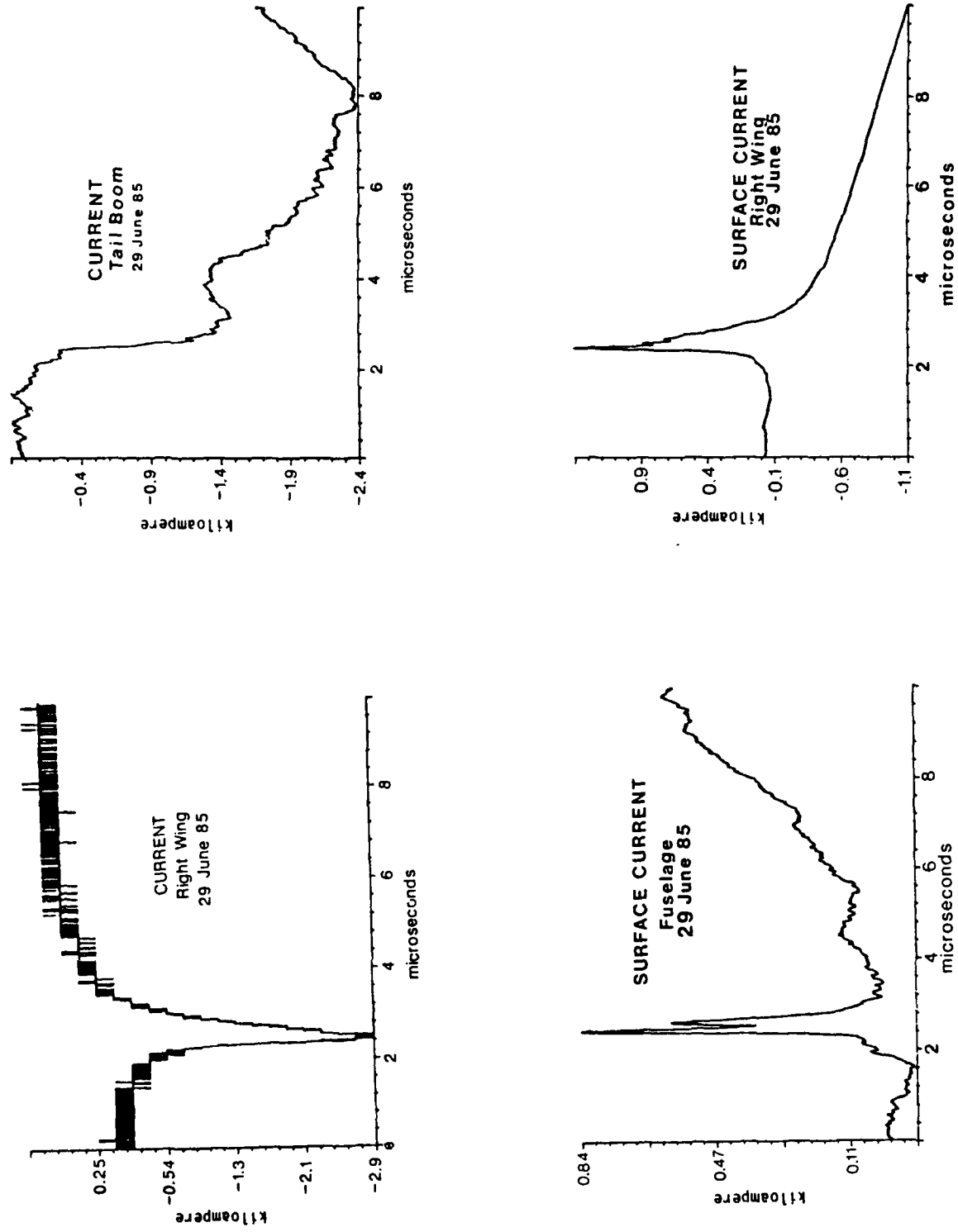


Figure 52. Digital Data Recorded on the Aircraft at the Time of the Cloud-to-Ground Event Shown in Figure 51.

this case, the trigger must have occurred as a leader attached. The digital data set was incomplete, so current levels from the left wing sensors are not available for this event. The video cameras, however, showed streamers at both wingtips.

The aircraft data is consistent with negative charge movement onto the aircraft, as would be expected during a negative cloud-to-ground flash. Current levels apparently ranged from 1.5 to 3 kA at the time of the attachment.

Another example of simultaneous airborne and ground data was the aircraft-triggered intracloud flash, part of which was already shown in Fig. 30. The entire flash, as recorded in both locations (100 km apart), is shown in Fig. 53. Inspection of the electric field waveform on the ground shows that the two prominent negative excursions at the end of the event ( $R_1$  and  $R_2$ ) are a first and subsequent return stroke, indicating an intracloud event which became cloud to ground.

Electric fields from the first and subsequent return strokes are shown in Fig. 54. The first return stroke is extremely large, scaling out to 133 kA. The subsequent stroke scales out to 40 kA. No current is on the aircraft at the time of the subsequent stroke. This is to be expected since the aircraft was no longer involved in the discharge, as discussed further in Section IV.

### 3. SCALE MODEL STUDIES

To attain some of the objectives of the program, we needed to measure some characteristics of the lightning channel prior to attachment to the aircraft. To make this measurement, a magnetic field sensor was selected, but a suitable location on the aircraft had to be determined to avoid field distortion and measurement inaccuracy caused by the geometry of the aircraft. The aircraft would produce scattering within the bandwidth of interest if a suitable location was not selected. Theoretical considerations suggested that the best location would be in the plane of symmetry either fore or aft of the aircraft and near the axis of the fuselage. Thus, scale model tests were conducted to determine a suitable sensor location (Reference 33). At the University of Michigan Radiation Laboratory facility described in Reference 34, a 1:74-scale model of the CV-580 was used to determine the error at positions 1 to 9 in the plane of symmetry, shown in Fig. 55. Analysis

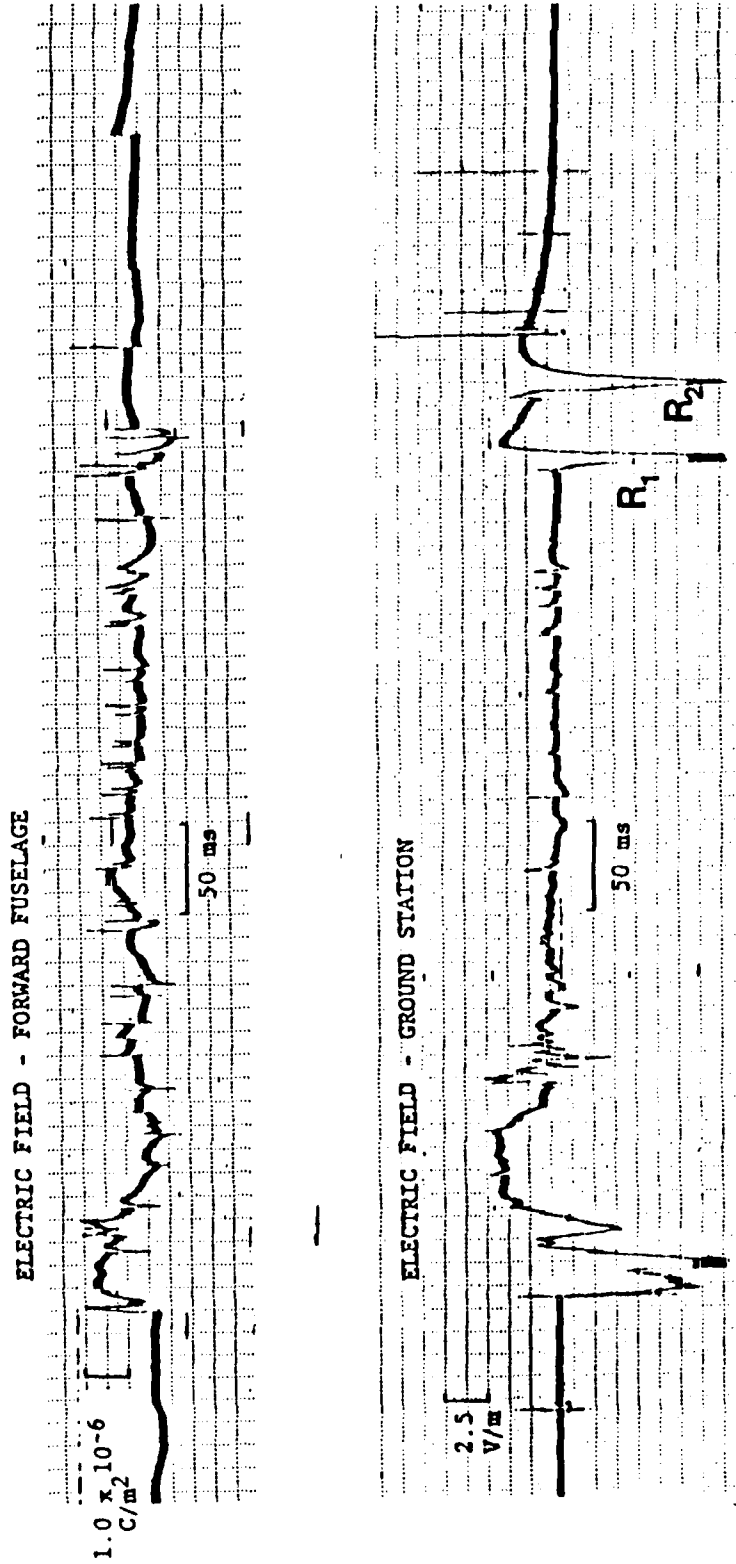


Figure 53. Simultaneous Recordings of the Electric Field on the Aircraft and at the Ground Station During an Event Triggered by the Aircraft

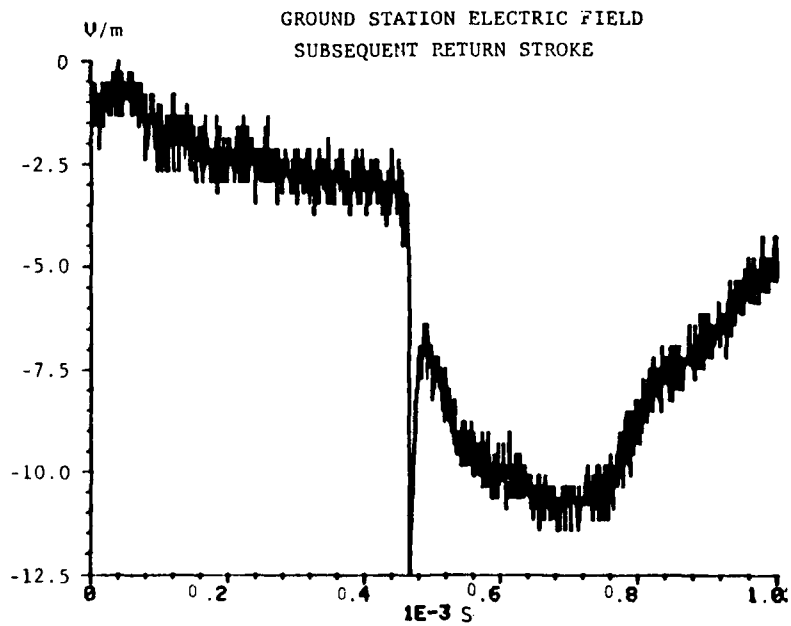
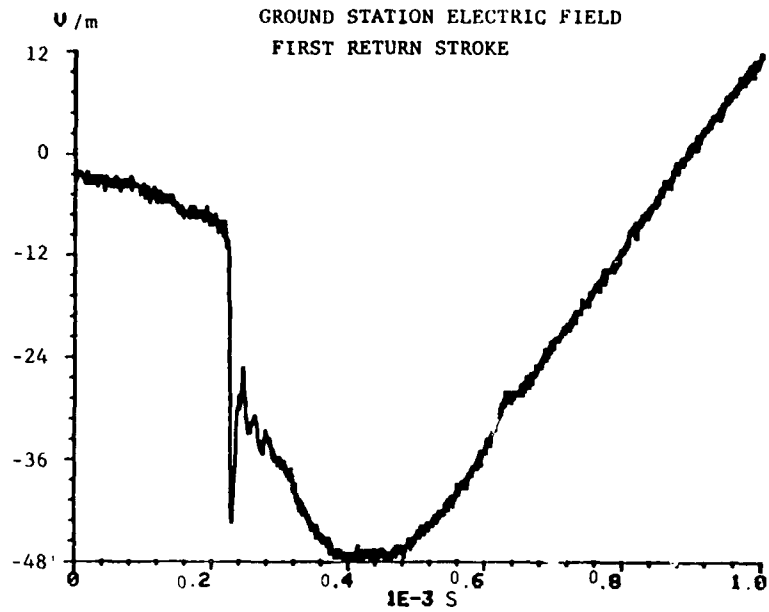


Figure 54. First and Subsequent Return Strokes Recorded at the Ground Station at the End of an Intracloud Event Triggered by the Aircraft.

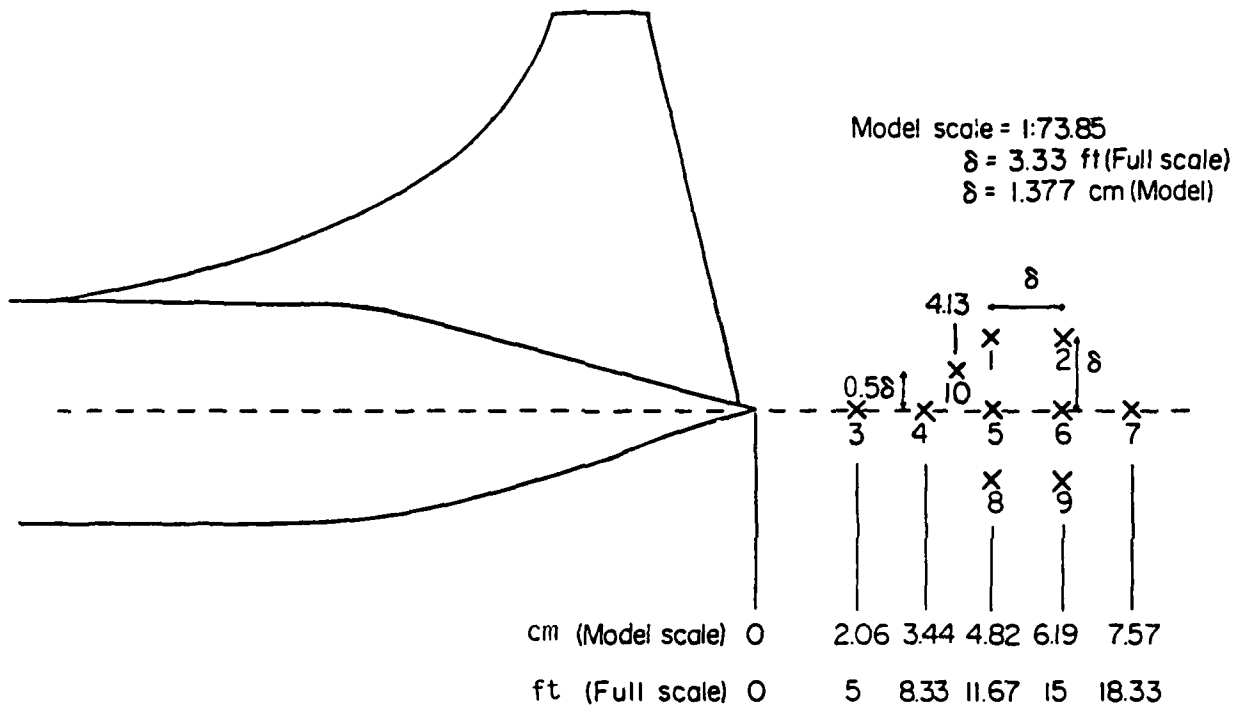


Figure 55. Scale Model Study Measurement Locations (Not to Scale)

of the results at these points revealed that a "quieter" position may exist between some of the original nine points. This resulted in additional measurements at point 10 in Fig. 55. This position corresponded roughly to a plane defined by the axis of the wings and horizontal tail. Figure 56 compares the results of measurements at points 1, 4 and 10 of Fig. 55 and illustrates the reason for selecting position 10 for the sensor.

Since the overall intent of the program included comparing responses to both lightning and EMP threats, the scale model tests were expanded to include measurements at the various electromagnetic sensor locations. These measurements were made at the University of Michigan Radiation Laboratory to develop transfer functions at these locations (Reference 35). The transfer functions were then used to predict aircraft responses, at these same locations, from standard lightning and EMP threats (Reference 36). These data might then be used for comparison with simulated ground test data and actual in-flight measurements. Figure 57, which is taken from Reference 35, shows the response at the bottom of the left wing with the electric field perpendicular to the fuselage. Table 18 summarizes the aircraft sensor locations and the excitation description for each location. The responses that were measured at these locations are documented in Reference 35.

The Dikewood Division of Kaman Sciences, Corp. used the data from Reference 35 and calculated predicted responses at each of the sensor locations, for the given excitation orientations, to an NCGS-84-1 Criteria High-Altitude EMP threat and also to typical reciprocal double exponential waveforms (Reference 36). Figure 58 is the predicted response to the reciprocal double exponential waveform at the same location of Fig. 57.

Figure 59 shows a typical reciprocal double exponential waveform used to predict aircraft responses and a representative excitation received during simulated NEMP tests. The reciprocal double exponential input assumed a 60-kV/m peak field strength with a 5-ns time constant and a 250-ns decay time to 50 percent of peak value. Typical simulated NEMP excitations had comparable peak magnitudes with 7 to 8-ns rise and decay times. Extrapolated scale model and measured responses for the forward fuselage surface current sensor are shown in Fig. 60. In this case, the applied field was oriented in a direction parallel to the aircraft fuselage. Figure

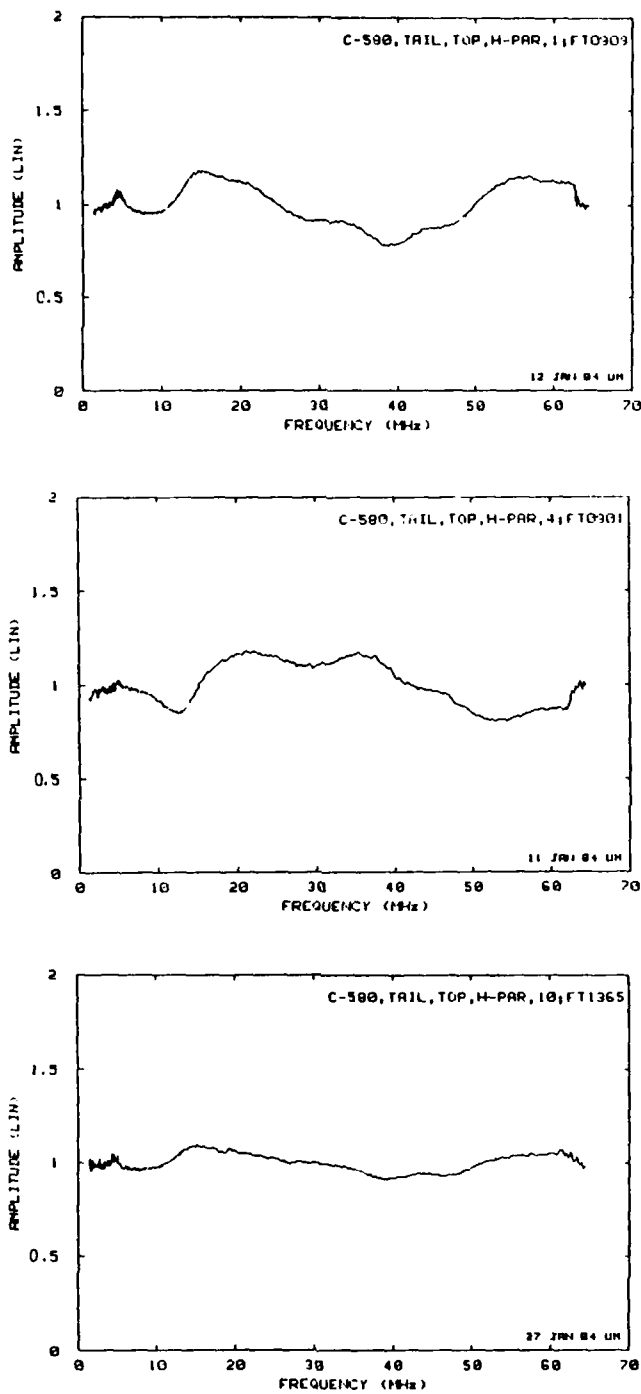


Figure 56. Comparison of Scale Model Measurements at Three Positions in the Plane of Symmetry Aft of the Aircraft

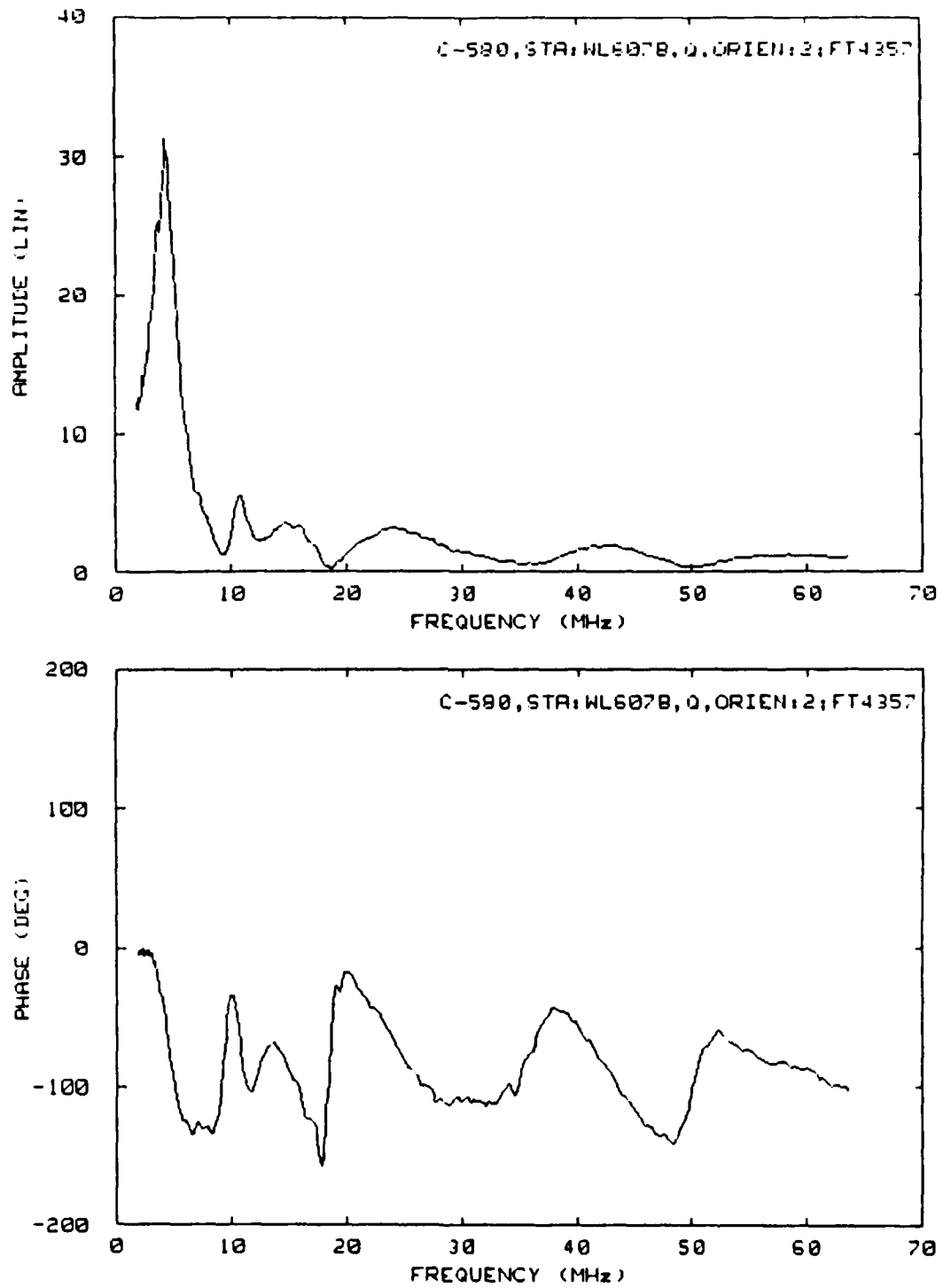


Figure 57. Typical CV-580 Response (Taken From Reference 35)

TABLE 18. CV-580 Measurement Stations and Excitation Description

NO.	STATION	MEASUREMENT	SENSOR LOCATION	EXCITATION DESCRIPTION
1	WL9SB	J <sub>a</sub>	Left wing, bottom, W9B, F357 (approx.)	Top incidence, E parallel to fuselage; E direction from tail to nose
2	WL607B	E <sub>n</sub>	Left wing, bottom, center wing, W607, F405 (approx.)	Top incidence, E perpendicular to fuselage; E direction from right-to-left wing
3	WL75T	J <sub>a</sub>	Left wing, top, W75, F384 (approx.)	Nose-on incidence, E vertical
4	WR75T	E <sub>n</sub>	Right wing, top, W75 F384 (approx.)	Left-side incidence, E vertical
5	F264.5T	J <sub>a</sub>	Fuselage centerline, top, F264.5	Left-side incidence, 30° below, E vertical
6	F455.5T	J <sub>a</sub>	Fuselage centerline, top, F455.5	Nose-on incidence, 30° below, E vertical
7	F185T	E <sub>n</sub>	Fuselage centerline, top, F185	Tail-on incidence, 30° below, E vertical
8	VS185L	E <sub>n</sub>	Vertical Stabilizer, left, VS185, F854 (approx.)	Bottom incidence, E perpendicular to fuselage; E direction from right-to-left wing
9	WR607B	E <sub>n</sub>	Right wing, bottom, center wing, W607, F405 (approx.)	Bottom incidence, E parallel to fuselage; E direction from tail to nose

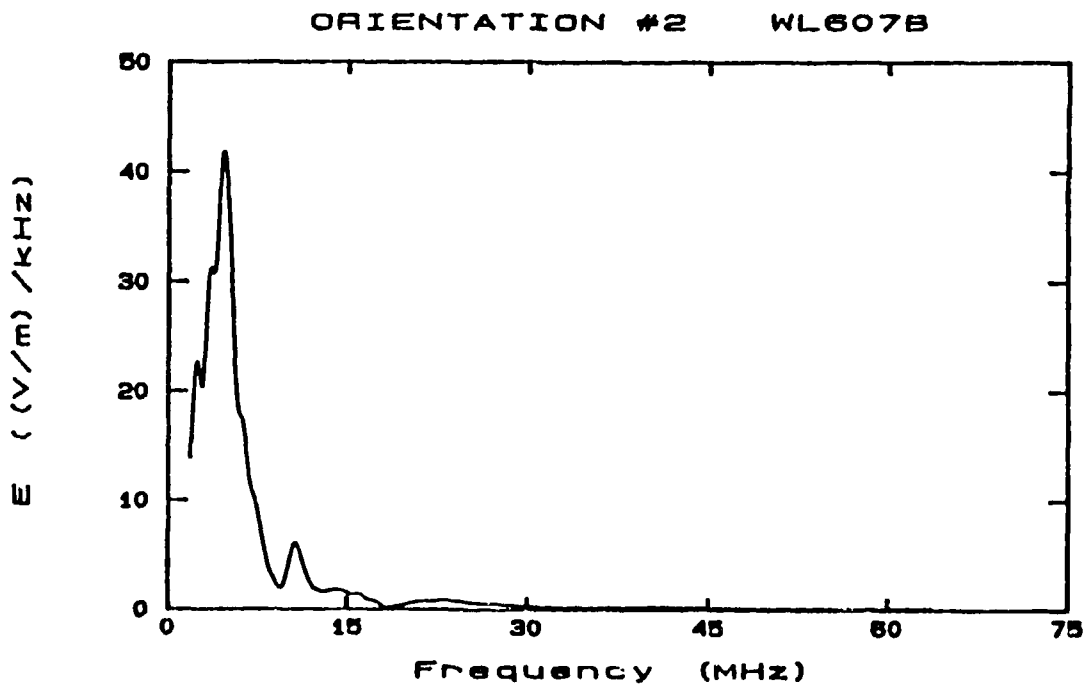
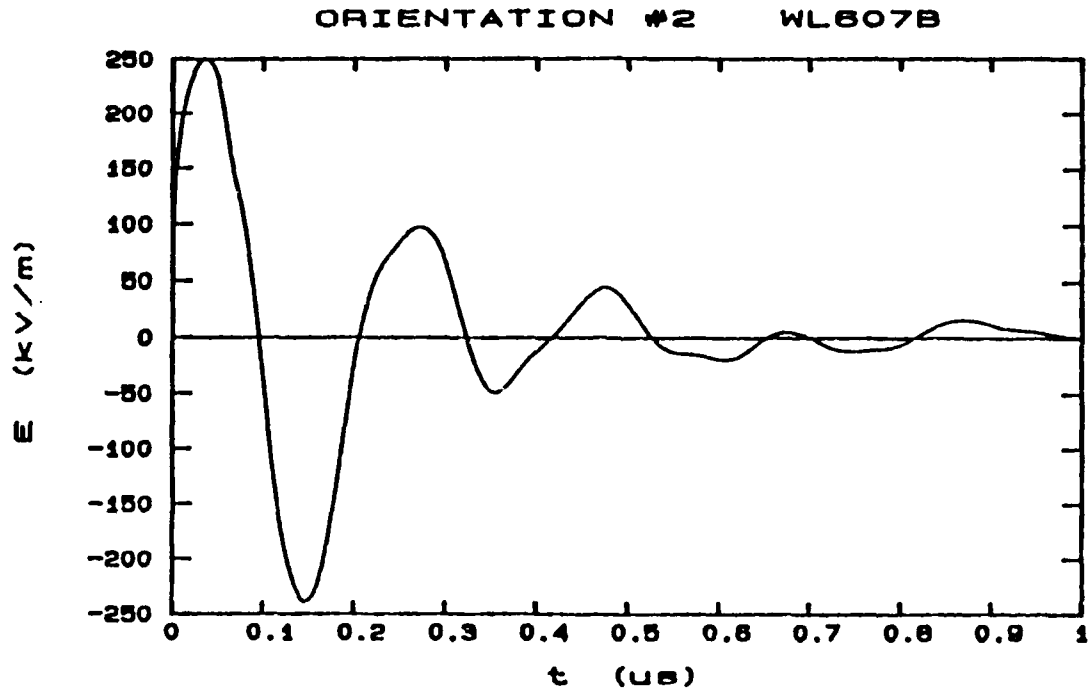


Figure 58. Predicted Response to the Reciprocal Double Exponential Waveform for the Sensor Location of Figure 57

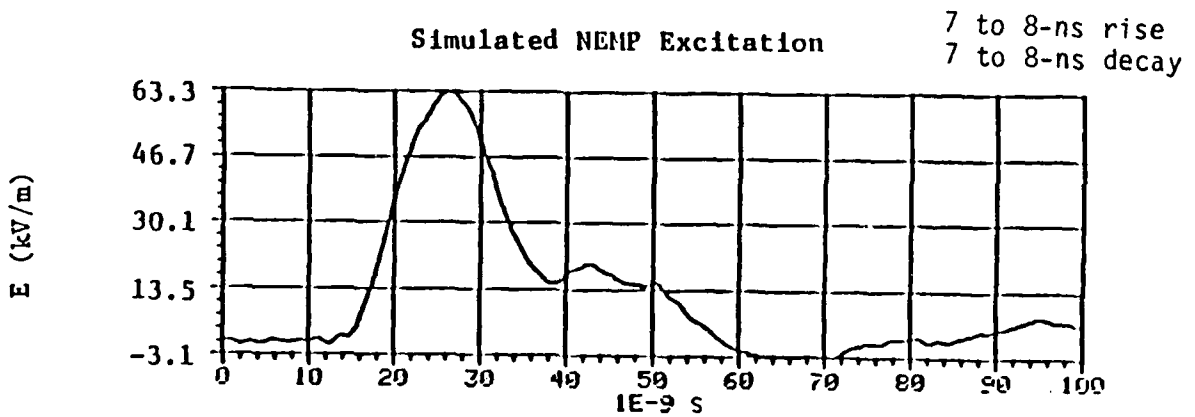
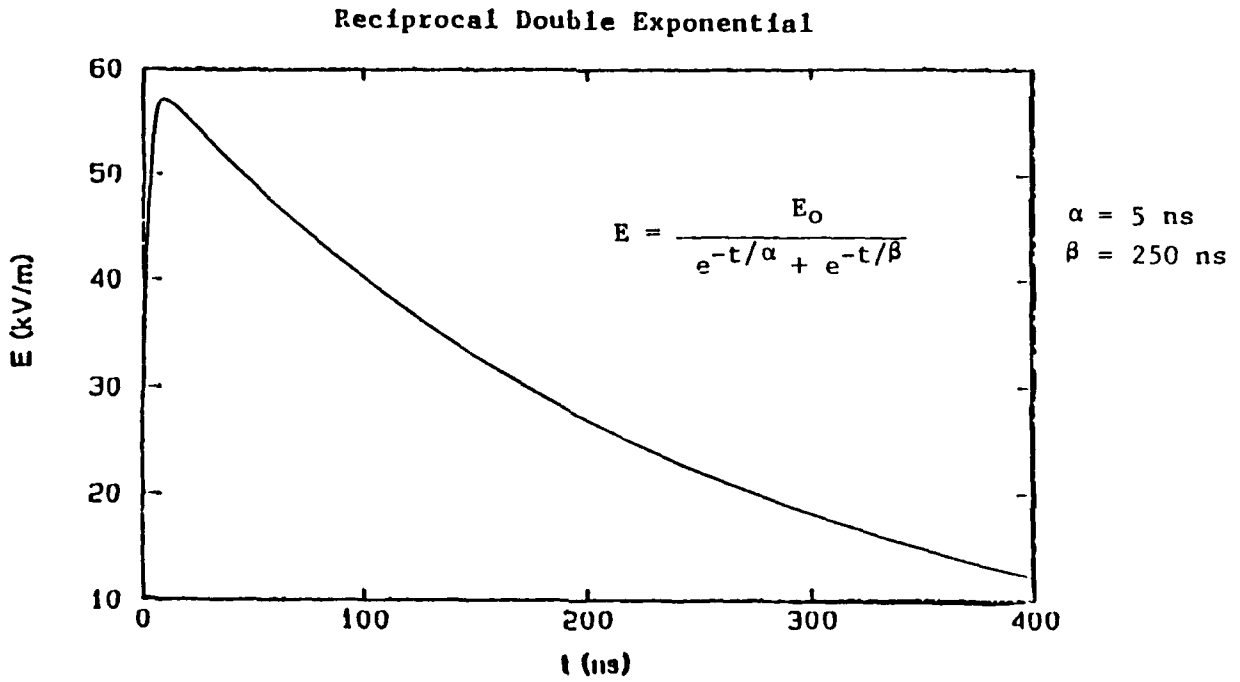
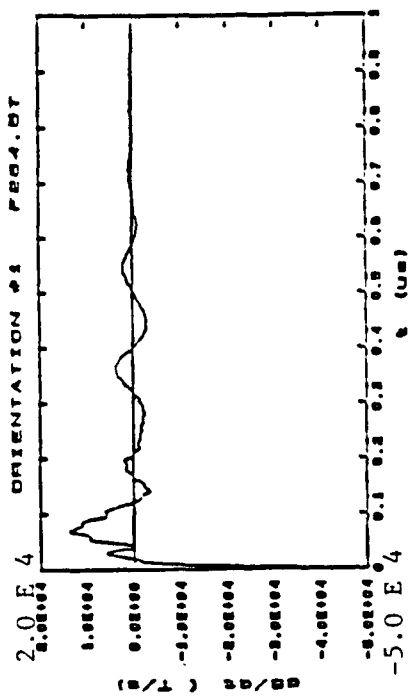
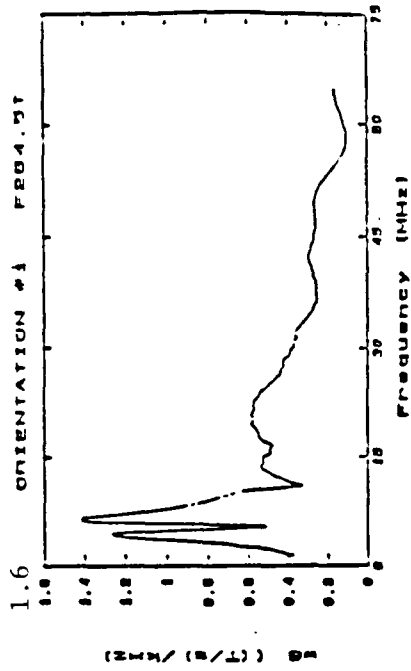


Figure 59. Reciprocal Double Exponential and Simulated NEMP Input Waveforms



Measured Response

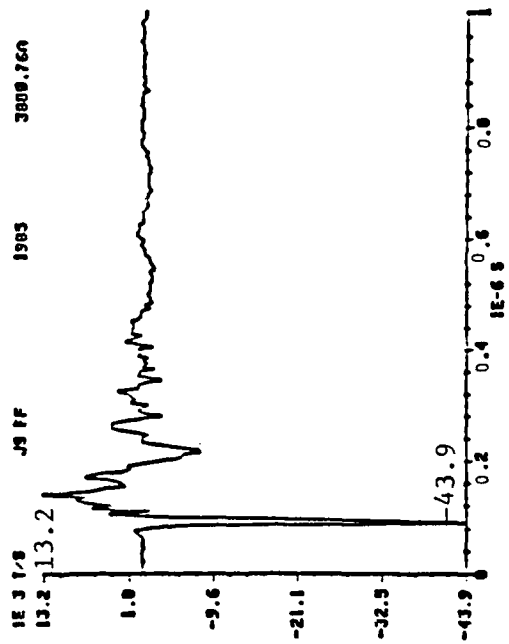
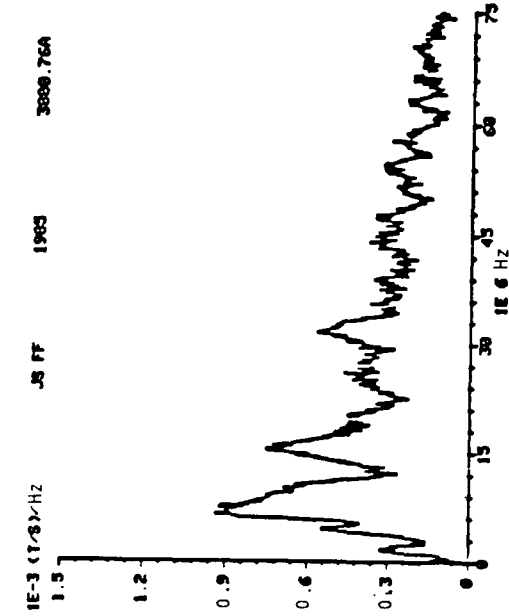


Figure 60. Extrapolated Scale Model and Measured Responses of Surface Current Sensor on the Forward Fuselage - Parallel Configuration

61 gives the responses of the left-wing electric field sensor to a field applied in a direction perpendicular to the aircraft fuselage. In both cases, the extrapolated and measured responses display similar characteristics and aircraft resonances.

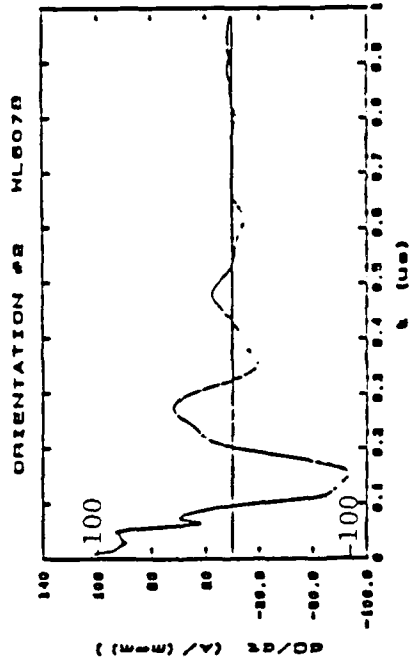
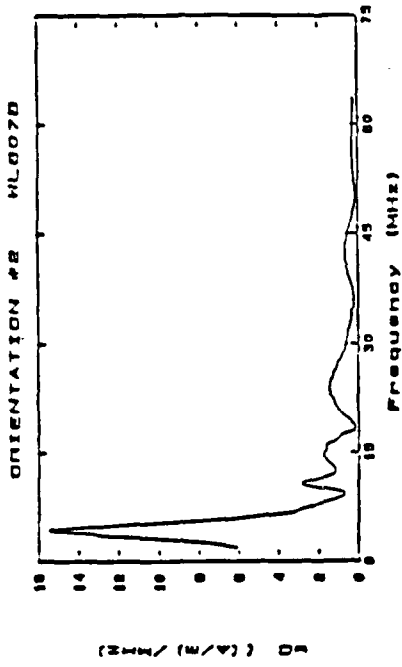
Comparison of nearby lightning measurements to the data derived from the scale model testing and the reciprocal double exponential waveforms is not practical for a number of reasons. The instrumentation on the aircraft was setup for measurement of lightning parameters during a direct strike, not nearby lightning. Although the electromagnetic sensors will respond to nearby lightning radiated fields, without knowing the orientation of the lightning channel, we cannot possibly know the orientation of the fields exciting the sensors. This would require orthogonal free field measurements. A second reason is that the lightning event itself must be representative of the reciprocal double exponential used for comparison. No such events were recorded with the digital wideband system. Thus, the only meaningful comparisons that can be made are between the simulated EMP measurements and the corresponding reciprocal double exponential predicted responses.

#### 4. GROUND SIMULATION TESTS

##### a. Lightning

Figure 62 shows the surface currents on the aircraft due to the unipolar output of a 4  $\mu$ F, 200-kV generator used with a wire mesh return path for the ground tests in June 1984. The applied unipolar current pulse simulated the lightning return stroke current as it flowed on the aircraft. The slow rise time of the applied waveform, 14  $\mu$ s, was not adequate to verify the complete response of the aircraft, but was suitable for noise testing, trigger level determination, and operator training.

Figure 63 shows the surface currents due to a unipolar current pulse from a fast submicrosecond current generator with a quasi-coaxial return path. A 13-kA peak current pulse was applied nose to tail and produced a calculated current of 12 kA at the forward fuselage and 11.1 kA at the aft fuselage, based on multiplying the surface current by the fuselage circumference (9.3 m) and assuming uniform current distribution. The uniform current distribution assumption is considered valid with the quasi-coaxial return path configuration. This configuration also produced some



Measured Response

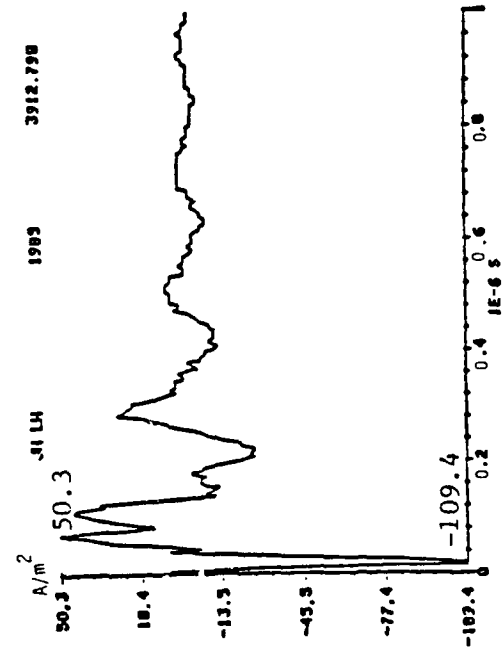
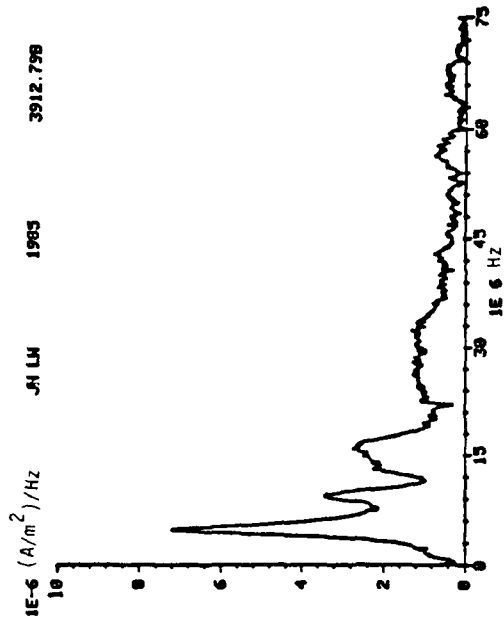


Figure 61. Extrapolated Scale Model and Measured Responses of Left-Wing Electric Field Sensor - Perpendicular Configuration

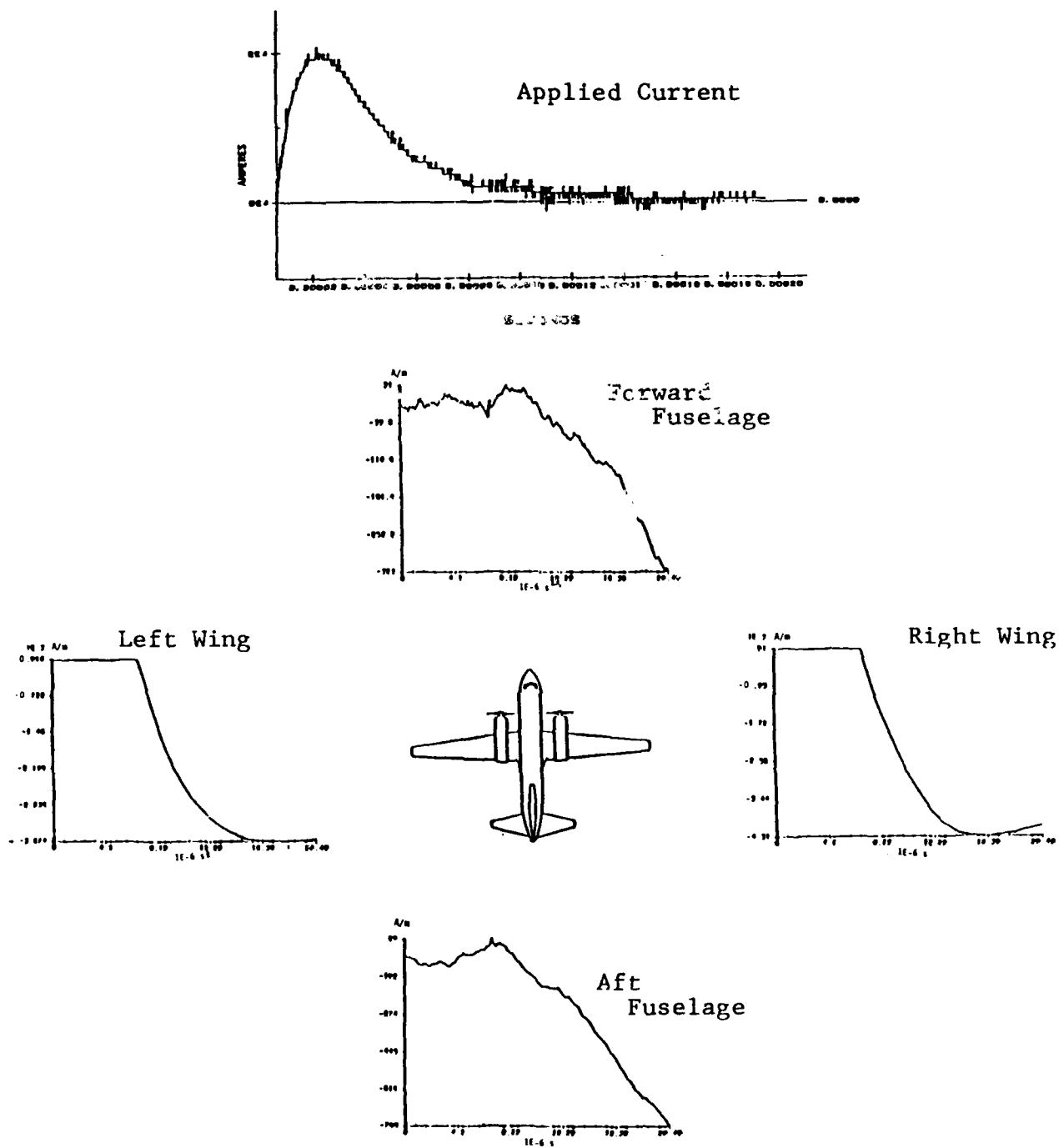


Figure 62. Response of the Surface Current Sensors to a Unipolar Current From the 4 μf, 200-kV Generator Applied to the Left Wing of the Aircraft

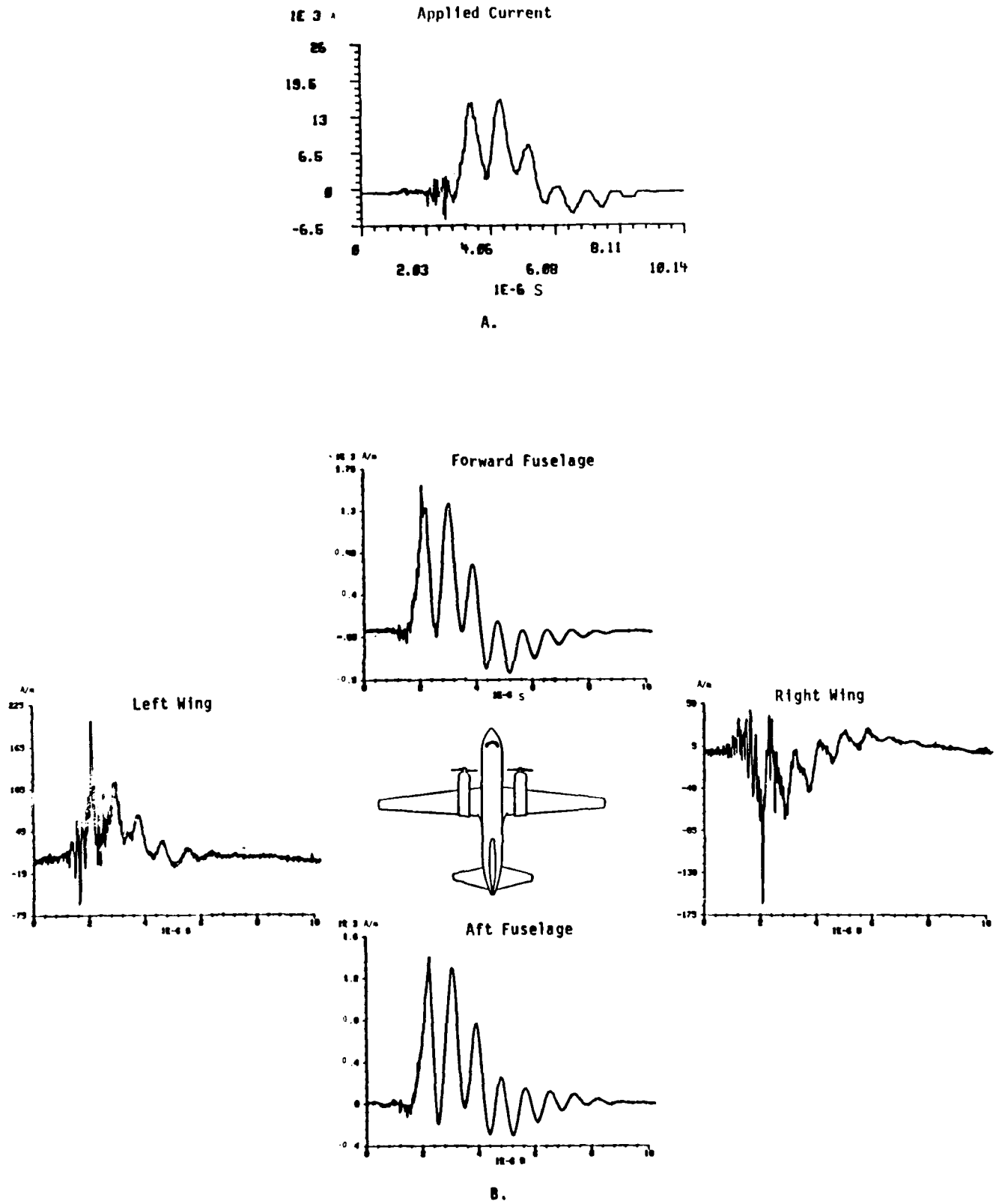


Figure 63. Response of the Surface Current Sensors to a Unipolar Current From the Fast Rise Time Generator Applied to the Nose of the Aircraft.

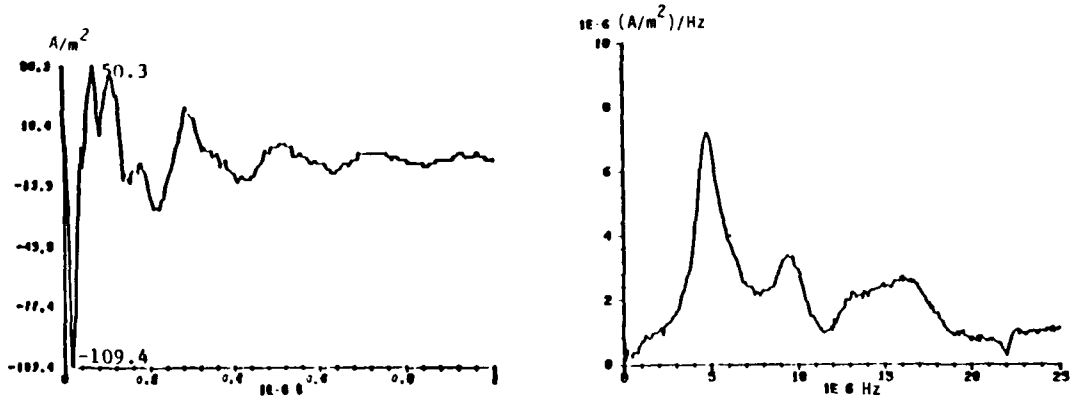
current flow to the wings, an effect which is also seen in the airborne data (see Table 11) for nose-to-tail attachments.

An extensive discussion of the time and frequency domain techniques developed for processing the ground simulation data is reported in Reference 37. A preliminary analysis using these techniques showed that the choice of lightning generators and return path configurations had a pronounced effect on the current levels and distributions experienced on the aircraft. The transfer functions from each configuration showed that the fast rise time generator and quasi-coaxial return path provided the best simulation of the airborne event.

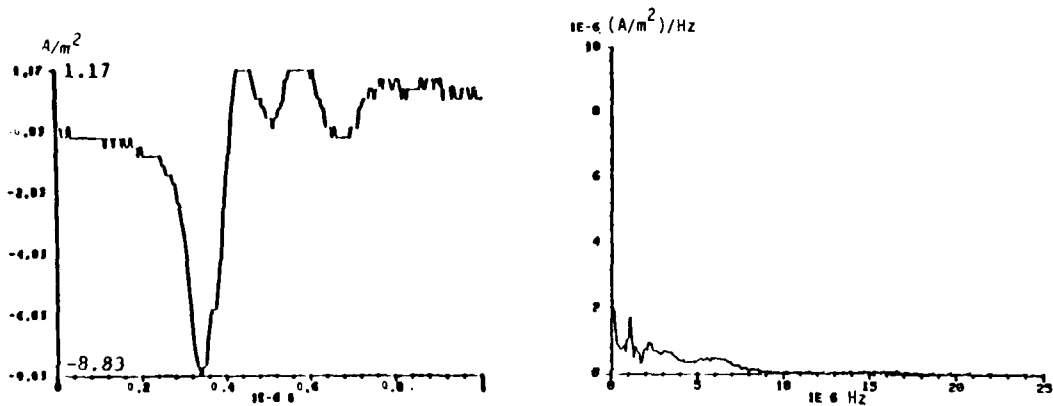
#### b. Simulated Nuclear Electromagnetic Pulse

In Reference 38, two lightning attachments recorded in 1984 were compared with simulated NEMP test measurements where current propagation along the aircraft in those events most closely matched the two NEMP configurations. Subsequent improvements in our ability to analyze the data have confirmed that neither of these events involved a cloud-to-ground return stroke in which the aircraft was part of the channel. One direct comparison that can be made between the two types of data is between the displacement currents induced by the electric field change. Figure 64 shows a comparison of the time and frequency domain responses of the left wing displacement current sensor due to lightning and NEMP for the wing-to-wing/perpendicular configuration. The Fig. 64b airborne data is believed to be due to an initial interaction between the aircraft and a positive charge center and therefore is only a low level lightning-related event which is not representative of a return stroke. Figure 64c is the response at the left wing displacement current sensor due to a return stroke which attached to the tail boom and exited through the left wing at 14,000 ft. The displacement current amplitude is much lower for the lightning event (than in the simulated NEMP case) due, in part, to the slower rate of change of electric field. The induced displacement currents were not sufficient to excite the aircraft resonances.

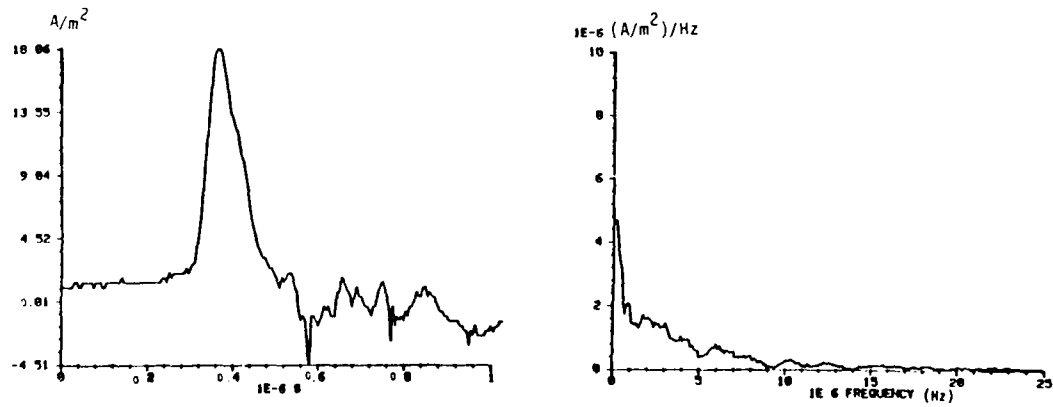
Figure 65 shows three sets of waveforms at the aft fuselage surface current sensor; one produced by simulated NEMP (65a), the second (65b) by the attachment of a stepped leader to the nose at low altitude (4500 ft), and the third (65c) by the attachment of a return stroke to the tail at high altitude (14,000 ft). Comparison



a. Simulated NEMP Response

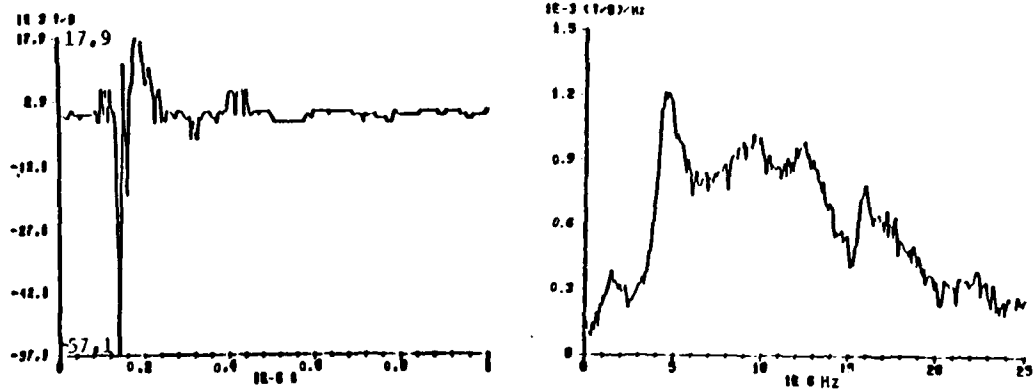


b. Response to Lightning Attachment to Wing — Initial Attachment Process

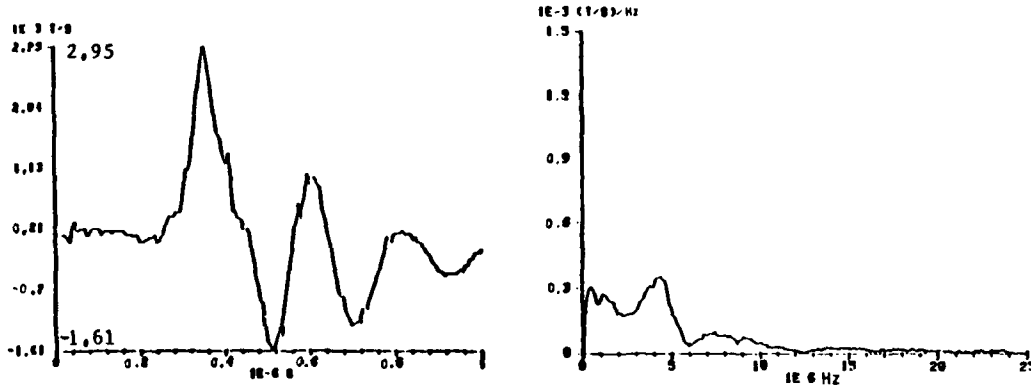


c. Response to Lightning Attachment to Wing — Cloud-to-Ground Return Stroke

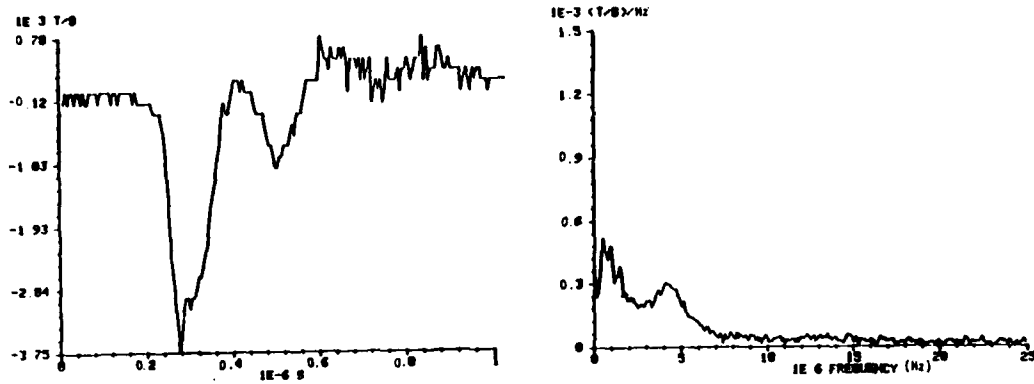
Figure 64. Time and Frequency Domain Responses of the Left Wing Displacement Current Sensor to Simulated NEMP, an Initial Attachment Pulse and a Return Stroke at Altitude



a. Simulated NEMP Response



b. Response to Lightning Attachment to Nose — Stepped Leader



c. Response to Lightning Attachment to Tail — Cloud-to-Ground Return Stroke

Figure 65. Time and Frequency Domain Responses of the Aft Fuselage Surface Current Sensor to Simulated NEMP, a Stepped Leader and a Return Stroke at Altitude

of surface current data is complicated by the fact that the NEMP response of the aircraft is due to rate of change of the radiated magnetic field, while the lightning event response is due to conducted current on the aircraft. The comparison is further complicated by the low amplitude of the lightning event. However, the surface current frequency domain data, even at this low level, shows excitation of the aircraft resonance. If the frequency domain data were to be scaled (assuming linearity) to an average lightning threat level, the amplitudes at the aircraft resonances would be higher at low frequencies than for the NEMP threat used.

#### 5. CV-580/F-106 JOINT MISSIONS

The CV-580 was flown with the NASA F-106 aircraft in an attempt to get simultaneous data of the same event (Reference 39). The intent was to compare strike probabilities at different altitudes in the same storm and to measure electromagnetic fields and currents from the same lightning event on two different airplanes.

The aircraft are substantially different in physical configuration and performance since the F-106 is a fighter and the CV-580 a commercial transport. Because of lower gust limits and susceptibility to radome damage in heavy precipitation, the CV-580 was unable to penetrate areas with a radar reflectivity greater than 40 dBZ while the F-106 could penetrate areas with reflectivities up to 50 dBZ. Penetration speed for the CV-580 was 185 knots compared to 300 knots for the F-106. Time on station also varied significantly: 45 min for the F-106 vs 120 min for the CV-580.

The performance factors combined with the need to coordinate with Air Traffic Control, differences in storm environments between the penetration altitudes for each aircraft and real and apparent differences in the appearance of the storm on the various radar displays made it very difficult to place both aircraft safely in a thunderstorm at the same time. The two aircraft were able to record six strikes during joint operations but none of these strikes were correlated with an event on the other plane. Reference 39 concludes that "coordinated thunderstorm research operations of two airplanes with significantly different penetration capabilities were counterproductive to both airplanes in terms of gathering electromagnetic data while maintaining range safety."

## SECTION IV DISCUSSION OF RESULTS

### 1. GENERAL

The lightning data reported here represent a significant increase in the data base available for characterization of lightning attachments to aircraft. The analyses performed represent a first step in describing the aircraft/ lightning interaction using real data. These analyses will be discussed in more detail in this section.

Although the data represent the most comprehensive set of airborne strike data to aircraft available to date, several desirable improvements have been identified and should be incorporated into future lightning characterization programs. These areas are also discussed in this section, as are gaps in the data base and alternatives available to eliminate them. These suggestions should be carefully considered before other programs are implemented, particularly because of the *inherent hazard that exists in airborne lightning characterization measurements of direct strikes to aircraft.*

### 2. AIRBORNE DIRECT STRIKES

As a result of this program, we find it now possible to measure electromagnetic field and current responses of an aircraft and determine whether the strike was triggered or intercepted. For intercepted strikes, these responses show whether the strike was positive or negative and if the aircraft was in a branch or in the main channel of the event.

#### a. Intercepted Strikes

Intercepted strikes are easily identified by the characteristic hooked shape of the electric field produced by the leader as it approaches the aircraft (Reference 9). In the case of a negative cloud-to-ground or intracloud event, the hook indicates positive charge increasing at the sensor, followed by a sharp

negative increase in charge on the aircraft at attachment. The opposite is true for a positive intracloud or cloud-to-ground event.

An aircraft in a branch of a cloud-to-ground event records the initial attachment of a leader followed by the opposite field and current indications when the branch collapses. It does not experience any cloud-to-ground return strokes since it is not in the main channel. An aircraft in the main channel does experience these return strokes, with their magnitude and rise time depending on the altitude when struck.

In 2 yr and approximately 100 h of thunderstorm flying, the CV-580 recorded only three positive and six negative intercepted strikes. All three positive strikes occurred in the same storm in 1984 at altitudes above 14,000 ft. Of the six negative events, four occurred at low altitude, two in 1984 and two in 1985. In all four of these cases, the aircraft was in a branch of the event, not the main channel. The other two negative intercepts occurred above 14,000 ft. In one case, the aircraft was in the main channel of a cloud-to-ground event. This appears to be true of the second event also, but not enough evidence is available to be sure.

Obviously, the data base for intercepted strikes is very small. These events occur infrequently as compared to triggered strikes, in spite of flying in very close proximity to thunderstorms at a variety of altitudes for extended lengths of time. In 20 h of flying below 4,000 ft, the CV-580 did not intercept the main channel of a cloud-to-ground strike at low altitude, which should produce the most severe return stroke current threat level. This suggests that few aircraft are subjected to this threat level. We must note, however, that the CV-580 experience is limited to central Florida summer thunderstorms and that flying in different areas, types of storms, etc., may produce different results.

The one (possibly two) occasions where the aircraft was in a cloud-to-ground event and in the main channel occurred above 14,000 ft. Perhaps this is because the main channel has not yet begun to branch at these high altitudes while at low altitudes it has developed many branches. Whatever the reason, both peak current levels and their rise times are reduced at high altitudes as compared to a strike at ground level. Measurements show that the aircraft is not subjected to anything close to the full level threat at these high altitudes.

b. Triggered Strikes

One of the most important results of this program is the information it provides on the mechanism by which an aircraft triggers a lightning strike. Much of this information was presented in the previous section. In this section, the relevant data are reviewed and discussed in more detail. A likely triggering mechanism is postulated and evidence is offered.

The first item for discussion is the quasi-static electric field record shown in Fig. 47. The record shows that the aircraft potential exhibited intermittent, small, negative excursions 2 s before the strike, which can be attributed to triboelectric charging. This is a phenomenon in which precipitation particles strike the aircraft, acquire a charge and leave an opposite charge on the aircraft (Reference 40). The charge deposited is almost always negative, as determined by many investigators, who also show that the charge magnitude is a function of particle type, particle size and work function of the metal (Reference 41). We well know that pilots often report radio interference and St. Elmo's Fire several seconds before a lightning strike, and that these phenomena are the result of triboelectric charging.

Point B in Fig. 48, marks a pronounced negative increase in aircraft potential on the field mill record and in the electric field record from the forward upper fuselage sensor. This increase is believed to be due to the sudden approach of a positive charge concentration, as would be expected for a streamer propagating from a positive charge volume towards the aircraft.

We feel it is important to emphasize that the streamer is not a leader at this point. The aircraft is able to accumulate negative charge rapidly because the streamer moves positive charge close to the aircraft, increasing the ambient field, and the aircraft is in conditions which allow triboelectric charging. No strike occurs at this point, however.

An expansion of the electric field record for an event triggered by the aircraft was given in Fig. 31. The exponential shape of the electric field record is similar to that of a charging capacitor. As shown in Fig. 32 and 33, the latter

stages of this charging process are accompanied by intermittent positive pulses on all the electric field sensors. These are attributed to the production of negative streamers as the charge level increases and breakdown begins to occur. Figure 41 shows that the magnetic field sensor also saw pulses, but they do not coincide with the electric field pulses until after the peak in the negative charge level. These first pulses are believed to be the result of more streamers (or additional steps of the original streamer) and once again, the aircraft can accumulate more charge. The streamers grow until breakdown occurs, as shown in Fig. 32, 42, and 43. As the negative streamer from the aircraft and a positive streamer from the positive charge volume move towards each other, a positive charge increase is evident on all the electric field sensors as negative charge flows off the aircraft. Initial, small current pulses on the aircraft due to the negative leader steps become much larger once the two leaders connect and a channel is established. Continuing current flow from the positive charge volume also begins at this time.

Further evidence of the aircraft interaction with a positive charge center comes from the digital triggers obtained just at the beginning of the collapse of the slow initial negative charge increase. (See Table 10 and Fig. 39.) In all cases, this data shows that negative charge is flowing off the aircraft from an attachment point so that the aircraft must be interacting with a positive charge volume. Similar results were obtained with the F-100 during Project Rough Rider (Reference 2).

Figure 12 shows that the latter stages of the strikes triggered by the aircraft feature a preponderance of pulses indicating negative charge increases on all electric field sensors. These are believed to be recoil streamers (also called K-changes) which occur when the leader through the aircraft intercepts negative charge volumes. This result is in agreement with Ogawa and Brook (Reference 27) who state that most intracloud events begin with a leader from a positive charge volume which taps successively lower pockets of negative charge.

Much of the above data and hypothesis has been reviewed with other investigators and their suggestions have been carefully considered. One idea, that the initial increase in negative charge reflects only the approach of a positive leader, was also our initial interpretation. In this case, however, we would expect

to see the type of initial curve shown in Fig. 11, where the aircraft does appear to be intercepting a positive leader. We find it difficult to see how an approaching leader could produce the type of curve shown in Fig. 31.

Another suggestion was that the initial change in negative charge was due to a positive leader leaving the aircraft under the influence of the external ambient field. This hypothesis is difficult to reconcile with our digital data at the time of the initial attachment which shows negative charge flow off the aircraft at the attachment point. Also, a positive leader should interact with a negative charge volume, producing a sharp negative charge increase on the aircraft when the two connect. Instead, there is a positive charge increase at this point.

There is also some circumstantial evidence to support the idea that triboelectric charging is an important part of the triggering process. First, none of the events triggered by the aircraft occurred below 14,000 ft, in spite of the fact that the aircraft was flown in thunderstorms below 14,000 ft for 41 h. Since 14,000 ft corresponds roughly to the freezing level in Florida during the summer, and since clouds containing ice particles produce more charge on the aircraft than clouds containing only liquid water (Reference 39), this provides indirect support for the suggestion that rapid triboelectric charging has an important role in the triggering process.

We find it also interesting to note that the aircraft experienced no strikes, either triggered or intercepted, during almost 17 h of flying between 5,000 and 13,000 ft. This may be due to a reduced rate of triboelectric charging at these warmer altitudes, a level too low to trigger a strike but high enough to keep the aircraft potential slightly negative and shield it from an on-coming negative leader.

Finally, we noted that the time required for the initial negative charge increase in 1984 averaged only 2.0 ms, while in 1985 it was 3.7 ms. Since the rate of triboelectric charging depends on airspeed, this difference could be due to the fact that the aircraft was flown over 50 knots faster in 1984 as compared to 1985 (See Tables 2 and 3.)

An extensive data base now exists on triggered strikes to aircraft. The above triggering mechanism, we realized, will be controversial and results of future programs such as the C-160 Transall program by ONERA should be of great interest. Since the majority of strikes to aircraft are triggered and these strikes seem to give warning of their impending occurrence, complete understanding of their phenomenology should improve methods of protecting against them.

### c. Intracloud Strike Current Measurements

The most common threat to the aircraft arises from recoil streamers (K-changes) during intracloud events triggered by the aircraft. Several of these pulses may occur in any given event; amplitudes, as shown in Section III, average 1 to 3 kA.

The largest current magnitude measured during both years of the program, 23 kA, occurred on a K-change but had the relatively slow rise time of 5  $\mu$ s. Another strong intracloud flash, which ended with a very large return stroke, produced several pulses of 10 to 15 kA on the aircraft during the K-changes, but showed very little current during the return stroke itself. Out of the hundreds of current pulses recorded on the aircraft during the program, only a dozen or so were above 5 kA.

It appears, therefore, that the commonly used scenario of a stepped leader intercepting the aircraft, proceeding to ground and initiating a series of return strokes which pass through the aircraft occurs only rarely. When it does occur, the aircraft often is at high altitudes so that current levels are low. When the aircraft is part of a cloud-to-ground event at low altitudes, it is usually in a branch and again experiences only low current levels. The most common type of event experienced by an aircraft is a triggered intracloud flash in which current pulses occur frequently but average only 1 to 3 kA.

## 3. INSTRUMENTATION CONSIDERATIONS

Because airborne lightning characterization programs are expensive, time-consuming and involve substantial risk, the aircraft must be carefully instrumented for the most return on investment.

The objective of the program must be carefully defined because unnecessary instrumentation ties up power and space, both of which are in short supply on an aircraft. It also can produce significant heat, which rapidly becomes a problem in an enclosed aircraft, particularly at low altitude.

The objective also must be defined and limited so that instrumentation data windows and input ranges can be selected and/or designed in a timely manner. For example, lightning events contain current pulses from milliamperes to tens of kiloamperes. Recording them all with favorable signal-to-noise ratios in one program is very difficult. Similarly, lightning events last from a few milliseconds to over a second, while individual current pulses may rise to peak in a few tens of nanoseconds. Again, recording them all successfully is a challenge that is difficult to meet in a single flight program.

A primary consideration is a digital data acquisition system with the fastest possible sample rate, longest window and greatest number of time-synchronized channels. The digital window for the CV-580 program was limited to 10  $\mu$ s at a 5-ns sample rate. Much better systems are now available and should be obtained for future programs.

Much valuable information was obtained from the electric field sensor on the forward fuselage, which was able to record frequencies down to 1 Hz. Future programs should be designed with similar electronics for all these sensors. On the CV-580, the other electric field sensors had a lower frequency response of about 1? kHz.

Two strengths of the CV-580 program were the time synchronization and the trigger system. Time synchronization made it possible to determine attachment and exit points, and current paths through the aircraft. The well-designed trigger system allowed digital windows to be obtained on different parts of the lightning events, i.e., a 10-kA return stroke rather than a 3-kA leader. Future programs should make use of these techniques.

Although much data on triggered strikes was obtained with the CV-580, there is still a need for careful study of the pretrigger and breakdown phenomena. Longer

digital windows of surface current and current shunt data synchronized with electric and magnetic field data would be extremely valuable.

Also missing to date are current and field measurements with the aircraft in a main channel at low altitude, the most severe threat. Obtaining data of this nature will be extremely expensive and time-consuming, and obviously is more dangerous than flying at higher altitudes.

#### 4. PREDICTED VERSUS SIMULATED NEMP RESPONSES

Measured responses to simulated NEMP were compared to scale model extrapolated predictions, for a given sensor and applied field orientation, in Figs. 60 and 61. Although no attempt was made to remove ground effects for the measured NEMP responses, both the predicted and measured responses contained similar characteristics and aircraft resonances. In most cases, the resonances correspond directly to reflections between aircraft structures on the wings or fuselage.

Extrapolated simulated NEMP responses based on scale models appear reasonably accurate for the limited number of measurements available for comparison. The responses of the surface current sensors mounted on the fuselage agreed more closely with scale model predictions when the incident electric field was parallel to the fuselage. Wing responses were quite comparable when the applied field was perpendicular to the fuselage. All measurements contained frequencies corresponding to major wing or fuselage resonances, depending on the orientation of the applied electric field. Predicted and simulated NEMP responses are compared in more detail in Reference 38.

#### 5. LIGHTNING VERSUS SIMULATED NEMP RESPONSES

A comparison of aircraft responses to lightning and simulated NEMP was made in Figs. 64 and 65, as well as in Reference 38. Such comparisons are complicated by the fact that the lightning responses were due to conducted current on the aircraft, while the simulated NEMP responses resulted from fast-changing radiated electric fields. The comparison was further complicated by the relatively low amplitude of the lightning events, whereas the simulated NEMP excitation represented a moderate level NEMP threat.

Although the lightning and NEMP responses both contained frequencies corresponding to wing and fuselage resonances, peak amplitudes for simulated NEMP measurements were 4 to 20 times higher than those of the lightning events compared. The lightning responses often contained spectral components below 4 MHz that were not present in simulated NEMP, and seldom indicated significant frequencies higher than 10 MHz. This is due, in part, to the slower rate of change and low magnitude of the lightning excitation.

Unfortunately, digital data from a moderate level lightning strike was not obtained for comparison with the simulated NEMP threat used. However, even low level lightning shows excitation of primary aircraft resonances. If the frequency domain lightning data were to be scaled (assuming linearity) to even an average threat level, the amplitudes at low frequencies would be higher than for the NEMP threat used.

SECTION V  
CONCLUSIONS

The principal conclusions resulting from this 2-yr CV-580 aircraft lightning characterization program are as follows:

1. The most common lightning threat to an aircraft is a strike triggered by the aircraft which then continues as an intracloud discharge. Such attachments may produce current pulses as high as 25 kA, but recorded current levels more often ranged from 1 to 3 kA.

2. In 7 of the 41-lightning events analyzed, the lightning channel was intercepted rather than triggered by the aircraft. In five of these cases, the aircraft was in a branch of a cloud-to-ground discharge rather than in the main channel. On one (or possibly two) occasions, the aircraft was in the main channel but at high altitude where the full return stroke current was not experienced. There were no cases in which the aircraft was in the main channel of a cloud-to-ground return stroke at low altitude.

3. The intercepted strikes produced current levels of 3 to 4 kA on the aircraft. Due to the lack of data for the main channel at low altitude, however, information on current levels during this most severe lightning threat was not obtained.

4. Existing engineering models and threat definitions of lightning based on ground measurements (such as MIL-STD-1757) are not contradicted by this program. Current amplitudes, rise times, durations, etc., measured on the aircraft fall within previously established ranges.

5. Penetration of a thundercloud at or above the freezing level almost always resulted in the triggering of an intracloud strike. A possible mechanism for this triggering process is presented after detailed study of the correlated electromagnetic field and current records during the preattachment, breakdown and attachment phases of each event.

6. The electric field records from wideband sensors with near dc frequency response contain different characteristics depending on whether the strike is triggered or intercepted. Possibly, these characteristic signatures could be exploited to enhance aircraft system protection against lightning. Analytical models also could be improved by incorporating these signatures.

7. Pulse repetition rates exceeding 10 pulses per second were often observed for short intervals. The effects of such high pulse repetition rates on aircraft microelectronics should be investigated and addressed in existing lightning protection specifications.

8. Predicted simulated NEMP responses based on scale model studies are considered reasonably accurate in that they display major aircraft resonances contained in actual simulated NEMP ground measurements.

9. Low level lightning measurements often contained significant frequency responses below 4 MHz not apparent in simulated NEMP. If frequency domain data were to be scaled (assuming linearity) to even an average threat level, the amplitudes at low frequencies would exceed that of the moderate level NEMP threat compared.

## SECTION VI RECOMMENDATIONS

This report makes a substantial contribution to understanding the preattachment and attachment phases of triggered lightning strikes. Much more information could be extracted from this data by investigators who can apply more advanced analysis techniques. Identification of the phenomenology involved in the triggering process would be of considerable value in developing lightning warning systems for aircraft and should improve methods of diverting lightning strikes from sensitive aircraft components to less vulnerable areas. In addition, digital control systems could be programmed to disregard data during an impending lightning strike that may be polluted by induced transients.

Even though this program did not produce measurements of low altitude cloud-to-ground return stroke currents thought to represent the most severe lightning threat, there is not sufficient evidence to suggest that the probability of a 200-kA return stroke is too low to warrant a change in current protection standards. However, the fact remains that a vast majority of the lightning strikes to the CV-580 aircraft appear to be triggered and are of greatly lower magnitudes. A point of contention for aircraft designers will continue to be the extent to which it is prudent to view the amount of lightning protection required in terms of flight environment, probability of lightning attachment, probable current levels, radar cross section, cost of replacement, etc. This topic requires continued research and clarification.

As successful as this program may have been in contributing to the understanding of lightning interaction with aircraft, practically all recorded airborne data involve metallic aircraft. The degree to which these results can be readily applied to next generation composite aircraft is an area that requires extensive investigation. For example, can composite aircraft be expected to trigger lightning attachments in a manner similar to the CV-580 as presented in this report? Direct effects damage to aircraft surfaces and structures, often minimal for metal conductive materials, can create significant problems for even low amplitude lightning currents. Furthermore, composite aircraft would not offer the degree of electromagnetic shielding against induced transients that is provided by their

metallic counterparts. Such issues are not restricted to aircraft, but extend to all forms of aerospace vehicles.

Future airborne lightning characterization programs should be conducted with comparable sensors, instrumentation and recording systems to those used in this program with the following enhancements:

1. The analog channels should be recorded using FM techniques. Since the analog data is already bandwidth limited, it is considered preferable to record all parameters on analog channels with dc response.
2. All sensor outputs interfaced to the analog recorder should be recorded using two channels with overlapping ranges. This will provide greater dynamic range and considerably improved signal-to-noise ratios.
3. The memory for the digital recording system should be expanded to the *maximum* available without sacrificing vertical resolution. Consideration should be given to increasing sample intervals to 10 ns to obtain a longer window, or to "daisy chaining" recorder channels.
4. The electric field mill data should be recorded on the same analog recorder as other sensor outputs to improve time synchronization.
5. Consideration should be given to using innovative recording techniques for high resolution digital data on analog tape. Techniques are available which could speed up the transfer rate from the digitizing instruments to permanent storage, thus achieving almost continuous recording of entire lightning events.
6. The analog data should be processed using more sophisticated methods, including digitizing of the entire event rather than only selected portions. Noise filtering and auto and cross correlation methods could be applied to extract signals from noise.

## REFERENCES

1. Perala, R.A., A Program Plan for In-Flight Characterization of Cloud to Ground Lightning Strikes to Aircraft, Electromagnetic Applications, Inc. Report No. EMA-84-12-14, February 1984, prepared under contract no. DTFA03-84-C-00010.
2. Petterson, B.J. and Wood, W.R., Measurements of Lightning Strikes to Aircraft, Sandia Laboratory Report No. SC-M-67-549, January 1968.
3. Pitts, F.L., Thomas, M.E., Campbell, R.E., Thomas, R.M., and Zaepfel, K.P., In-Flight Lightning Characteristics Measurement System, Federal Aviation Administration - Florida Institute of Technology Workshop on Grounding and Lightning Technology, FAA-RD-79-6, pp. 105-111, March 1979.
4. Fisher, F.A. and Plumer, J.A., Lightning Protection of Aircraft, NASA Reference Publication 1008, October 1977.
5. Corbin, J.C., Lightning Interaction With USAF Aircraft, presented at the 8th International Aerospace and Ground Conference on Lightning and Static Electricity, June 21-23, 1983, Report No. DOT/FAA/CT-83/25.
6. Air Force Systems Command (AFSC) Design Handbook DH 1-4, Electromagnetic Compatibility, March 1984.
7. Corn, P.B., An Overview of Lightning Hazards to Aircraft, March 1978.
8. Cianos, N. and Pierce, E.T., A Ground Lightning Environment for Engineering Usage, Stanford Research Institute Technical Report No.1, August 1972.
9. Uman, M.A., Lightning, Dover Publications, Inc., 1969.
10. Golde, R.H., Lightning, Vol. 1 Physics of Lightning, Academic Press, 1977.
11. MIL-STD-1757A, Lightning Qualification Test Techniques for Aerospace Vehicles and Hardware, 20 July 1983.
12. McEachron, K.B., "Phenomena of Lightning," Journal of the Western Society of Engineers, Vol. 47, No. 2, pp.43-58, April 1942. +
13. Fitzgerald, D.R., USAF Flight Lightning Research, Proceedings, Lightning and Static Electricity Conference, 3-5 December 1968, Technical Report AFAL-TR-68-290, Part II, pp. 123-134, May 1969.
14. Fitzgerald, D.R., "Probable Aircraft Triggering of Lightning in Certain Thunderstorms," Monthly Weather Review, Vol. 95, No. 12, December 1967.
15. Imyanitov, I.M., Aircraft Electrification in Clouds and Precipitation, Elektrizatsiya Samoletov v Oklakakh i Osadkakh, 1970. (Translation by Foreign Technology Division, Wright-Patterson Air Force Base).

16. Anderson, R.V. and Bailey, J.C., Vector Electric Fields Measured in a Lightning Environment, NRL Memorandum Report No. 5899, January 1987.
17. Pryzby, J.E., FAA CV-580 Lightning Protection Program, Memoranda 1-14, October 1983-August 1984, Lightning Technologies, Inc., prepared under Technology/Scientific Services P.O. No. 162-12-531S.
18. Pryzby, J.E., Lightning Safety Inspection and Test on Convair CV-580 N49 Integral Fuel Tanks, Lightning Technologies, Inc. Report No. LT-84-201, June 1984, prepared under Technology/Scientific Services P.O. No. 162-12-513S.
19. Liepa, V., Lightning Assessment Studies—Scale Model Measurements on the Convair 580, Test Results, University of Michigan Radiation Laboratory submitted to Technology Scientific Services under Purchase Order 162-13-116S, September 1984.
20. Arora, S. and Snow, F.E., Substantiative CV-580 Tail Boom Installation, Aircraft Technical Service, Inc. Report No. 1345, April 1985.
21. Frilzner, S., Ground Vibration and Flight Flutter Test of a Modified C-131 Aircraft, Specialized Testing Service, Report No. 8553, April 1985.
22. Nanevicz, J. and Vance, E., Instrumentation Design Tradeoffs for the Airborne Characterization of Lightning, SRI International, Menlo Park, CA.
23. Rustan, P., Kuhlman, B., Burket, H., Reazer, J. and Serrano, A., Low Altitude Lightning Attachment to an Aircraft, AFWAL-TR-86-3009, February 1986.
24. Bailey, J.C. and Anderson, R.V., Experimental Calibration of a Vector Electric Field Measurement System on an Aircraft, NRL Memorandum Report No. 5900, March 1987.
25. Reazer, J. and Richmond, R.D., Simultaneous Airborne and Ground Measurement of Low Altitude Cloud-to-Ground Strike on CV-580 Aircraft, 1986 International Aerospace and Ground Conference on Lightning and Static Electricity, Dayton, OH, June 1986, AFWAL-TR-86-3098, Oct. 1986.
26. Fisher, R.J. and Uman, M.A., "Measured Electric Field Rise Times for First and Subsequent Lightning Return Strokes," Journal of Geophysical Research, Vol. 77, pp. 399-405, 1972.
27. Ogawa, T. and Brook, M., "Mechanism of the Intracloud Lightning Discharge," Journal of Geophysical Research, Vol. 69, pp. 5141-5153, December 1964.
28. Reazer, J. and Serrano, A., Spatial and Temporal Description of Strikes to the FAA CV-580, 1986 International Aerospace and Ground Conference on Lightning and Static Electricity, Dayton, OH, June 1986.
29. Krider, E. and Radda, G., "Radiation Field Waveforms Produced by Lightning Stepped Leaders," Journal of Geophysical Research, Vol. 80, No. 18, June 1975.
30. Anderson, R.V. and Bailey, J.C., Vector Electric Fields Measured in a Lightning Environment, NRL Memorandum Report No. 5899, April 1987.

31. Uman, M.A., "Lightning Return Stroke Electric and Magnetic Fields," Journal of Geophysical Research, Vol. 90, June 1985.
32. Idone, V.P. and Orville, R.E., "Lightning Return Stroke Velocities in the Thunderstorm Research International Program (TRIP)," Journal of Geophysical Research, Vol. 87, pp. 4903-4915, 1982.
33. Liepa, A.V., Kuhlman, B., and Serrano, A., Effects of Aircraft Interaction on Performance of B-Dot Sensor for Delta-Wing and Cargo-Type Aircraft, presented at Nuclear EMP Meeting, University of New Mexico, Albuquerque, NM, May 19-23, 1986.
34. Lee, K.S.H. (Ed.), EMP Interaction: Principles, Techniques and Reference Data, AFWAL-TR-80-402, pp. 267-276, December 1980.
35. Liepa, A.V., Miksell, M., and Pierce, L., Exterior Electromagnetic Response of CV-580 Aircraft, Dikwood Division of Kaman Sciences Corp., Report No. DC-FR-4088, pp. 340-2, October 1985.
36. Chiu, I.L. and Yang, F.C., External Response of CV-580 Aircraft to NCGS-84-1 Criteria High-Altitude Electromagnetic Pulse and to Typical Reciprocal Double Exponential Waveforms (U), Dikwood Division of Kaman Sciences Corp., Report No. DC-FR-4088, pp. 340-1, October 1985, SECRET-Restricted.
37. Hebert, J.L., Reazer, J.S., Schneider, J.G., Risley, M.D., and Serrano, A.V., Current Levels and Distributions on an Aircraft During Ground Lightning Simulation Data and In-Flight Attachments, 1986 International Aerospace and Ground Conference on Lightning and Static Electricity, Dayton, OH, June 1986, AFWAL-TR-86-3098, October 1986.
38. Burket, H.D., Comparison of Electromagnetic Measurements on an Aircraft From Direct Lightning Attachment and Simulated Nuclear Electromagnetic Pulse, 1986 International Aerospace and Ground Conference on Lightning and Static Electricity, Dayton, OH, June 1986, AFWAL-TR-86-3098, October 1986.
39. Fisher, B.D., Brown, P.W., Wunschel, A.J., Jr., Burket, H.D., and Terry, J.S., Joint Thunderstorm Operations Using the NASA F-106B and FAATC/AFWAL Convair 580 Airplanes, 1986 International Aerospace and Ground Conference on Lightning and Static Electricity, Dayton, OH, June 1986, AFWAL-TR-86-3098, October 1986.
40. Nanevicz, J.E., Static Charging and Its Effects on Avionics Systems, IEEE Transactions on Electromagnetic Compatibility, Vol. EMC-24, May 1982.
41. Illingworth, A.J. and Marsh, S.J., Static Charging of Aircraft by Collisions With Ice Crystals, 10th International Aerospace and Ground Conference on Lightning and Static Electricity, 10-13 June 1985.

APPENDIX A  
PROGRAM ORGANIZATIONAL ELEMENTS, RESPONSIBILITIES  
AND KEY PERSONNEL

1. U.S. Air Force - The U.S. Air Force had the lead responsibility for the program. This included coordination with each of the other agencies and responsibility for design, installation, operation and maintenance for most of the equipment needed for this program. In addition, the Air Force (AF) was responsible for processing, analyzing and reporting the corresponding data. The program was managed by the Atmospheric Electricity Hazards Research Group of the Air Force Wright Aeronautical Laboratories, Aeronautical Systems Division, Air Force Systems Command (AFWAL/FIESL) at Wright-Patterson Air Force Base. The program manager was Mr. Gary A. DuBro in 1984 and Major Pedro L. Rustan, Ph.D. in 1985. Maj. Rustan served as technical manager during the data acquisition periods and initial data processing, analysis, and reporting phases. Capt. Brian Kuhlman was the AF project officer in charge of instrumentation development. Capt. Harold D. Burket served as technical program manager during the final data processing, analysis and documentation phase. Both Maj. Rustan and Capt. Burket participated as data acquisition directors and operators during data acquisition missions.

The Air Force Weapons Laboratory (AFWL) provided transient recording systems, technical assistance, and predictions of the electromagnetic response of the CV-580. The AFWL support was under the direction of senior scientist Dr. Carl E. Baum and Capt. Dennis Andersh. The Air Force Eastern Space and Missile Center (ESMC) at Patrick AFB provided support under the direction of Mr. Cy Golub and Capt. Rudy Heller. This support included aircraft ground support, aircraft instrumentation maintenance facilities for AFWAL and FAA support personnel, a radio frequency for aircraft/ground controller communications, a weather radar display with aircraft position and Lightning Location System overlays, a site for the triggered lightning ground station, a field mill system for the ground station, and general weather support.

2. Department of Transportation/FAA - Administration of the FAA Technical Center Support was under the direction of Mr. N. Rasch. Mr. Michael Glynn served as the

FAA operations project manager. The Technical Center provided the Convair CV-580 as well as the pilots and maintenance personnel. In addition, they were responsible for aircraft maintenance support, modifications, flight test and certification. The FAA also provided funds to the Air Force for contracting the installation of the tail boom in 1985. The chief pilots were Mr. Jesse Terry and Mr. Al Bazer.

3. U.S. Navy - The Navy Research Laboratory was responsible for the primary instrumentation needed for measuring and recording ambient electric field data. This included design, fabrication, test and calibration of the field mill system; providing installation requirements to the FAA; operation and maintenance of the system during the missions; and processing analyzing and reporting the data. Key NRL personnel were Dr. Lothar Ruhnke and Messrs. Robert V. Anderson and Jeffrey Bailey. Mr. Anderson and Mr. Bailey were the system operators during the missions and were responsible for analyzing and reporting the data. In addition to the NRL, the Naval Air Development Center (NADC) provided some financial support to help ensure that the main objectives of the program were accomplished.

4. NASA - The NASA Kennedy Space Center (KSC) was responsible for personnel and supplies needed for the rocket-triggered lightning equipment, coordinating AF/ESMC operations at the rocket-triggering station, helping provide ground lightning strike locations from the lightning location system and electric field information from the ground field mill systems, tracking the aircraft during operations near KSC, and providing meteorological information. Mr. William Jafferis was the key individual for KSC.

5. ONERA - The French Government research organization (Office National d'Etudes et de Recherches Aeronautiques) supported both the rocket-triggered lightning experiments and the aircraft lightning characterization program. Support included the rockets and rocket launching system, along with installation, operation and maintenance of the rocket launching system and data acquisition system at the ground station. ONERA supplemented the Air Force and NRL aircraft instrumentation systems with additional electromagnetic sensors, transient digitizers, induced transient measurements on special nonstandard aircraft circuits, and a second quasi-static measuring and recording system. In addition, ONERA provided an operator for the aircraft system operation and maintenance. ONERA operations were under the

direction of Dr. Joseph Taillet who was supported by Messrs. J.L. Boulay and J.C. Alliot at the rocket-triggered lightning site and Dr. J.P. Moreau on the aircraft.

6. CONTRACTORS - Participating contractors during the program were, in alphabetical order:

a. Aero Specialties of Van Nuys, CA was responsible (under subcontract to Aircraft Technical Service) for the actual aircraft modifications needed for installation of the tail boom. The work was accomplished under the direction of Mr. Roger Oeland.

b. Aircraft Technical Service (ATS), Inc. of Van Nuys, CA designed the tail boom installation and aircraft structural modification, and supervised subcontractors for aircraft modification and ground vibrations and flutter testing. ATS did this work under subcontract to Technology/Scientific Services. The work was performed under the direction of Mr. Floyd Snow, Structural Designated Engineering Representative.

c. Dikewood Division of Kaman Sciences Corp. was contracted by AFWL to make aircraft response predictions at electromagnetic sensor locations using data generated by the University of Michigan during scale model tests. Messrs. Mr. Mikesell and L. Pierce performed the analysis jointly with the University of Michigan.

d. Electromagnetic Applications, Inc. of Albuquerque, NM was contracted by the FAA Technical Center to develop the operations plan for the program. This was accomplished under the direction of Dr. R. Perala.

e. Lightning Location and Protection, Inc. of Phoenix, AZ operated and maintained the lightning location systems used by NASA and provided the displays at ESMC, under contract to NASA.

f. Lightning Technologies, Inc. (LTI) of Pittsfield, MA was responsible for a safety survey of the aircraft design, a review of lightning strike experience on

this model aircraft, design protection, and for protection verification. This was done in 1984 under subcontract to Technology/Scientific Services, and in 1985 under a direct contract with the FAA Technical Center. The work was performed under the direction of Mr. J.A. Plumer.

g. Specialized Testing Service (STS) of North Hollywood, CA performed the CV-580 ground vibration and flight flutter test after installation of the tail boom. This was done under subcontract to Aircraft Technical Service, Inc. under the direction of Mr. Sanford Friezner.

h. Technology/Scientific Services (T/SS) of Dayton, OH was the in-house contractor for the Atmospheric Electricity Hazards Group (AFWAL/FIESL). T/SS was responsible for the design, development, checkout, installation, maintenance and operation of the hybrid instrumentation system. T/SS was also responsible for processing the data and provided a major portion of the analysis in this report. In addition, T/SS was responsible for subcontracts to ATS, LTI, STS and the University of Michigan. Mr. Arturo V. Serrano was the program manager for T/SS. The data acquisition system software was developed by Mrs. Jean Reazer. Mrs. Reazer was also the system operator during data acquisition missions and was responsible for data processing, analysis, and documentation. The instrumentation system was developed under the direction of Mr. Martin D. Risley.

i. University of Michigan - The Radiation Laboratory of the Department of Electrical and Computer Engineering performed swept continuous waveform (CW) measurements on a CV-580 scale model and predicted aircraft responses to electromagnetic radiation at each of the electromagnetic sensor locations. This was done in 1984 under subcontract to T/SS. In 1985, under subcontract to Dikewood, they participated in predicting aircraft responses to a lightning threat at each sensor location. Dr. V. Liepa directed this effort and collaborated with Dikewood for subsequent predictions based on these data.

APPENDIX B  
ELECTRIC FIELD AT THE FORWARD FUSELAGE AND CURRENT SHUNT DATA  
FOR LIGHTNING ATTACHMENTS IN 1985

At the beginning of the data reduction effort, outputs from the analog tape channels were played back into a strip chart recorder to provide an initial review of the results obtained. Similar plots for the 1984 data were presented in Reference 23.

Each plot shows the charge change in the vicinity of the forward fuselage sensor scaled in  $(C/m^2)/cm$  and the currents at the left wing tip, right wing tip, tail and vertical tail boom sensors scaled in  $A/cm$ . The analog recorder was played back at  $7\frac{1}{2}$  in./s,  $1/16$ th of the recording speed of 120 in./s. With the strip chart moving at 25 mm/s, this resulted in a time of 25 ms/cm on the horizontal scale and allowed most of the events to be displayed with reasonable resolution in a report format. (See Fig. B-1 through Fig. B-25.)

Caution must be used in interpreting these charts. Amplitudes are reduced somewhat as compared to most of the data presented in the body of the report since the latter was usually obtained by playing the data back into digitizers at appropriate sample rates. Digitization of the data also often revealed cases where a pulse which appeared to be of one polarity actually had a fast rising initial portion of a different polarity followed by an overshoot. Finally, the current channels shown are the ones set to record current pulses with amplitudes of 2500 A or less. Any pulses higher than this would also be recorded on the current channels set for high amplitudes, where their correct amplitude would be recorded. Data on these pulses was presented in Section III.

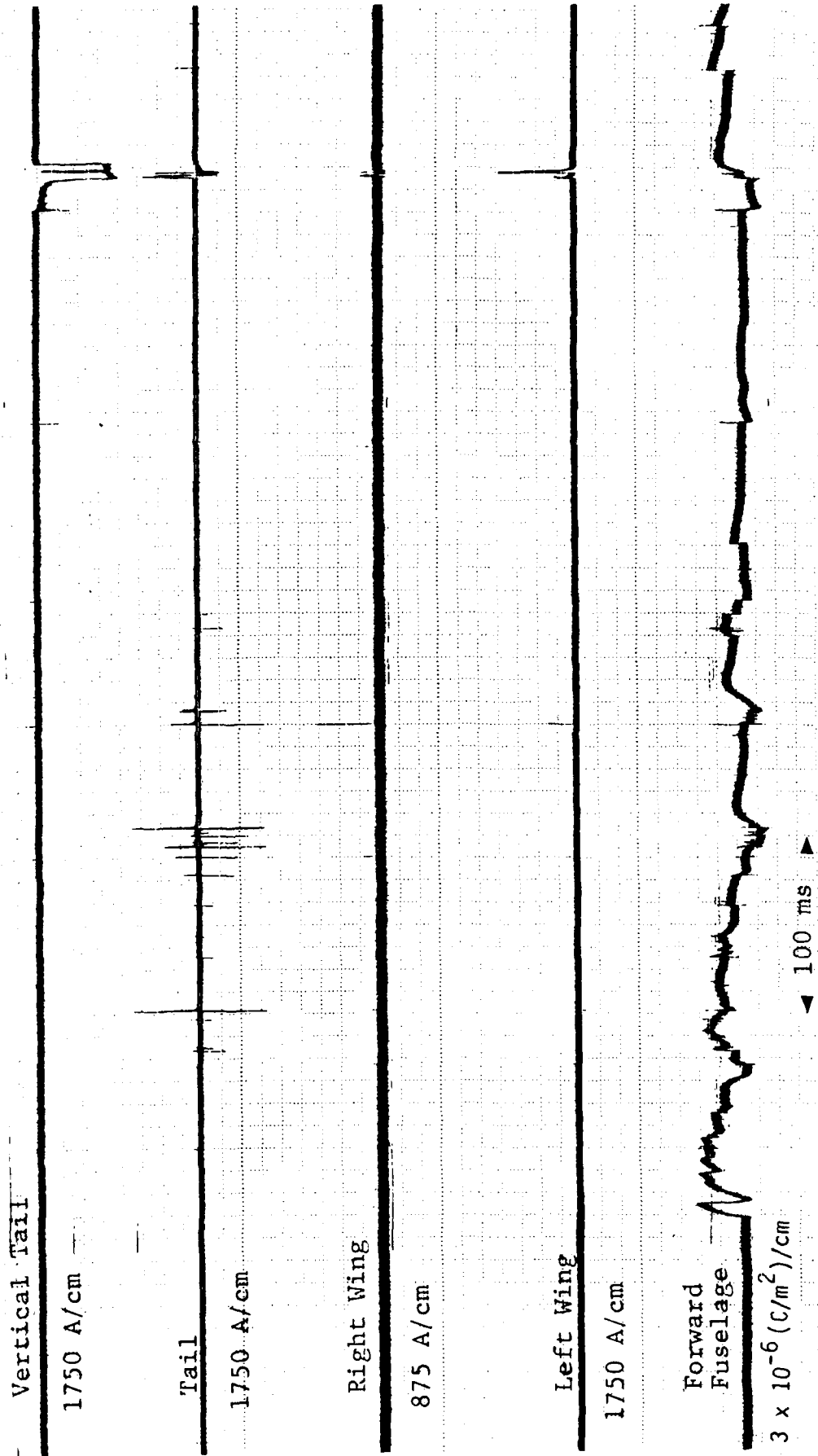


Figure B-1. Event 85-01

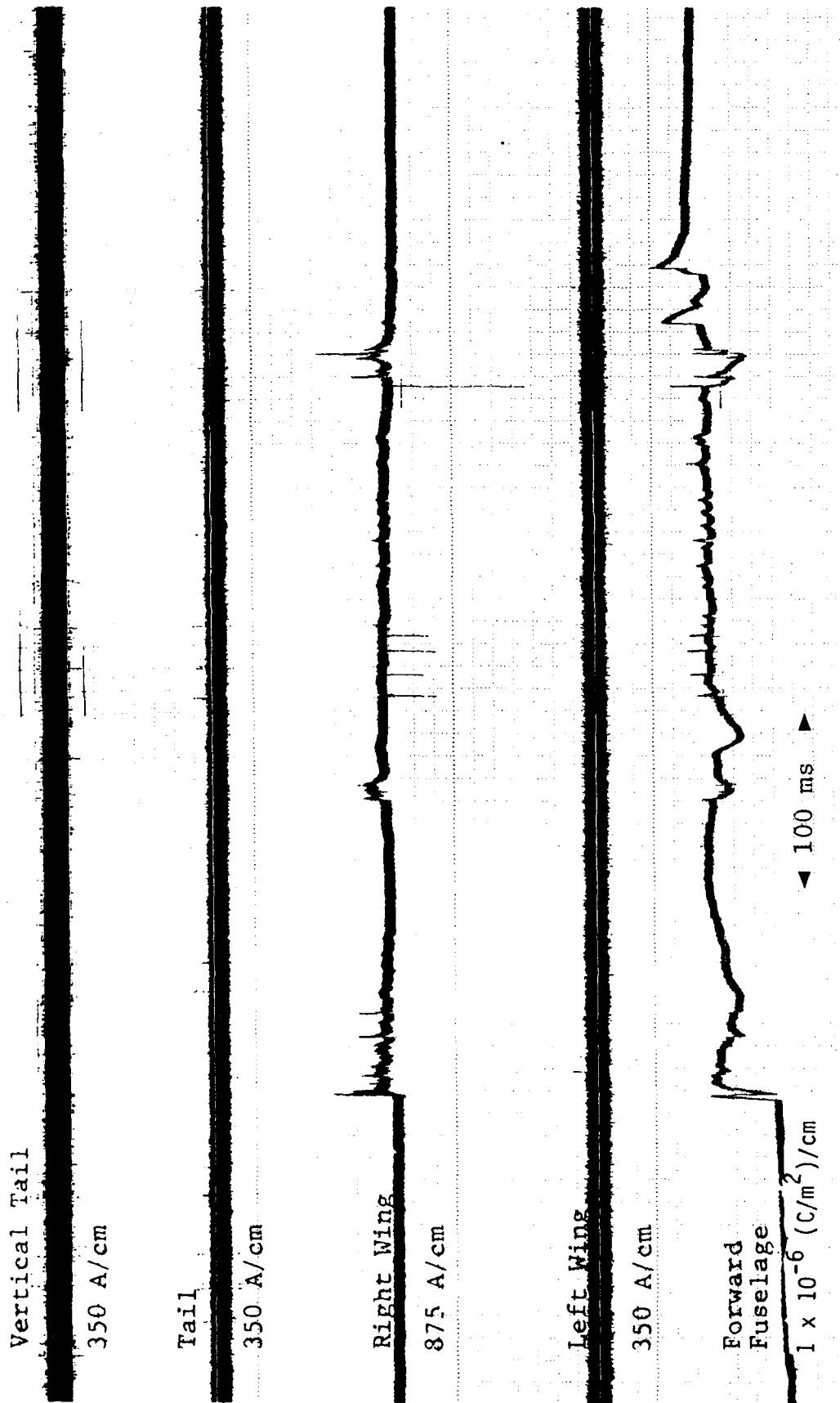


Figure B-2. Event 85-04



Figure B-3. Event 85-05

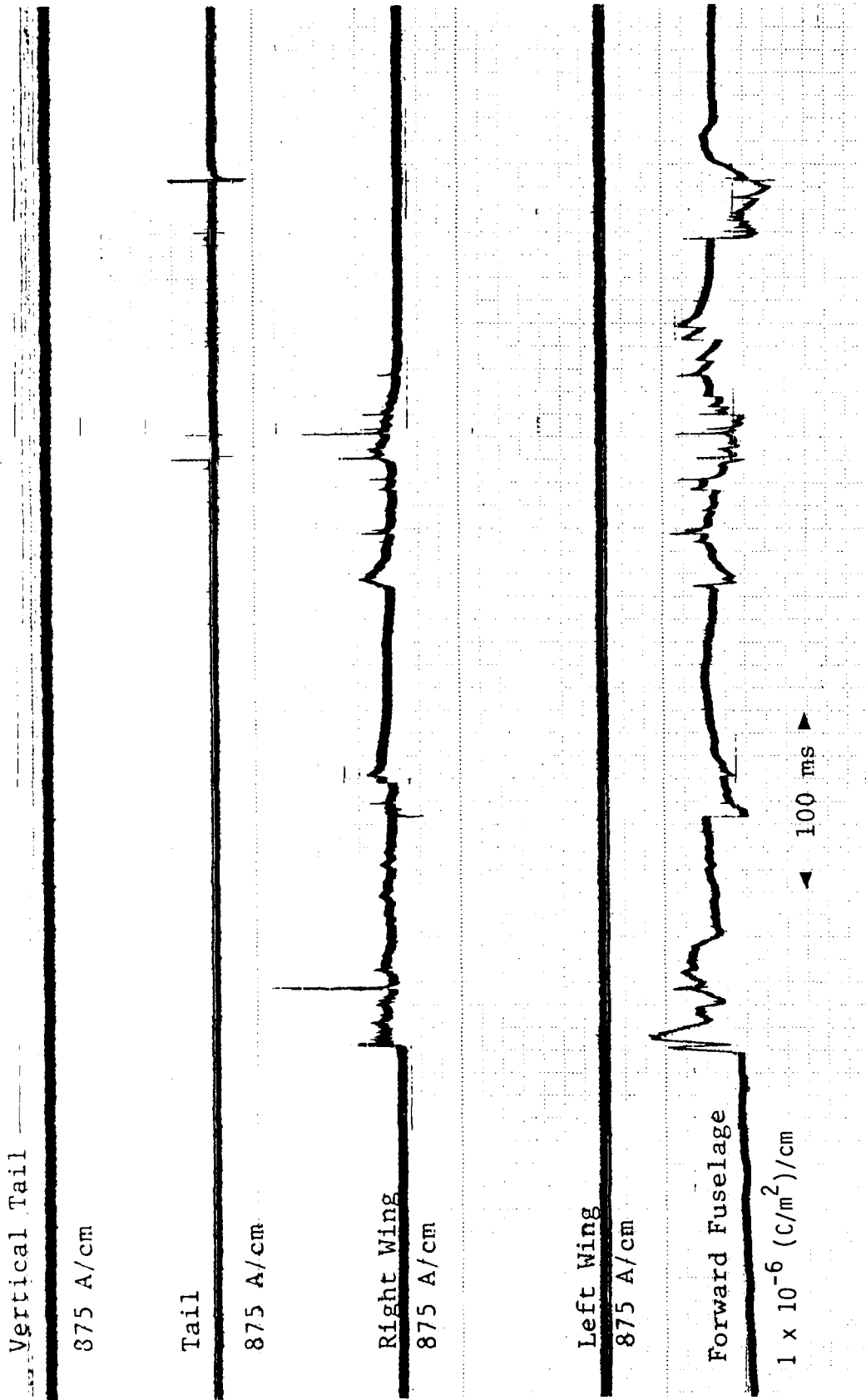


Figure B-4. Event 85-06

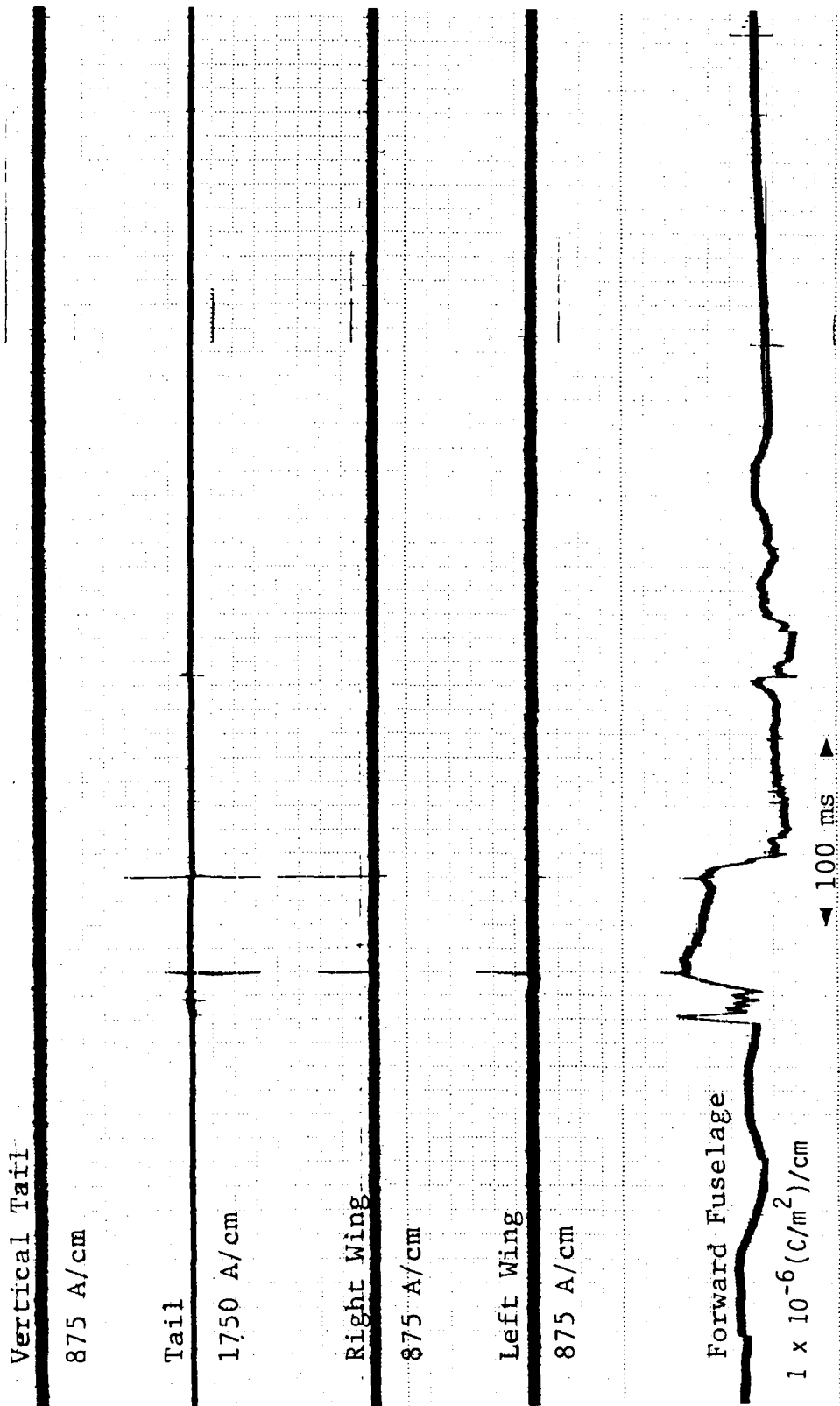


Figure B-5. Event 85-07

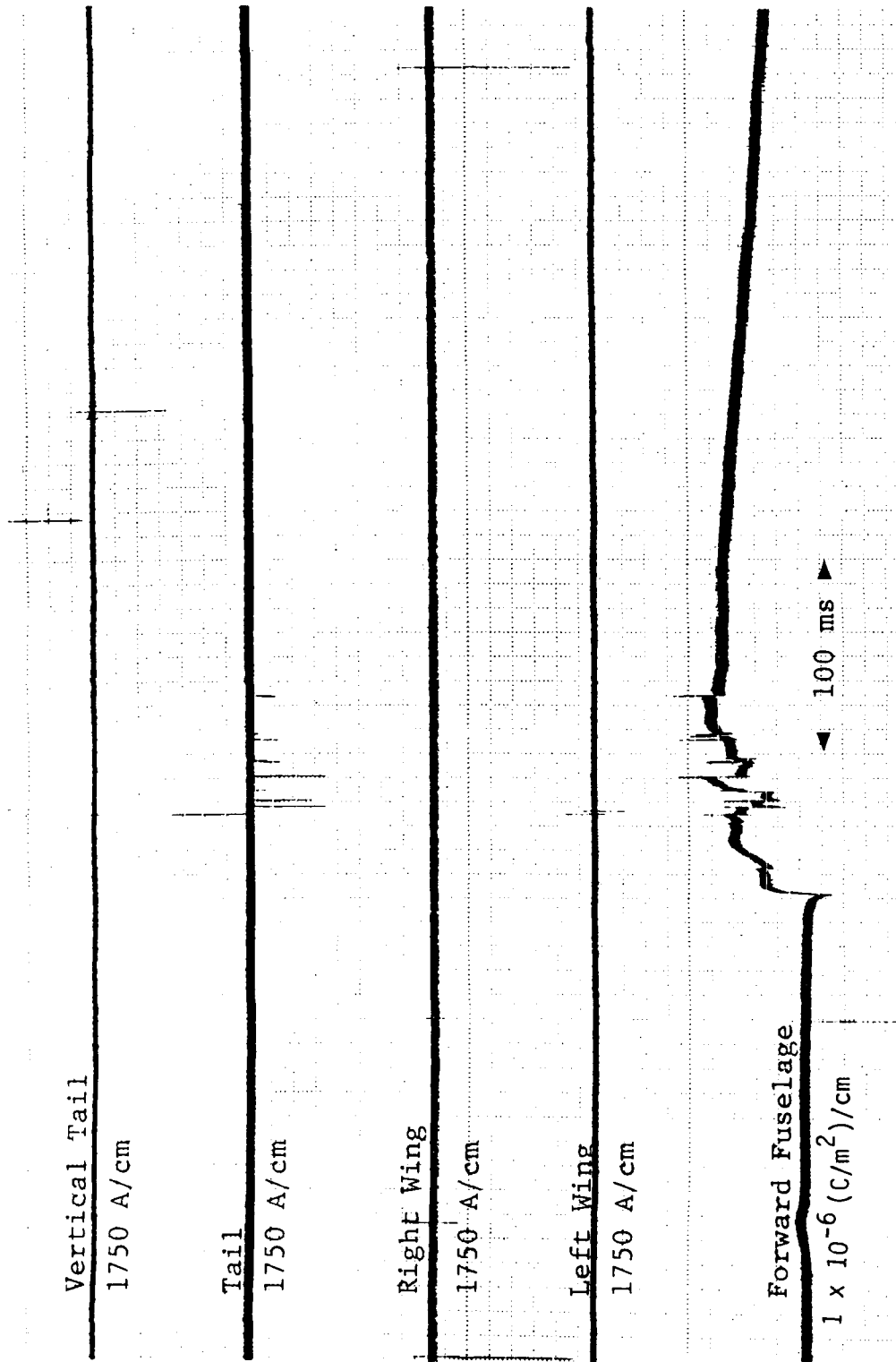


Figure B-6. Event 85-08

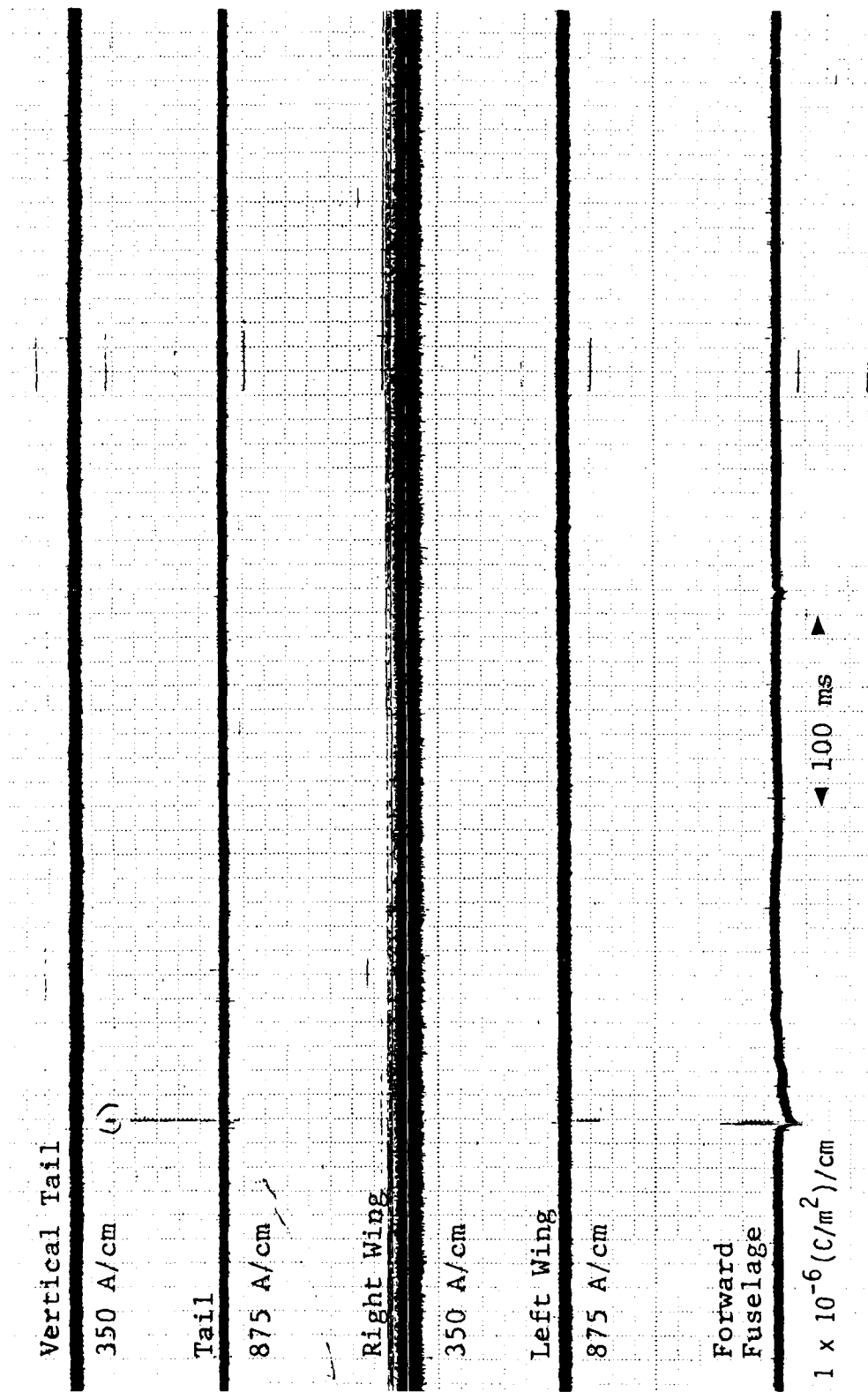


Figure B-7. Event 85-11

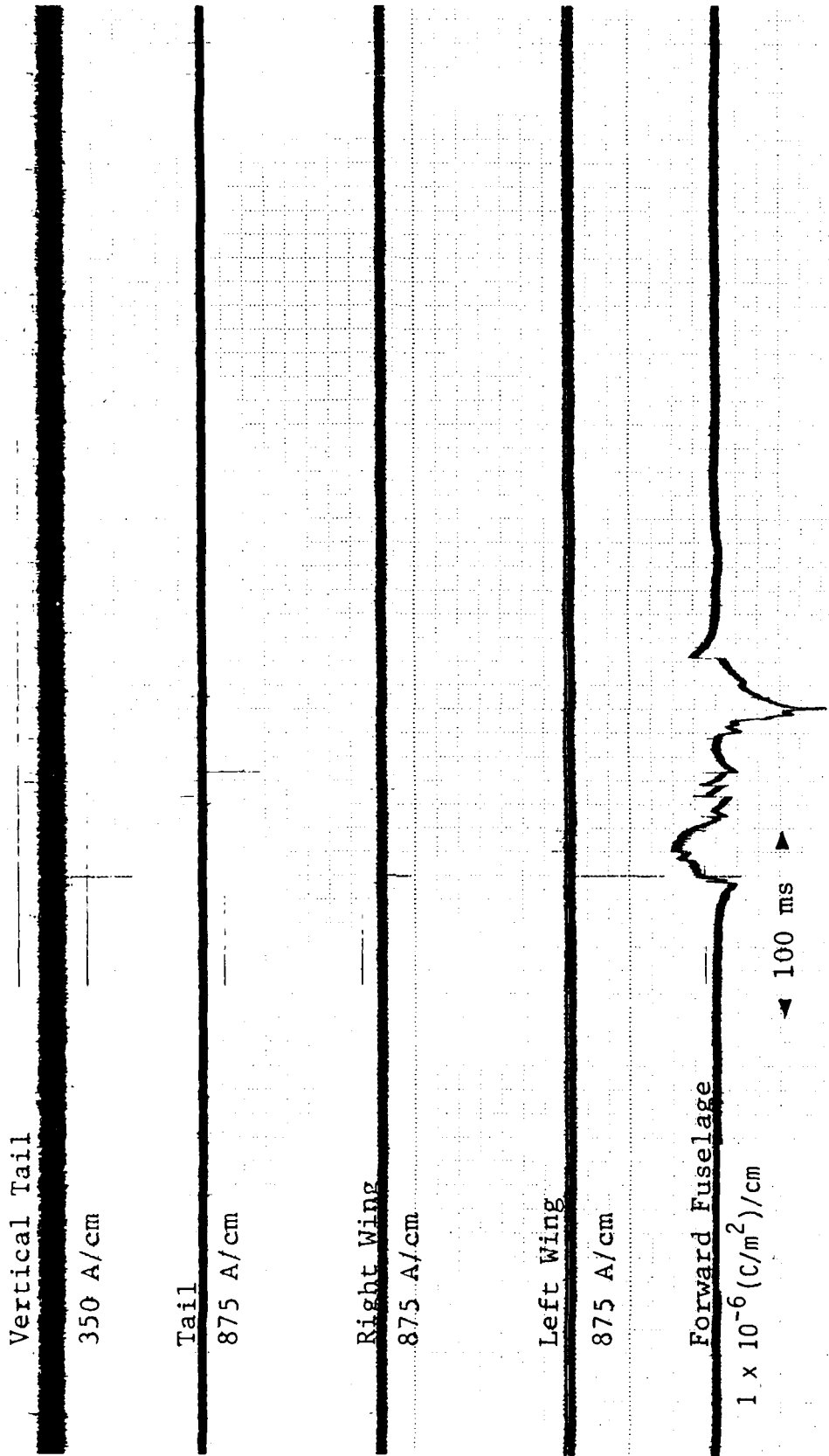


Figure B-8. Event 85-12



Figure B-9. Event 85-13

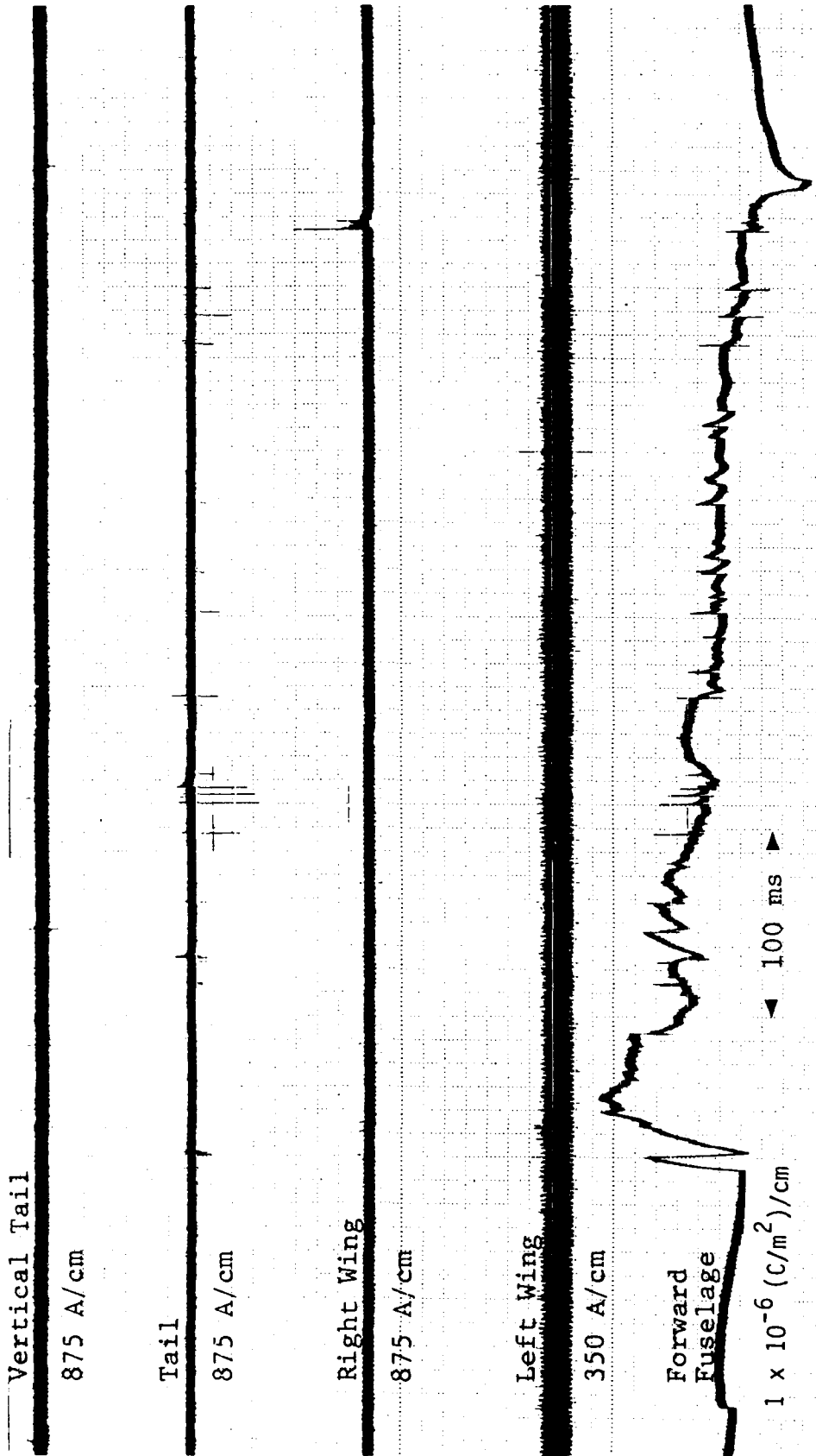


Figure B-10. Event 85-14

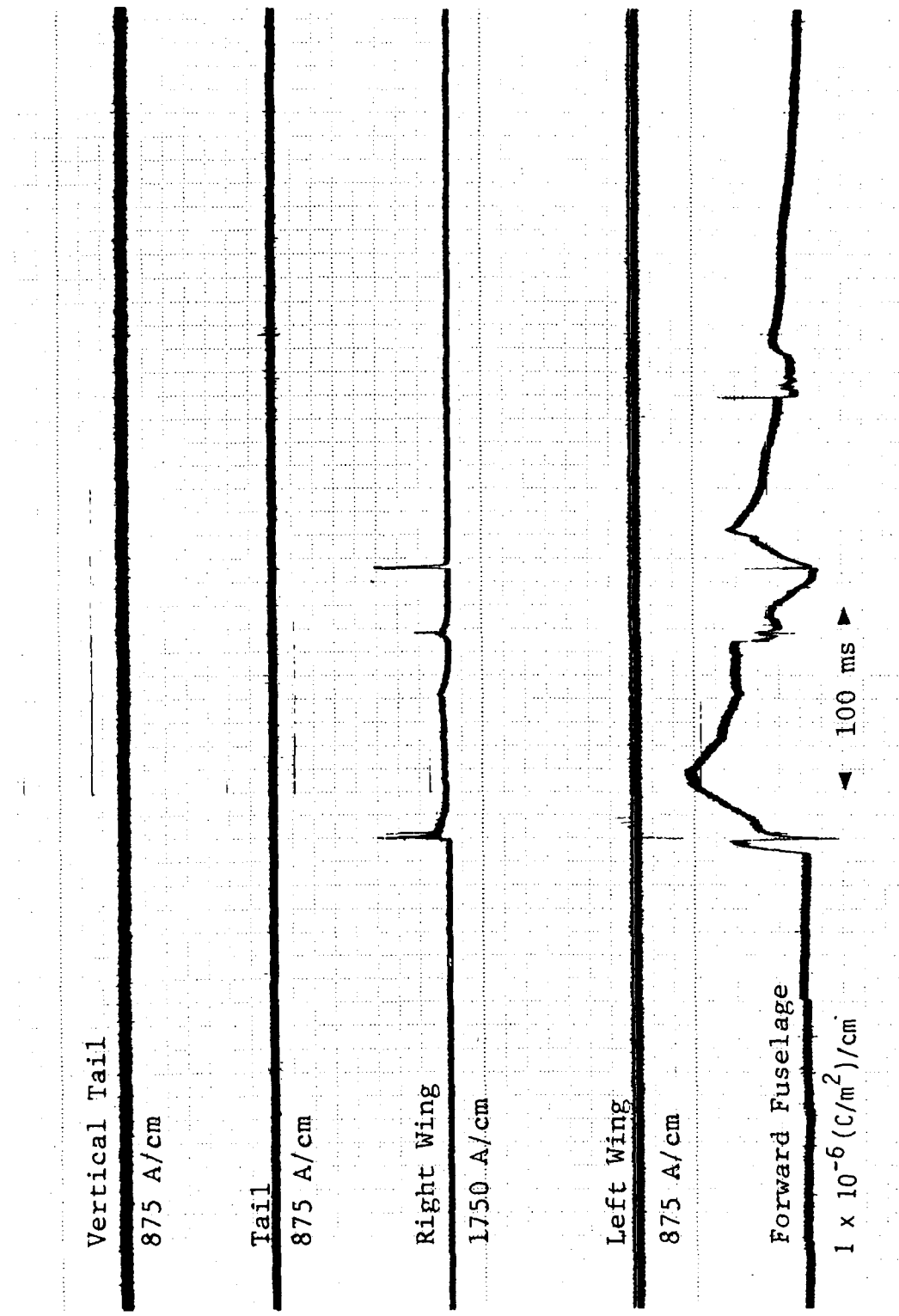


Figure B-11. Event 85-16

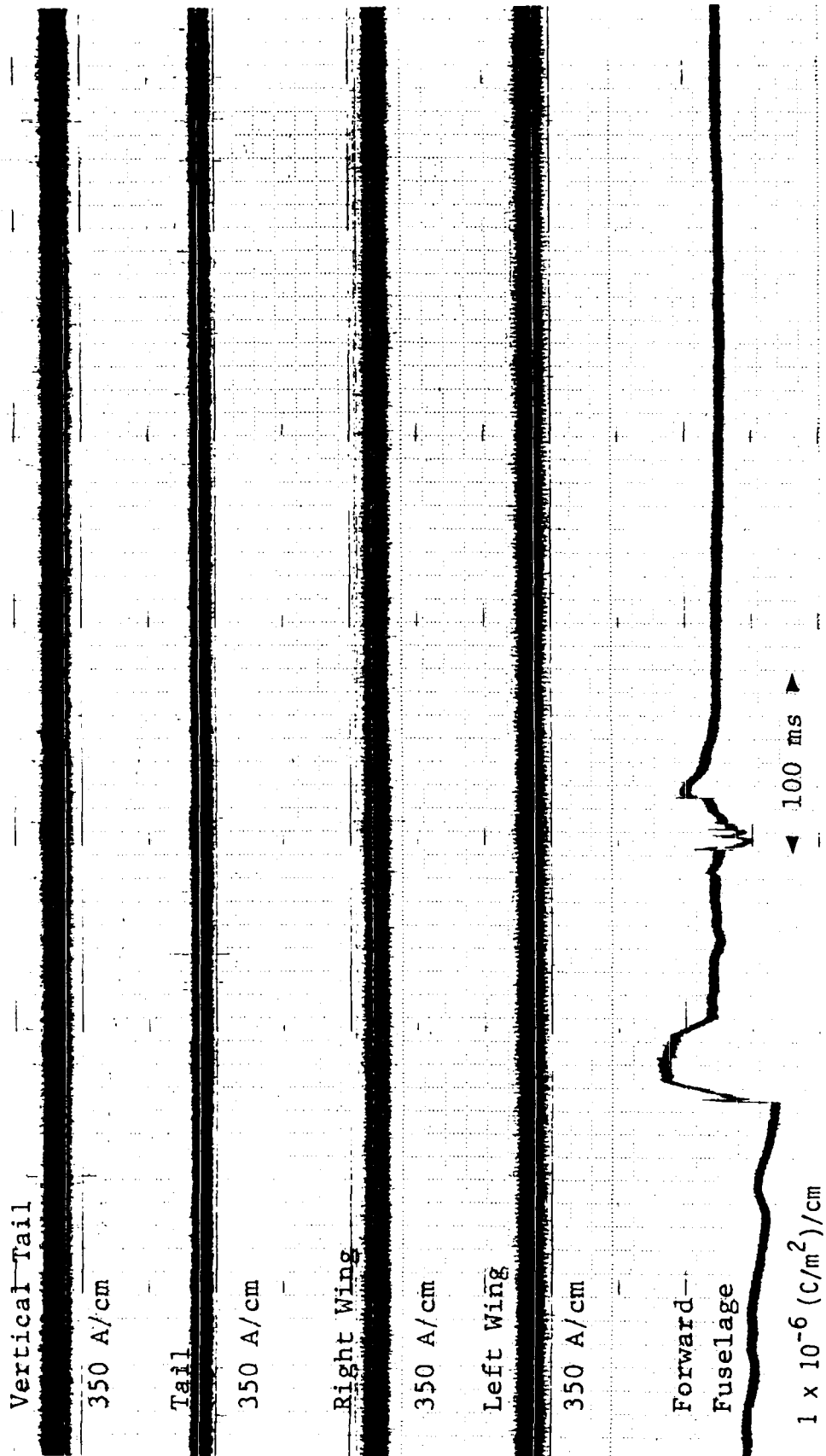


Figure B-12. Event 85-17

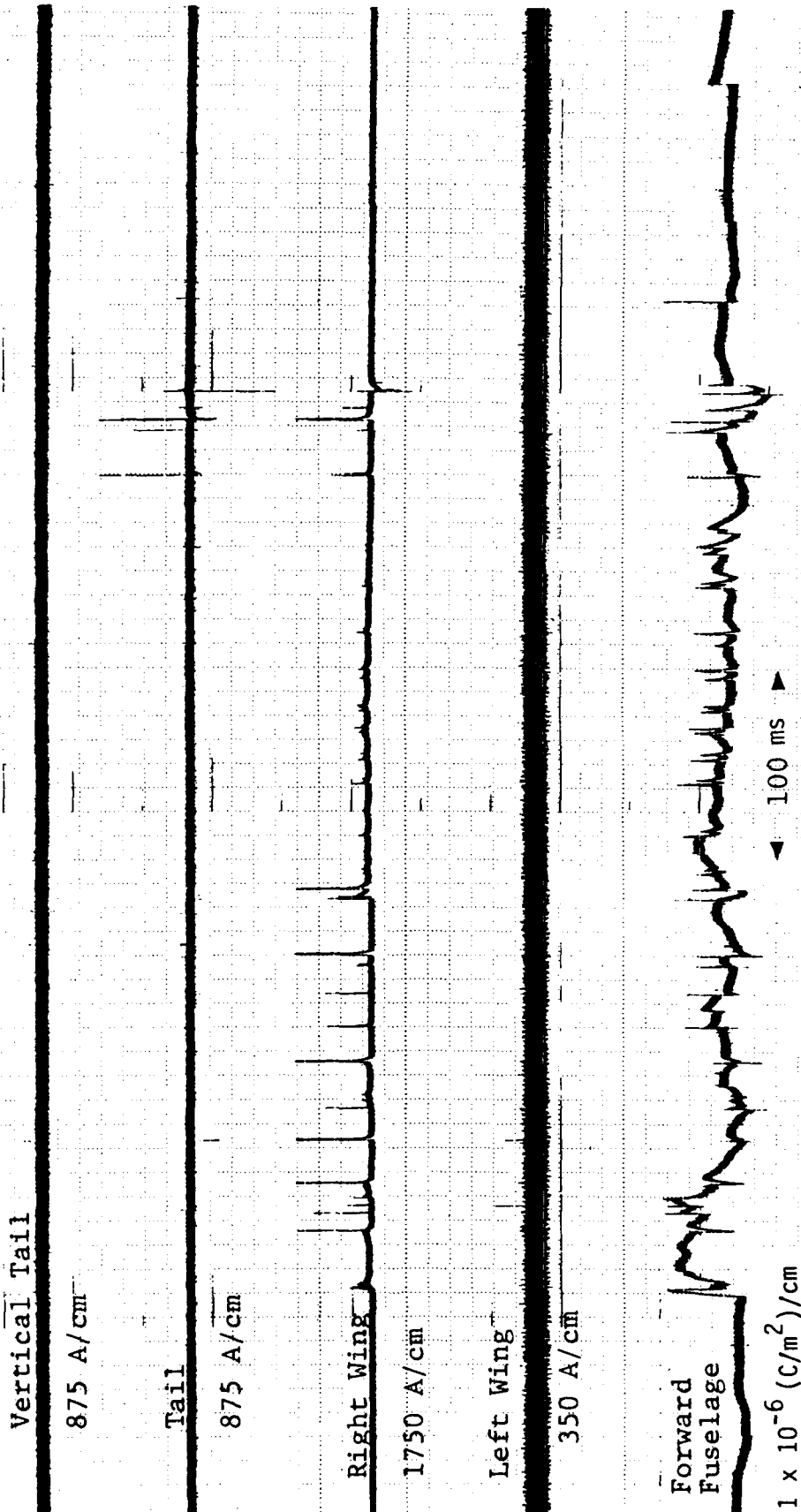


Figure B-13. Event 85-18

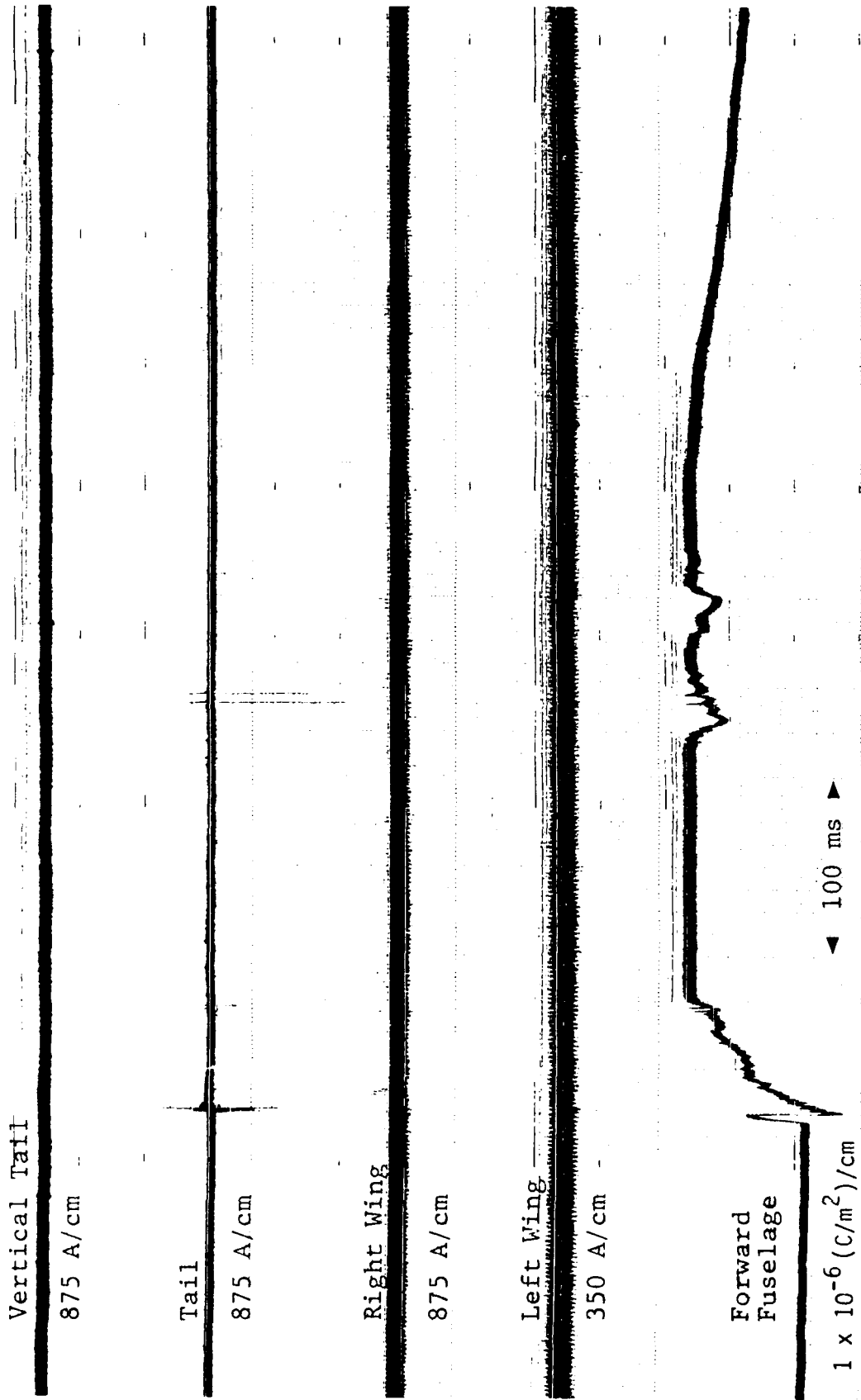


Figure B-14. Event 85-19

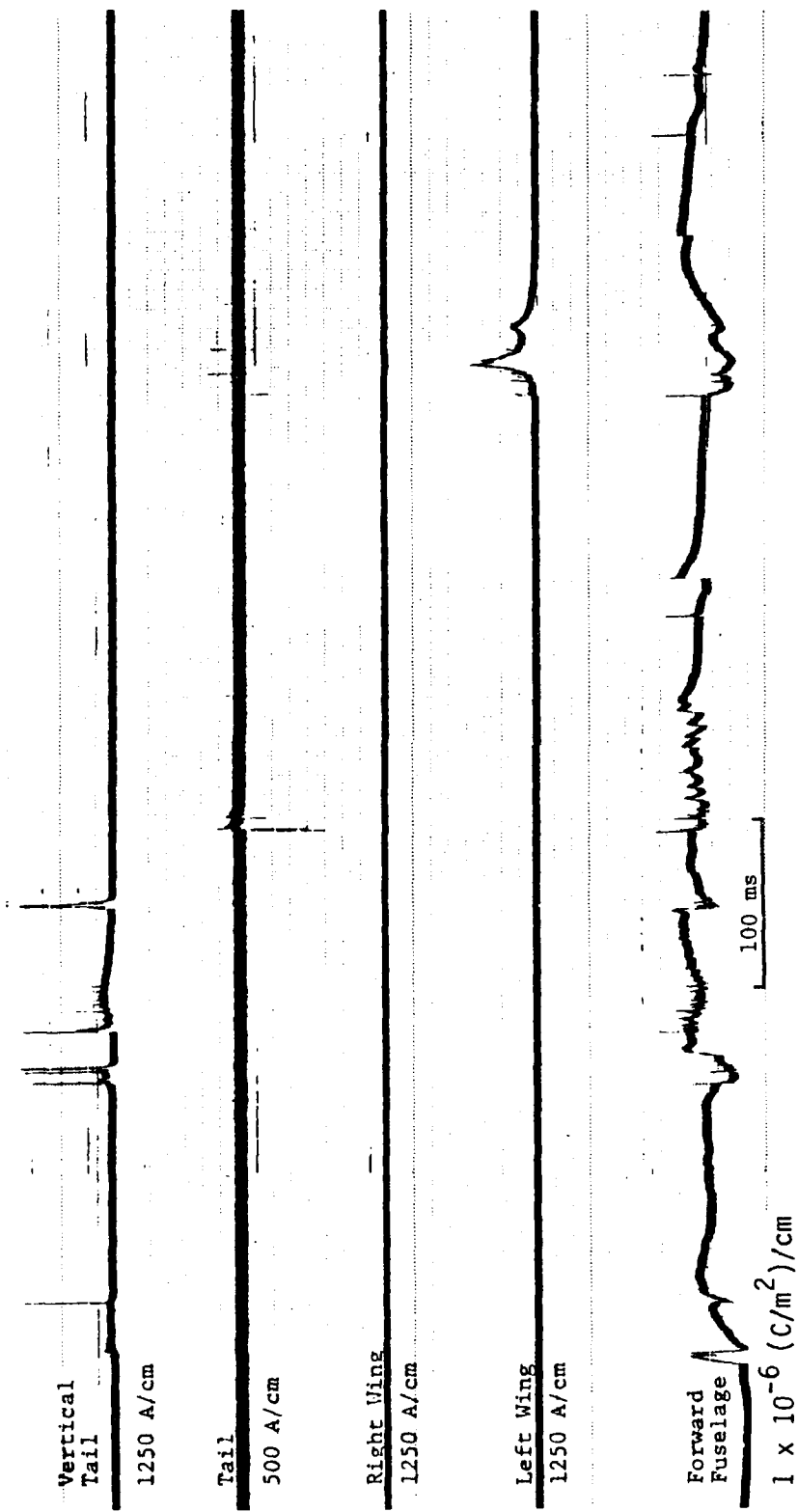


Figure B-15. Event 85-20

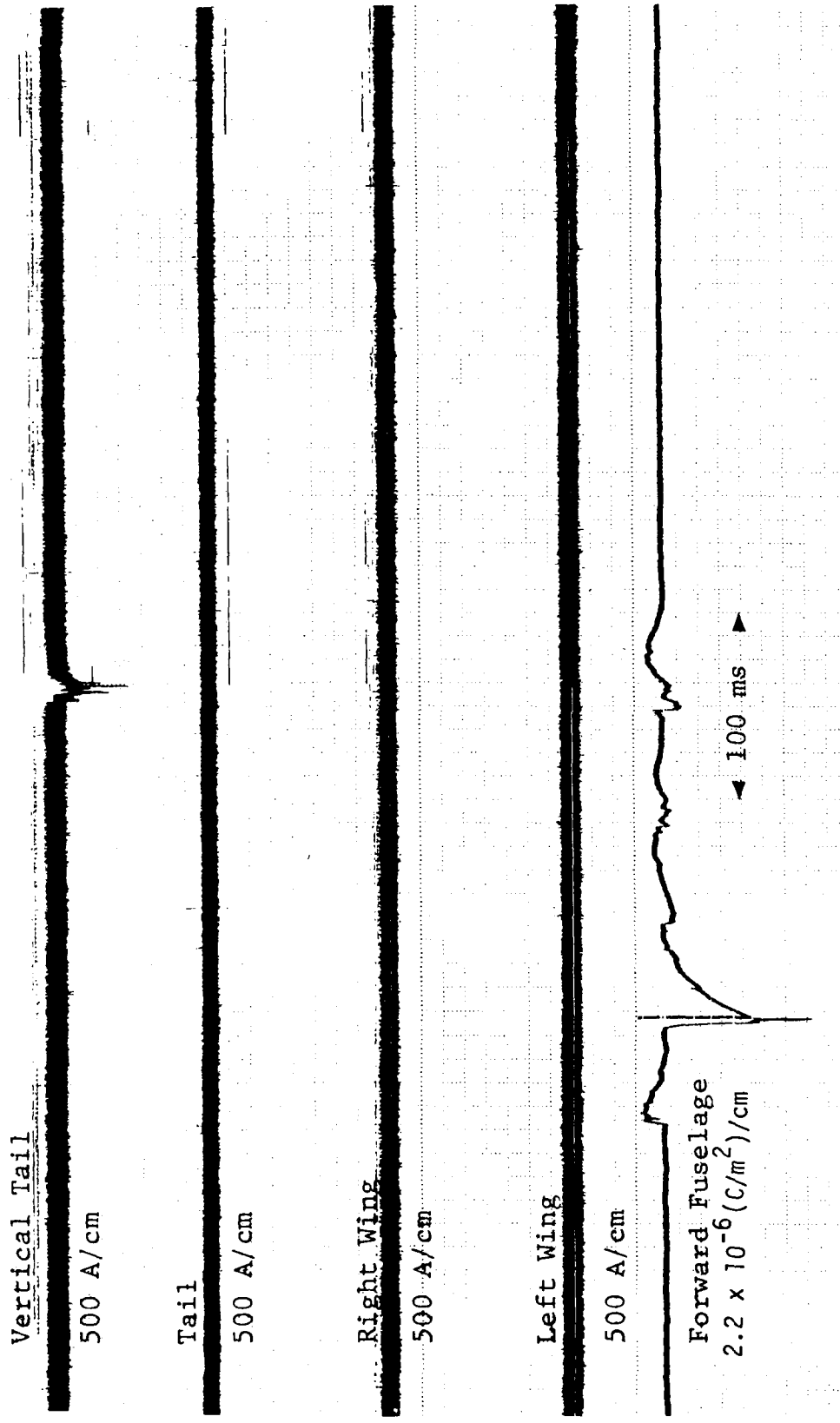


Figure B-16. Event 85-21

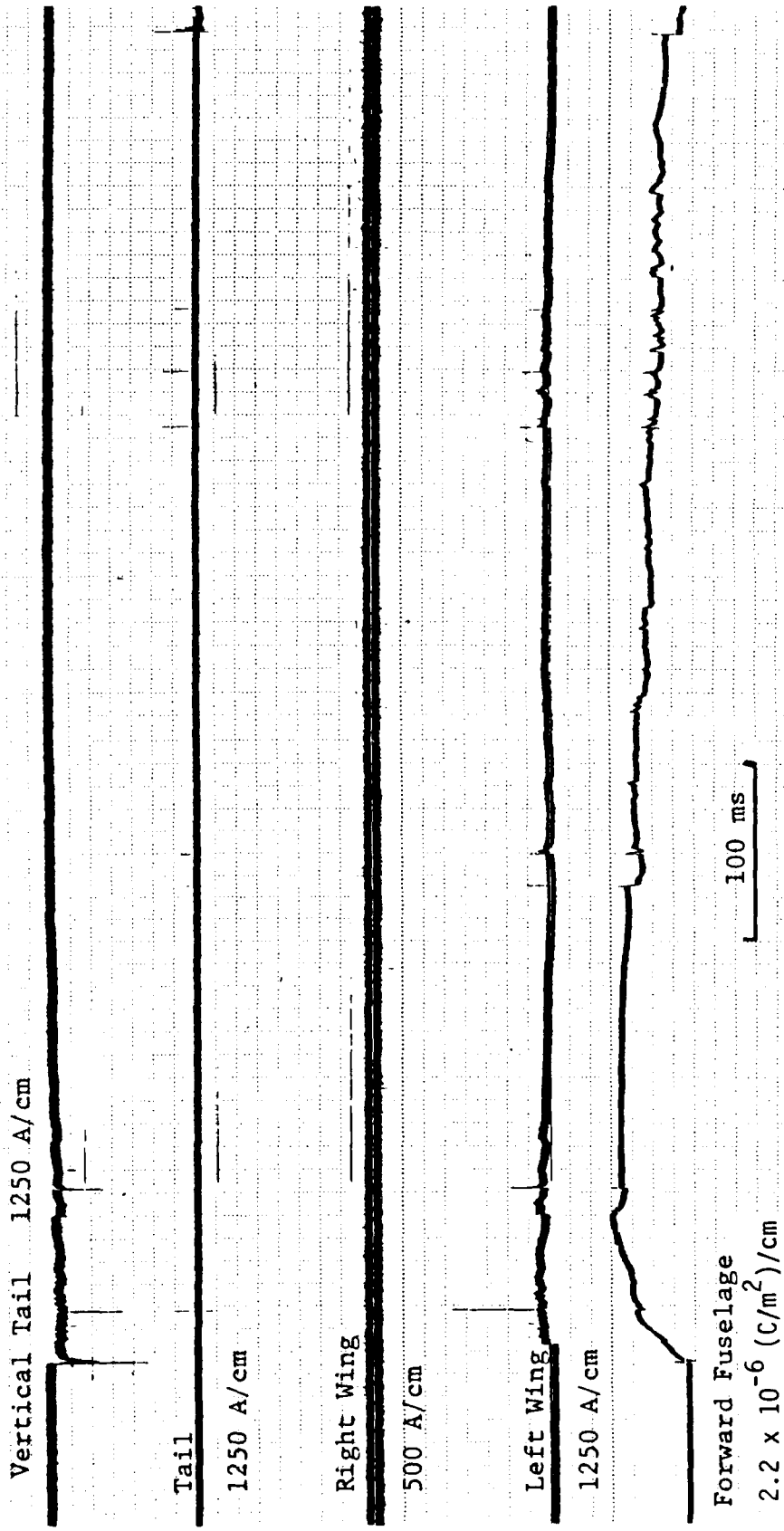


Figure B-17. Event 85-23

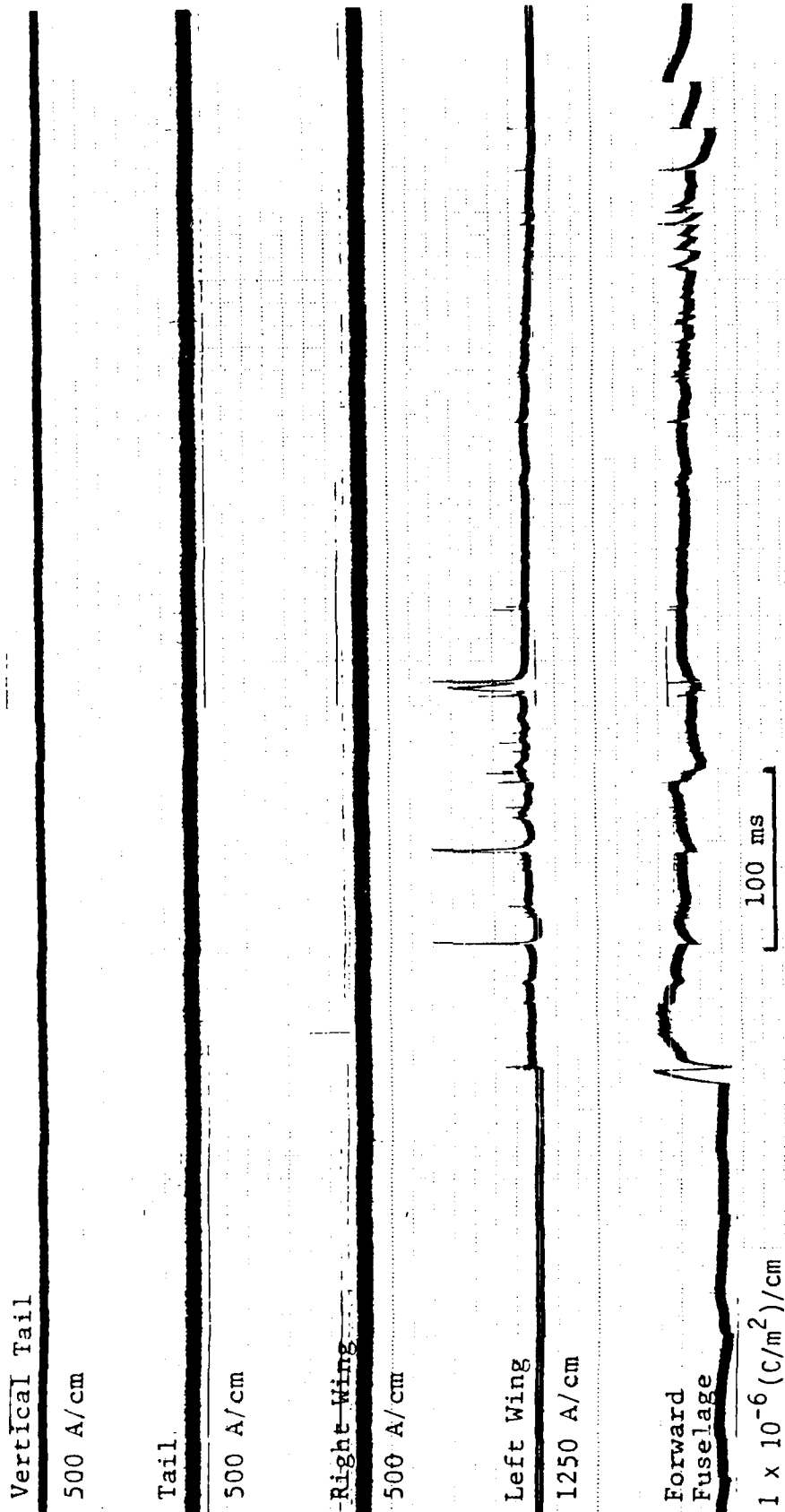


Figure B-18. Event 85-24

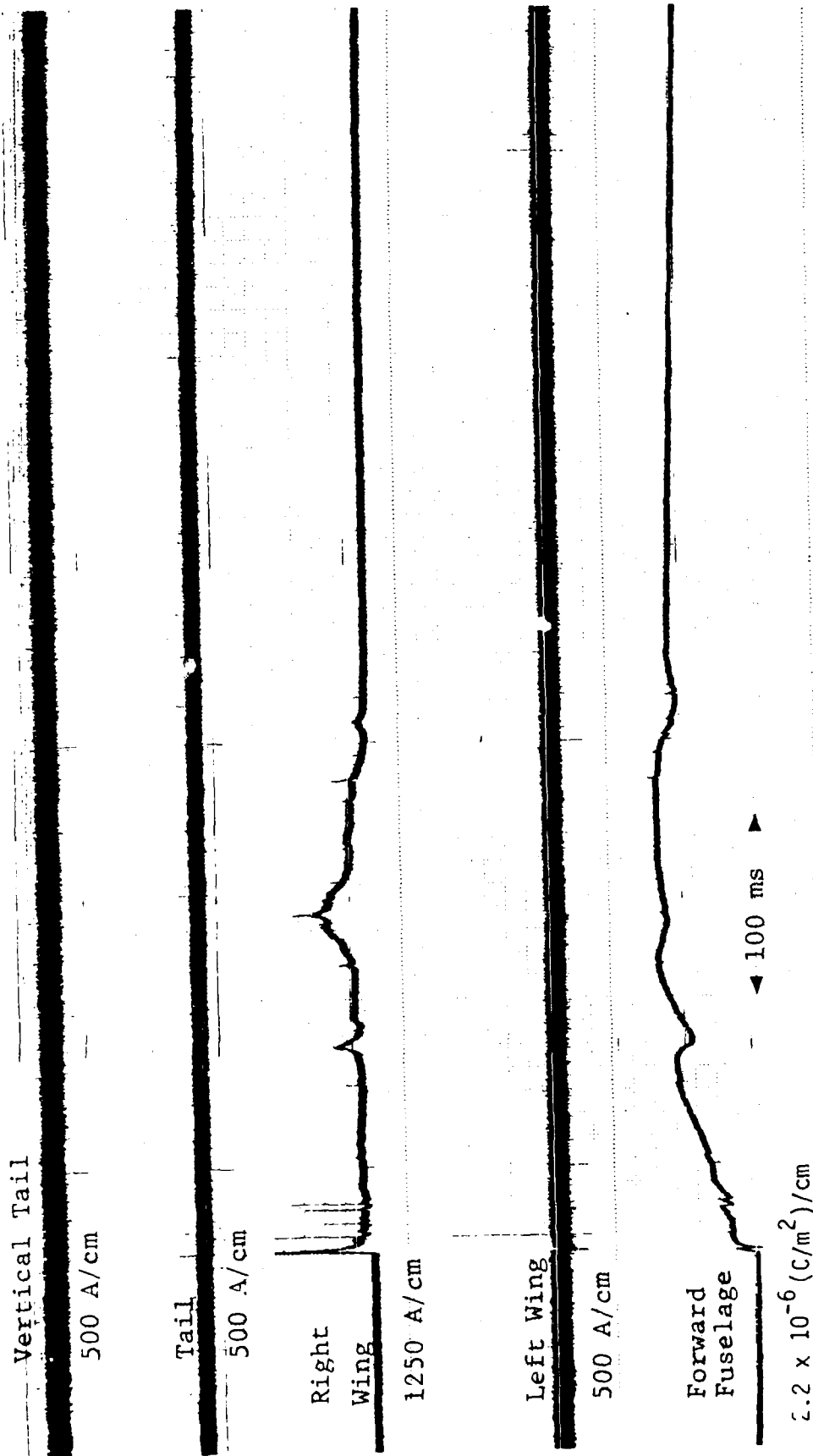


Figure B-19. Event 85-25

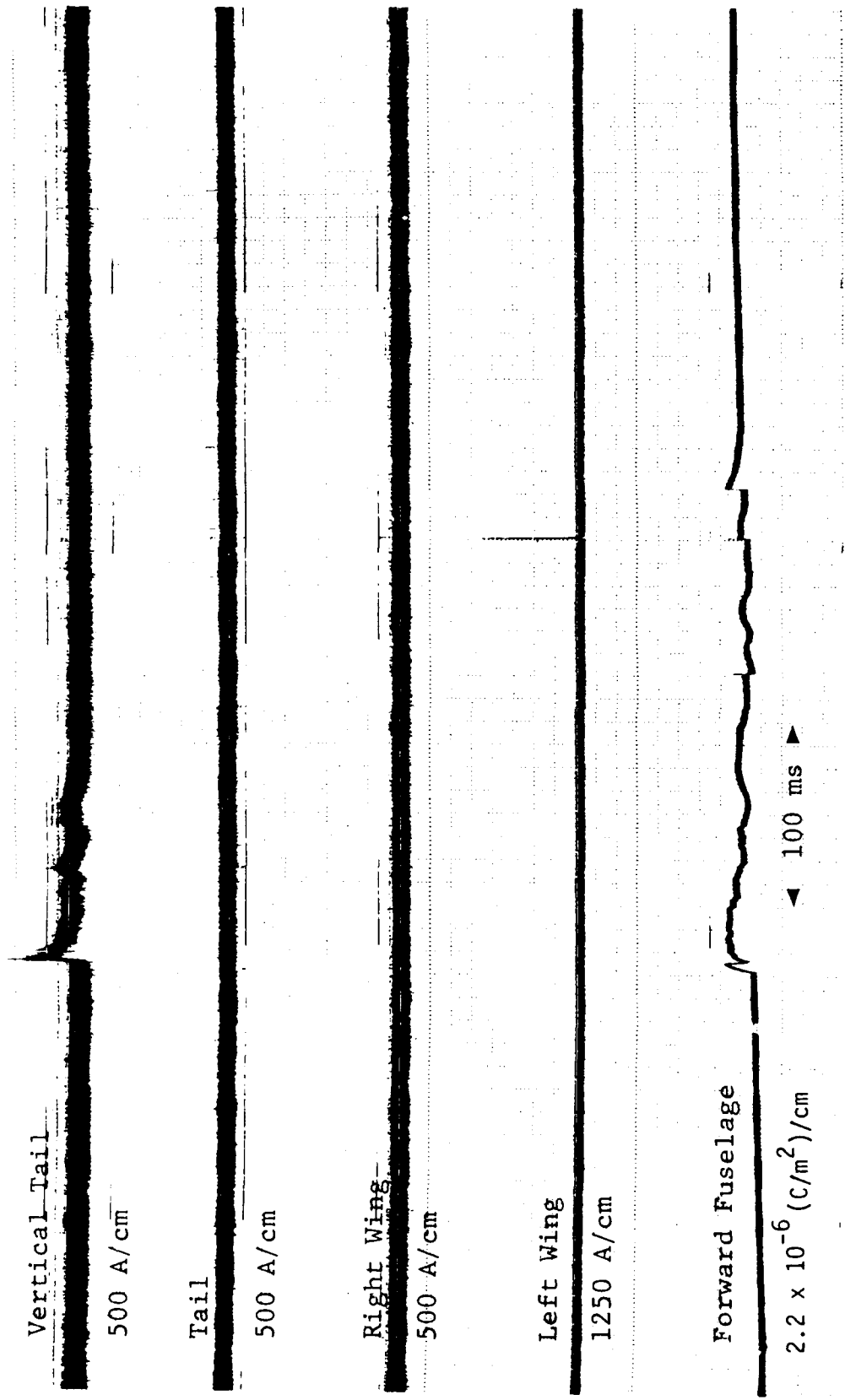


Figure B-20. Event 85-26

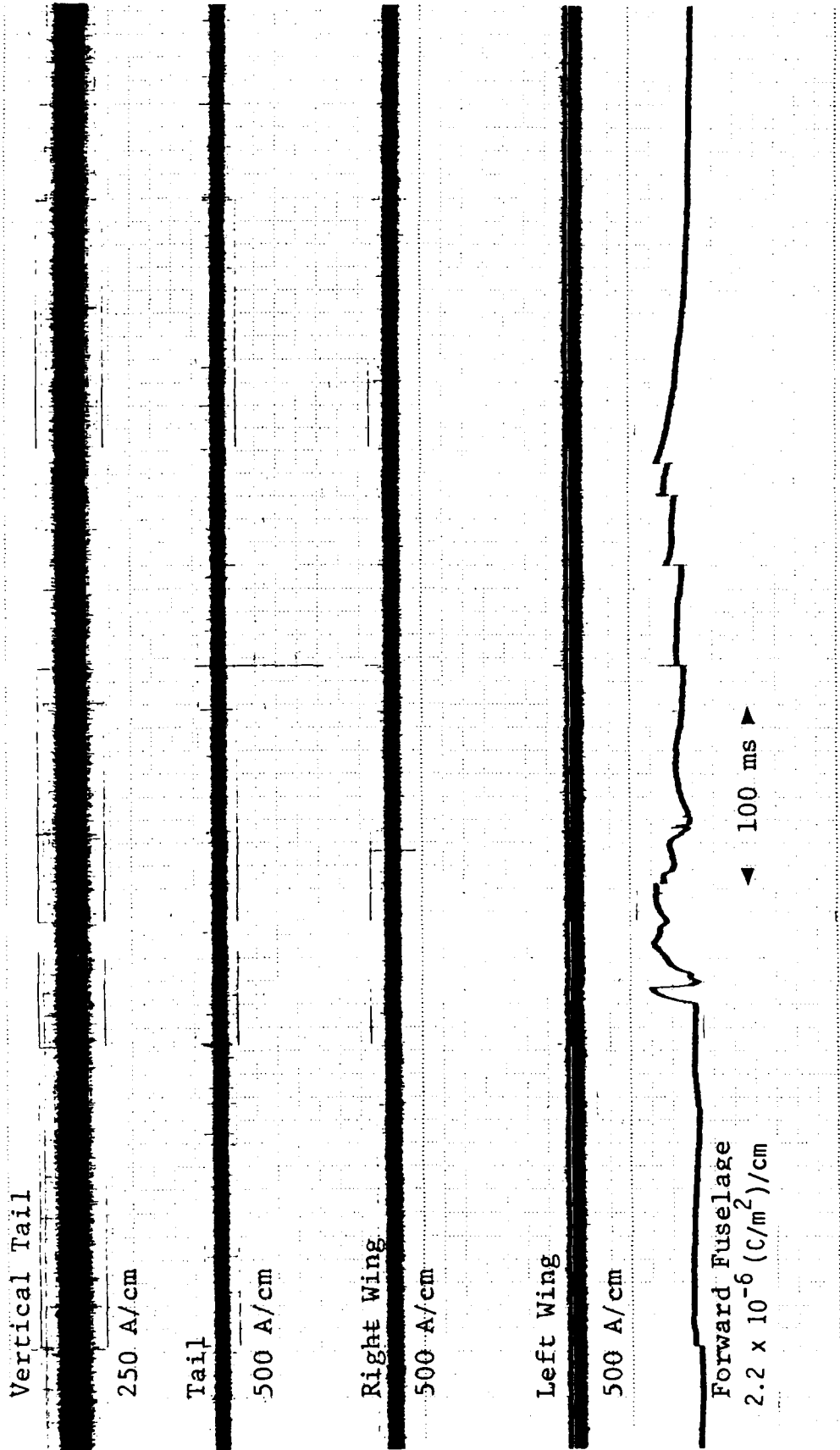


Figure B-21. Event 85-27

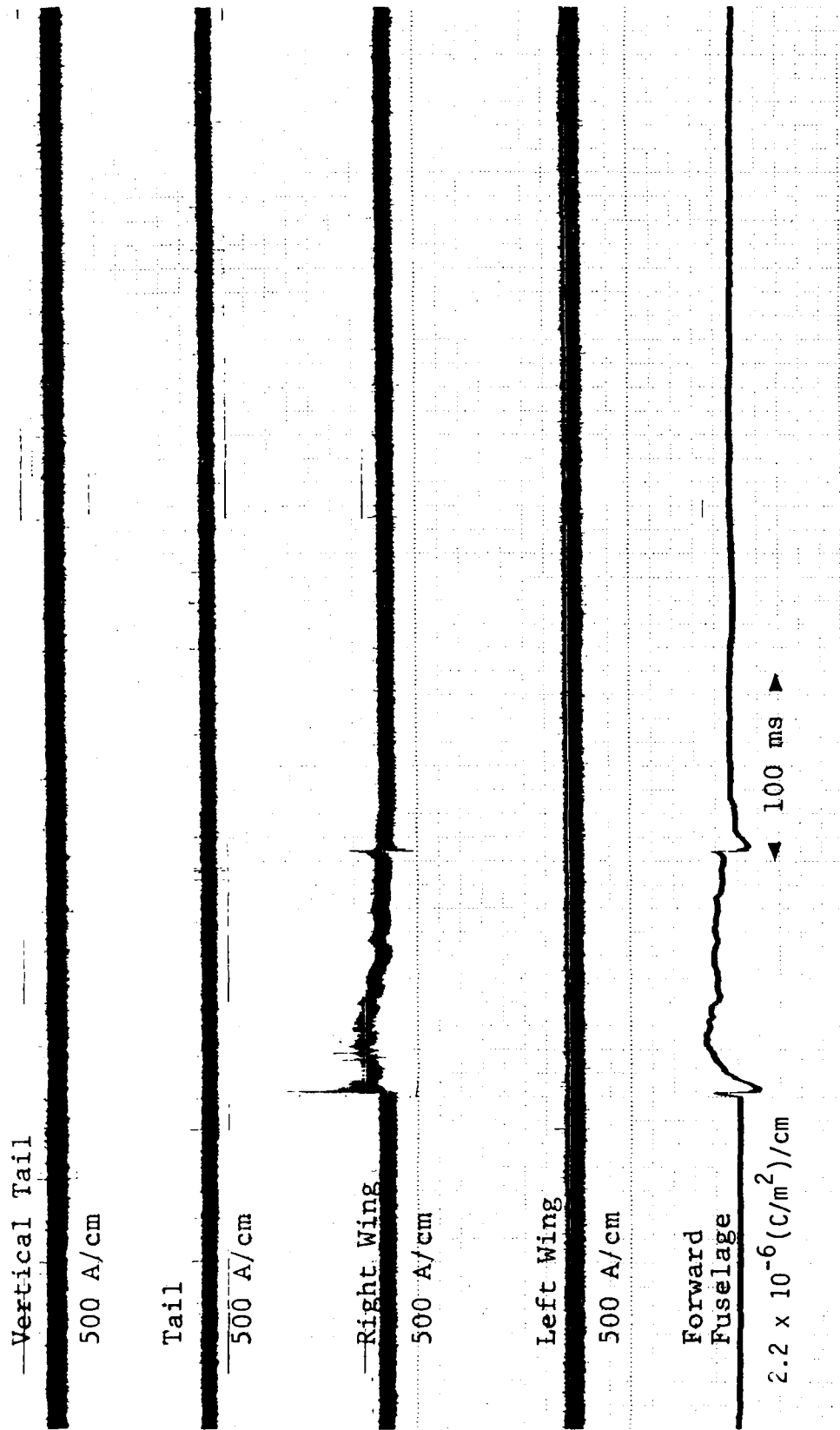


Figure B-22. Event 85-28

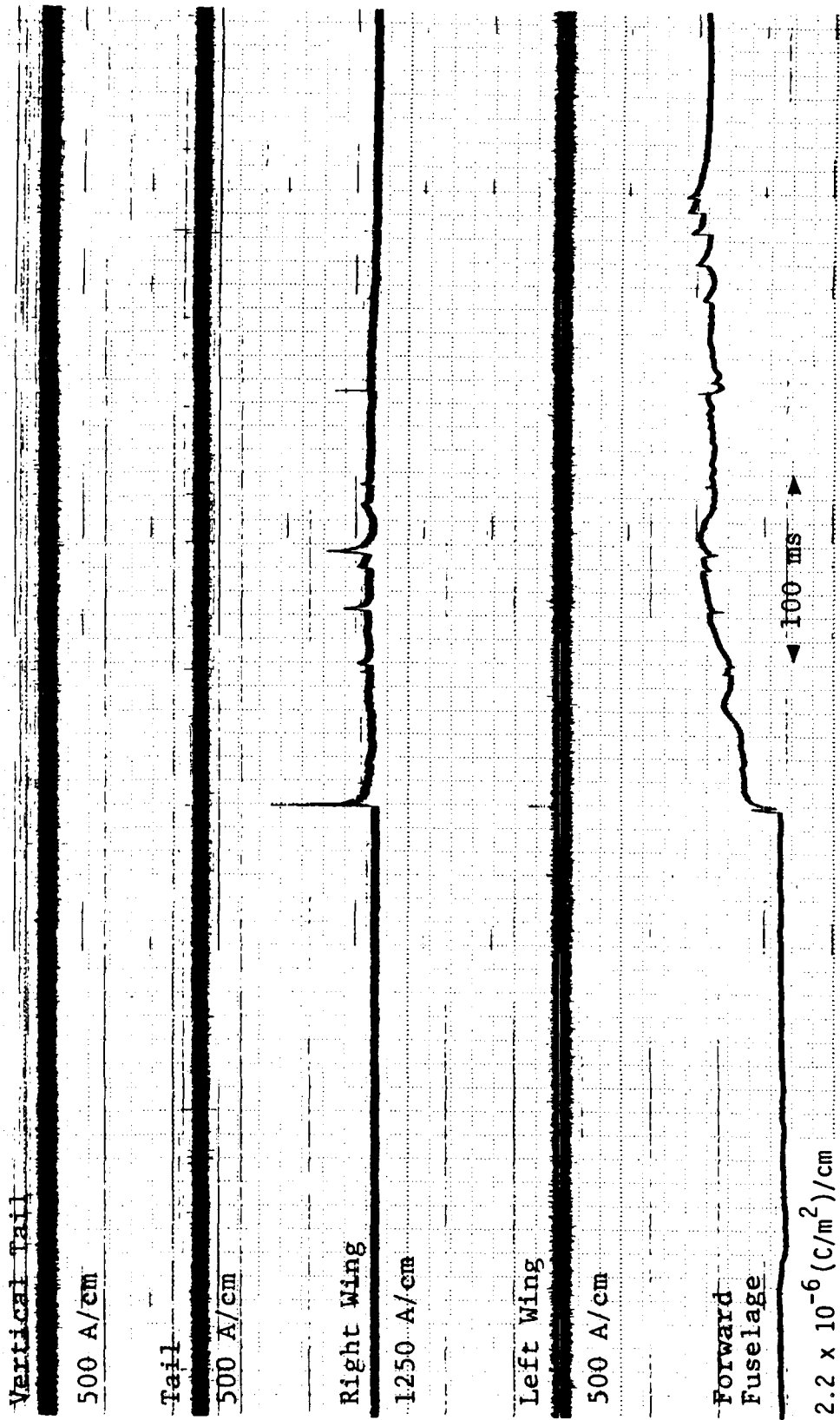


Figure B-23. Event 85-29



Figure B-24. Event 85-30

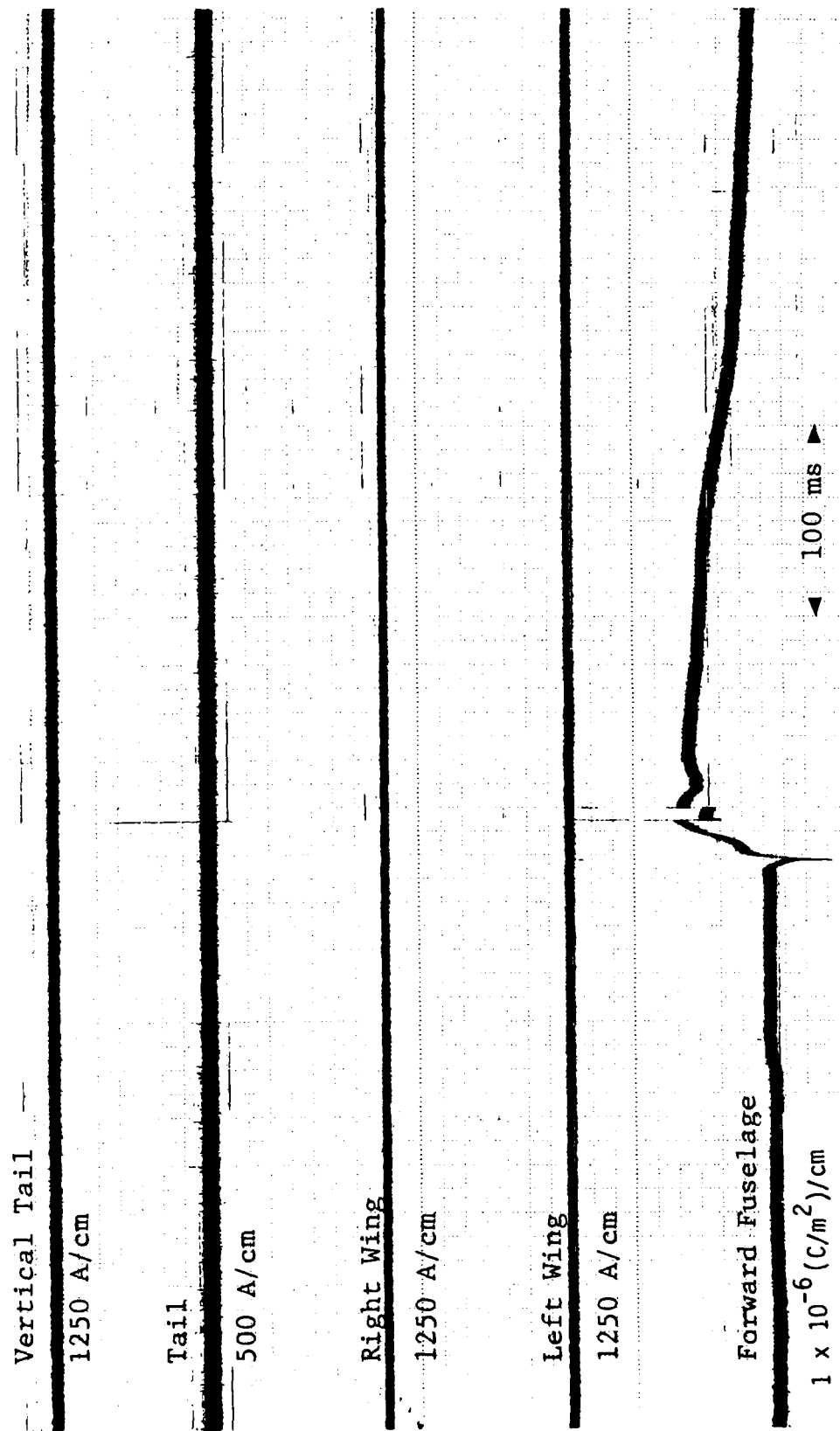


Figure B-25. Event 85-31